Electronic Supplementary Material (ESI) for Reaction Chemistry & Engineering.

Electricity-induced micro-flow C-H/N-H alkyne annulation: A greener approach to access heteroaromatic compounds

Sanjeev Kumar,[a,b] Bhushan Mahajan,[a,b] Bhanwar Kumar Malviya[a], Genji Sukumar[a], P. Srihari,*[a,b] Ajay K. Singh*[a,b]

[a] Department of Organic Synthesis & Process Chemistry, CSIR-Indian Institute of Chemical Technology, Hyderabad-500007, India.

[b] Academy of Scientific and Innovative Research (AcSIR), CSIR-Human Resource Development Centre (CSIR-HRDC) Campus, Ghaziabad-201002, Uttar Pradesh, India.

E-mail: ajaysingh015@gmail.com.

Table of Contents

1: General

1.1. Material and method used in experiments.

Most of the reagents and chemicals were purchased from Sigma-Aldrich and AVRA chemicals, which were used without further purification and demineralized water (18.2 mS conductivity) was used for the all experiments. All work-up and purification procedures were carried out with the reagent-grade solvents. Thin-layer chromatography (TLC) was performed using analytical chromatography silica gel 60 F254 precoated plates (0.25 mm). The developed chromatogram was analysed by UV lamp (254 nm). Polytetrafluoroethylene (PTFE) (id = 100-1000 μm) tubing, T-junction, high-purity Perfluoro alkoxy alkanes (PFA) tubing were also purchased from Upchurch IDEX HEALTH &SCIENCE. Graphite electrode, platinum electrode, heating reactor bought from the SmartChemSynth Pvt. Ltd. Hyderabad, India.

1.2. Measurement Method.

Nuclear magnetic resonance (NMR) spectra were recorded on a Bruker 600, 500, 400 or 300 MHz in $CDCl_3$, DMSO-d_6 or CD_3OD solvent. Chemical shifts for ^1H NMR were expressed in parts per million (ppm) relative to tetramethylsilane (δ 0.00 ppm). Chemical shifts for ^{13}C NMR were expressed in ppm relative to $CDCl_3$ (δ 77.0 ppm) or CD_3OD (49.00) and data were reported as follows: chemical shift, multiplicity (s = singlet, d = doublet, dd = doublet of doublets, t = triplet, q = quartet, quin = quintet, sext = sextet, m = multiplet), coupling constant (Hz), and integration. High-resolution mass spectra (HRMS) were obtained from a JMS-T100TD instrument (DART) and Thermo Fisher Scientific Exactive (APCI). Power Sonic 405 sonication instrument was used for washing the metal surface. ATR analysis was conducted on portable FTIR spectrometer Bruker ALPHA and Datalog model DCS-PS-6401 power supply system was used to supply the constant current. Melting point was conducted on POLMAN MP-96. Han's

Yueming laser series (model CMA0604-B-A, Carbon dioxide based, laser power 60W) equipment was used for the fabrication of micro-channel.

2. Preparation of starting materials: The following starting materials were synthesized according to previously described methods.[1] A 50 mL round bottomed-flask was charged with (0.01 M) o-phenylenediamine **(1a),** methanol (10 mL) and (0.01 M) substituted benzaldehyde (**2**). The open round bottomed-flask was placed under blue LED and stirred at room temperature until disappearance of starting material as checked by thin layer chromatography (TLC and/or ^{1}H NMR). The reaction mixture was concentrated under reduced pressure and purified by recrystallization or by silica gel column chromatography.

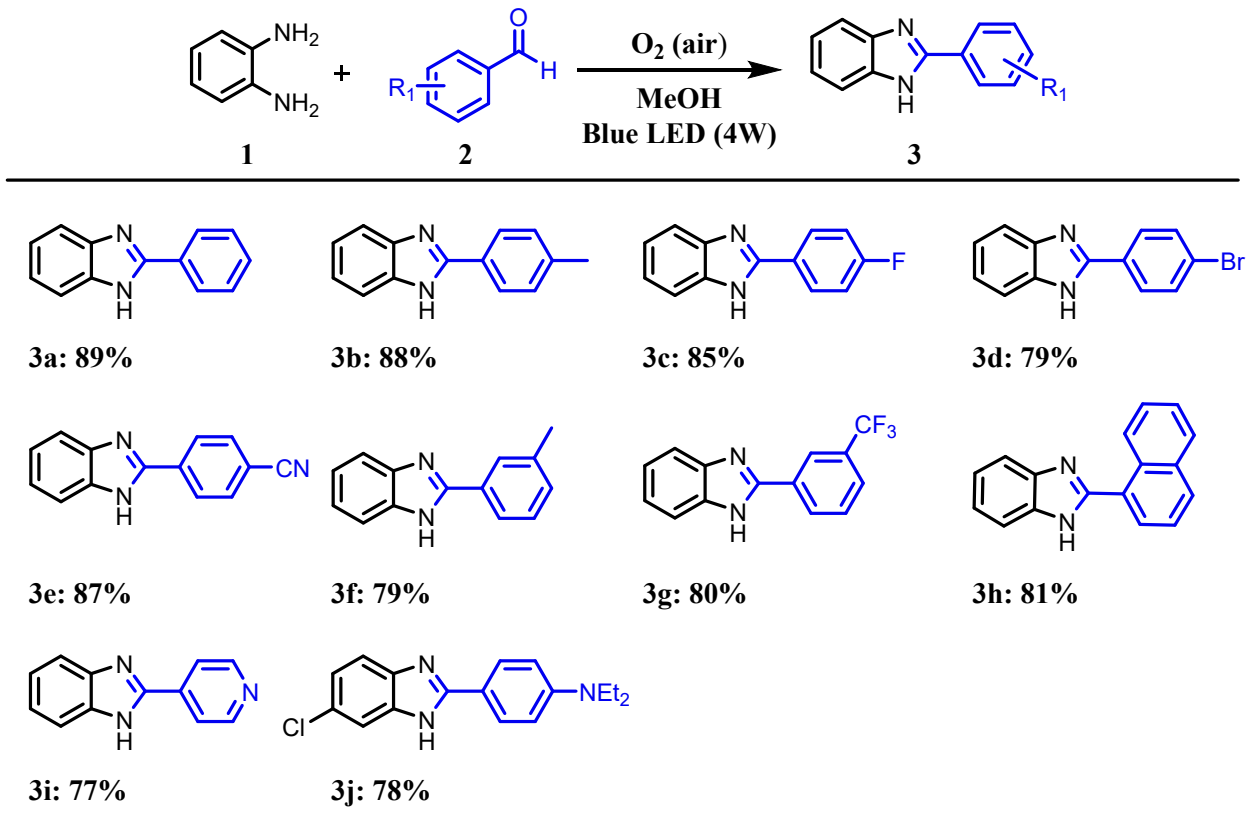

Fig. S1. Synthesis of substituted fused Imidazole (2-aryl benzimidazoles) reaction Condition: o-phenylenediamine, (0.01M); substituted benzaldehyde (0.01M); 10 mL methanol, blue LED 4-watt, time 12 h under open air condition. Yields are based on isolated yield.

2-Phenyl-1H-benzo[d] imidazole (3a): Take a 50 mL round bottomed-flask and charge with

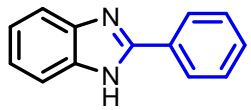

(0.01 M) o-phenylenediamine **(1a)** in methanol (10 mL) and to this was added (0.01 M) benzaldehyde (**2a)**. The open round bottomed-flask was placed under blue LED and stirred at room temperature until the consumption of starting material was observed as checked by thin layer chromatography (TLC). The reaction mixture was concentrated under reduced pressure and the crude material was purified by silica gel column chromatography (n-Hexane: EtOAc = 80:20), yield **3a** (345 mg, 89%) as a white solid and melting point is 288−291 °C. **^{1}H NMR (400 MHz, DMSO-*d*$_6$):** δ 12.93 (s, 1H), 8.24 – 8.17 (m, 2H), 7.69 (d, *J* = 7.5 Hz, 1H), 7.62 – 7.47 (m, 4H), 7.28 – 7.17 (m, 2H). **^{13}C NMR (101 MHz, DMSO-*d*$_6$):** δ 151.22, 143.80, 134.99, 130.16, 129.84, 128.95, 126.43, 122.54, 121.68, 118.88, 111.33. **IR (V_{max}):** 3687, 3023,2361, 1520, 1215, 1175, 1021, 740, 671. **HRMS (ESI):** *m/z* calcd for $C_{13}H_{10}N_2$ $[M+H]^+$: 195.0922, found: 195.0916. Verified the analytical data with those reported in the literature.[2-4]

2-(*p*-Tolyl)-1H-benzo[d]imidazole (3b): Starting material **3b** was prepared according to general

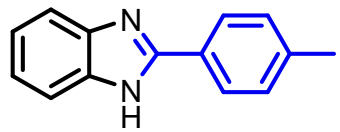

procedure mentioned in section **2**. The crude material was purified by silica gel column chromatography (n-Hexane: EtOAc = 80:20), yield **3b** (366 mg, 88%) as a white solid and melting point is 280−281°C. **^{1}H NMR (400 MHz, DMSO-*d*$_6$):** δ 8.07 (d, *J* = 8.2 Hz, 2H), 7.60 (dd, *J* = 6.0, 3.2 Hz, 2H), 7.38 (d, *J* = 7.9 Hz, 2H), 7.22 (dd, *J* = 6.0, 3.1 Hz, 2H), 2.39 (s, 3H). **^{13}C NMR (101 MHz, DMSO-*d*$_6$):** δ 161.38, 151.16, 140.06, 138.58, 129.61, 126.69, 126.57, 122.39, 114.86, 21.03. **IR (V_{max}):** 3023, 2405, 1523, 1427, 1215, 741, 670. **HRMS (ESI):** *m/z* calcd for $C_{14}H_{12}N_2$ $[M+H]^+$: 209.1079, found: 209.1073. Verified the analytical data with those reported in the literature.[5]

2-(4-Fluorophenyl)-1H-benzo[d]imidazole (3c): Starting material **3c** was prepared according to general procedure mentioned in section **2**. The crude material was purified by silica gel column chromatography (n-Hexane: EtOAc = 80:20), yield **3c** (360 mg, 85%) as a white solid and melting point is 180−181 °C. **^{1}H NMR (400 MHz, DMSO-d_6):** δ 12.93 (s, 1H), 8.26 – 8.19 (m, 2H), 7.60 (dd, *J* = 52.6, 7.3 Hz, 2H), 7.44 – 7.37 (m, 2H), 7.20 (dd, *J* = 8.6, 6.9 Hz, 2H). **^{13}C NMR (101 MHz, DMSO-d_6):** δ 163.07 (d, $J_{C\text{-}F}$ = 248.46 Hz), 150.39, 143.76, 135.02, 128.73 (d, $J_{C\text{-}F}$ = 8.08 Hz), 126.81 (d, $J_{C\text{-}F}$ = 2.02 Hz), 122.56, 121.73, 118.84, 116.01 (d, $J_{C\text{-}F}$ = 22.22 Hz), 111.33. **^{19}F NMR (377 MHz, DMSO-d_6):** δ -106.24. **IR (V_{max}):** 3021, 1521, 1427, 1216, 740, 671. **HRMS (ESI):** *m/z* calcd for $C_{13}H_9FN_2$ $[M+H]^+$: 213.0822, found: 213.0820. Verified the analytical data with those reported in the literature.[4]

2-(4-Bromophenyl)-1H-benzo[d]imidazole (3d): Starting material **3d** was prepared according to general procedure mentioned in section **2**. The crude material was purified by silica gel column chromatography (n-Hexane: EtOAc = 80:20), yield **3d** (428 mg, 79%) as a brown solid and melting point is 295−297 °C. **^{1}H NMR (400 MHz, DMSO-d_6):** δ 13.00 (s, 1H), 8.14 (d, *J* = 8.5 Hz, 4H), 7.78 (d, *J* = 8.5 Hz, 4H), 7.63 (dd, *J* = 5.8, 3.2 Hz, 4H), 7.24 (dd, *J* = 6.0, 3.1 Hz, 4H). **^{13}C NMR (101 MHz, DMSO-d_6):** δ 150.19, 139.49, 131.97, 131.70, 130.97, 129.33, 128.36, 127.95, 123.27, 122.34, 115.10. **IR (V_{max}):** 3021, 1529, 1427, 1215, 740, 671. **HRMS (ESI):** *m/z* calcd *for* $C_{13}H_9BrN_2$ $[M+H]^+$: 273.0021, found: 273.0023. Verified the analytical data with those reported in the literature.[4]

4-(1H-benzo[d]imidazol-2-yl) benzonitrile (3e): Starting material **3e** was prepared according to

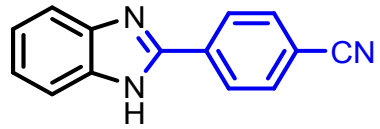

general procedure mentioned in section **2**. The crude material was purified by silica gel column chromatography (n-Hexane: EtOAc = 80:20), yield **3e** (381 mg, 87%) as a white solid and melting point is 266−267 °C. **^{1}H NMR (400 MHz, DMSO-d_6):** δ 8.36 (d, *J* = 8.4 Hz, 1H), 8.05 (d, *J* = 8.4 Hz, 1H), 7.67 (dd, *J* = 5.9, 3.2 Hz, 1H), 7.28 (dd, *J* = 6.0, 3.1 Hz, 1H). **^{13}C NMR (101 MHz, DMSO-d_6):** δ 161.03, 159.45, 149.34, 134.19, 132.99, 127.00, 122.86, 118.61, 115.45, 112.05, 111.93. **IR (V_{max}):** 3021, 1215, 741, 670. **HRMS (ESI):** *m/z* calcd for $C_{14}H_9N_3$ $[M+H]^+$: 220.0869, found: 220.0870. Verified the analytical data with those reported in the literature.[6]

2-(*m*-Tolyl)-1H-benzo[d]imidazole (3f): Starting material **3f** was prepared according to general

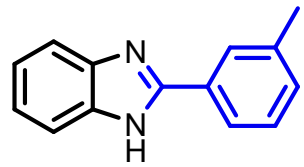

procedure mentioned in section **2**. The crude material was purified by silica gel column chromatography (n-Hexane: EtOAc = 80:20), yield **3f** (328 mg, 79%) as a white solid and melting point is 234-237°C. **^{1}H NMR (400 MHz, DMSO-d_6):** δ 12.87 (s, 1H), 8.04 (s, 1H), 7.98 (d, *J* = 7.8 Hz, 1H), 7.67 (d, *J* = 7.1 Hz, 1H), 7.54 (d, *J* = 7.1 Hz, 1H), 7.45 (t, *J* = 7.6 Hz, 1H), 7.33 (d, *J* = 7.5 Hz, 1H), 7.22 (dd, *J* = 8.5, 6.1 Hz, 2H), 2.44 (s, 3H). **^{13}C NMR (101 MHz, DMSO-d_6):** δ 151.30, 143.78, 138.14, 134.96, 130.46, 130.08, 128.83, 126.99, 123.57, 122.44, 121.60, 118.79, 111.27, 21.06. **IR (V_{max}):** 3057, 2921, 2871, 2782, 1602, 1535, 1440, 1279, 749. **HRMS (ESI):** m/z calcd for $C_{14}H_{12}N_2$ $[M+H]^+$: 209.1073, found: 209.1070. Verified the analytical data with those reported in the literature.[6]

2-(3-(Trifluoromethyl) phenyl)-1H-benzo[d]imidazole (3g): Starting material **3g** was prepared according to general procedure mentioned in section **2**. The crude material was purified by silica gel column chromatography (n-Hexane: EtOAc = 70:30), yield **3g** (419 mg, 80%) as a white solid and melting point is 209−211 °C. **^{1}H NMR (400 MHz, DMSO-*d*$_6$):** δ 8.59 – 8.49 (m, 1H), 7.84 (dt, *J* = 15.5, 7.8 Hz, 1H), 7.70 – 7.64 (m, 1H), 7.30 – 7.24 (m, 1H). **^{13}C NMR (101 MHz, DMSO-*d*$_6$):** δ 149.59, 139.14, 130.94, 130.27, 130.00, 129.68, 129.37, 126.34, 126.31, 125.42, 122.91, 122.87, 122.69, 115.35. **^{19}F NMR (377 MHz, DMSO-*d*$_6$):** δ -61.34 (s). **IR (V_{max}):** 3455, 3394, 3196, 3074, 2765, 1426, 1327, 1132, 754, 696. **HRMS (ESI):** *m/z* calcd for $C_{14}H_9F_3N_2$ $[M+H]^+$: 263.0790, found: 263.0785.

2-(Naphthalen-1-yl)-1H-benzo[d]imidazole (3h): Starting material **3h** was prepared according to general procedure mentioned in section **3**. The crude material was purified by silica gel column chromatography (n-Hexane: EtOAc = 80:20), yield **3h** (395 mg, 81 %) as a white solid and melting point is 216−218 °C. **^{1}H NMR (400 MHz, DMSO-*d*$_6$):** δ 13.00 (s, 2H), 9.12 (d, *J* = 8.2 Hz, 3H), 8.16 – 8.02 (m, 9H), 7.76 – 7.59 (m, 15H), 7.33 – 7.24 (m, 6H). **^{13}C NMR (101 MHz, DMSO-*d*$_6$):** δ 151.31, 133.61, 130.49, 130.18, 128.40, 127.90, 127.43, 127.09, 126.36, 126.31, 125.28, 122.18. **IR (V_{max}):** 3644, 3206, 3102, 3115, 2915, 2712, 1397, 765. **HRMS (ESI):** *m/z* calcd for $C_{13}H_{12}N_2$ $[M+H]^+$: 245.1073, found: 245.1071.

2-(Pyridin-4-yl)-1H-benzo[d]imidazole (3i): Starting material **3i** was prepared according to general procedure mentioned in section **2**. The crude material was purified by silica gel column chromatography (n-Hexane: EtOAc = 70:30), yield **3i** (300 mg, 77 %) as a pale yellow and melting point is 218-219 °C. **^{1}H NMR (400 MHz, DMSO-*d*$_6$):** δ 8.77 (dd, *J* = 4.5, 1.6 Hz, 1H), 8.13 (dd, *J* = 4.5, 1.6 Hz, 1H), 7.68 (dd, *J* = 6.1, 3.2 Hz, 1H), 7.28 (dd, *J* = 6.1, 3.2 Hz, 1H). **^{13}C NMR (101 MHz, DMSO-*d*$_6$):** δ 150.48, 149.34, 148.95, 139.50, 137.29, 122.80, 120.36, 115.68. **IR (V_{max}):** 3022, 1606, 1525, 1431, 1215, 740, 671. **HRMS (ESI):** *m/z* calcd for $C_{12}H_9N_3$ $[M+H]^+$: 196.0869, found: 196.0868. Verified the analytical data with those reported in the literature.[7]

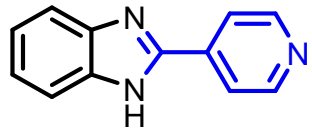

4-(6-Chloro-1H-benzo[d]imidazol-2-yl)-N, N-diethyl aniline (3j): Starting material **3i** was prepared according to general procedure mentioned in section **2**. The crude material was purified by silica gel column chromatography (n-Hexane: EtOAc = 70:30), yield **3i** (466 mg, 78 %) as a brown yellow and melting point is 106-107 °C. **^{1}H NMR (400 MHz, DMSO-*d*$_6$)**: δ 12.67 (s, 1H), 7.96 (d, *J* = 8.9 Hz, 2H), 7.57 – 7.46 (m, 2H), 7.15 (dd, *J* = 8.5, 2.0 Hz, 1H), 6.80 (d, *J* = 8.8 Hz, 2H), 3.48 – 3.41 (m, 4H), 1.15 (t, *J* = 6.9 Hz, 6H). **^{13}C NMR (101 MHz, DMSO-*d*$_6$):** δ 153.81, 150.36, 148.77, 143.74, 131.25, 128.05, 125.50, 124.06, 121.34, 115.68, 111.05, 110.09, 43.70, 12.46. **IR (V_{max}):** 3076, 2973, 1608, 1501, 1450, 1357, 1272, 1205, 1076, 813, 757. **HRMS (ESI):** *m/z* calcd for $C_{17}H_{18}ClN_3$ $[M+H]^+$: 300.1262 found: 300.125.

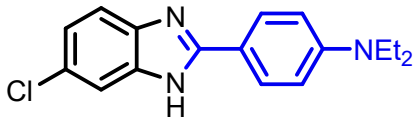

3: General reaction procedure and fabrication of micro electro flow reactor (µ-EFR).

3.1. Design of micro-electro flow reactor (µ-EFR): Electro-flow reactor (µ-EFR) outer body was fabricated with a Bakelite body Fig. S2. (60 mm length x 60 mm width x 10 mm thickness). The second layer was fabricated with PTFE film (60 mm length x 60 mm width x 1 mm thickness) layer made with a laser cutter. Next, platinum electrode was customized as per the reactor size (60 mm length x 60 mm width 0.2 mm thickness) and the solution flow under the constant current, the fourth layer incorporated of a laser scratch PTFE flexible plastic (60 mm x 60 mm x 1 mm thickness) zig-zag groove with a rectangular shape (2 mm x 80.0 mm). Graphite (Gr) electrode was customized as per the reactor size (60 mm length x 60 mm width x 2 mm thickness) and the solution flow under the constant current after that heating plate customized as per the reactor size (60 mm length x 60 mm width x 2 mm thickness). After construction of each layer and to align the patterns, the 4-corners of each two PTFE Teflon films were instructed to make a hole (1 mm diameter). Eventually, both the electrodes were sandwiched by Teflon zig-zag channel sheets with identical dimension to fit groove channels and integrate by inserting metal pins through the holes at the film corners Fig. S2. bakelite holders, the set was aligned by inserting metal pins through the holes at the film corners. Finally, the bakelite holder was tightly pressed by screw to seal the device with no leak Fig. S2.

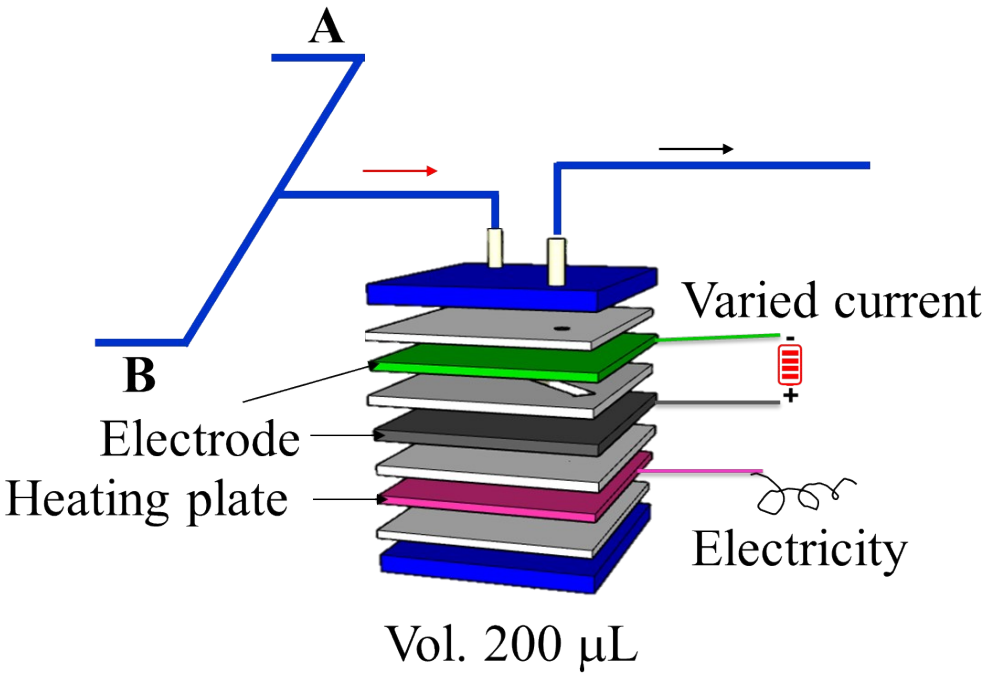

Fig. S2. Schematic set-up for the electrolysis reaction.

4. An integrated continuous micro electro flow platform for the synthesis, extraction and separation of annulated product.

4.1. Optimization of μ-EFR platform for annulation reaction:

We were proceeded the model reaction of a solution containing fused Imidazole **3a**: alkyne **4a**: $[RuCl_2(p\text{-cymene})]_2$ in *t*-AmOH: DMF and KOAc dissolved in H_2O + DMF was connected with above designed μ-EFR as described in Fig. S2. The two-solutions phase was mixed with stoichiometric molar ratio of **3a**: **4a**: $[RuCl_2(p\text{-cymene})]_2$) in *t*-AmOH: DMF and KOAc in H_2O: DMF at T-mixer and then flowed by μ–EFR (reactor volume 200 μL) with constant 4 mA current was placed in between the reactor Fig. S2. The product mixture from the end of μ–EFR reactor as an outlet was collected into a flask. As mentioned in table 1, S1-3, various reaction parameters (retention time, temperature, current, catalyst, electrolyte and solvent,) were regulated to optimize reaction performance.

Table S1. Screening of catalyst.

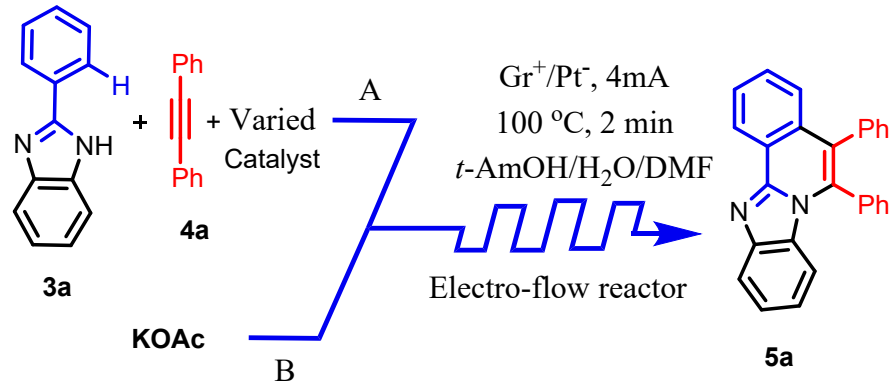

Entry	Catalyst	% Yield
1	$Co(OAc)_2 \cdot 4H_2O$	NA
2	$Ni(OAc)_2 \cdot 4H_2O$	NA
3	$Ni(OAc)_2 \cdot H_2O$	NA
4	$NiBr_2(dme)$	NA
5	CuI	NA
6	$Pd(OAc)_2$	NA
7	$[RuCl_2(p\text{-cymene})]_2$	96

Reaction Condition: The stock solution **(A)** containing **3a**:**4a**:catalyst:*t*-AmOH:DMF in a molar ratio 1:2:0.05:137:65 and the stock solution; **(B)** having an electrolyte KOAc:H_2O:DMF as a molar ratio 1:415:32.5. Yields are based on isolated yield.

Table S2. Screening of temperature.

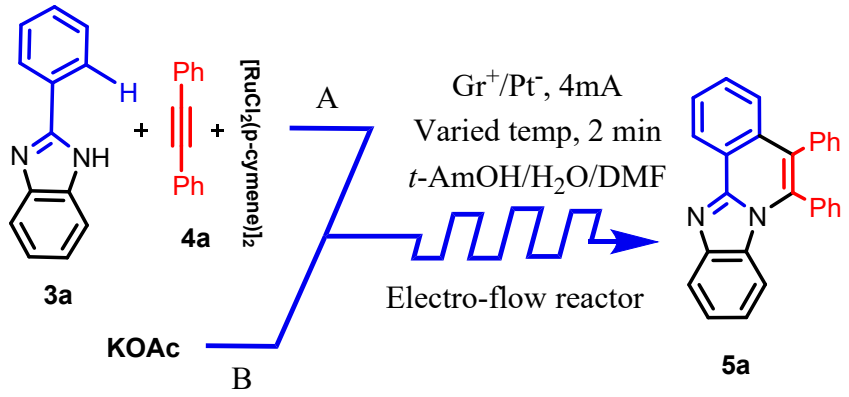

Entry	Temperature (^{0}C)	% Yield
1	80	60
2	100	96
3	120	66

Reaction condition: The stock solution **(A)** containing **3a**:**4a**:[$RuCl_2$(cymene)]$_2$:*t*-AmOH:DMF in a molar ratio 1:2:0.05:137:65 and the stock solution; **(B)** having an electrolyte KOAc:H_2O:DMF as a molar ratio 1:415:32.5. Yields are based on isolated yield.

Table S3. Screening of electrolyte.

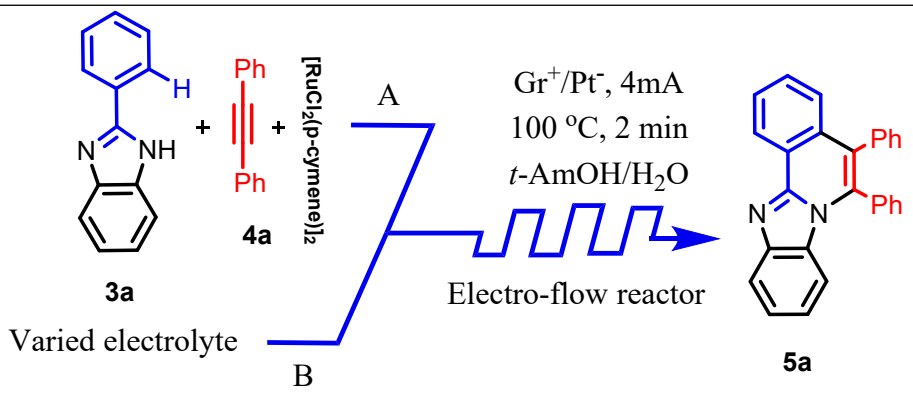

Entry	Electrolyte	% Yield
1	LiCl	69
2	KPF_6	40
3	KOAc	96
4	-	48

Reaction condition: The stock solution **(A)** containing **3a**:**4a**:$[RuCl_2(cymene)]_2$:*t*-AmOH: DMF in a molar ratio 1:2:0.05:137:65 and the stock solution; **(B)** having an electrolyte in H_2O:DMF as a molar ratio 1:415:32.5. Yield are based on isolated product.

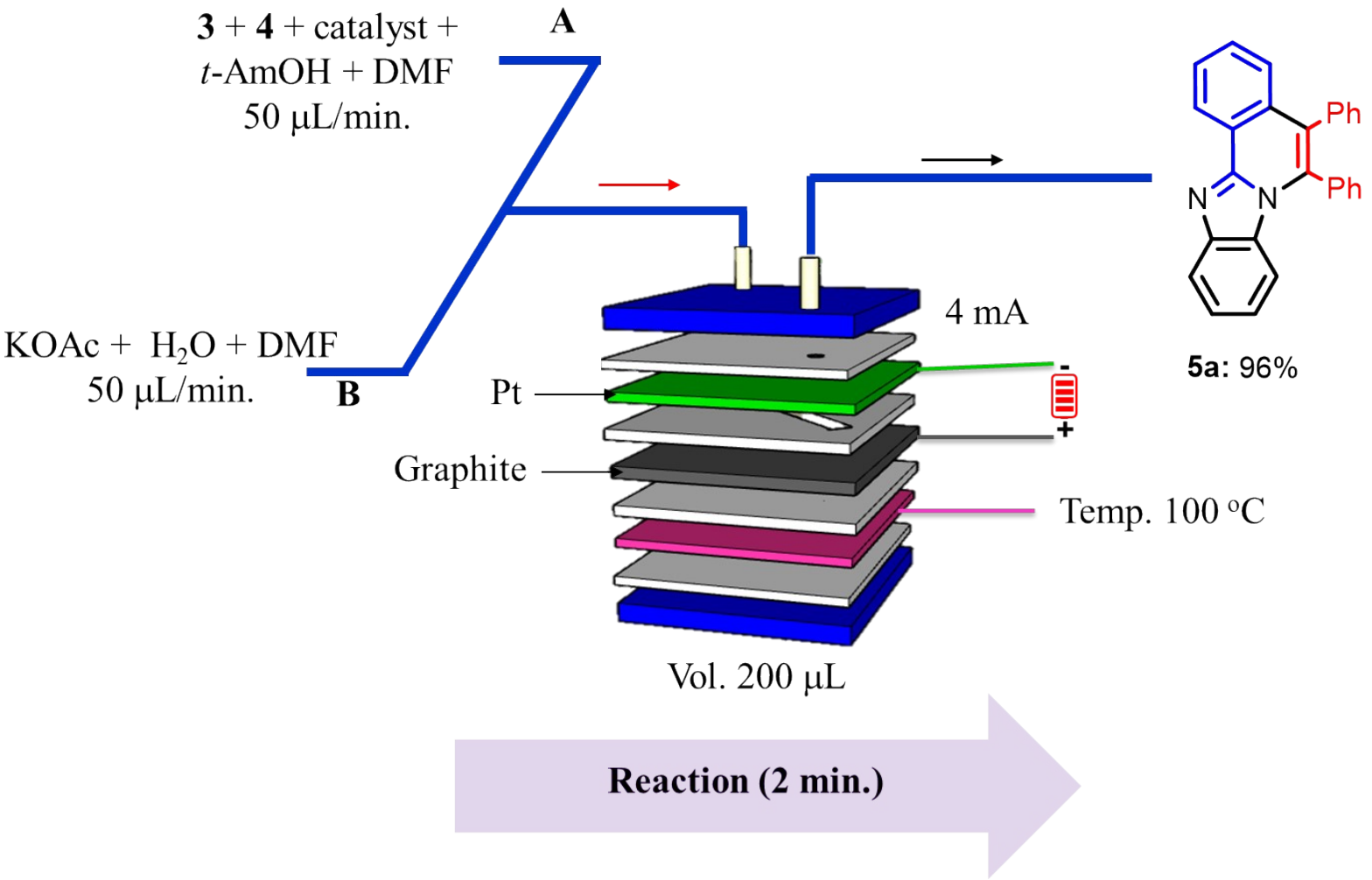

Fig. S3. Basic set up for the synthesis of imidazoisoquinolines. The stock solution (**A**) containing **3a**:**4a**:$[RuCl_2(cymene)]_2$:*t*-AmOH: DMF in a molar ratio 1:2:0.05:137:65; (**B**) having an electrolyte KOAc dissolved in H_2O:DMF as a molar ratio 1:415:32.5.

4.2. Fabrication of a dual channel micro-separator: As shown in Fig. S4, laser ablation on PTFE film was employed to fabricate the proposed dual-channel device. First and foremost, layers of 1000 μm thick PTFE films were ablated by UV laser 355 nm, to form a serpentine microchannel (1000 μm width, 1000 μm depth, and 80 cm length) as per our previously reported procedure[8]. The 4-corners of each film were holed (1 mm dia.) to align the film patterns. After laser ablation, the films were cleaned by washing with acetone under ultrasonic and dried. Polytetrafluoroethylene (PTFE) membrane (Whatman, 0.45 μm pore, 47 mm dia.) sandwiched by two sheets of PTFE film with the identical dimension of microchannel were placed between metal holders, which were aligned with each other by inserting metal pins through the holes at the film corners. Finally, the metal holder was tightly pressed by the screw to seal the device with no leak.

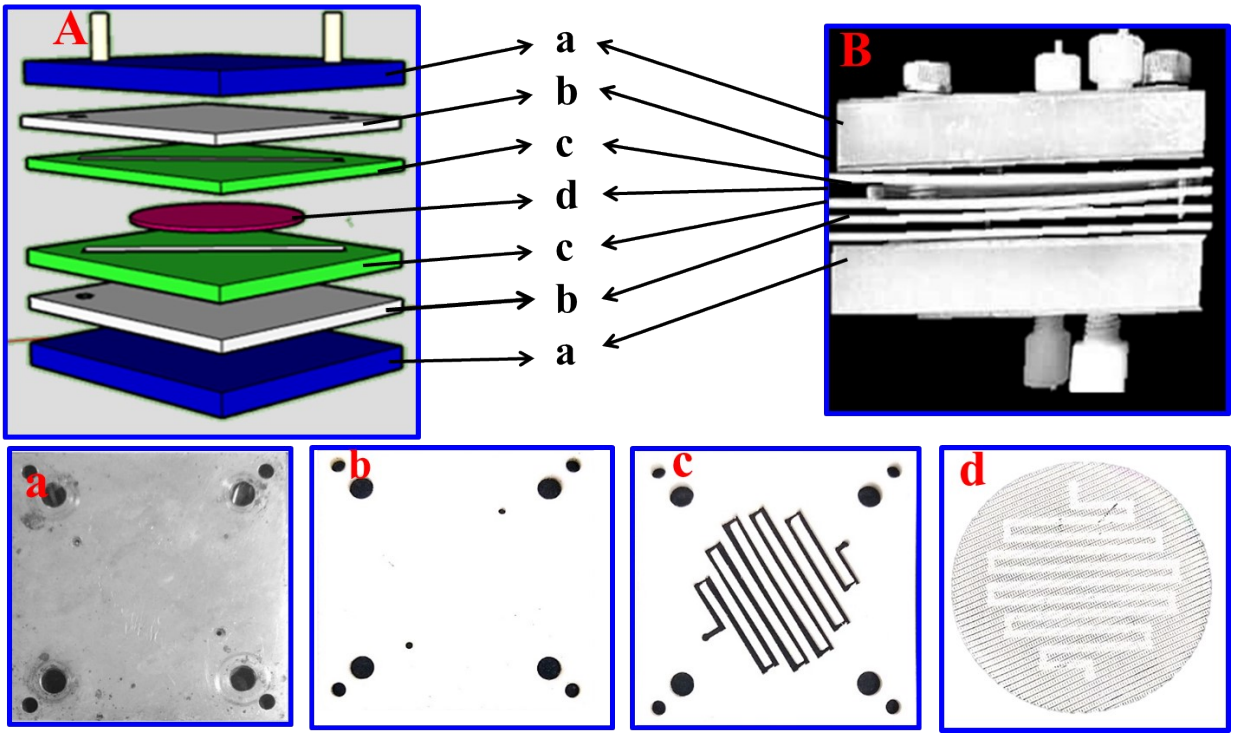

Fig. S4. Diagram of a fluoropolymer PTFE membrane based micro-separator (A) 3D model; (B) original photograph; (a) SS-metal body; (b) metal protecting PTFE layer; (c) laser grooved PTFE channel; (d) propylene coated PTFE membrane.

4.3. Solvent exchange optimization: To exchange the solvent containing product from *t*-AmOH:H_2O:DMF to solvent ethyl acetate, the additional PTFE membrane embedded phase separator was connected to the outlet of the μ-EFR reactor as shown in table S4. A serial process of droplet formation, extraction and separation for purification of the imidazoisoquinolines was conducted in droplet microfluidics equipped with the PTFE membrane micro-separator, as explained in a stepwise manner. At first, formation of alternating organic-aqueous droplets by introducing water into the product mixture in ethyl acetate through X-junction was done. Secondly, extraction of reaction waste into aqueous stream by passing through a length of 0.2 m capillary during 1.3 min. Finally, completion of the separation of the mixture of reactant, catalyst and product containing organic phase by wetting and crossing through thin PTFE membrane to the bottom of the separator wherein, the waste aq. *t*-AmOH:DMF containing aqueous phase did not wet the membrane and passed through as the original stream.

Table S4. Solvent exchange through the micro-separator.

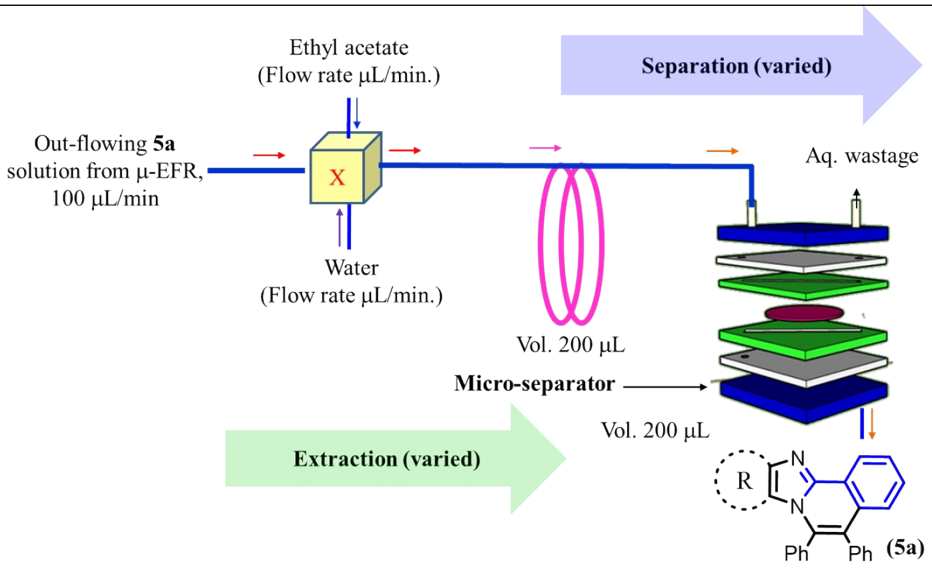

Entry	Flow rate (µL/min.)		Extraction time (min.)	Separation time (min.)	%Yield 5a
	Water	Ethyl acetate			
1	25	25	1.3	1.3	91
2	**50**	**50**	**1.0**	**1.0**	**96**
3	100	100	0.66	0.66	90
4	150	150	0.5	0.5	85

Isolated yields are based on average of two experiments, data errors ±1%.

4.4. An integrated continuous flow synthesis of 5,6-diphenylbenzo [4,5] imidazo [2,1-a] isoquinoline (5a):

The stock solution (**A**) containing **3a**:**4a**:[$RuCl_2$(p-cymene)]$_2$:*t*-AmOH:DMF in a molar ratio 1:2:0.05:137:65 and the stock solution (**B**) having an electrolyte KOAc dissolved in H_2O:DMF as a molar ratio 1:415:32.5 was taken in two syringes and connected with designed micro-electro-flow reactor to perform the reaction. The solution was introduced into capillary micro-reactor with T-junction and passed through an electro-flow reactor (reactor volume 200 μL) containing platinum (Pt) electrode (cathode) and Graphite (Gr-) electrode (anode) held at 100 °C with current of 4 mA, and residence time of two minutes. The μ-EFR solution delivers to the micro separator by introducing water and ethyl acetate through additional X-junction to form organic-aqueous droplets. Complete extraction between organic-aqueous segments was accomplished for 1.3 min retention time by flowing through a PTFE capillary (id = 1000 μm, length = 0.2 m, vol. = 200 μL). The complete separation was achieving by passing through the micro separator under the optimized reaction condition. The extracted waste aqueous layer was further extracted with ethyl acetate and analyzed by NMR and confirmed by the absence of the corresponding peaks in the crude NMR analysis (^{1}H and ^{13}C NMR spectra) which showed no product. The ethyl acetate layer was concentrated under vacuum to give the product and subsequent purification by column chromatography(*n*-Hexane: EtOAc = 5:1) on silica gel afforded the corresponding product **5a**, (96%) as a white solid and melting point is 275-277 °C. **^{1}H NMR (400 MHz, $CDCl_3$):** δ 8.99 (dd, *J* = 8.0, 0.8 Hz, 1H), 7.99 (d, *J* = 8.2 Hz, 1H), 7.72 – 7.67 (m, 1H), 7.60 – 7.55 (m, 1H), 7.43 – 7.32 (m, 7H), 7.29 (dd, *J* = 7.7, 6.0 Hz, 2H), 7.26 – 7.18 (m, 3H), 6.93 (ddd, *J* = 8.4, 7.2, 1.1 Hz, 1H), 6.01 (d, *J* = 8.5 Hz, 1H). **^{13}C NMR (101 MHz, $CDCl_3$):** δ 147.7, 144.2, 135.6, 135.1, 133.7, 132.6, 131.5, 131.2, 130.6, 129.9, 129.2, 128.7,

128.0, 127.7, 127.2, 126.4, 125.0, 124.1, 123.5, 122.9, 121.2, 119.5, 114.1. **IR (V_{max}):** 3027, 1712, 1501, 1438, 1360, 1221, 748 cm^{-1}. **HRMS (ESI):** *m/z* calcd for $C_{27}H_{18}N_2$ $[M+H]^+$: 371.1543, found: 371.1541. The analytical data corresponds with those reported in the literature.[9-12]

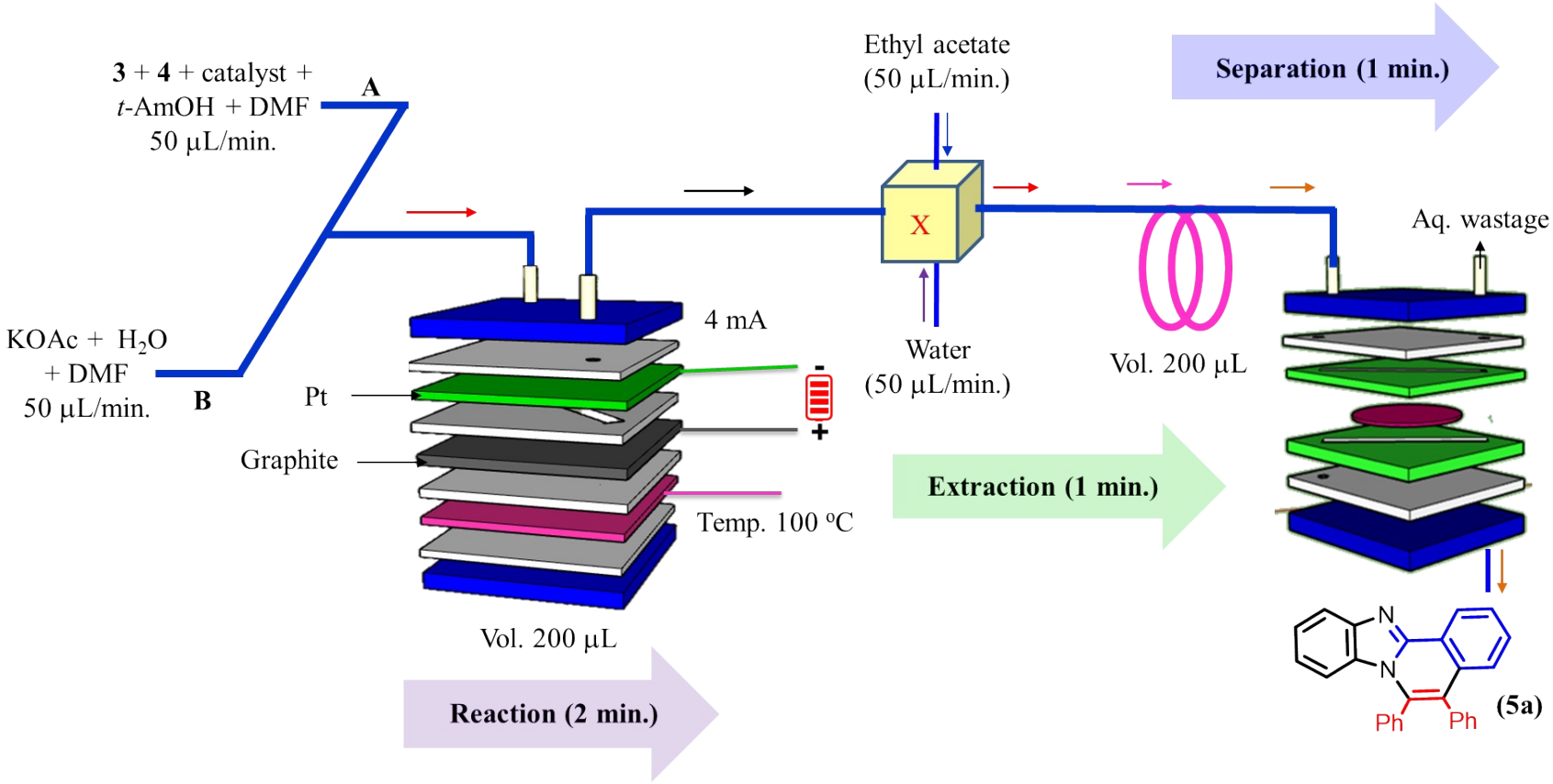

Fig. S5. Integrated continuous set-up for annulation reaction.

Table S5. Comparative table for C-H/N-H annulation reaction.

Product	Reaction condition				Ref.
	Temp (°C)	Time (min.)	Oxidant	Additive	
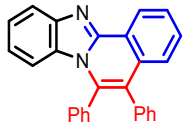	100	240	electricity	1-AdCO$_2$H	[12]
	110	720	Cu (II)	no	[11]
	160	1200	KOBu^t	no	[9]
	50	2888	Ag	no	[1]
	60	300	Ag	no	[10]
	100	**2**	**electricity**	**no**	**This study**

Productivity per day:

Molar solution = 0.05 M

Flow rate = 50µL/min

Product molecular weight = 370

Product yield = 96 %

$$Productivity\ g/day\ = \frac{0.05 \times 0.05 \times 60 \times 24 \times 370 \times 0.96}{1000}$$

Productivity g/day =1.278 g/day

3-Methyl-5,6-diphenylbenzo [4,5] imidazo [2,1-a] isoquinoline (5b): The product **(5b)** was

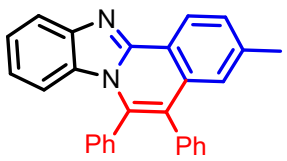

prepared according to the general procedure as described in section **4.4.** The extracted mixture was concentrated under vacuum and purified by silica gel column chromatography (n-Hexane: EtOAc = 5:1), 65% yield of **5b** as a white solid and melting point is 264-264 °C, **^{1}H NMR (500 MHz, $CDCl_3$):** δ 8.87 (d, *J* = 8.2 Hz, 1H), 7.96 (d, *J* = 8.1 Hz, 1H), 7.53 (dd, *J* = 8.2, 1.1 Hz, 1H), 7.42 – 7.27 (m, 8H), 7.26 – 7.15 (m, 3H), 7.11 (s, 1H), 6.91 (ddd, *J* = 8.4, 7.1, 1.1 Hz, 1H), 5.98 (d, *J* = 8.5 Hz, 1H), 2.42 (s, 3H). **^{13}C NMR (101 MHz, $CDCl_3$):** δ 147.9, 144.3, 140.3, 135.7, 135.1, 133.8, 132.7, 131.5, 131.2, 130.6, 129.3, 129.1, 128.8, 128.0, 127.2, 126.1, 125.0, 124.00, 123.4, 121.0, 120.6, 119.4, 114.0, 22.0. **IR (V_{max}):** 3050, 2929, 1620, 1453, 1340, 1268, 745 cm^{-1}. **HRMS (ESI):** *m/z* calcd for: $C_{28}H_{20}N_2$ $[M+H]^+$: 385.1705, found: 385.1697. Verified the analytical data with those reported in the literature.[10-12]

3-Fluoro-5,6-diphenylbenzo [4,5] imidazo[2,1-a] isoquinoline (5c): The product **(5c)** was

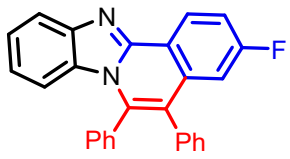

prepared according to the general procedure as described in section **4.4.** The extracted mixture was concentrated under vacuum and purified by silica gel column chromatography (n-Hexane: EtOAc = 5:1), 85% yield of **5c** as a white solid and melting point is 251-253 °C. **^{1}H NMR (400 MHz, $CDCl_3$):** δ 8.98 (dd, *J* = 8.9, 5.7 Hz, 1H), 7.96 (d, *J* = 8.1 Hz, 1H), 7.47 – 7.36 (m, 5H), 7.36 – 7.26 (m, 5H), 7.23 – 7.17 (m, 2H), 7.02 – 6.88 (m, 2H), 5.99 (d, *J* = 8.5 Hz, 1H). **^{13}C NMR (101 MHz, $CDCl_3$):** δ 163.6 (d, $^{1}J_{C\text{-}F}$ = 251 Hz), 147.3, 144.20, 136.3, 135.1, 134.8 (d, $^{3}J_{C\text{-}F}$ = 10 Hz), 133.4, 131.3, 131.1, 130.4, 129.4, 128.8, 128.2, 127.7 (d, $^{3}J_{C\text{-}F}$ =9.0 Hz), 127.5, 124.3, 122.9 (d, $^{4}J_{C\text{-}F}$ = 3.0 Hz), 121.3, 119.5, 119.5, 116.4 (d, $^{2}J_{C\text{-}F}$ = 23 Hz), 114.1, 111.7 (d, ^{2}JC-F = 23 Hz). **^{19}F NMR (377 MHz, $CDCl_3$):** δ -108.4 (s). **IR (V_{max}):** 2986, 1738, 1451, 1318, 1269, 1154, 1033 cm^{-1}. **HRMS**

(ESI): *m/z* calcd for $C_{27}H_{17}FN_2$ $[M+H]^+$: 389.1449, found: 389.1449. Verified the analytical data with those reported in the literature.[10-12]

3-Bromo-5,6-diphenylbenzo [4,5] imidazo[2,1-a] isoquinoline(5d): The product **5d** was

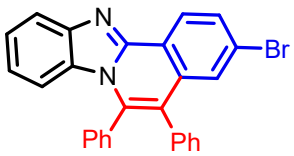

prepared according to the general procedure as described in section **4.4.** The extracted mixture was concentrated under vacuum and purified by silica gel column chromatography (n-Hexane: EtOAc = 5:1), 65% yield of yield **5d** as a white solid and melting point is 297-299 °C. **^{1}H NMR (400 MHz, $CDCl_3$):** δ 8.84 (d, *J* = 8.6 Hz, 1H), 7.97 (d, *J* = 8.1 Hz, 1H), 7.79 (dd, *J* = 8.6, 1.9 Hz, 1H), 7.47 (d, *J* = 1.8 Hz, 1H), 7.44 – 7.36 (m, 4H), 7.34 – 7.27 (m, 5H), 7.22 – 7.18 (m, 2H), 6.94 (ddd, *J* = 8.4, 7.2, 1.2 Hz, 1H), 5.99 (d, *J* = 8.5 Hz, 1H). **^{13}C NMR (101 MHz, $CDCl_3$):** δ 147.2, 144.2, 136.3, 134.8, 134.1, 133.4, 131.4, 131.1, 131.0, 130.4, 129.4, 128.8, 128.8, 128.2, 127.6, 126.7, 124.6, 124.4, 122.5, 121.66, 121.6, 119.6, 114.1. **IR (V_{max}):** 2937, 1603, 1524, 1435, 1335, 1260, 747 cm^{-1}. **HRMS (ESI):** *m/z* calcd for $C_{27}H_{17}BrN_2$ $[M+H]^+$: 449.0653, found: 449.0652. Verified the analytical data with those reported in the literature.[10-12]

5,6-Diphenylbenzo[4,5]imidazo[2,1-a]isoquinoline-3-carbonitrile (5e): The product **5e** was

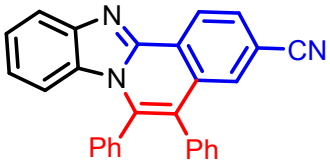

prepared according to the general procedure as described in section **4.4.** The extracted mixture was concentrated under vacuum and purified by silica gel column chromatography (n-Hexane: EtOAc = 5:1), 85% yield of **5e** as a white solid and melting point is 272-274 °C. **^{1}H NMR (400 MHz, $CDCl_3$):** δ 9.07 (d, *J* = 8.3 Hz, 1H), 8.01 (d, *J* = 8.2 Hz, 1H), 7.88 (d, *J* = 8.3 Hz, 1H), 7.66 (s, 1H), 7.43 (dd, *J* = 16.0, 8.3 Hz, 4H), 7.37 – 7.29 (m, 5H), 7.19 (d, *J* = 6.8 Hz, 2H), 7.00 (t, *J* = 7.8 Hz, 1H), 6.03 (d, *J* = 8.5 Hz, 1H). **^{13}C NMR (101 MHz, $CDCl_3$):** δ 146.1, 144.3, 137.0, 134.2, 133.0, 132.5, 131.3, 131.1, 131.1, 130.3, 129.6, 129.5, 128.9, 128.4, 127.9, 125.9, 125.6,

124.8, 122.5, 122.4, 120.0, 118.7, 114.3, 113.0. **IR (V_{max}):** 2927, 1448, 1215, 752, 671 cm^{-1}. **HRMS (ESI):** *m/z* calcd for $C_{28}H_{17}N_3$ $[M+H]^+$: 396.1501, found: 396.1494. Verified the analytical data with those reported in the literature.[10]

2-Methyl-5,6-diphenylbenzo [4,5] imidazo[2,1-a] isoquinoline (5f): The product **5f** was

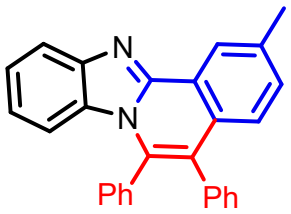

prepared according to the general procedure as described in section **4.4.** The extracted mixture was concentrated under vacuum and purified by silica gel column chromatography (n-Hexane: EtOAc = 5:1), 52% yield of **5f** as a white solid and melting point is 291-293 °C. **^{1}H NMR (500 MHz, $CDCl_3$):** δ 8.81 (s, 1H), 7.98 (d, *J* = 8.1 Hz, 1H), 7.44 – 7.32 (m, 7H), 7.28 – 7.19 (m, 6H), 6.92 (dd, *J* = 11.5, 4.1 Hz, 1H), 6.01 (d, *J* = 8.4 Hz, 1H), 2.60 (s, 3H). **^{13}C NMR (101 MHz, $CDCl_3$):** δ 147.72, 144.2, 138.0, 135.8, 134.2, 133.8, 131.4, 131.4, 131.2, 130.7, 130.4, 129.1, 128.7, 127.9, 127.2, 126.3, 124.7, 124.0, 123.5, 122.8, 121.1, 119.5, 114.1, 21.5. **IR (V_{max}):** 3050, 2940, 1619, 1502, 1442, 1340, 1265, 1023, 828, 753 cm^{-1}. **HRMS (ESI):** *m/z* calcd for $C_{28}H_{20}N_2$ $[M+H]^+$: 385.1705, found: 385.161698.

5,6-Diphenyl-2-(trifluoromethyl) benzo [4,5] imidazo [2,1-a] isoquinoline (5g): The product

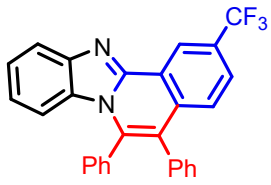

5g was prepared according to the general procedure as described in section **4.4.** The extracted mixture was concentrated under vacuum and purified by silica gel column chromatography (n-Hexane: EtOAc = 5:1), 55% yield of **5g** as a white solid and melting point is 285-287 °C. **^{1}H NMR (400 MHz, $CDCl_3$):** δ 9.29 (s, 1H), 8.01 (d, *J* = 8.2 Hz, 1H), 7.75 (dd, *J* = 8.5, 1.4 Hz, 1H), 7.47 – 7.38 (m, 5H), 7.37 – 7.27 (m, 5H), 7.21 (dd, *J* = 7.6, 1.6 Hz, 2H), 7.00 – 6.95 (m, 1H), 6.02 (d, *J* = 8.5 Hz, 1H). **^{13}C NMR (126 MHz, $CDCl_3$):** δ 146.9, 144.2, 137.2, 134.9, 134.8, 133.2, 131.4, 131.1, 130.3, 129.6 (q, $^2J_{C-F}$ = 25 Hz), 129.5, 128.9, 128.2, 127.6, 127.1, 125.8 (q, $^3J_{C-F}$ = 2.5 Hz), 125.1, 124.6,

124.6, 122.8 (q, $^{1}J_{C\text{-}F}$ = 10 Hz), 122.6 (q, $^{3}J_{C\text{-}F}$ = 3.8 Hz), 121.9, 119.8, 114.2. **^{19}F NMR (376 MHz, $CDCl_3$):** δ -62.20 (s). **IR (V_{max}):** 2925, 2859, 1439, 1315, 1132, 750 cm^{-1}. **HRMS (ESI):** *m/z* calcd for $C_{28}H_{17}F_3N_2$ $[M+H]^+$: 439.1422, found: 439.1417 found: 439.1417. Verified the analytical data with those reported in the literature.[10-12]

5,6-Dipropylbenzo [4,5] imidazo[2,1-a] isoquinoline (5h): The product **5h** was prepared according to the general procedure as described in section **4.4.** The extracted mixture was concentrated under vacuum and purified by silica gel column chromatography (n-Hexane: EtOAc = 5:1), 71% yield of **5h** as a white solid and melting point is 140-142 °C. **^{1}H NMR (400 MHz, $CDCl_3$):** δ 8.92 (dd, *J* = 8.0, 1.1 Hz, 1H), 8.03 (d, *J* = 7.7 Hz, 1H), 7.92 (d, *J* = 8.5 Hz, 1H), 7.86 (d, *J* = 8.1 Hz, 1H), 7.70 (ddd, *J* = 8.3, 7.2, 1.5 Hz, 1H), 7.66 – 7.57 (m, 1H), 7.55 – 7.43 (m, 1H), 7.37 (ddd, *J* = 8.4, 7.2, 1.2 Hz, 1H), 3.41 – 3.32 (m, 2H), 3.01 – 2.94 (m, 2H), 1.96 – 1.86 (m, 2H), 1.76 – 1.68 (m, 2H), 1.24 (t, *J* = 7.4 Hz, 3H), 1.14 (t, *J* = 7.3 Hz, 3H). **^{13}C NMR (101 MHz, $CDCl_3$):** δ 148.1, 144.4, 135.7, 131.5, 130.8, 129.9, 126.8, 125.6, 123.9, 123.5, 122.8, 121.6, 119.9, 118.6, 114.3, 31.07, 29.6, 23.8, 21.6, 14.5, 13.9. **IR (V_{max}):** 3063, 2956, 2878, 1625, 1526, 1455, 1354, 1281, 752 cm^{-1}. **HRMS (ESI):** *m/z* calcd for $C_{21}H_{22}N_2$ $[M+H]^+$: 303.1861, found: 303.1855. Verified the analytical data with those reported in the literature.[9]

3-Methyl-5,6-dipropylbenzo [4,5] imidazo[2,1-a] isoquinoline (5i): The product **5i** was prepared according to the general procedure as described in section **4.4.** The extracted mixture was concentrated under vacuum and purified by silica gel column chromatography (n-Hexane: EtOAc = 5:1), 63% yield of **5i** as a white solid and melting point is 124-126 °C. **^{1}H NMR (500 MHz, $CDCl_3$):** δ 8.80 (d, *J* = 8.1 Hz, 1H), 8.00 (dd, *J* = 8.1, 0.6 Hz, 1H), 7.91 (d, *J* = 8.5 Hz, 1H), 7.63 (s, 1H), 7.50 – 7.43

(m, 2H), 7.35 (ddd, J = 8.4, 7.1, 1.2 Hz, 1H), 3.40 – 3.34 (m, 2H), 2.99 – 2.93 (m, 2H), 2.58 (s, 3H), 1.97 – 1.86 (m, 2H), 1.78 – 1.70 (m, 2H), 1.24 (t, J = 7.3 Hz, 3H), 1.15 (t, J = 7.3 Hz, 3H). **^{13}C NMR (101 MHz, $CDCl_3$):** δ 148.3, 144.4, 140.1, 135.8, 131.7, 130.8, 128.4, 125.5, 123.8, 123.3, 121.3, 120.5, 119.8, 118.5, 114.2, 31.1, 29.5, 23.8, 22.3, 21.6, 14.5, 13.9. **IR (V_{max}):** 3060, 2955, 2876, 1626, 1526, 1454, 1350, 1281, 752 cm^{-1}. **HRMS (ESI):** *m/z* calcd for $C_{20}H_{26}N_2$ $[M+H]^+$: 317.2018, found: 317.2017

3-Fluoro-5,6-dipropylbenzo [4,5] imidazo [2,1-a] isoquinoline (5j): The product **5j** was

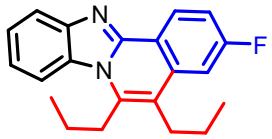

prepared according to the general procedure as described in section **4.4.** The extracted mixture was concentrated under vacuum and purified by silica gel column chromatography (n-Hexane: EtOAc = 5:1), 75% yield of **5j** as a white solid and melting point is 155-157 °C. **^{1}H NMR (400 MHz, $CDCl_3$):** δ 8.91 (dd, J = 8.9, 6.0 Hz, 1H), 8.00 (d, J = 8.1 Hz, 1H), 7.91 (d, J = 8.5 Hz, 1H), 7.53 – 7.44 (m, 2H), 7.40 – 7.31 (m, 2H), 3.41 – 3.32 (m, 2H), 2.95 – 2.87 (m, 2H), 1.96 – 1.86 (m, 2H), 1.72 (m, 2H), 1.25 (t, J = 7.3 Hz, 3H), 1.15 (t, J = 7.3 Hz, 3H). **^{13}C NMR (101 MHz, $CDCl_3$):** δ 164.0 (d, $^{1}J_{C\text{-}F}$ = 249 Hz), 147.63, 144.34, 137.08, 133.81 (d, $^{3}J_{C\text{-}F}$ = 9 Hz), 130.72, 128.2 (d, $^{3}J_{C\text{-}F}$ = 9 Hz), 124.15, 121.69, 119.91 119.41, 118.03 (d, $^{4}J_{C\text{-}F}$ = 3 Hz), 115.4 (d, $^{2}J_{C\text{-}F}$ = 23 Hz), 114.22, 109.0 (d, $^{2}J_{C\text{-}F}$ = 23 Hz), 31.13, 29.71, 23.61, 21.49, 14.46, 13.88. **^{19}F NMR (376 MHz, $CDCl_3$):** δ -108.89 (s). **IR (V_{max}):** 2955, 2881, 1622, 1453, 1345, 1370, 1191, 832, 749 cm^{-1}. **HRMS (ESI):** *m/z* calcd for $C_{21}H_{21}FN_2$ $[M+H]^+$: 321.1767, found: 321.1760.

3-Bromo-5,6-dipropylbenzo [4,5] imidazo[2,1-a] isoquinoline (5k): The product **5k** was

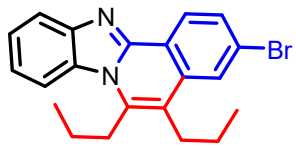

prepared according to the general procedure as described in section **4.4.** The extracted mixture was concentrated under vacuum and purified by silica gel column chromatography (n-Hexane: EtOAc = 5:1), 70% yield

of **5k** as a white solid and melting point is 158-160°C**. ^{1}H NMR (500 MHz, $CDCl_3$):** δ 8.77 (d, *J* = 8.6 Hz, 1H), 8.01 (d, *J* = 7.7 Hz, 1H), 7.97 (d, *J* = 1.8 Hz, 1H), 7.91 (d, *J* = 8.5 Hz, 1H), 7.72 (dd, *J* = 8.5, 1.8 Hz, 1H), 7.50 (ddd, *J* = 8.1, 7.2, 0.8 Hz, 1H), 7.41 – 7.35 (m, 1H), 3.41 – 3.31 (m, 2H), 2.95 – 2.88 (m, 2H), 1.95 – 1.87 (m, 2H), 1.7-1.69 (m, 2H), 1.25 (t, *J* = 7.3 Hz, 3H), 1.15 (t, *J* = 7.3 Hz, 3H). **^{13}C NMR (101 MHz, $CDCl_3$):** δ 147.5, 144.3, 137.1, 133.1, 130.7, 130.0, 127.2, 126.2, 124.7, 124.2, 121.9, 121.5, 120.1, 117.6, 114.3, 31.1, 29.4, 23.7, 21.5, 14.5, 13.8. **IR (V_{max}):** 2953, 1707, 1617, 1528, 1450, 1341, 1265, 1090, 825, 754 cm^{-1}. **HRMS (ESI):** *m/z* calcd for $C_{21}H_{21}BrN_2$ $[M+H]^+$: 381.0966, found: 381.0964.

5,6-Dipropylbenzo [4,5] imidazo [2,1-a] isoquinoline-3-carbonitrile (5l): The product **5l** was

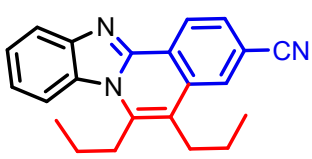

prepared according to the general procedure as described in section **4.4.** The extracted mixture was concentrated under vacuum and purified by silica gel column chromatography (n-Hexane: EtOAc = 5:1), 69% yield of **5l** as a white solid and melting point is 194-196 °C. **^{1}H NMR (500 MHz, $CDCl_3$):** δ 9.01 (d, *J* = 8.3 Hz, 1H), 8.16 (d, *J* = 1.0 Hz, 1H), 8.06 (dd, *J* = 8.2, 0.5 Hz, 1H), 7.95 (d, *J* = 8.5 Hz, 1H), 7.82 (dd, *J* = 8.3, 1.4 Hz, 1H), 7.57 – 7.52 (m, 1H), 7.45 (ddd, *J* = 8.4, 7.1, 1.2 Hz, 1H), 3.40 (dd, *J* = 9.5, 7.2 Hz, 2H), 3.00 – 2.93 (m, 2H), 1.97 – 1.89 (m, 2H), 1.76 – 1.68 (m, 2H), 1.27 (t, *J* = 7.4 Hz, 3H), 1.17 (t, *J* = 7.3 Hz, 3H). **^{13}C NMR (101 MHz, $CDCl_3$):** δ 146.4, 144.4, 137.9, 131.4, 130.7, 128.6, 128.4, 126.5, 125.6, 124.7, 122.8, 120.5, 119.0, 117.6, 114.4, 113.1, 31.1, 29.4, 23.9, 21.4, 14.4, 13.9. **HRMS (ESI):** *m/z* calcd for $C_{22}H_{21}N_3$ $[M+H]^+$: 328.1814, found: 328.1807.

2-Methyl-5,6-dipropylbenzo [4,5] imidazo[2,1-a] isoquinoline (5m): The product **5m** was prepared according to the general procedure as described in section **4.4.** The extracted mixture was concentrated under vacuum and purified by silica gel column chromatography (n-Hexane: EtOAc = 5:1), 61% yield of **5m** as a white solid and melting point is 168-170 °C. **^{1}H NMR (400 MHz, $CDCl_3$):** δ 8.73 (s, 1H), 8.02 (d, *J* = 8.1 Hz, 1H), 7.92 (d, *J* = 8.5 Hz, 1H), 7.75 (d, *J* = 8.4 Hz, 1H), 7.49 (dd, *J* = 17.6, 8.5 Hz, 2H), 7.36 (t, *J* = 7.8 Hz, 1H), 3.42 – 3.31 (m, 2H), 2.99 – 2.91 (m, 2H), 2.58 (s, 3H), 1.96 – 1.86 (m, 2H), 1.76-1.71 (m, 2H), 1.24 (t, *J* = 7.3 Hz, 3H), 1.13 (t, *J* = 7.3 Hz, 3H). **^{13}C NMR (101 MHz, $CDCl_3$):** δ 148.1, 144.3, 136.9, 134.8, 131.5, 130.8, 129.3, 125.2, 123.9, 123.4, 122.7, 121.4, 119.9, 118.7, 114.2, 31.0, 29.6, 23.9, 21.6, 21.3, 14.5, 13.8. **IR (V_{max}):** 2954, 1625, 1518, 1454, 1353, 749 cm^{-1}. **HRMS (ESI):** *m/z* calcd for $C_{22}H_{24}N_2$ $[M+H]^+$: 317.2018, found: 317.2008.

5,6-Dipropyl-2-(trifluoromethyl) benzo [4,5] imidazo [2,1-a] isoquinoline (5n): The product **5n** was prepared according to the general procedure as described in section **4.4.** The extracted mixture was concentrated under vacuum and purified by silica gel column chromatography (n-Hexane: EtOAc = 5:1), 65% yield of **5n** as a white solid and melting point is 137 °C. **^{1}H NMR (400 MHz, $CDCl_3$):** δ 9.22 (s, 1H), 8.09 – 8.01 (m, 1H), 7.95 (t, *J* = 8.0 Hz, 2H), 7.88 (dd, *J* = 8.7, 1.7 Hz, 1H), 7.57 – 7.49 (m, 1H), 7.42 (ddd, *J* = 8.4, 7.2, 1.2 Hz, 1H), 3.45 – 3.34 (m, 2H), 3.04 – 2.93 (m, 2H), 1.99 – 1.88 (m, 2H), 1.78-1.68 (m, 2H), 1.26 (t, *J* = 7.3 Hz, 3H), 1.16 (t, *J* = 7.3 Hz, 3H). **^{13}C NMR (101 MHz, $CDCl_3$)**: δ 147.29, 144.34, 138.09, 133.77, 130.75, 128.89, 128.56, 125.9 (q, $^3J_{C-F}$ = 3 Hz) 124.50, 124.33, 123.2 (q, $^3J_{C-F}$ = 4 Hz), 122.75, 122.30, 120.31, 118.07, 114.39, 31.22, 29.60, 23.82, 21.50, 14.49, 13.93. **^{19}F NMR (376 MHz, $CDCl_3$):** δ -62.14 (s). **IR**

(V_{max}): 2952, 1441, 1328, 1135, 752 cm^{-1}. **HRMS (ESI):** *m/z* calcd for$C_{22}H_{21}F_3N_2$ $[M+H]^+$: 371.1735, found: 371.1727.

5-Methyl-6-phenylbenzo [4,5] imidazo[2,1-a] isoquinoline (5o): The product **5o** was prepared

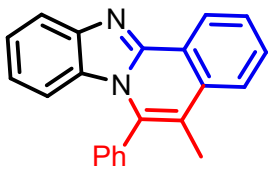

according to the general procedure as described in section **4.4.** The extracted mixture was concentrated under vacuum and purified by silica gel column chromatography (n-Hexane: EtOAc = 5:1), 85% yield of **5o** as a white solid and melting point is 238-240 °C. **^{1}H NMR (500 MHz, $CDCl_3$):** δ 8.97 (dd, *J* = 7.9, 1.2 Hz, 1H), 7.94 (t, *J* = 7.3 Hz, 2H), 7.78-7.63 (m, 5H), 7.52 – 7.46 (m, 2H), 7.35 – 7.31 (m, 1H), 6.92 – 6.89 (m, 1H), 5.93 (d, *J* = 8.5 Hz, 1H), 2.32 (s, 3H)**. ^{13}C NMR (101 MHz, $CDCl_3$):** δ 147.5, 143.9, 134.5, 134.3, 132.3, 131.1, 130.2, 130.0, 129.7, 129.5, 127.6, 125.4, 124.0, 123.8, 123.1, 121.0, 119.4, 115.5, 113.8, 14.5. **IR (V_{max}):** 2929, 1626, 1456, 1354, 1273, 1194, 757 cm^{-1}. **HRMS (ESI):** *m/z* calcd for $C_{22}H_{16}N_2$ $[M+H]^+$: 309.1392, found: 309.1391. Verified the analytical data with those reported in the literature.[9, 12]

3,5-Dimethyl-6-phenylbenzo [4,5] imidazo[2,1-a] isoquinoline (5p): The product **5p** was

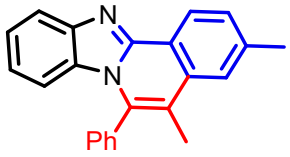

prepared according to the general procedure as described in section **4.4.** The extracted mixture was concentrated under vacuum and purified by silica gel column chromatography (n-Hexane: EtOAc = 5:1), 77% yield of **5p** as a white solid and melting point is 179-181 °C**. ^{1}H NMR (500 MHz, $CDCl_3$):** δ 8.84 (d, *J* = 8.2 Hz, 1H), 7.93 – 7.90 (m, 1H), 7.71 (s, 1H), 7.68 – 7.62 (m, 3H), 7.55 (dd, *J* = 8.2, 1.1 Hz, 1H), 7.49 – 7.46 (m, 2H), 7.32 (ddd, *J* = 8.2, 7.1, 1.0 Hz, 1H), 6.89 (ddd, *J* = 8.4, 7.1, 1.2 Hz, 1H), 5.92 (d, *J* = 8.5 Hz, 1H), 2.61 (s, 3H), 2.29 (s, 3H). **^{13}C NMR (101 MHz, $CDCl_3$):** δ 147.7, 144.0, 140.3, 134.6, 134.3, 132.4, 131.1, 130.2, 129.7, 129.5, 129.1, 125.3, 124.0, 123.7, 120.8,

120.8, 119.2, 115.3, 113.7, 22.2, 14.5. **IR (V_{max}):** 3192, 2930, 2862, 1721, 1627, 1453, 1350, 1273, 754 cm^{-1}. **HRMS (ESI):** *m/z* calcd for $C_{23}H_{18}N_2$ $[M+H]^+$: 322.1549, found: 322.1547.

3-Fluoro-5-methyl-6-phenylbenzo [4,5] imidazo[2,1-a] isoquinoline (5q): The product **5q** was

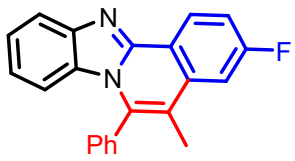

prepared according to the general procedure as described in section **4.4.** The extracted mixture was concentrated under vacuum and purified by silica gel column chromatography (n-Hexane: EtOAc = 5:1), 82% yield of **5q** as a white solid and melting point is 168-170 °C. **^{1}H NMR (400 MHz, $CDCl_3$)** δ 8.96 (dd, *J* = 8.9, 5.8 Hz, 1H), 7.92 (d, *J* = 8.1 Hz, 1H), 7.72 – 7.62 (m, 3H), 7.55 (dd, *J* = 10.5, 2.4 Hz, 1H), 7.51 – 7.37 (m, 3H), 7.34 (ddd, *J* = 8.2, 7.2, 1.0 Hz, 1H), 6.91 (ddd, *J* = 8.4, 7.2, 1.1 Hz, 1H), 5.92 (d, *J* = 8.5 Hz, 1H), 2.27 (s, 3H). **^{13}C NMR (101 MHz, $CDCl_3$):** δ 163.9 (d, $^1J_{C\text{-}F}$ = 250 Hz), 147.1, 144.0, 135.5, 134.5 (d, $^3J_{C\text{-}F}$ = 9 Hz), 134.2, 131.0, 130.0, 129.9, 129.6, 128.0 (d, $^3J_{C\text{-}F}$ = 10 Hz), 124.0, 121.1, 119.7, 119.4, 116.1 (d, $^4J_{C\text{-}F}$ = 24 Hz), 114.8 (d, $^2J_{C\text{-}F}$ = 3 Hz), 113.8, 109.7 (d, $^2J_{C\text{-}F}$ = 22 Hz), 14.5. **IR (V_{max}):** 3022, 1433, 1256, 743, 671 cm^{-1}. **HRMS (ESI):** *m/z* calcd for $C_{22}H_{15}FN_2$ $[M+H]^+$: 327.1298, found: 327.1298.

7, 8-Diphenylbenzo[h]benzo [4,5] imidazo[2,1-a] isoquinoline (5r): The product **5r** was

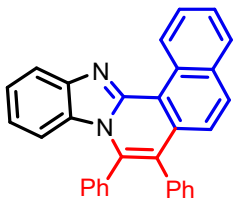

prepared according to the general procedure as described in section **4.4.** The extracted mixture was concentrated under vacuum and purified by silica gel column chromatography (n-Hexane: EtOAc = 5:1), 61% yield of **5r** as a white solid and melting point is 236-238 °C**. ^{1}H NMR (400 MHz, $CDCl_3$):** δ 11.14 (d, *J* = 8.5 Hz, 1H), 8.12 (d, *J* = 8.1 Hz, 1H), 8.00 – 7.91 (m, 3H), 7.75 – 7.70 (m, 1H), 7.45-7.34 (m, 7H), 7.33-7.28 (m, 3H), 7.25 – 7.23 (m, 2H), 6.97-6.93 (m 1H), 6.08 (d, *J* = 8.5 Hz, 1H). **^{13}C NMR (101 MHz, $CDCl_3$):** δ 147.8, 144.7, 136.4, 136.0, 134.0, 132.5, 132.4, 131.7, 130.7, 130.5, 130.2, 129.8, 129.1, 128.7, 128.2, 128.2, 128.0, 127.2, 126.8, 124.3, 123.9, 121.0,

119.8, 118.1, 114.4. **IR (V_{max}):** 3058, 2927, 2855, 1482, 1375, 1278, 1088, 1029, 753 cm^{-1}. **HRMS (ESI):** *m/z* calcd for $C_{31}H_{20}N_2$ $[M+H]^+$: 421.1699, found: 421.1695. Verified the analytical data with those reported in the literature.[10-12]

7,8-Dipropylbenzo[h]benzo [4,5] imidazo[2,1-a] isoquinoline (5s): The product **5s** was prepared according to the general procedure as described in section **4.4.** The extracted mixture was concentrated under vacuum and purified by silica gel column chromatography (n-Hexane: EtOAc = 5:1), 63% yield of **5s** as a white solid and melting point is 117-119 °C. **^{1}H NMR (400 MHz, $CDCl_3$):** δ 11.09 (d, *J* = 8.7 Hz, 1H), 8.17 (d, *J* = 7.8 Hz, 1H), 8.09 (d, *J* = 9.0 Hz, 1H), 8.03 (d, *J* = 8.5 Hz, 1H), 7.98 (t, *J* = 8.7 Hz, 2H), 7.91 (ddd, *J* = 8.5, 6.9, 1.4 Hz, 1H), 7.71 – 7.66 (m, 1H), 7.57-7.54 (m, 1H), 7.43-7.39 (m, 1H), 3.54 – 3.45 (m, 2H), 3.14 – 3.06 (m, 2H), 2.03 – 1.92 (m, 2H), 1.84 – 1.74 (m, 2H), 1.28 (t, *J* = 7.3 Hz, 3H), 1.18 (t, *J* = 7.3 Hz, 3H). **^{13}C NMR (101 MHz, $CDCl_3$):** δ 148.1, 144.8, 136.9, 132.1, 131.7, 131.1, 130.6, 129.4, 129.2, 128.1, 128.0, 126.4, 124.2, 121.5, 121.5, 120.4, 119.1, 117.9, 114.6, 31.4, 30.2, 24.1, 21.5, 14.6, 14.0. **IR (V_{max}):** 3062, 2951, 1728, 1461, 1373, 1278, 1090, 810, 747 cm^{-1}. **HRMS (ESI):** *m/z* calcd for $C_{25}H_{24}N_2$ $[M+H]^+$: 352.2018, found: 352.2018.

5,6-Diphenylindolo[2,1-a] isoquinoline (5t): The product **5t** was prepared according to the general procedure as described in section **4.4.** The extracted mixture was concentrated under vacuum and purified by silica gel column chromatography (n-Hexane: EtOAc = 5:1), 69% yield of **5t** as a green solid and melting point is 225-227 °C. **^{1}H NMR (400 MHz, $CDCl_3$):** δ 8.30 (dd, *J* = 8.0, 0.7 Hz, 1H), 7.78 (d, *J* = 8 Hz, 1H), 7.54 – 7.46 (m, 1H), 7.41 (d, *J* = 0.5 Hz, 1H), 7.33 (m, 6H), 7.25 – 7.05 (m, 7H), 6.80 (m, 1H), 5.99 (dd, *J* = 8.7, 0.6 Hz, 1H). **^{13}C NMR (101 MHz, $CDCl_3$):** δ

136.7, 136.0, 135.9, 135.3, 132.7, 131.8, 130.8, 130.2, 129.6, 128.7, 128.6, 127.8, 127.3, 127.0, 126.7, 126.1, 125.4, 123.2, 121.6, 121.4, 120.2, 120.1, 114.6, 94.2. **IR (V_{max}):** 3295, 3053, 2703, 1603, 1449, 1346, 751, 696 cm^{-1}. **HRMS (ESI):** *m/z* calcd for $C_{28}H_{17}N$ $[M+H]^+$: 370.1595 found: 370.1587. Verified the analytical data with those reported in the literature.[9, 13]

5,6-Diphenylbenzo [4,5] imidazo [2,1-a] [2,6] naphthyridine (5u): The product **5u** was

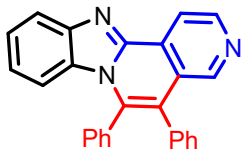

prepared according to the general procedure as described in section **4.4.** The extracted mixture was concentrated under vacuum and purified by silica gel column chromatography (n-Hexane: EtOAc = 5:1), 71% yield of **5u** as a white solid and melting point is 268-270 °C. **^{1}H NMR (500 MHz, $CDCl_3$):** δ 8.85 (d, *J* = 5.3 Hz, 1H), 8.75 – 8.69 (m, 2H), 8.03 (d, *J* = 8.2 Hz, 1H), 7.48 – 7.40 (m, 4H), 7.36 – 7.28 (m, 5H), 7.25 – 7.23 (m, 2H), 7.03 – 6.99 (m, 1H), 6.06 (d, *J* = 8.5 Hz, 1H). **^{13}C NMR (101 MHz, $CDCl_3$):** δ 149.4, 146.9, 145.5, 144.2, 136.7, 133.9, 132.9, 131.3, 131.1, 130.4, 129.6, 128.9, 128.2, 127.9, 127.7, 127.0, 124.7, 122.5, 121.8, 120.2, 117.2, 114.4. **IR (V_{max}):** 3055, 2932, 1593, 1533, 1439, 1330, 847, 757 cm^{-1}. **HRMS (ESI):** *m/z* calcd for C_{26} $H_{17}N_3$ $[M+H]^+$: 372.1501, found: 372.1494. Verified the analytical data with those reported in the literature.[10]

5,6-Dipropylbenzo [4,5] imidazo[2,1-a] [2,6] naphthyridine (5v): The product **5v** was

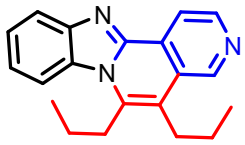

prepared according to the general procedure as described in section **4.4.** The extracted mixture was concentrated under vacuum and purified by silica gel column chromatography (n-Hexane: EtOAc = 5:1), 61% yield of **5v** as a white solid and melting point is 167-169 °C. **^{1}H NMR (400 MHz, $CDCl_3$):** δ 9.27 (s, 1H), 8.78 (d, *J* = 5.1 Hz, 1H), 8.64 (d, *J* = 5.3 Hz, 1H), 8.06 (d, *J* = 8.1 Hz, 1H), 7.94 (d, *J* = 8.5 Hz, 1H), 7.54 (t, *J* = 7.6 Hz, 1H), 7.44 (t, *J* = 7.9 Hz, 1H), 3.42 – 3.33 (m, 2H), 3.09 – 2.99 (m, 2H), 1.96 - 1.86 (m, 2H), 1.82 – 1.72 (m, 2H), 1.26 (t, *J* = 7.3 Hz, 3H), 1.16 (t, *J* = 7.3 Hz, 3H). **^{13}C NMR**

(101 MHz, $CDCl_3$): δ 146.9, 145.9, 145.7, 144.2, 137.4, 130.7, 127.8, 125.8, 124.5, 122.8, 120.6, 117.6, 117.2, 114.4, 30.8, 28.8, 24.1, 21.4, 14.4, 13.8 cm^{-1}. **IR (V_{max}):** 3050, 2954, 1529, 1435, 1359, 846, 746 cm^{-1}. **HRMS (ESI):** *m/z* calcd for $C_{20}H_{21}N_3$ $[M+H]^+$: 304.1814, found: 304.1811.

***N, N* Diethyl-5,6-diphenylbenzo [4,5] imidazo[2,1-a] isoquinolin-3 amine (5w):** The product

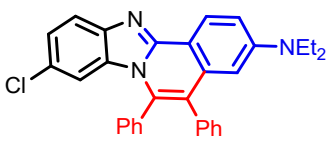

5w was prepared according to the general procedure as described in section **4.4.** The extracted mixture was concentrated under vacuum and purified by silica gel column chromatography (n-Hexane: EtOAc = 5:1), 75% yield of **5w** as a white solid and melting point is 260-262 °C. **^{1}H NMR (400 MHz, $CDCl_3$):** δ 8.71 (d, *J* = 9.0 Hz, 1H), 7.83 (d, *J* = 2.0 Hz, 1H), 7.42 – 7.26 (m, 6H), 7.25 – 7.19 (m, 4H), 7.08 (dd, *J* = 9.1, 2.6 Hz, 1H), 6.78 (dd, *J* = 8.9, 2.1 Hz,1H), 6.31 (d, *J* = 2.5 Hz, 1H), 5.77 (d, *J* = 8.9 Hz, 1H), 3.30 (q, *J* = 7.1 Hz, 4H), 1.08 (t, *J* = 7.1 Hz, 6H). **^{13}C NMR (101 MHz, $CDCl_3$):** δ 149.7, 149.0, 145.6, 136.0, 134.9, 134.6, 133.8, 131.3, 131.3, 130.6, 129.9, 129.1, 128.7, 127.9, 127.1, 126.7, 123.8, 120.2, 118.1, 114.2, 113.5, 111.5, 106.1, 44.6, 12.3. **IR (V_{max}):** 2962, 1610, 1480, 1355, 1259, 754 cm^{-1}. **HRMS (ESI):** *m/z* calcd for $C_{31}H_{26}ClN_3$ $[M+H]^+$: 476.1894, found: 476.1887.

5,6-Diphenylimidazo[2,1-a] isoquinoline (5x): The product **5x** was prepared according to the

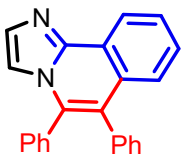

general procedure as described in section **4.4.** The extracted mixture was concentrated under vacuum and purified by silica gel column chromatography (n-Hexane: EtOAc = 5:1), 65% yield of **5x** as a white solid and melting point is 237-239 °C. **^{1}H NMR (500 MHz, $CDCl_3$)**: δ 8.76 (d, *J* = 7.5 Hz, 1H), 7.66 – 7.63 (m, 1H), 7.54 (d, *J* = 1.2 Hz, 1H), 7.50 – 7.46 (m, 1H), 7.39 (d, *J* = 8.1 Hz, 1H), 7.33 -7.31 (m, 3H), 7.31 – 7.27 (m, 4H), 7.25 – 7.19 (m, 4H). **^{13}C NMR (101 MHz, $CDCl_3$):** δ 143.1, 135.9, 133.5, 133.4,

131.404, 130.824, 130.6, 130.2, 128.8, 128.6, 128.0, 127.8, 127.3, 126.4, 124.4, 123.2, 123.2, 113.9. **IR (V_{max}):** 2934, 1490, 1449, 1311, 760, 704 cm^{-1}. **HRMS (ESI):** *m/z* calcd for $C_{23}H_{16}N_2$ $[M+H]^+$: 321.1392, found: 321.1389. Verified the analytical data with those reported in the literature.[9] [10]

5. Mechanistic studies:

Control experiment.

Step 1. H/D exchange experiment: The stock solution **(A)** containing **3a**:**4a**:catalyst: *t*-AmOH: DMF in a molar ratio 1:2:0.05/137:65 and the stock solution **(B)** having an electrolyte KOAc dissolved in D_2O:DMF as a molar ratio 1:415:32.5 was taken in two syringes and connected with designed electro-flow reactor to perform the reaction as described in Fig. S6. The solution was introduced into capillary micro reactor with T-junction and passed through an electro-flow reactor (reactor volume 200 µL) containing platinum (Pt) electrode and graphite electrode (Gr) held at 100 °C with constant current of 4 mA, residence time 2 min. and the solution was removed under reduced pressure to give the residue and purified by column chromatography (*n*-hexane: EtOAc = 8:2), yield $[D]_n$-**3a** (58%) as a white solid and $[D]_n$-**5a** (39%) as a white solid. The D-incorporation was estimated by ^1H NMR spectroscopy.

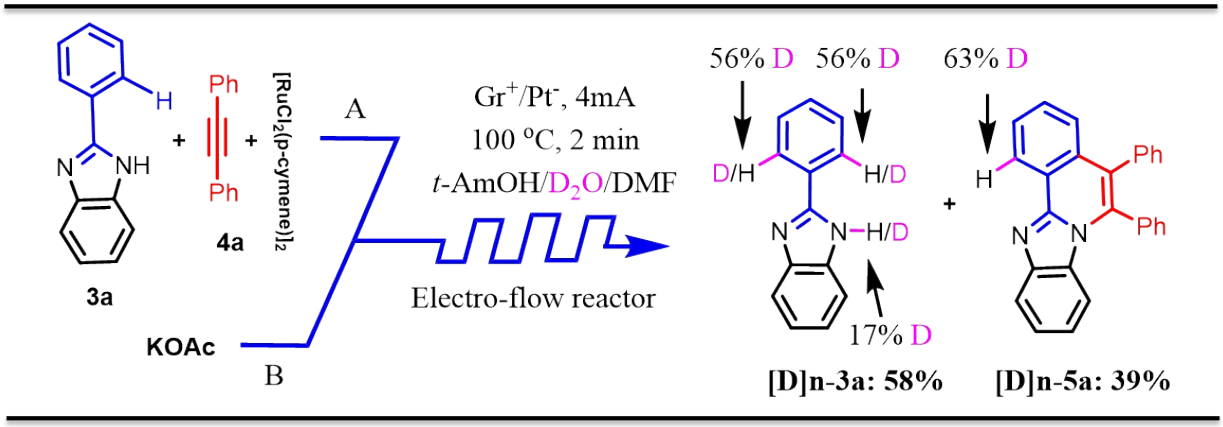

Fig. S6. The synthesis of H/D exchange: stock solution (**A**) containing **3a**:**4a**:$[RuCl_2(p\text{-cymene})]_2$: *t*-AmOH: DMF in a molar ratio 1:2:0.05:137:65; and the stock solution (**B**) having an electrolyte KOAc dissolved in D_2O + DMF as a molar ratio 1:415:32.5. Yields are based on isolated yield.

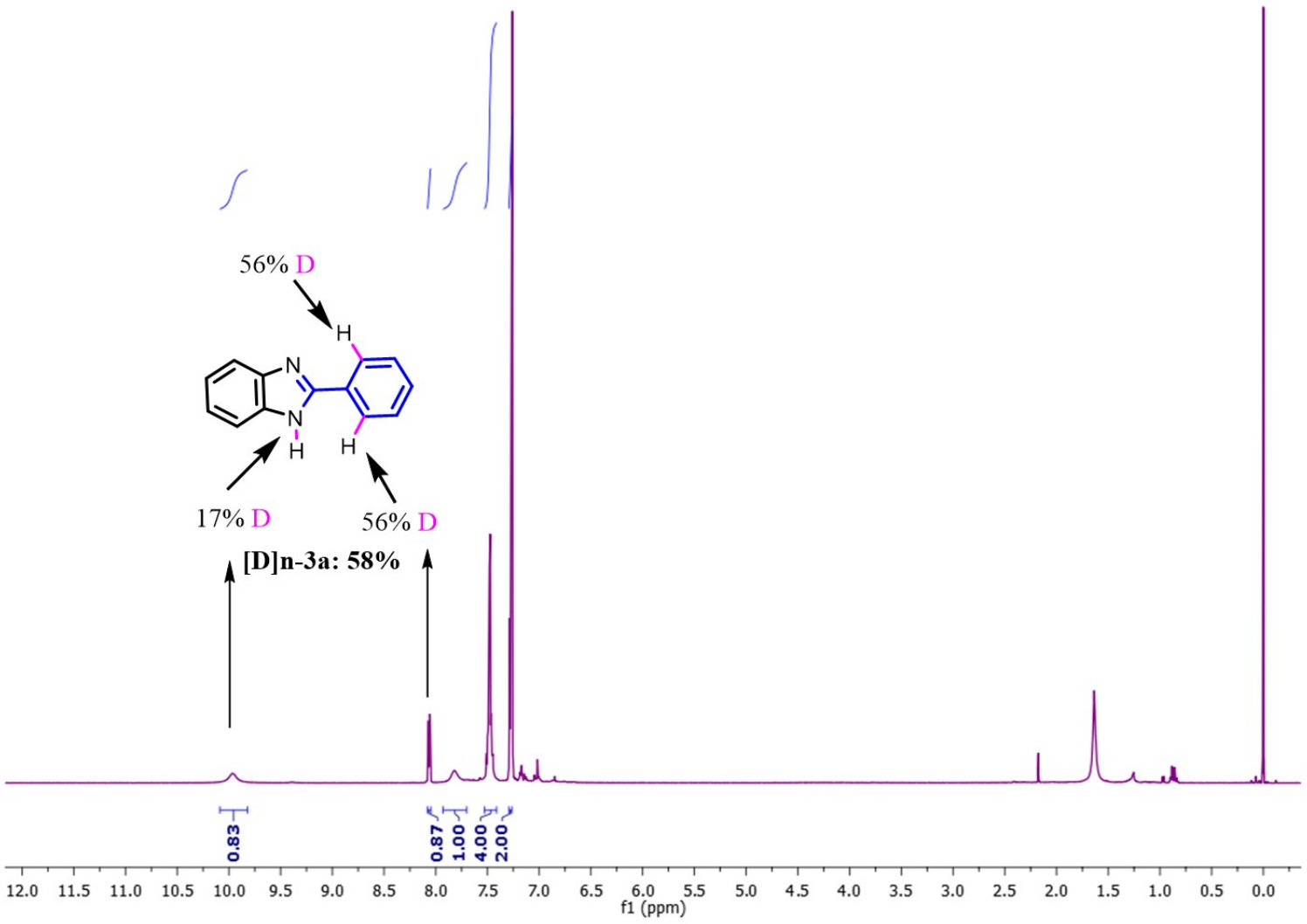

Fig. S7. ^{1}H NMR spectra of 2-(phenyl-2,6-d2)-1H-benzo[d]imidazole-1-d, in $CDCl_3$.

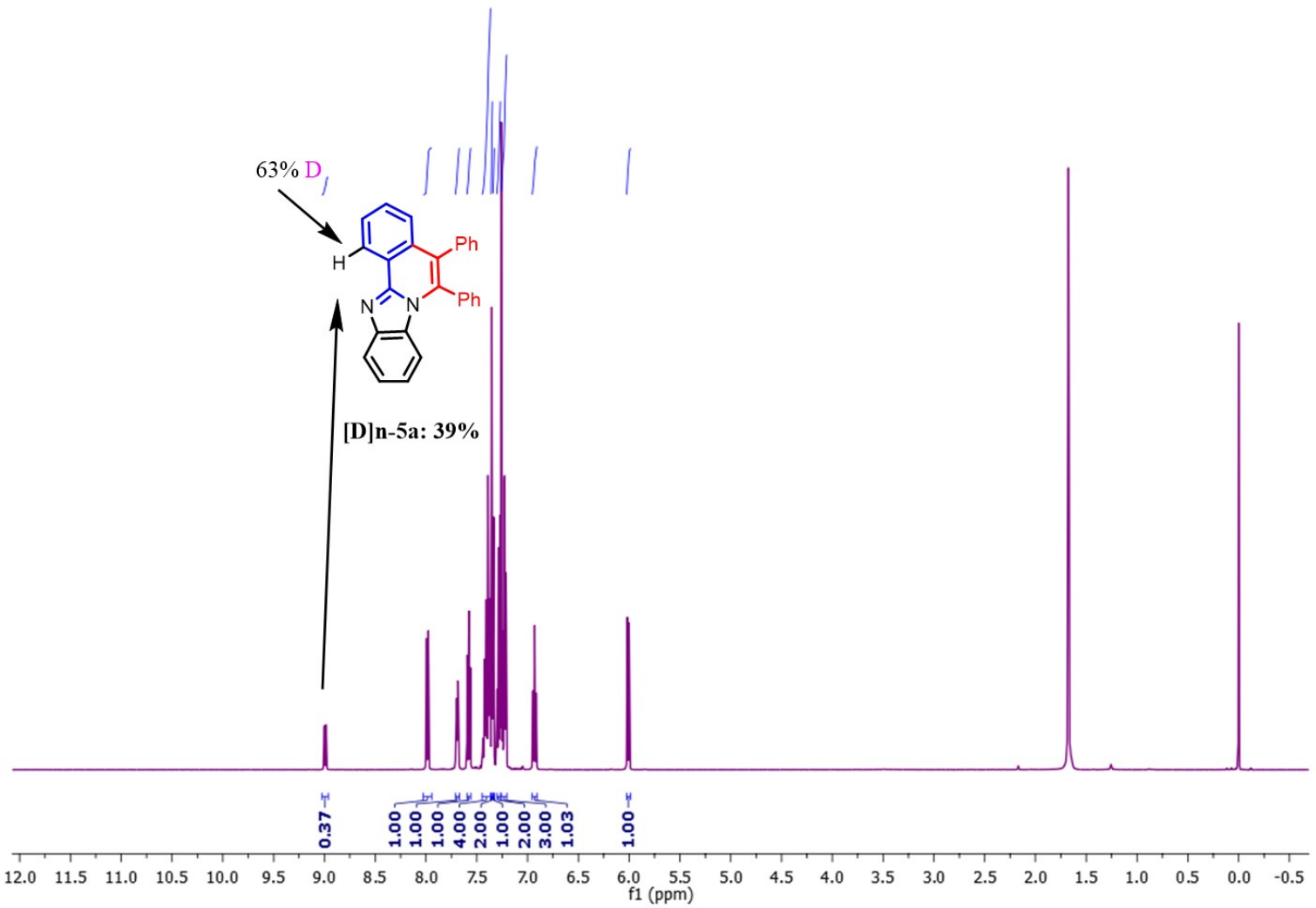

Fig. S8. ^{1}H NMR spectra of 5,6-diphenylbenzo [4,5] imidazo[2,1-a] isoquinoline-1-d, in $CDCl_3$.

Step 2: Synthesis of key intermediate of Ru-II.

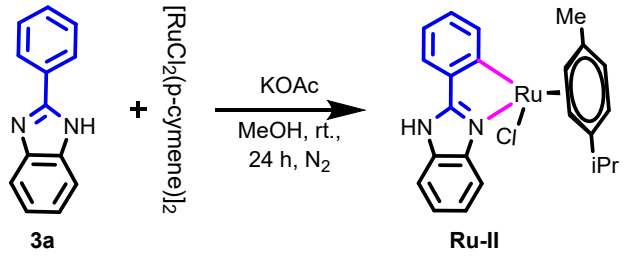

A 15 mL Schlenk tube was charged with **3a** (39 mg, 0.2 mmol), $[RuCl_2(p\text{-cymene})]_2$ (61.5 mg, 0.1 mmol), KOAc (39 mg, 0.40 mmol), and MeOH (20 mL). The mixture was stirred at ambient temperature for 24 h under N_2 and then MeOH was removed in vacuum. After column chromatography on silica gel (CH_2Cl_2:MeOH = 50:1) and crystallization (CH_2Cl_2 and n-hexane), **Ru-II** was isolated as a red solid (83 mg, 89%). **^{1}H NMR (500 MHz, $CDCl_3$):** δ 11.06 (s, 1H), 8.15 (d, *J* = 7.4 Hz, 1H), 7.67 (d, *J* = 8.0 Hz, 1H), 7.15 (t, *J* = 7.6 Hz, 1H), 6.86 – 6.80 (m, 2H), 6.72 (d, *J* = 7.3 Hz, 1H), 6.65 (d, *J* = 7.9 Hz, 1H), 6.14 (s, 1H), 5.85 (d, *J* = 5.8 Hz, 1H), 5.72 (d, *J* = 5.7 Hz, 1H), 5.39 (d, *J* = 5.8 Hz, 1H), 5.17 (d, *J* = 5.7 Hz, 1H), 2.2 – 2.14 (m 1H), 2.06 (s, 3H), 0.82 (d, *J* = 6.9 Hz, 3H), 0.68 (d, *J* = 6.9 Hz, 3H). **^{13}C NMR (101 MHz, $CDCl_3$):** δ 177.4, 159.0, 141.3, 138.6, 133.6, 133.4, 128.8, 123.5, 122.8, 122.6, 121.9, 114.7, 112.9, 100.5, 97.5, 89.5, 88.0, 81.6, 80.2, 30.7, 22.4, 21.7, 18.9. **IR (V_{max}):** 3102, 3052, 2964, 2922, 2859, 1593, 1458, 1378, 1276, 1012, 741, 668 cm^{-1}. **HRMS (ESI)** m/z calcd for $C_{23}H_{22}N_2Ru$ $[M\text{-}Cl]^+$: 429.0905 found: 429.0903.

Step 3. Synthesis of second key intermediate Ru-IV.

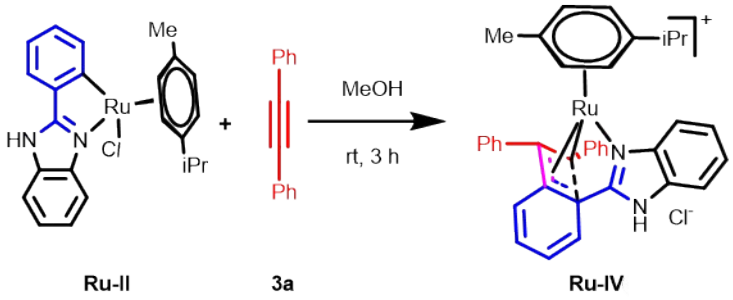

A 15 mL Schlenk tube was charged with **Ru-II** (93.0 mg, 0.20 mmol), **4a** (36.0 mg, 0.20 mmol) and MeOH (20 mL). The mixture was stirred at ambient temperature for 3 h, and then MeOH was removed in vacuo. After column chromatography on silica gel (CH_2Cl_2: MeOH = 50 : 1), **Ru-IV** was isolated as yellow solid (117.0 mg, 91%), **^{1}H NMR (700 MHz, CD_3OD):** δ 8.12 (d, *J* = 8.1 Hz, 1H), 7.82 (d, *J* = 7.1 Hz, 1H), 7.79 – 7.74 (m, 2H), 7.71 – 7.61 (m, 6H), 7.55 (d, *J* = 7.4 Hz, 1H), 7.49 (t, *J* = 7.4 Hz, 1H), 7.25 (d, *J* = 7.7 Hz, 2H), 7.15 (t, *J* = 7.4 Hz, 2H), 7.1 (t, *J* = 7.1 Hz, 1H), 5.25 (d, *J* = 5.2 Hz, 1H), 4.60 (d, *J* = 5.5 Hz, 1H), 4.29 (d, *J* = 5.0 Hz, 1H), 4.13 (s, 1H), 3.28 (d, *J* = 5.2 Hz, 1H), 2.24 (s, 3H), 1.31 (d, *J* = 6.4 Hz, 3H), 0.96 (d, *J* = 6.8 Hz, 3H). **^{13}C NMR (176 MHz, CD_3OD):** δ 175.8, 155.7, 143.7, 143.6, 141.3, 135.8, 135.4, 133.9, 133.8, 132.1, 131.9, 131.6, 130.7, 130.0, 129.2, 128.9, 128.4, 128.1, 125.96, 125.4, 119.5, 114.8, 114.0, 109.4, 92.4, 88.9, 84.3, 84.2, 83.4, 32.4, 25.2, 21.7, 18.7. **IR (V_{max}):** 3391, 3058, 3011, 2961, 1595, 1484, 1440, 1379, 1323, 1279, 1220, 866, 757, 699 cm^{-1}. **HRMS (ESI)** *m/z* calcd for $C_{37}H_{32}N_2Ru$ $[M\text{-}Cl]^+$: 607.1687 found: 607.1694.

Step 4. Cyclic voltammetry (CV) analysis.

Cyclic voltammetry (CV) measurement was conducted with HCH Instrument Model: CHI6005E electrochemical Workstation and CH Instr. ChI6005E software. For below the all experiments, a glassy carbon working electrode (disk, diameter: 3 mm), a platinum wire counter electrode (disk, diameter 1.5), and a saturated calomel reference electrode (SCE) (disk, diameter: 3mm), were operating. The voltammograms were recorded at room temperature in a mixture of *t*-AOH: H_2O: DMF at a substrate the concentration of 5 mmol/L and with 0.1 mol/L KOAc as supporting electrolyte. All solutions were saturated with N_2 before the measurement and an over-pressure of N_2 was maintained throughout the experiment. The scan rate is 100 mV/s. and Sensitivity (A/V) = $1e^{-4}$. Deviations from the general experimental setup as indicated in the respective Fig. S9-S14 and descriptions. When we are checking the Cyclic Voltammetry of $[RuCl_2(p\text{-cymene})]_2$ in absence of KOAc that time catalyst shows oxidative process. Due to the large peak to peak separation, it appears unlikely that these belong to one redox process. Upon addition of the KOAc salt, then peak will be disappeared (shown in Fig. S9) because of the oxidative process higher current is seen at the same potential due to increased solubility, while the reductive process intensifies and shifts to particularly more negative potentials due to formation of ruthenium potassium acetate complexes.[14] Additional voltammograms of the individual reagents and intermediate and their respective mixtures (Fig. S9-S14) were recorded to exclude misinterpretation of the catalysis mixture.

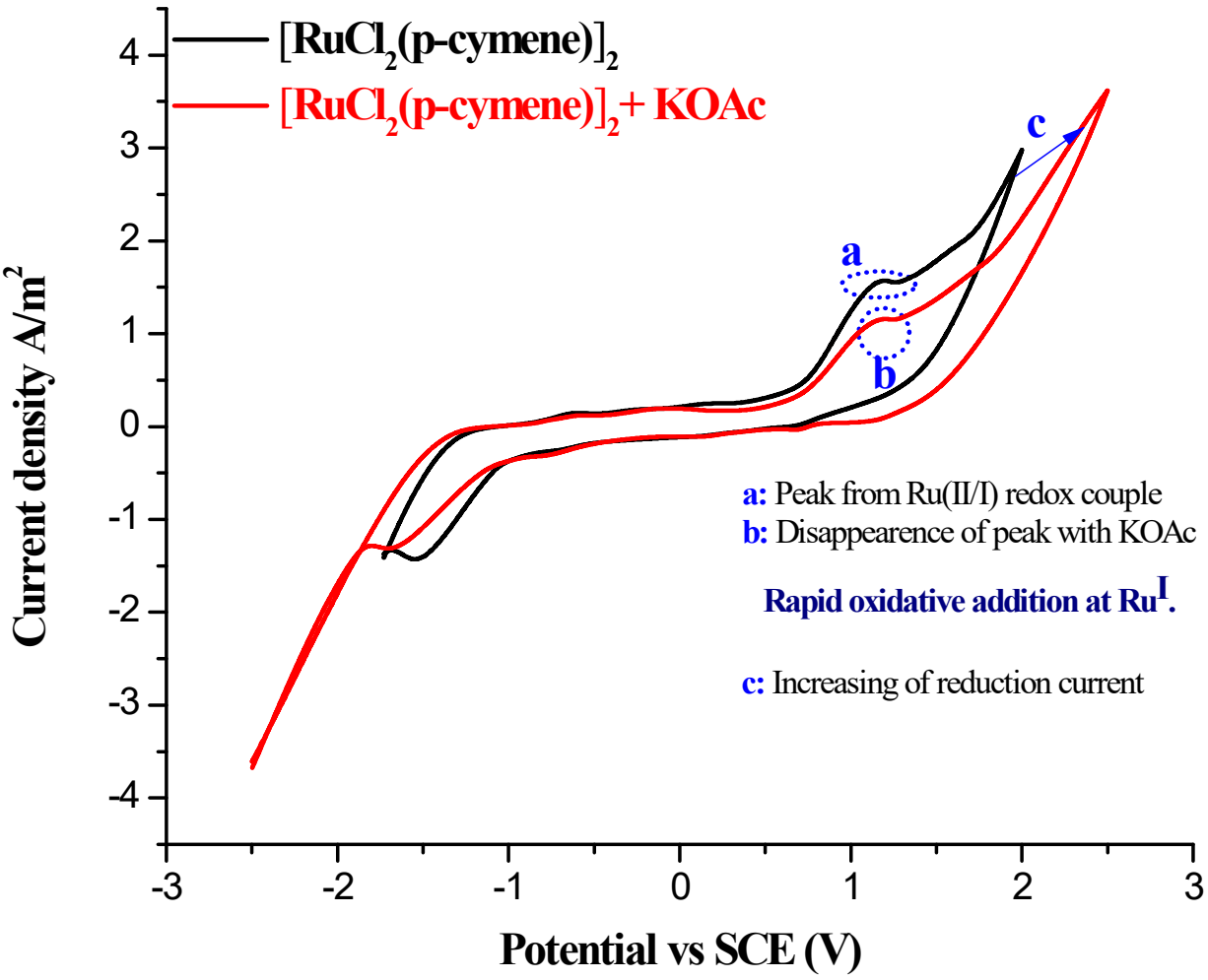

Fig. S9. Cyclic voltammograms of $[RuCl_2(p\text{-cymene})]_2$ (black line) and $[RuCl_2(p\text{-cymene})]_2$ + KOAc (red line) and room temperature at Scan Rate 100 mV/s.

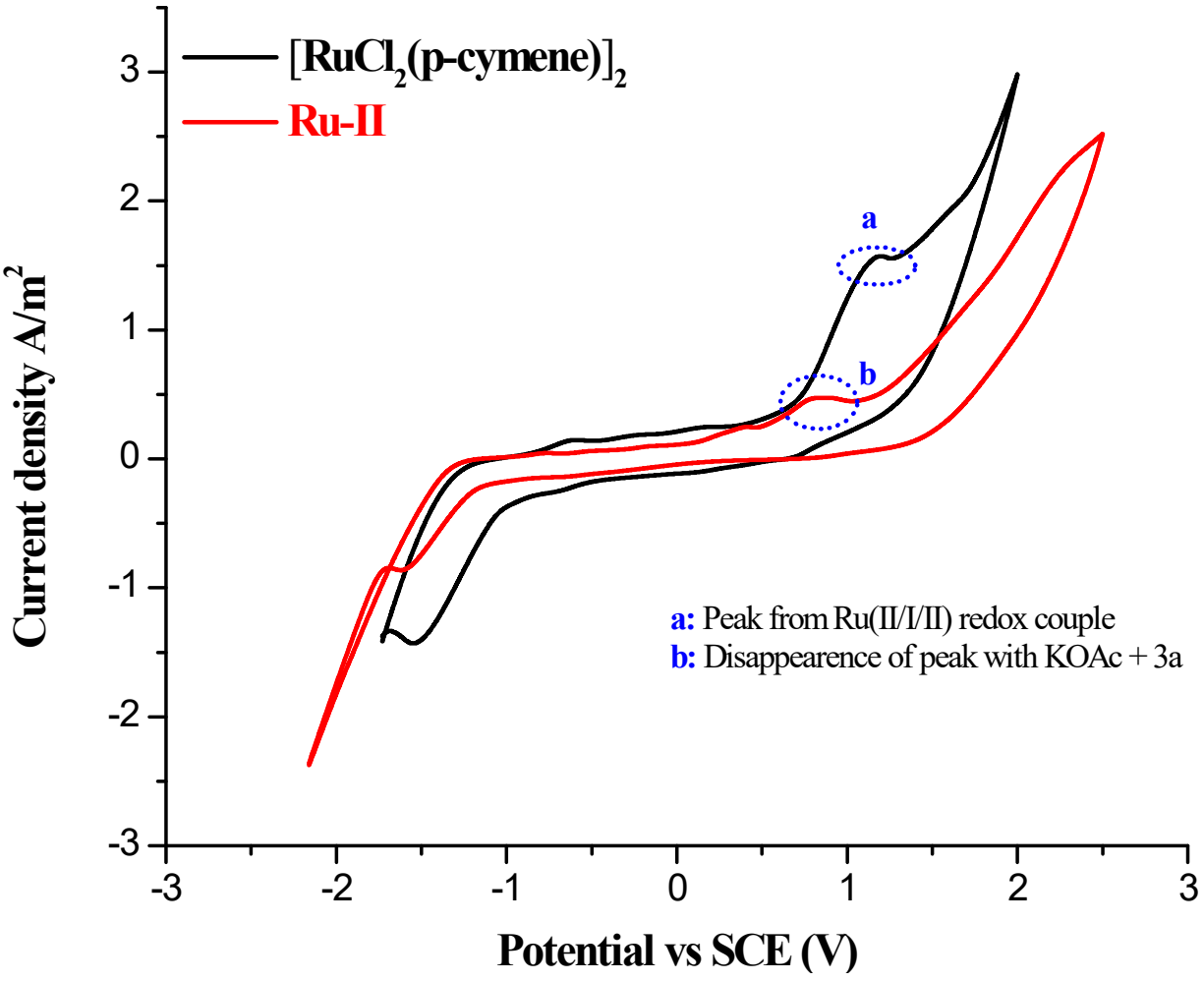

Fig. S10. Cyclic voltammograms of $[RuCl_2(p\text{-cymene})]_2$ (black line) and first intermediate complex **Ru-II** (red line) and room temperature at scan Rate 100 mV/s.

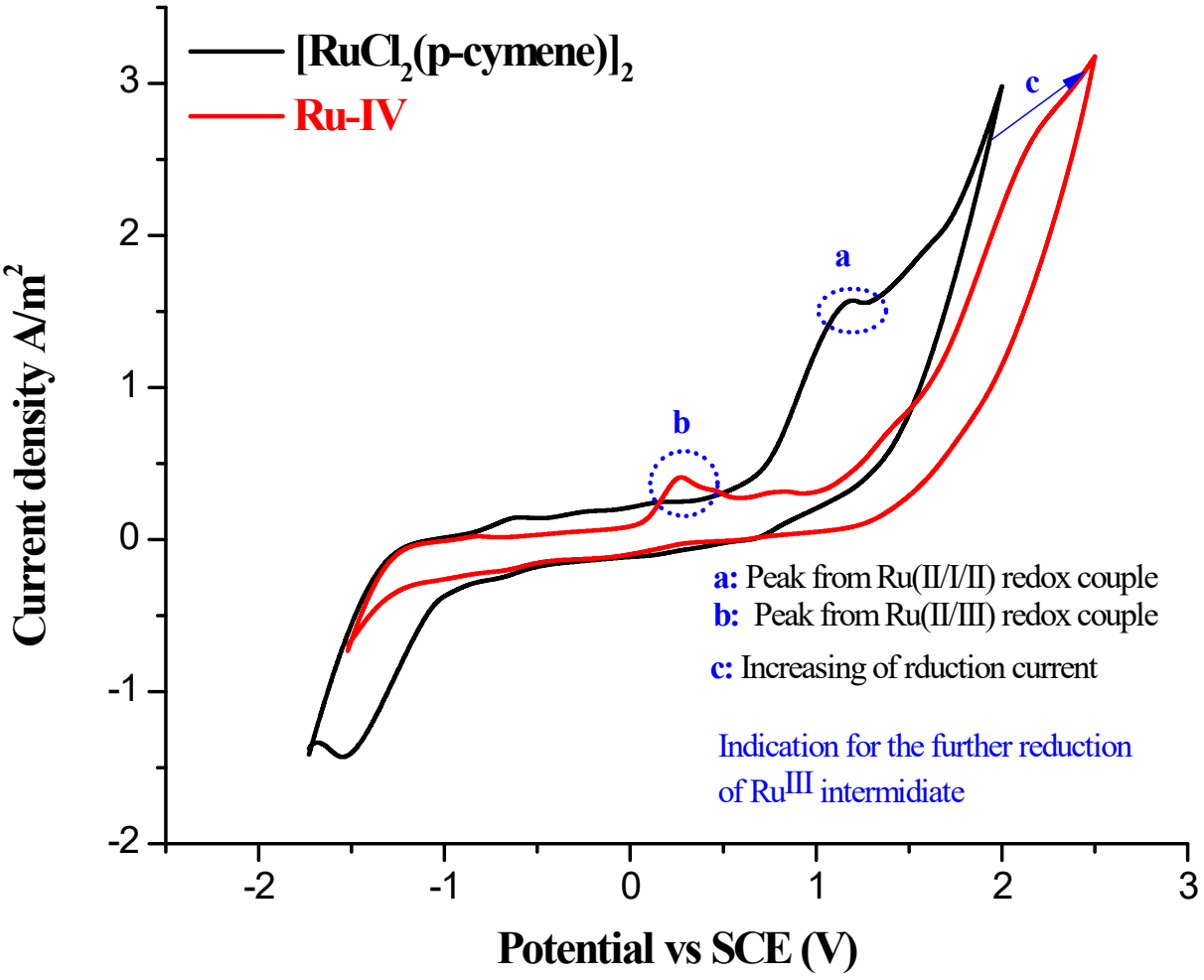

Fig. S11. Cyclic voltammograms of $[RuCl_2(p\text{-cymene})]_2$ (black line) and second intermediate complex **Ru-IV** (red line) and room temperature at scan rate 100 mV/s.

The screening of cyclic voltammetry of the electricity-induced C-H/N-H annulation Fig. S12. Thus, we observed the room temperature, The cyclic voltammetry of electrolyte KOAc (black line) the oxidation peak of 1.18V vs. SCE. The curve showed an oxidation peak of the $[RuCl_2(p\text{-cymene})]_2$ (red line, Fig. S12) at 1.26V vs. SCE. Interestingly, we found that the CV of **3a** (blue line, Fig. S12) and presented by single oxidation peak in the presence of KOAc, at 0.9V vs. SCE and the curve of **4a** (pink line, Fig. S12) and **5a** (green line, Fig. S12) in the presence of KOAc

showed no oxidation peak respectively. Furthermore, the electrochemical C-H/N-H annulation reaction analysis of cyclic voltammetry from mixture of the compounds Fig. S13. The cyclic voltammetry of electrolyte $[RuCl_2(p\text{-cymene})]_2$ the oxidation peak of 1.26V vs. SCE. (curve black line in Fig. S13). The curve showed an oxidation peak of the $[RuCl_2(p\text{-cymene})]_2$ at 1.20V vs. SCE. (red line) in the presence of KOAc. The cyclic voltammetry of the mixture of KOAc, $[RuCl_2(p\text{-cymene})]_2$ and **3a** demonstrated an apparent oxidation peak at 1.40 V vs. SCE. (curve blue line in Fig. S13) due to the possible chemical interaction between the three compounds. Further the mixture of cyclic voltammetry analysis of KOAc, $[RuCl_2(p\text{-cymene})]_2$, **3a** and **4a** showed the oxidation peak at 1.40 V vs. SCE (curve pink line in Fig. S13) due to the possible for four compounds.

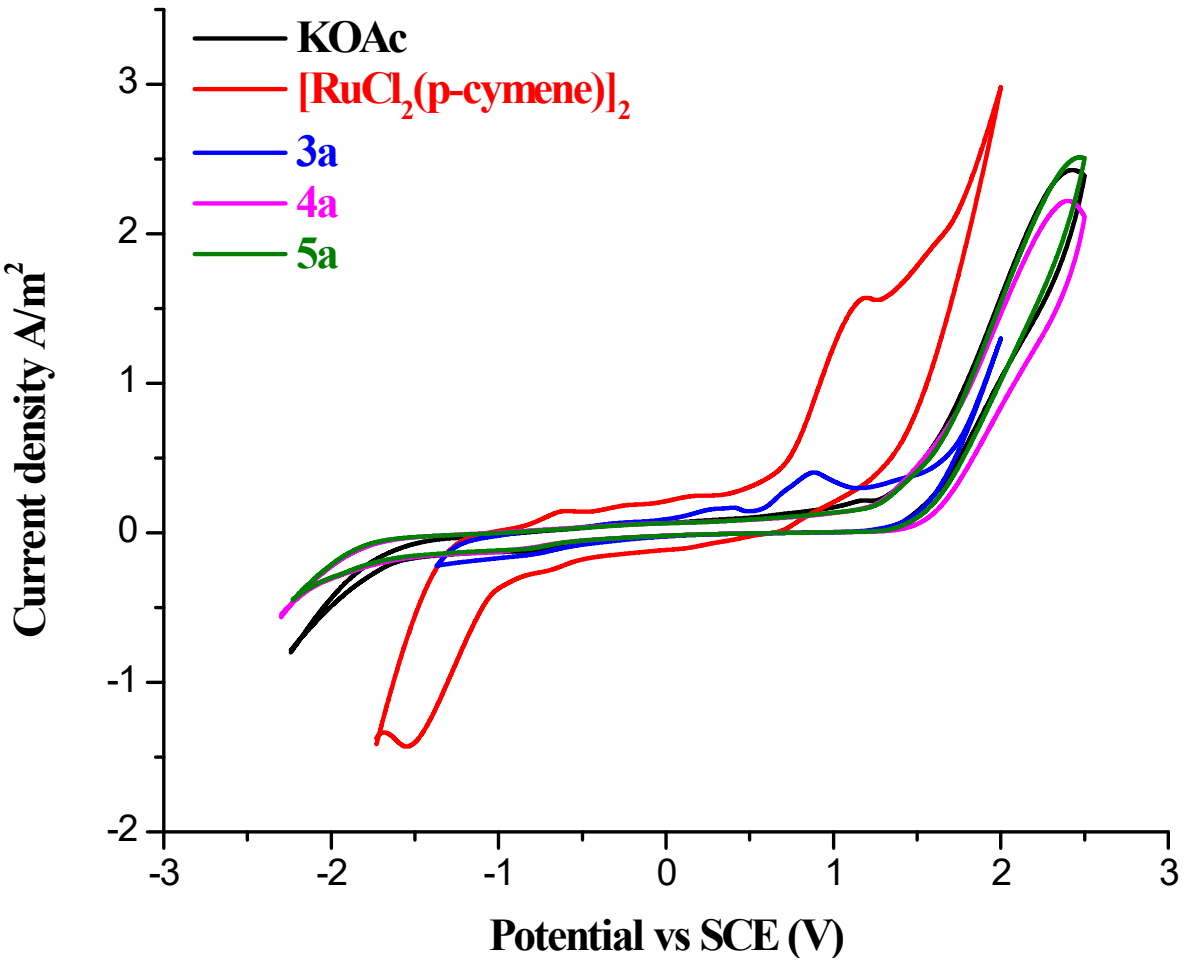

Fig. S12. Cyclic voltammograms of KOAc (black line), [$RuCl_2$(*p*-cymene)]$_2$ (red line), **3a** (blue line), **4a** (pink line), **5a** (green line) and room temperature at scan rate 100 mV/s.

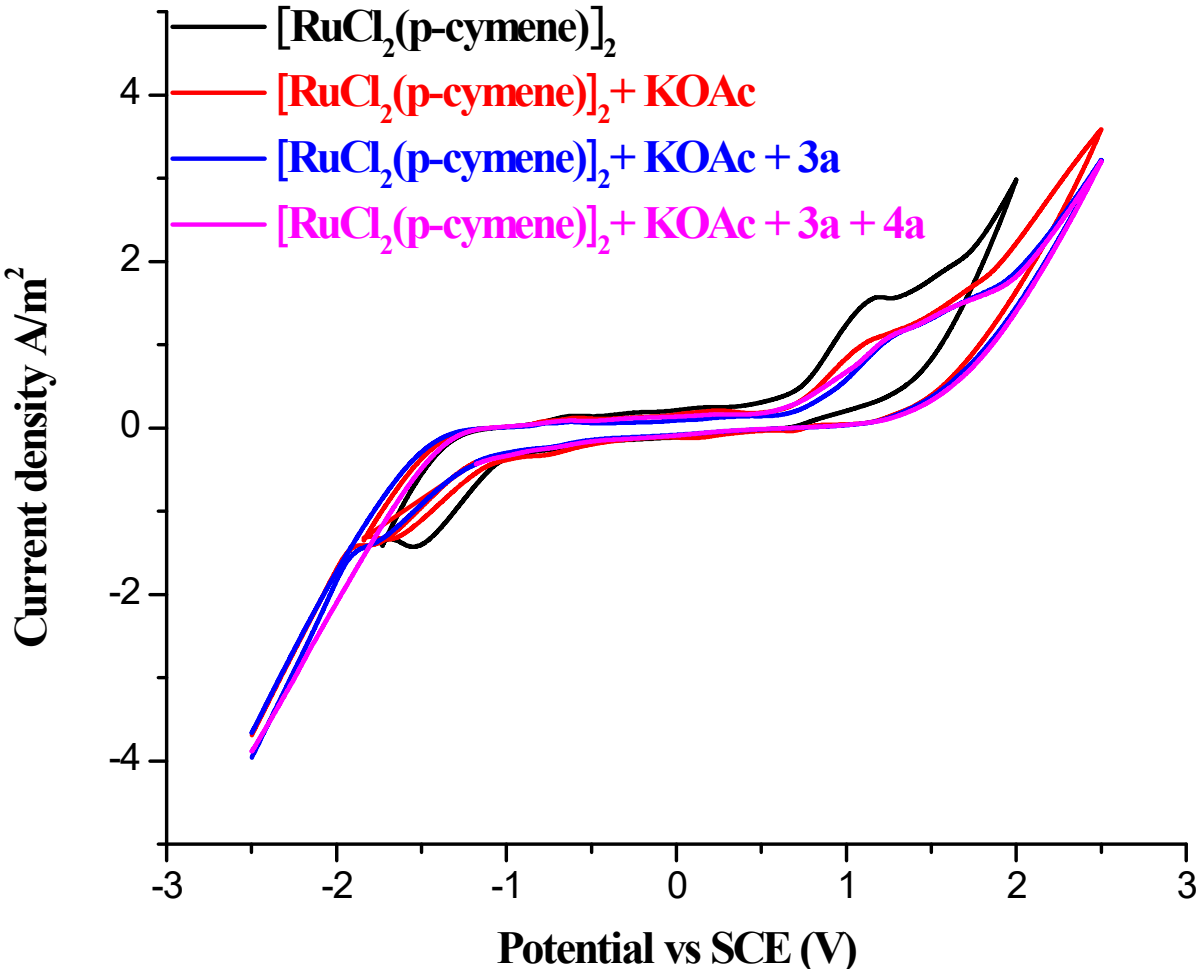

Fig. S13. Cyclic voltammograms of $[RuCl_2(p\text{-cymene})]_2$ (black line), KOAc + $[RuCl_2(p\text{-cymene})]_2$ (red line), KOAc + $[RuCl_2(p\text{-cymene})]_2$ + **3a** (blue line), and KOAc + $[RuCl_2(p\text{-cymene})]_2$ + **3a** + **4a** (pink line) and room temperature at scan rate 100 mV/s.

The analysis of electrochemical C-H/N-H annulation of cyclic voltammetry is well-marked ruthenium cycles Fig. S14. Thus, we observed room temperature irreversible oxidation of the ruthenium (II) complex, **Ru-II** (blue line) at 0.80V vs. SCE. The ruthenium (II), **Ru-IV** (red line) featured a considerably higher oxidation wave at 0.40 V vs. SCE, respectively.

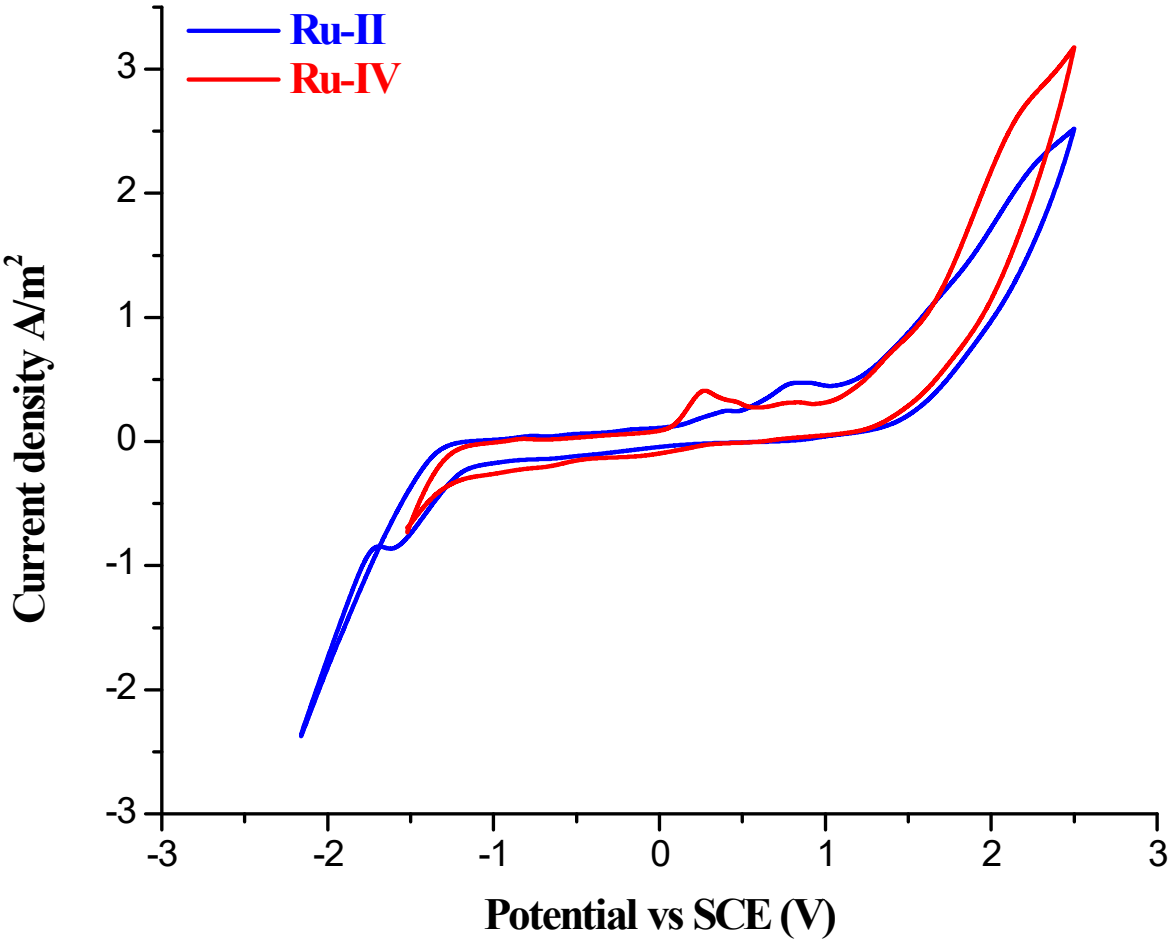

Fig. S14. Cyclic voltammetry of **Ru-II** (blue line), **Ru-IV** (red line) in *t*-AmOH/H_2O/DMF under N_2 at rt, electrolyte KOAc and room temperature at Scan Rate 100 mV/s.

6. Faradaic efficiency (ϕ) calculation

Experimental Charge (Q) = 0.0002 mol × 96485.33 $C.mol^{-1}$

Experimental Charge = 19.297C

Experimental Charge (96% yield) = 19.297C× 0.96

Experimental Charge (96% yield) = 18.525C

Theoretical charge (Q) = 0.004 × 60 × 80

= 19.2 C

$$Faradaic\ efficiency(\phi) = \frac{experimental\ charge(Qe)}{theoretical\ charge(Qt)} X\ 100$$

$$Faradaic\ efficiency(\phi) = \frac{18.525}{19.2} X\ 100$$

Faradaic efficiency (ϕ) = 96.48 %

7. Supporting references:

1 J. M. Villar, J. Suárez, J. A. Varela and C. Saá, *Org. Lett.*, 2017, **19**, 1702-1705.

2 W. Huang, N. Huber, S. Jiang, K. Landfester and K. A. I. Zhang, *Angew. Chem. Int. Ed.*, 2020, **59**, 18368-18373.

3 Z. Li, H. Song, R. Guo, M. Zuo, C. Hou, S. Sun, X. He, Z. Sun and W. Chu, *Green Chem.*, 2019, **21**, 3602-3605.

4 E. Skolia, M. K. Apostolopoulou, N. F. Nikitas and C. G. Kokotos, *Eur. J. Org. Chem.*, 2021, **2021**, 422-428.

5 R. R. Putta, S. Chun, S. H. Choi, S. B. Lee, D.-C. Oh and S. Hong, *J. Org. Chem.*, 2020, **85**, 15396-15405.

6 R. Zhang, Y. Qin, L. Zhang and S. Luo, *Org. Lett.*, 2017, **19**, 5629-5632.

7 T. B. Nguyen, L. Ermolenko and A. Al-Mourabit, *J. Am. Chem. Soc.*, 2013, **135**, 118-121.

8 S. Kumar, D. Aand, S. Pabbaraja, D.-P. Kim and A. K. Singh, *ACS Sustain. Chem. & Eng.*, 2019, **7**, 19605-19611.

9 A. Obata, A. Sasagawa, K. Yamazaki, Y. Ano and N. Chatani, *Chem. Sci.*, 2019, **10**, 3242-3248.

10 P. K. Dutta and S. Sen, *Eur. J. Org. Chem.*, 2018, **2018**, 5512-5519.

11 N. Kavitha, G. Sukumar, V. P. Kumar, P. S. Mainkar and S. Chandrasekhar, *Tetrahedron Lett.*, 2013, **54**, 4198-4201.

12 L. Yang, R. Steinbock, A. Scheremetjew, R. Kuniyil, L. H. Finger, A. M. Messinis and L. Ackermann, *Angew. Chem. Int. Ed.*, 2020, **59**, 11130-11135.

13 S. Thavaselvan and K. Parthasarathy, *Org. Lett.*, 2020, **22**, 3810-3814.

14 W.-J. Kong, L. H. Finger, A. M. Messinis, R. Kuniyil, J. C. A. Oliveira and L. Ackermann, *J. Am. Chem. Soc.*, 2019, **141**, 17198-17206.

8. Spectra:

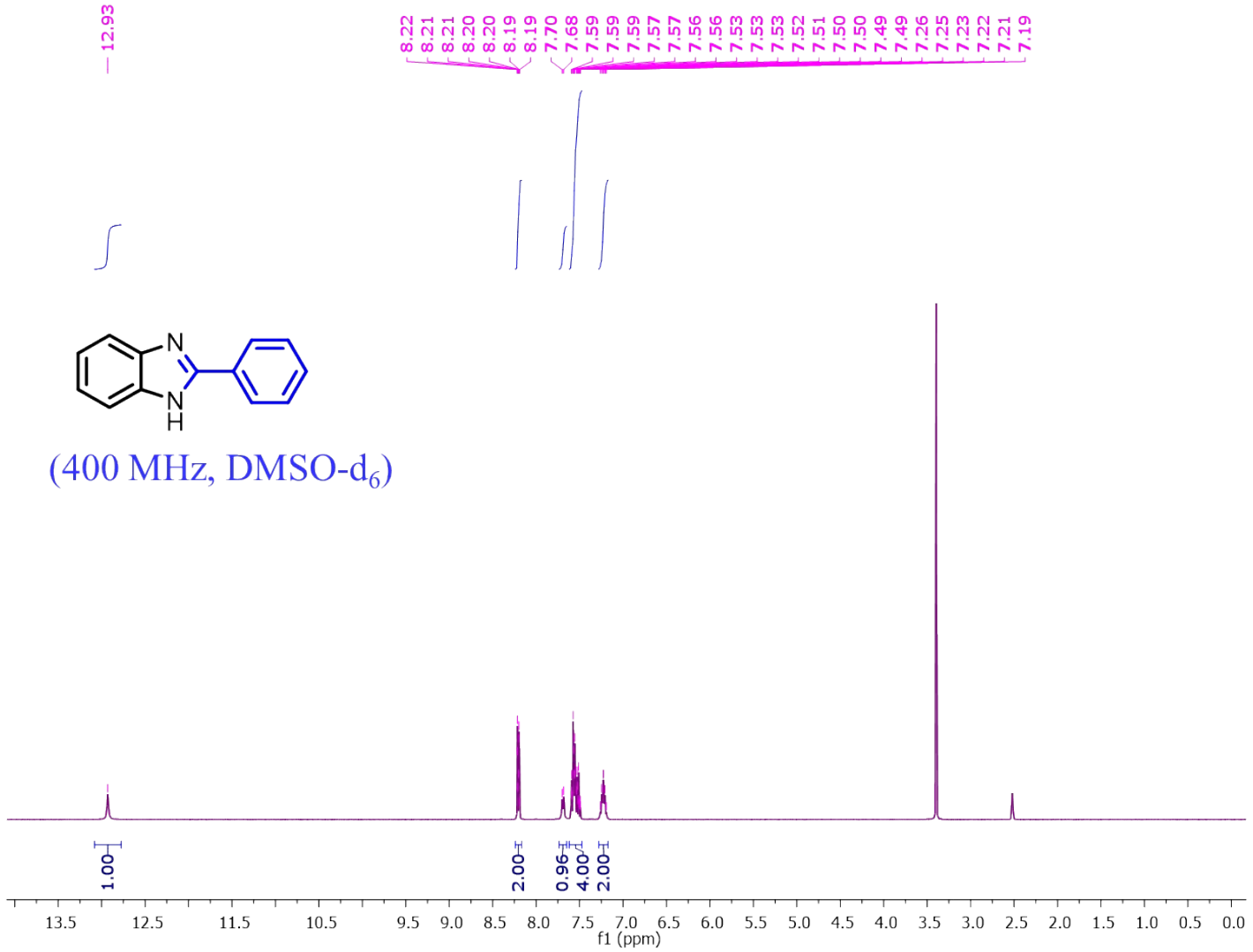

Fig. S15. ^{1}H NMR spectra of 2-phenyl-1H-benzo[d]imidazole (**3a**) in DMSO-d_6.

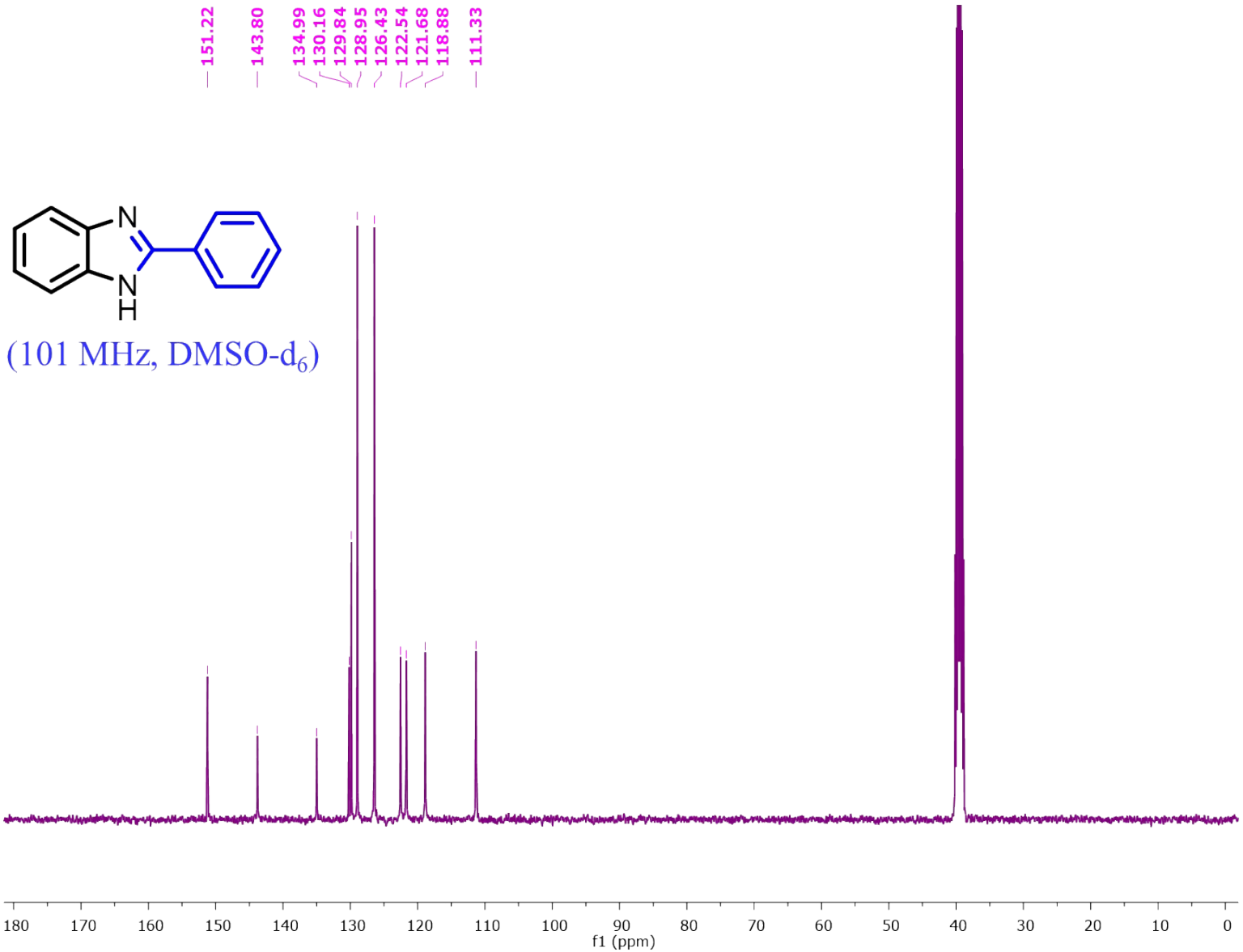

Fig. S16. ^{13}C NMR spectra of 2-phenyl-1H-benzo[d]imidazole (**3a**) in DMSO-d_6.

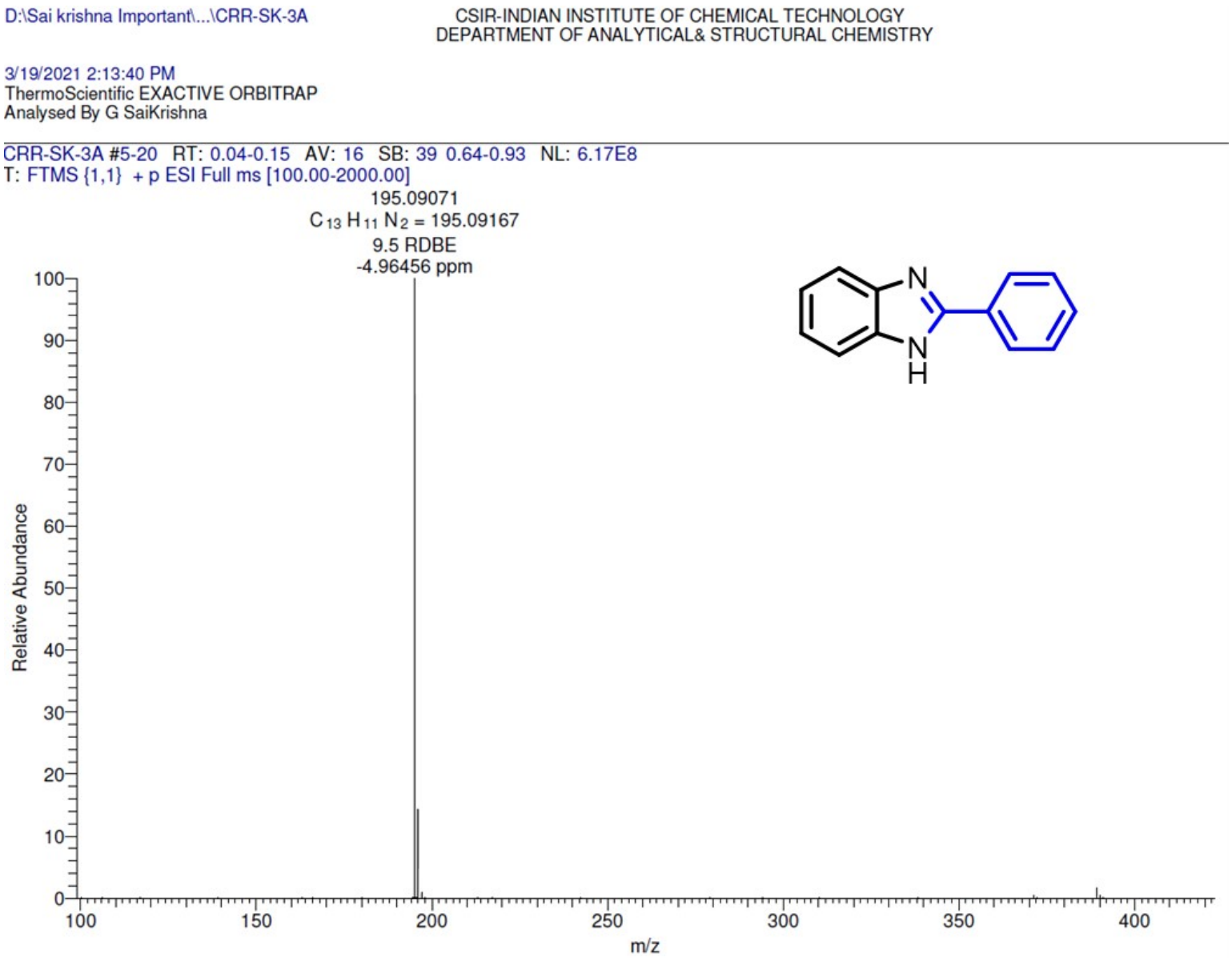

Fig. S17. IR spectra of 2-phenyl-1H-benzo[d]imidazole **(3a).**

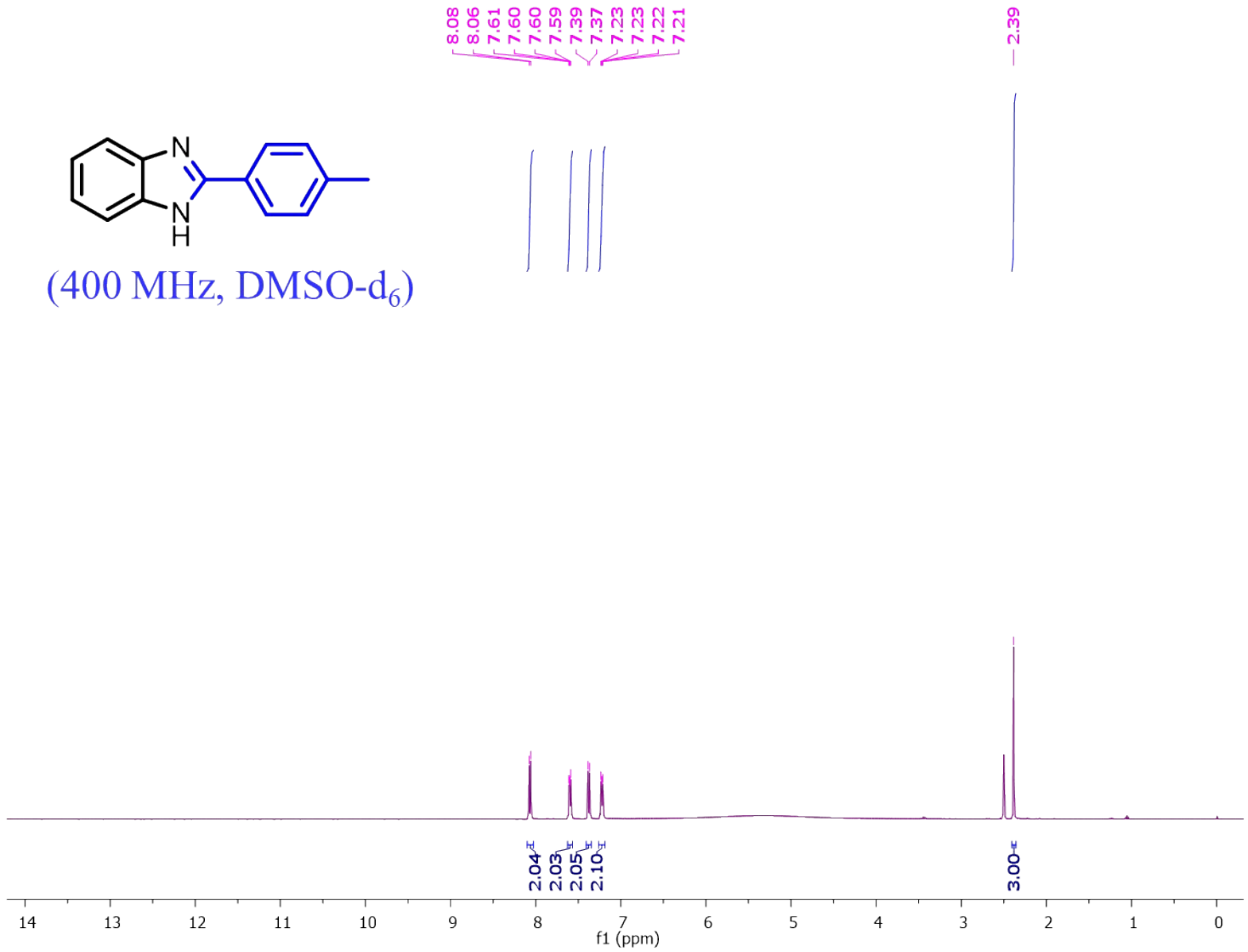

Fig. S18. [1]H NMR spectra of 2-(p-tolyl)-1H-benzo[d]imidazole (**3b**) in DMSO-d_6.

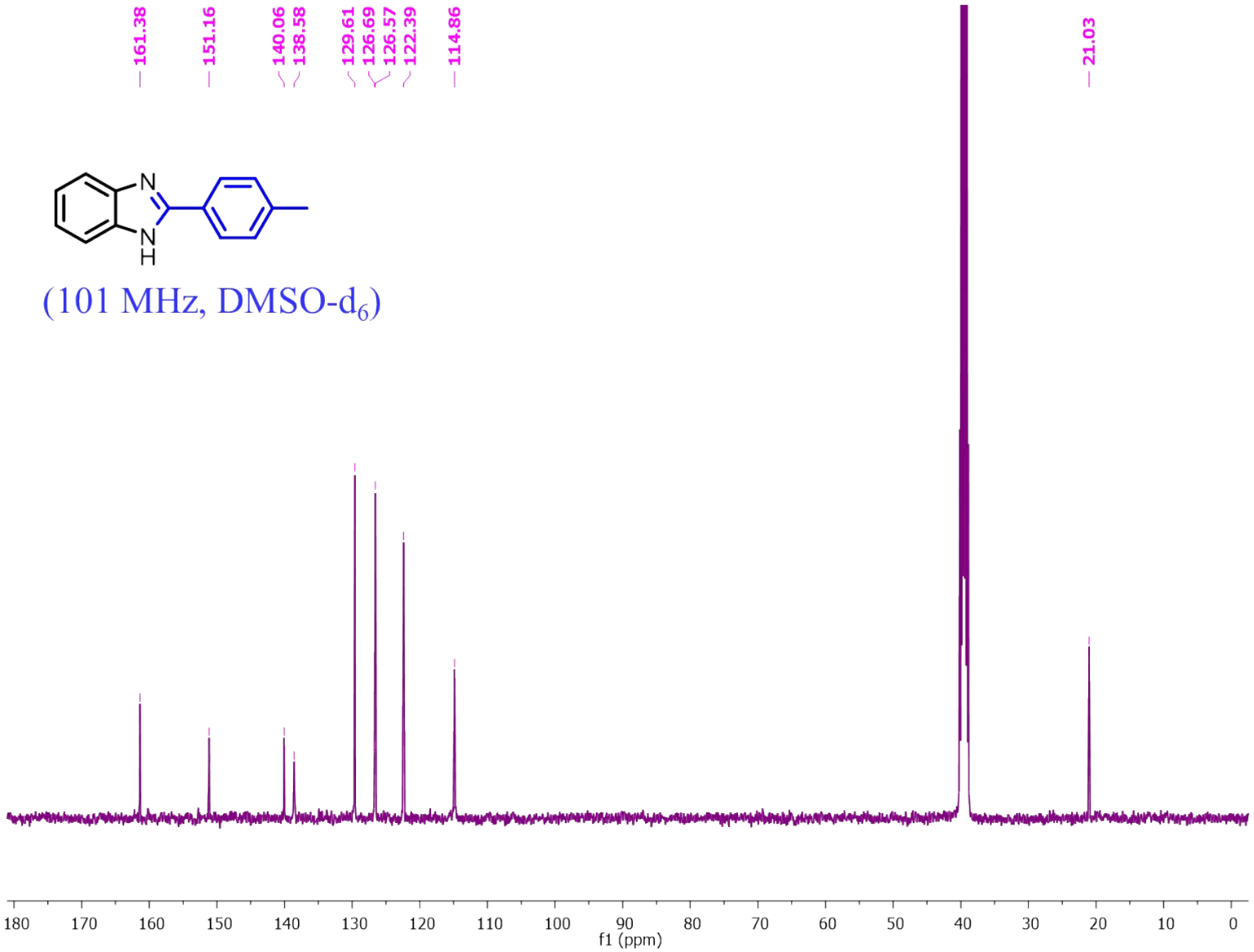

Fig. S19. ^{13}C NMR spectra of 2-(p-tolyl)-1H-benzo[d]imidazole (**3b**) in DMSO-d_6.

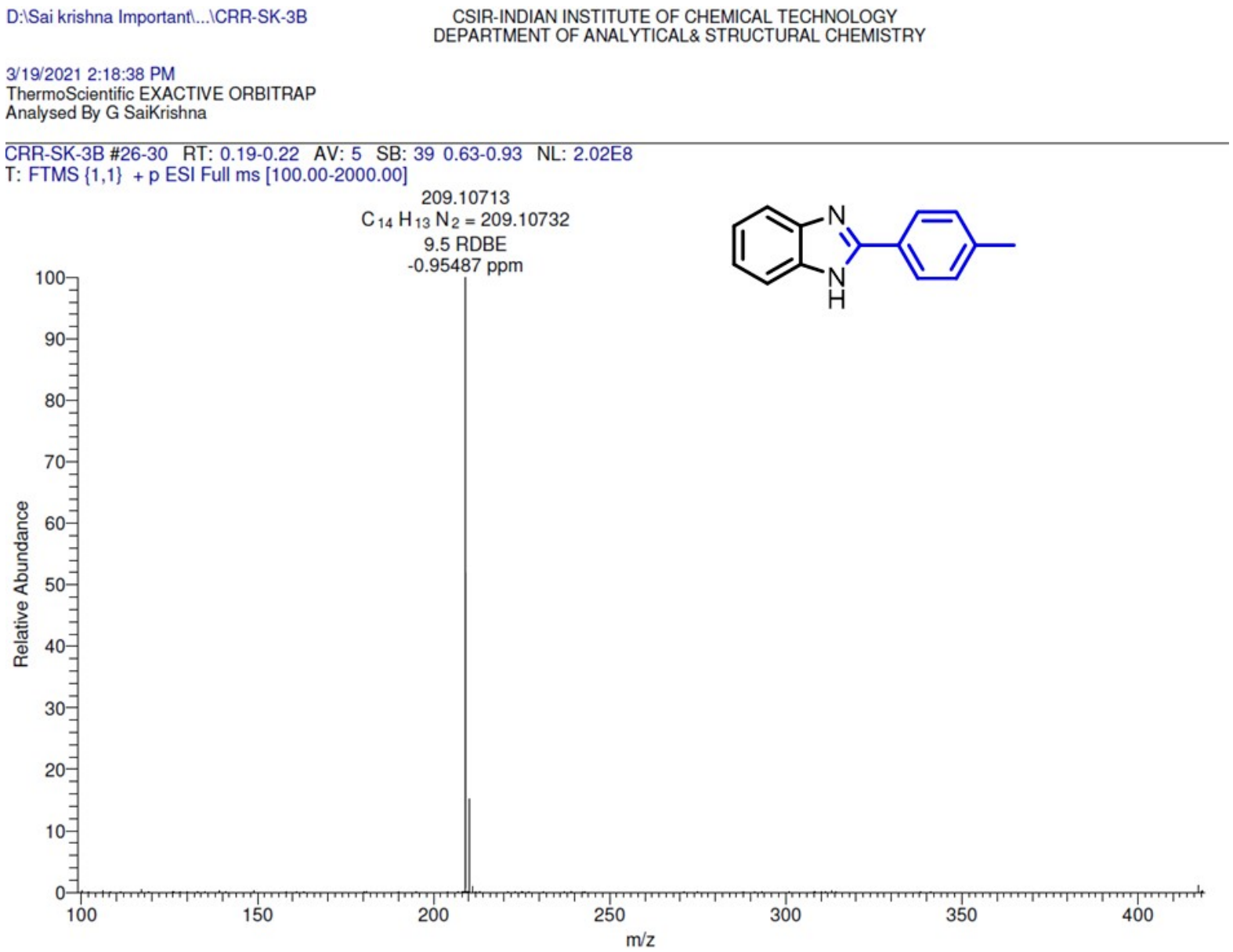

Fig. S20. IR spectra of 2-(p-tolyl)-1H-benzo[d]imidazole (**3b**).

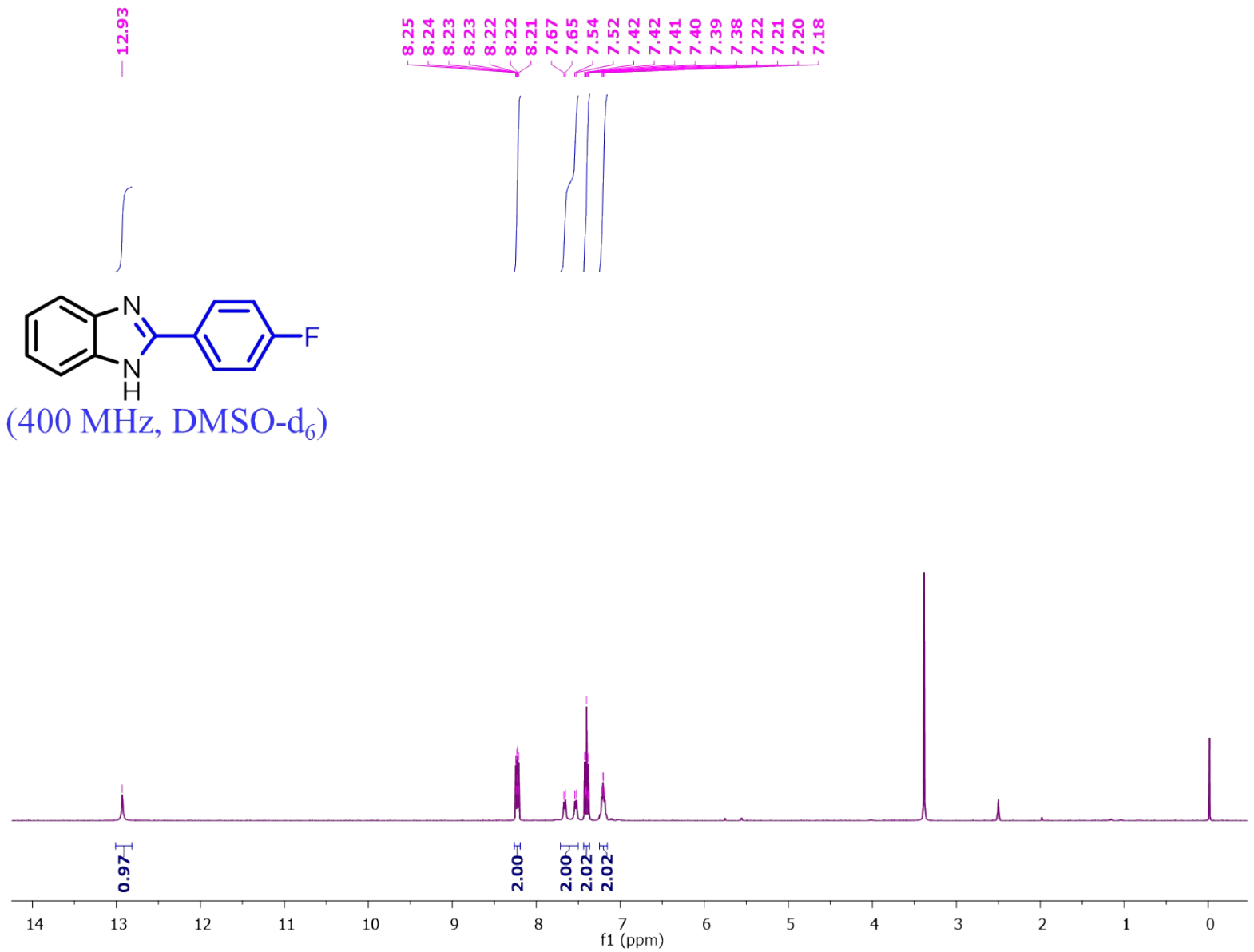

Fig. S21. [1]H NMR spectra of 2-(4-fluorophenyl)-1H-benzo[d]imidazole (**3c**) in DMSO-d_6.

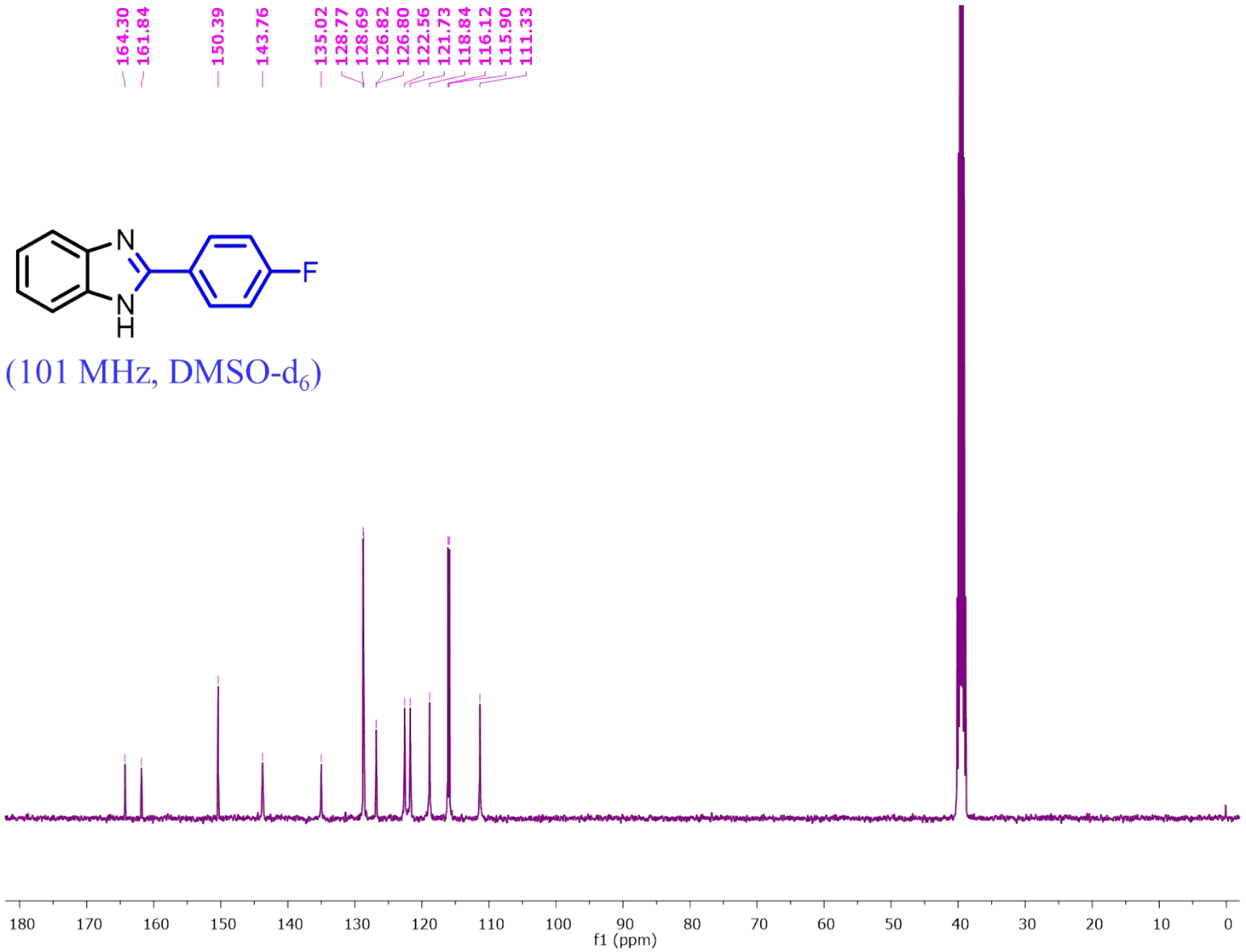

Fig. S22. ^{13}C NMR spectra of 2-(4-fluorophenyl)-1H-benzo[d]imidazole (**3c**) in DMSO-d_6.

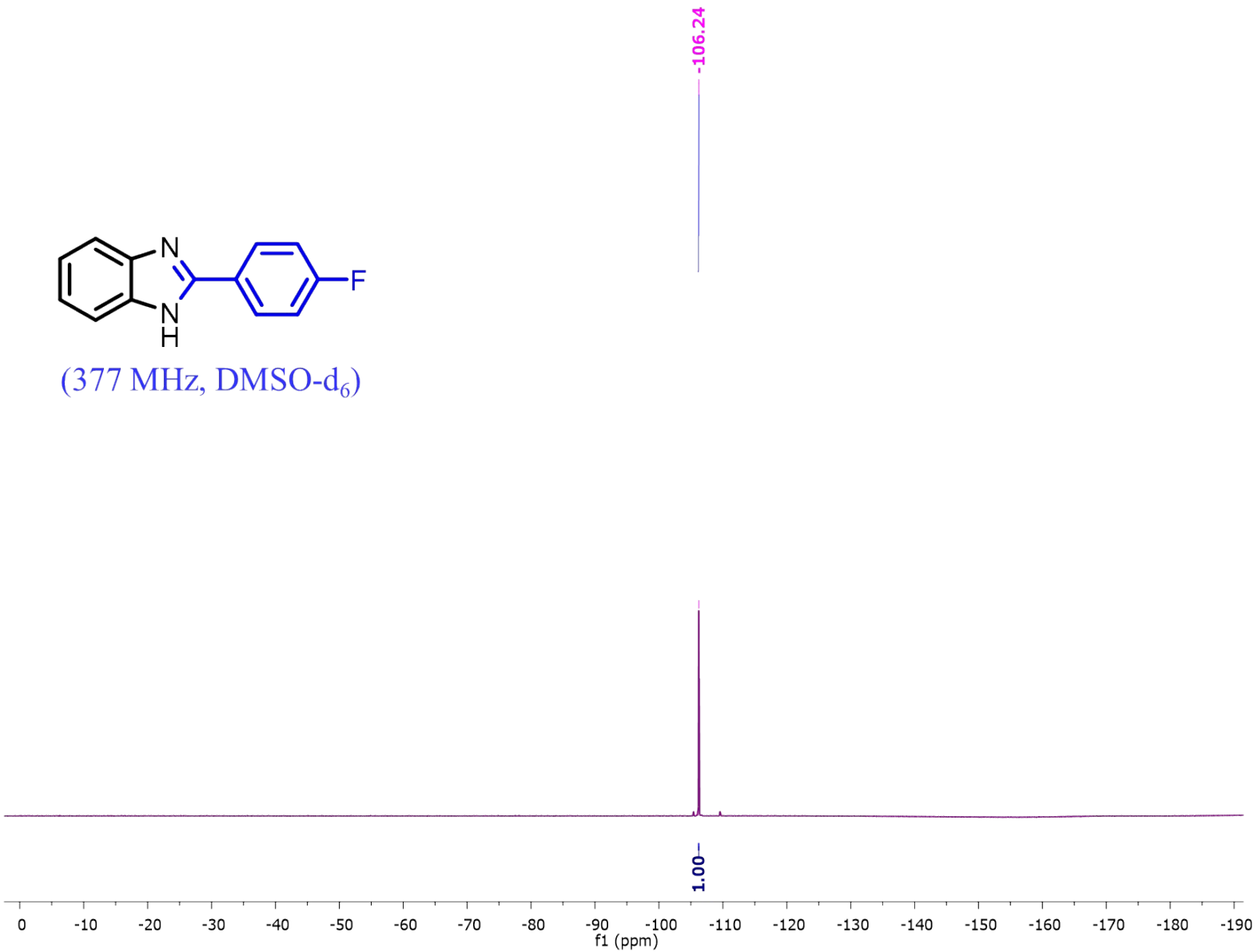

Fig. S23. ^{19}F NMR spectra of 2-(4-fluorophenyl)-1H-benzo[d]imidazole (**3c**) in DMSO-d_6.

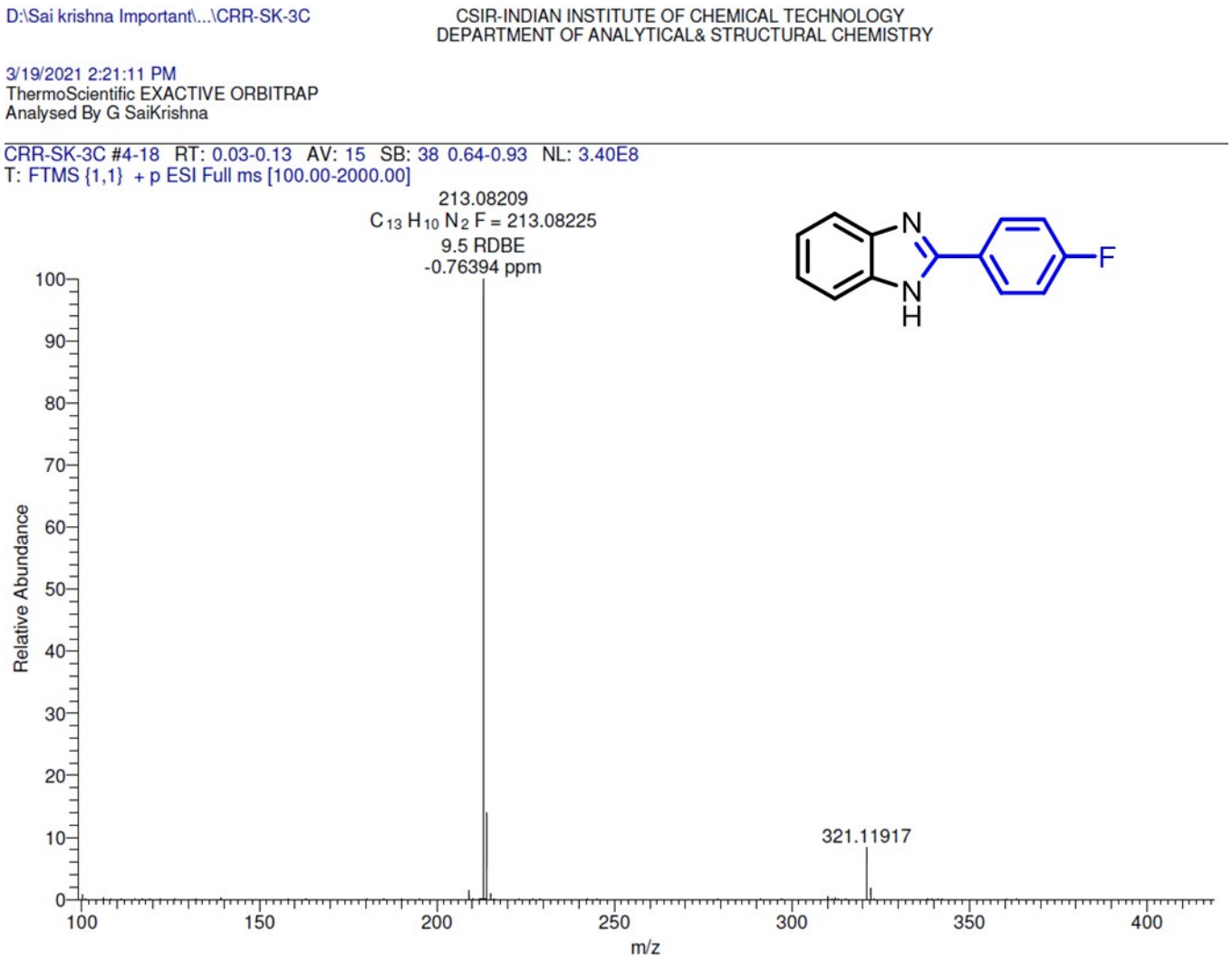

Fig. S24. HRMS spectra of 2-(4-fluorophenyl)-1H-benzo[d]imidazole **(3c)**.

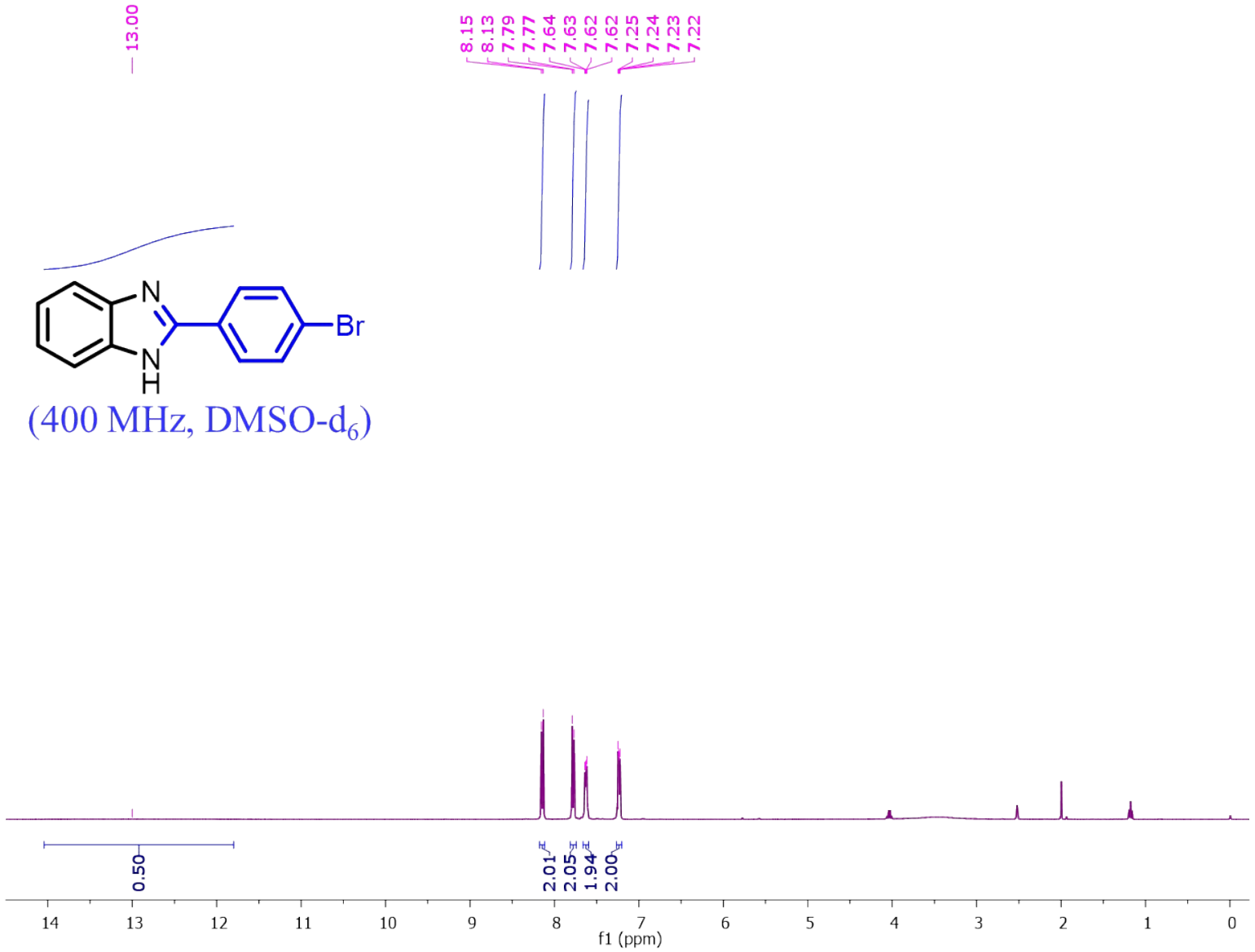

Fig. S25. [1]H NMR spectra of 2-(4-bromophenyl)-1H-benzo[d]imidazole **(3d)** in DMSO-d_6.

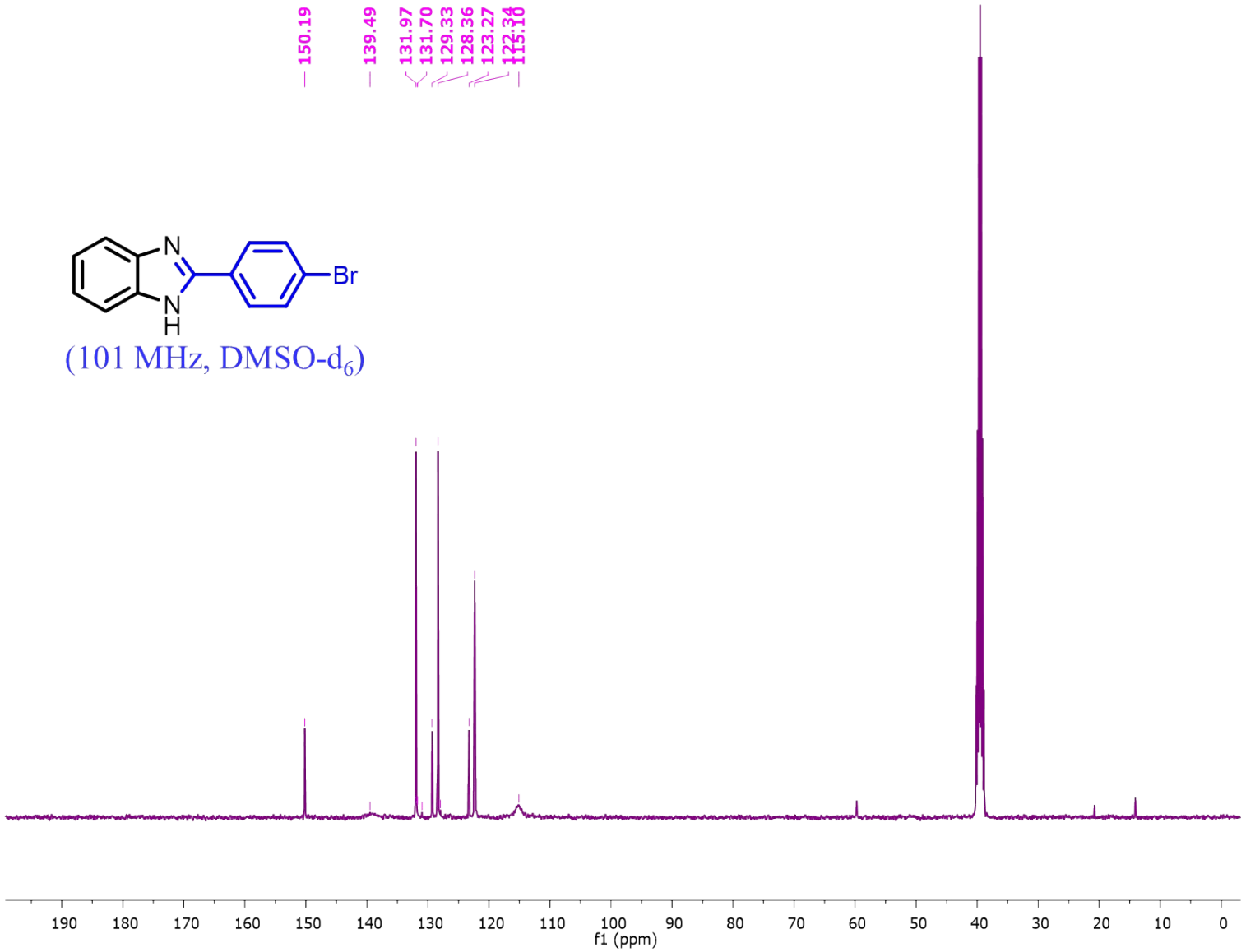

Fig. S26. ^{13}C NMR spectra of 2-(4-bromophenyl)-1H-benzo[d]imidazole **(3d)** in DMSO-d_6.

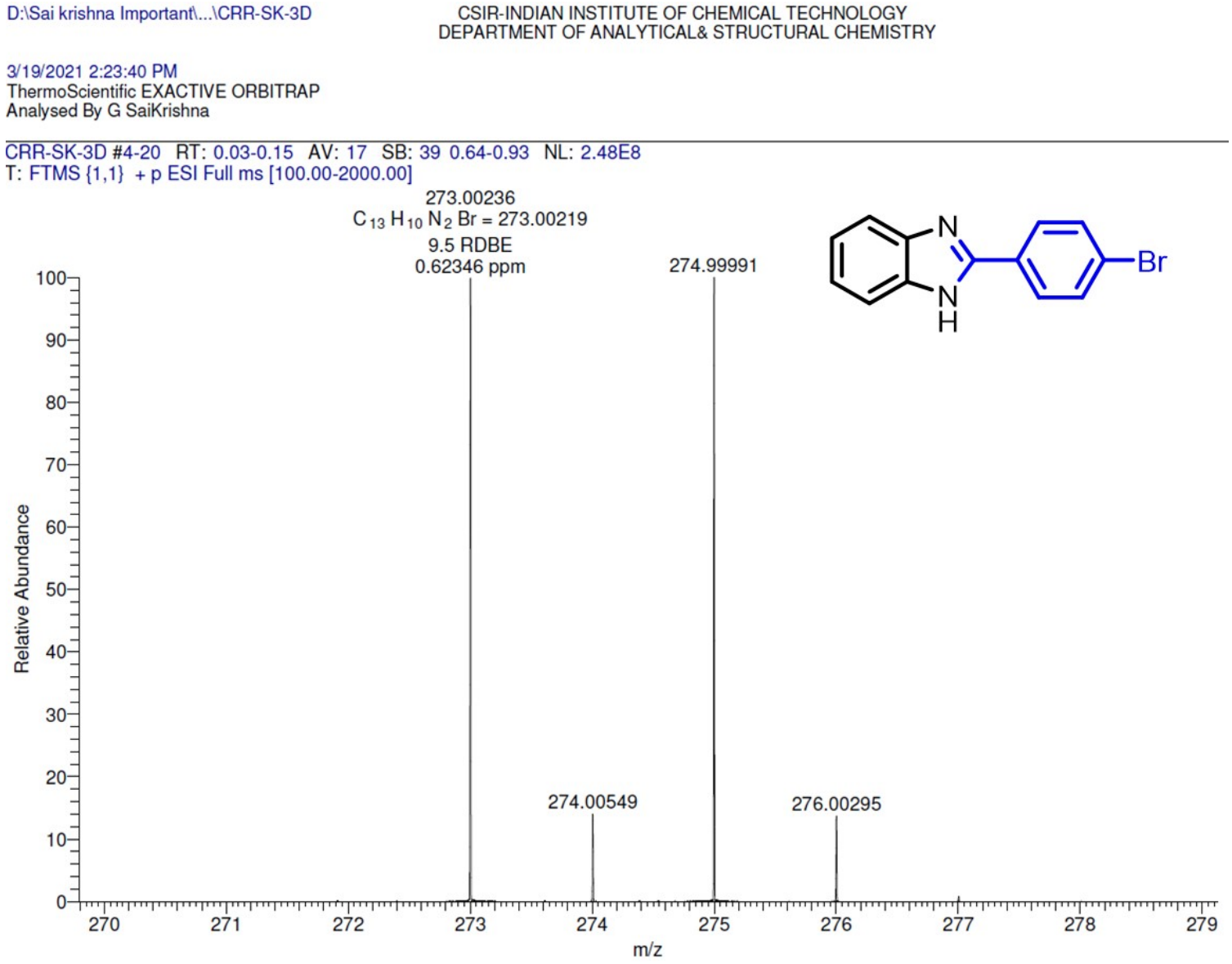

Fig. S27. HRMS spectra of 2-(4-bromophenyl)-1H-benzo[d]imidazole **(3d)**.

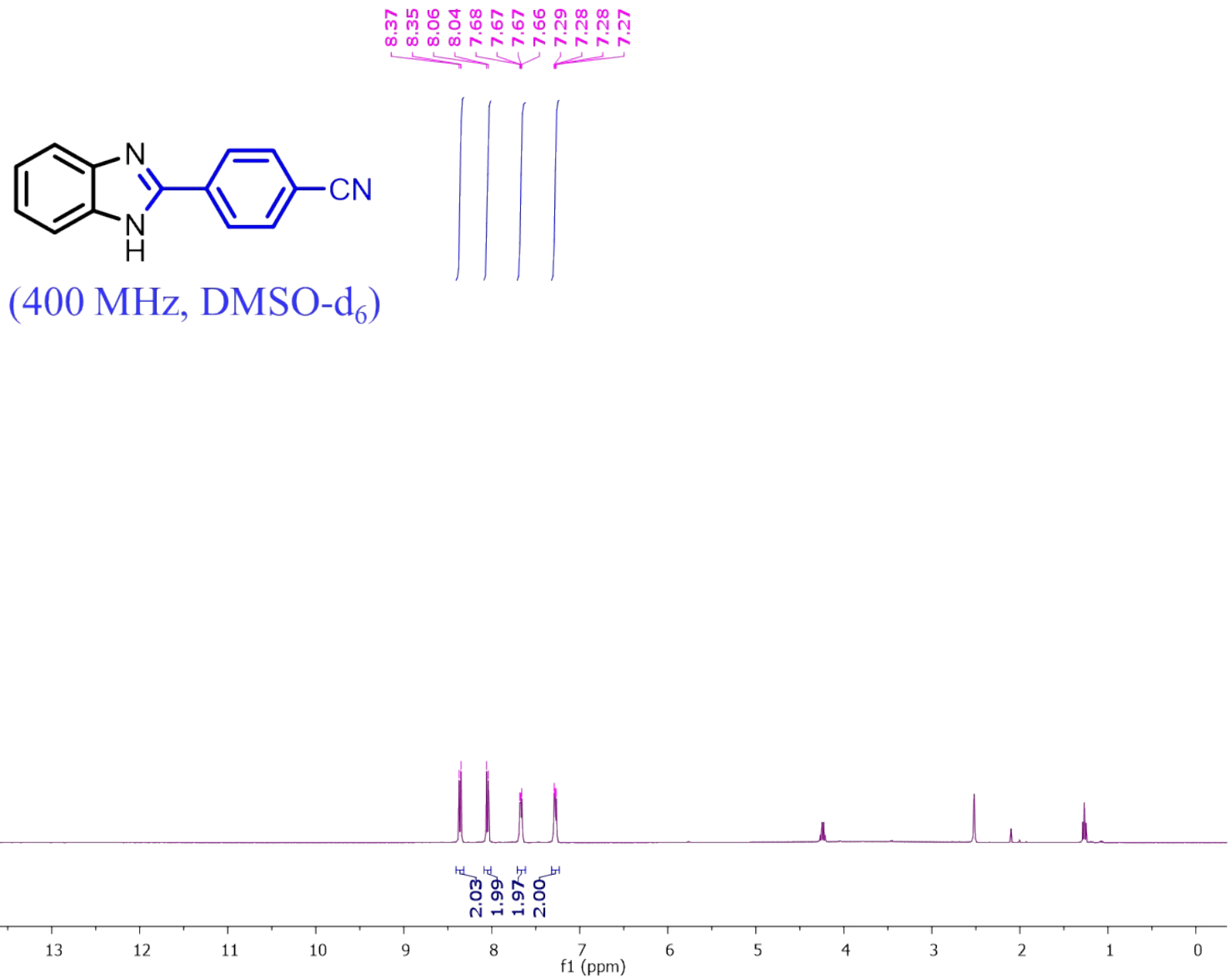

Fig. S28. [1]H NMR spectra of 4-(1H-benzo[d]imidazol-2-yl) benzonitrile **(3e)** in DMSO-d_6.

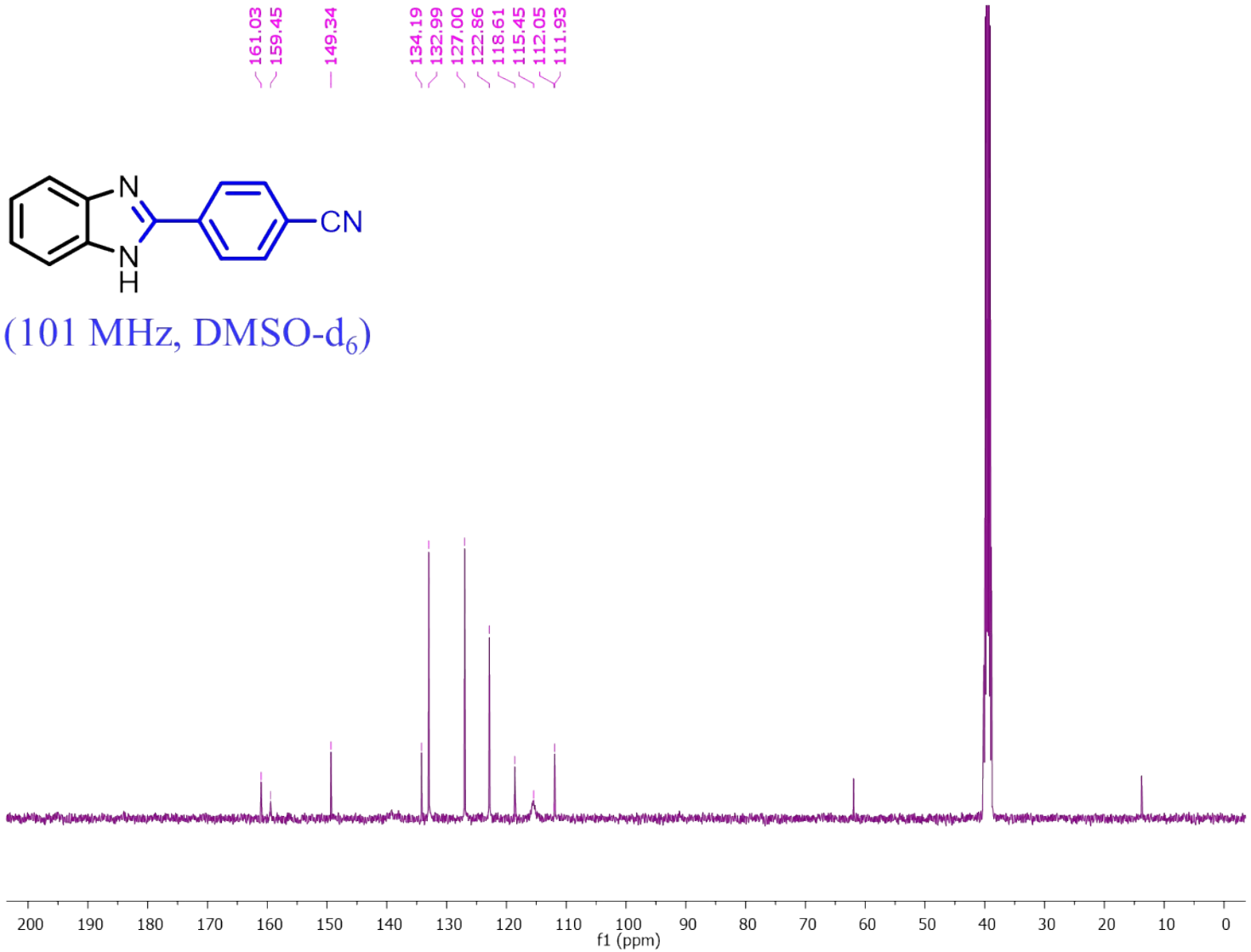

Fig. S29. ^{13}C NMR spectra of 4-(1H-benzo[d]imidazol-2-yl) benzonitrile **(3e)** in DMSO-d_6.

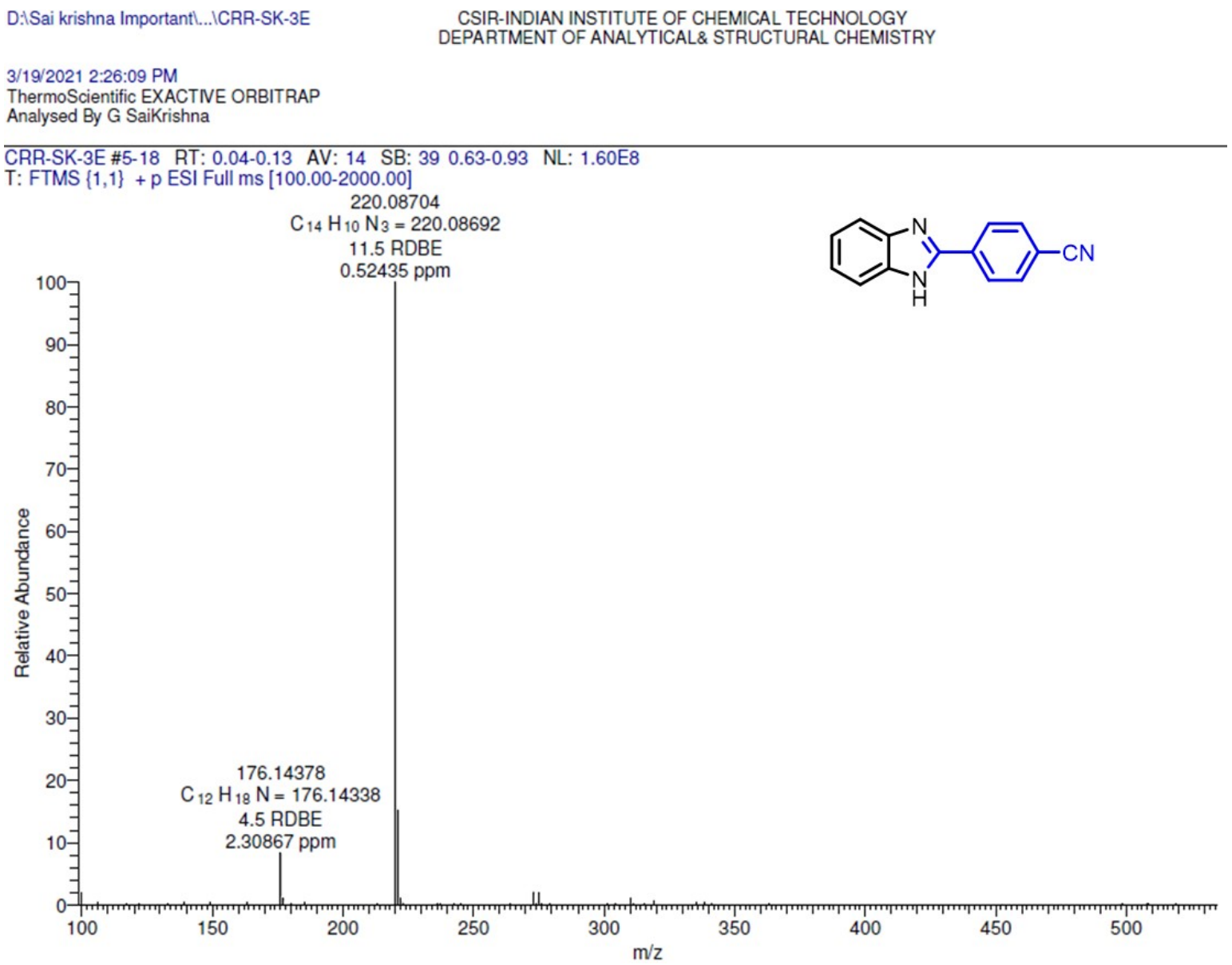

Fig. S30. HRMS spectra of 4-(1H-benzo[d]imidazol-2-yl) benzonitrile **(3e)**.

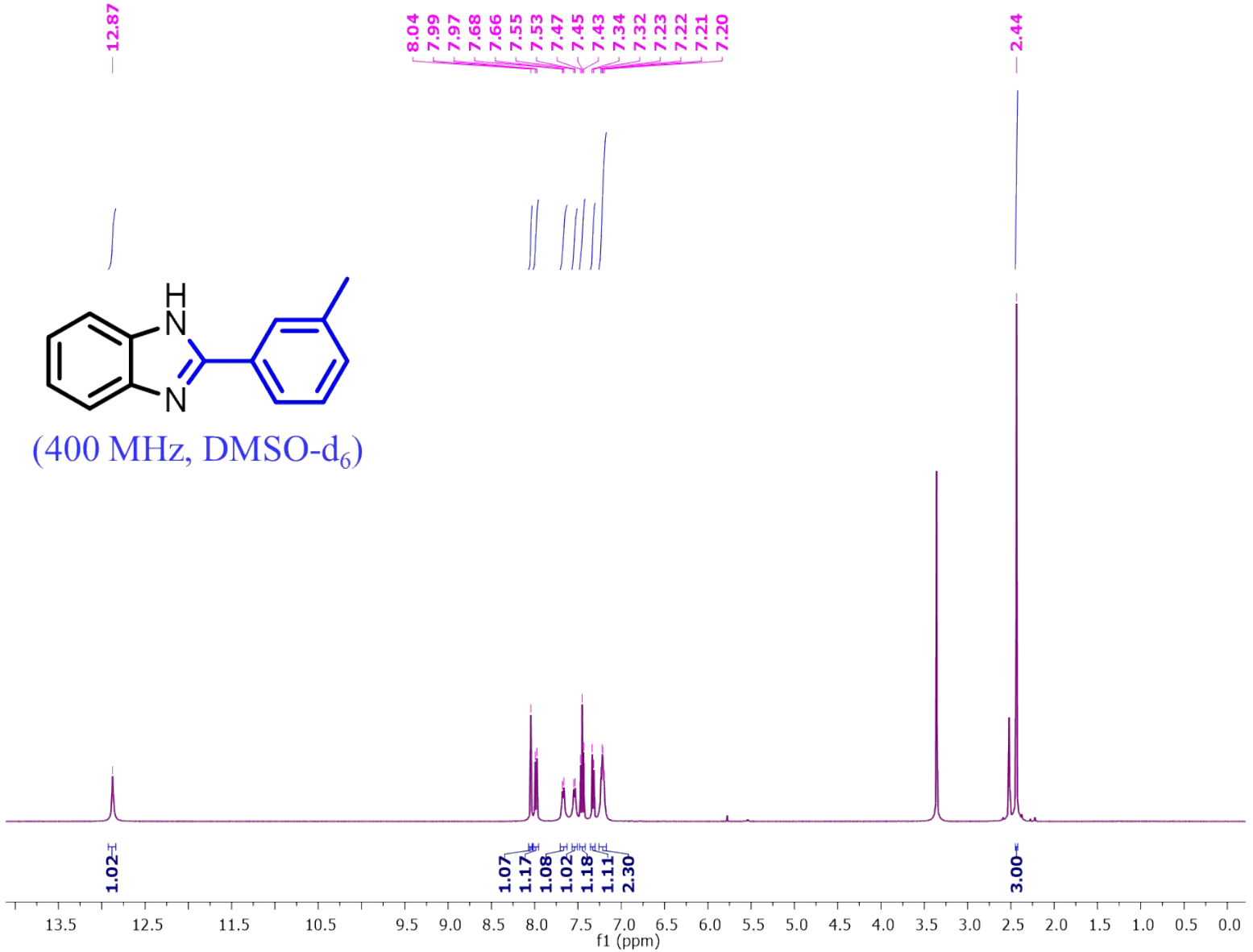

Fig. S31. [1]H NMR spectra of 2-(m-tolyl)-1H-benzo[d]imidazole (**3f)** in DMSO-d_6.

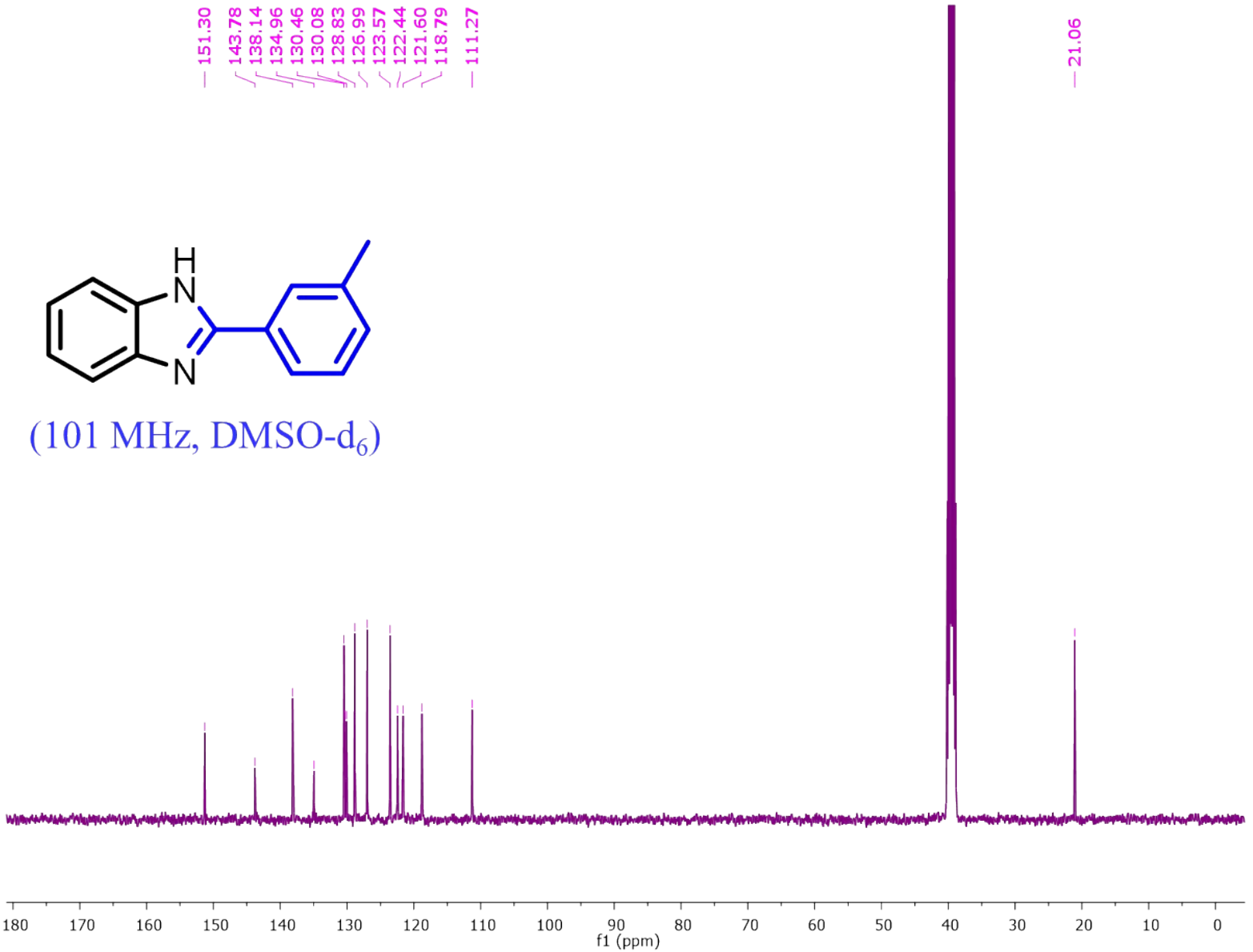

Fig. S32. ^{13}C NMR spectra of 2-(m-tolyl)-1H-benzo[d]imidazole (**3f**) in DMSO-d_6.

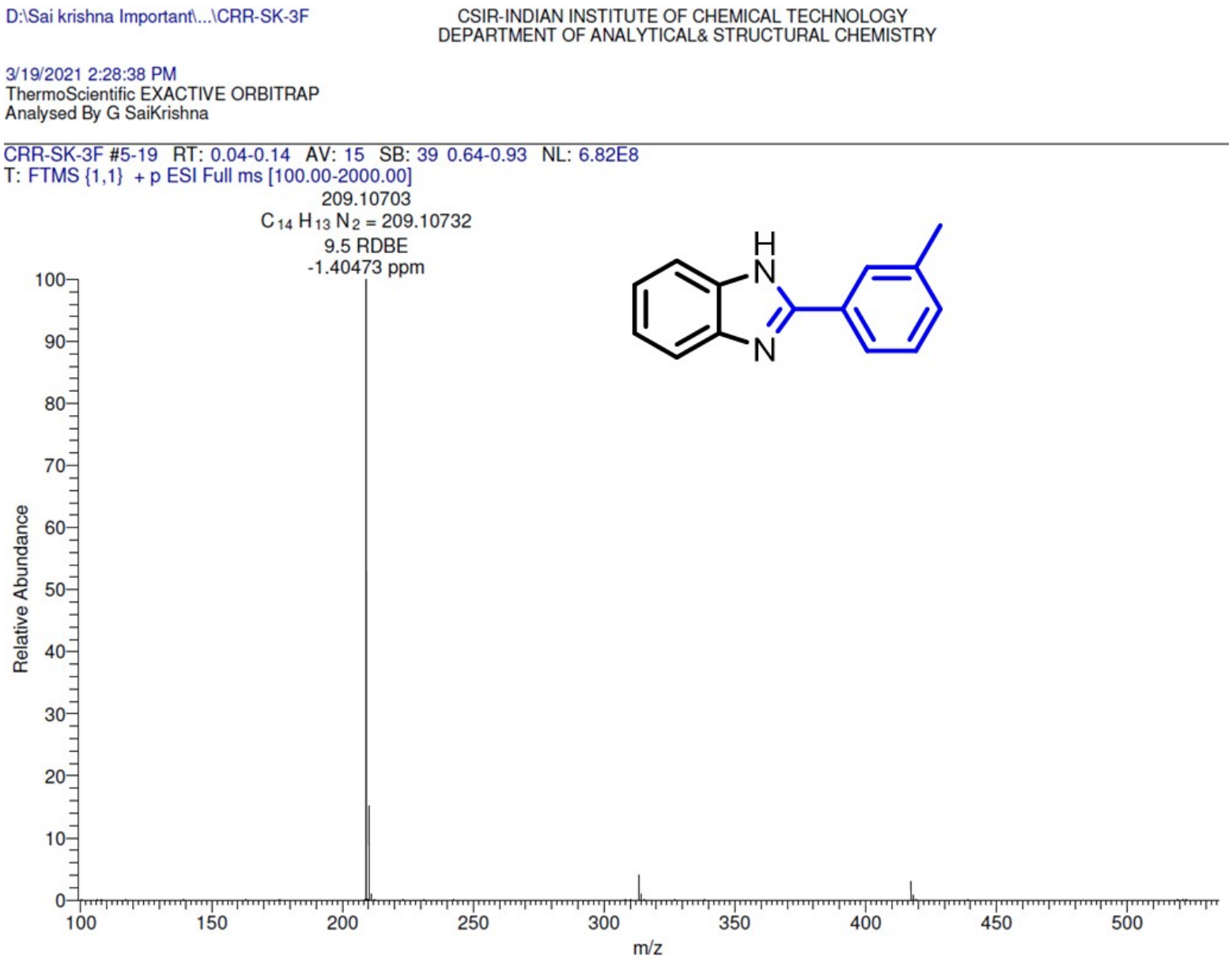

Fig. S33 HRMS spectra of 2-(m-tolyl)-1H-benzo[d]imidazole (**3f**).

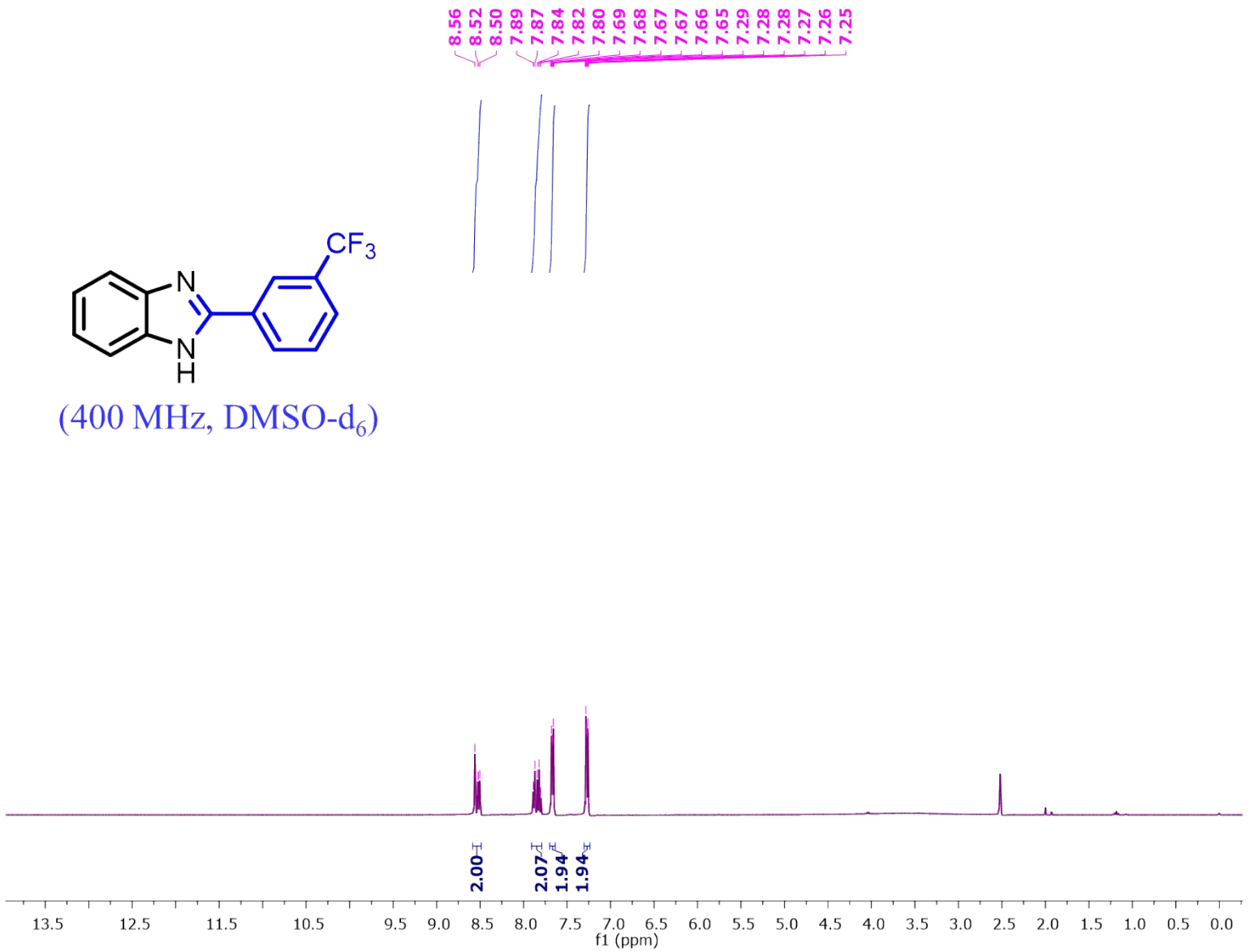

Fig. S34. [1]H NMR spectra of 2-(3-(trifluoromethyl) phenyl)-1H-benzo[d]imidazole (**3g**) in DMSO-d_6.

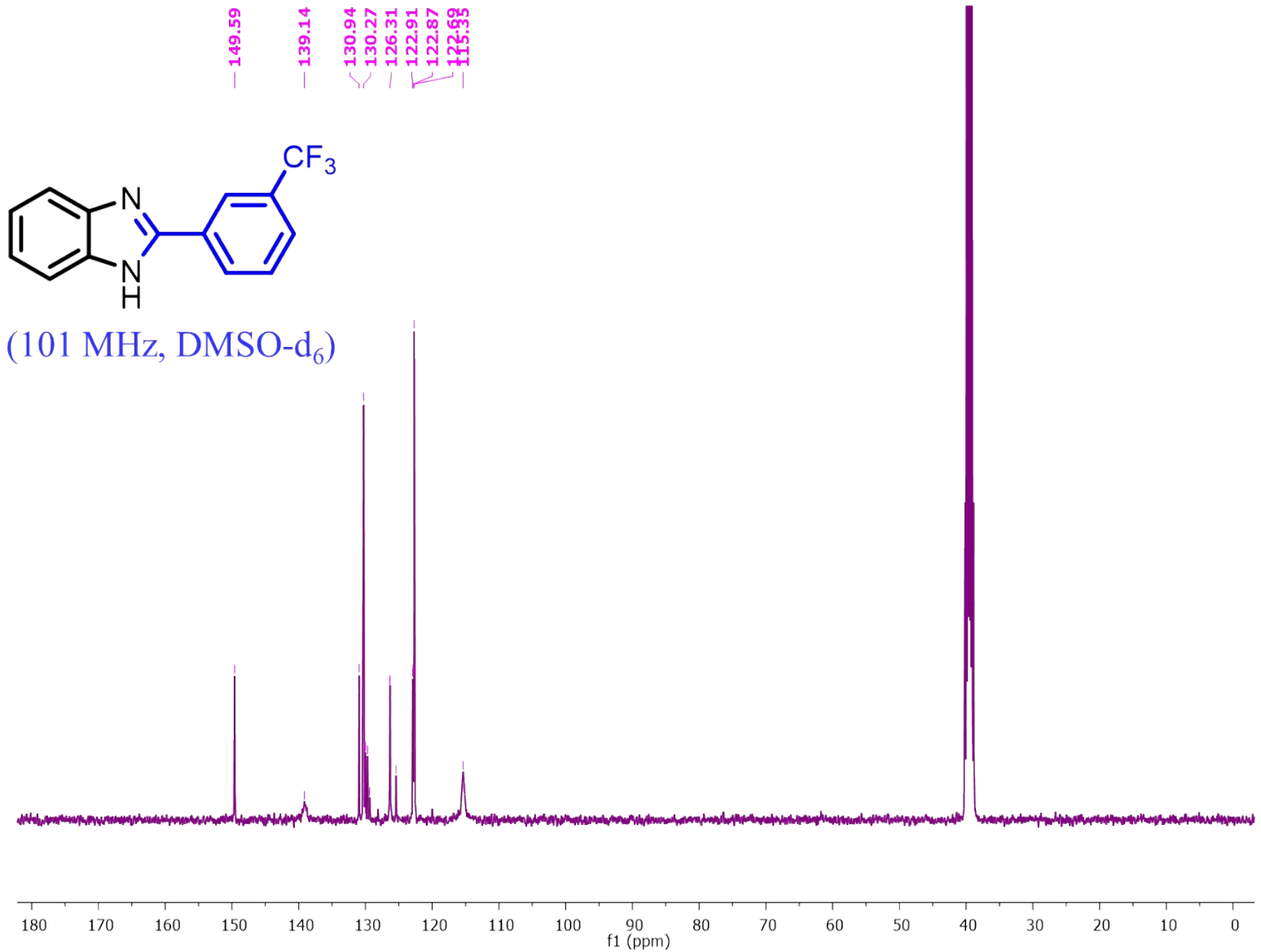

Fig. S35. ^{13}C NMR spectra of 2-(3-(trifluoromethyl) phenyl)-1H-benzo[d]imidazole (**3g**) in DMSO-d_6.

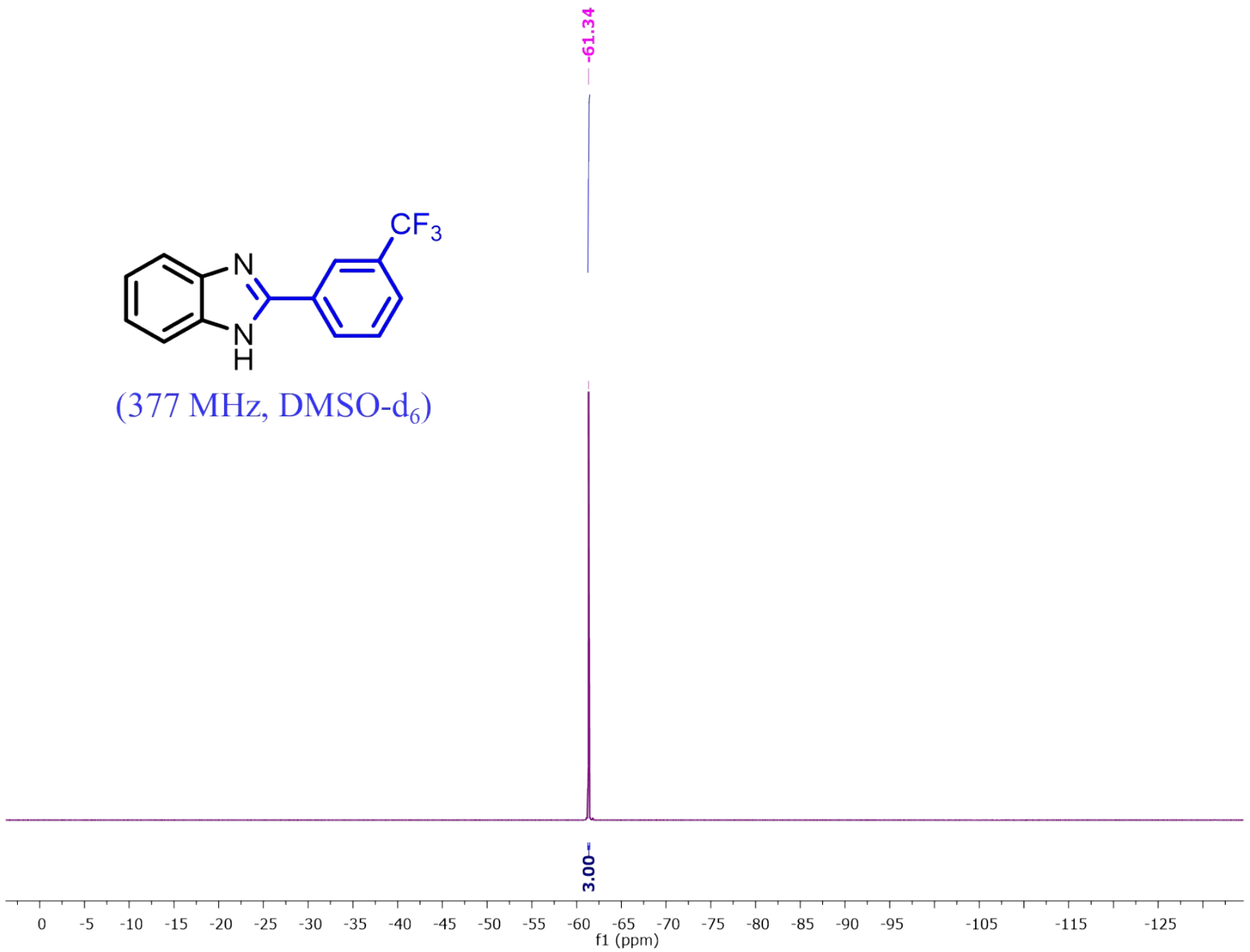

Fig. S36. ^{19}F NMR spectra of 2-(3-(trifluoromethyl) phenyl)-1H-benzo[d]imidazole (**3g**) in DMSO-d_6.

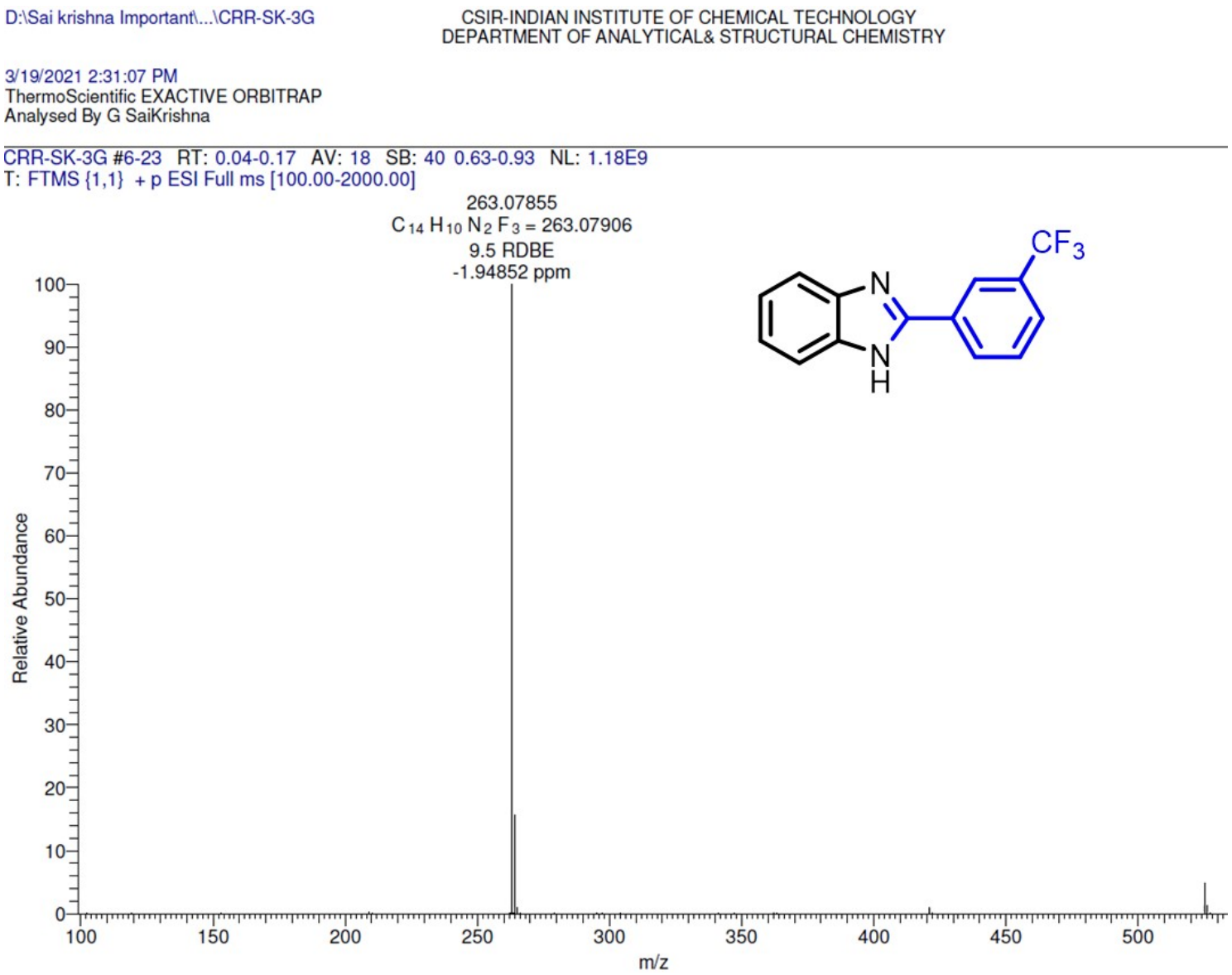

Fig. S37. HRMS spectra of 2-(3-(trifluoromethyl) phenyl)-1H-benzo[d]imidazole (**3g**).

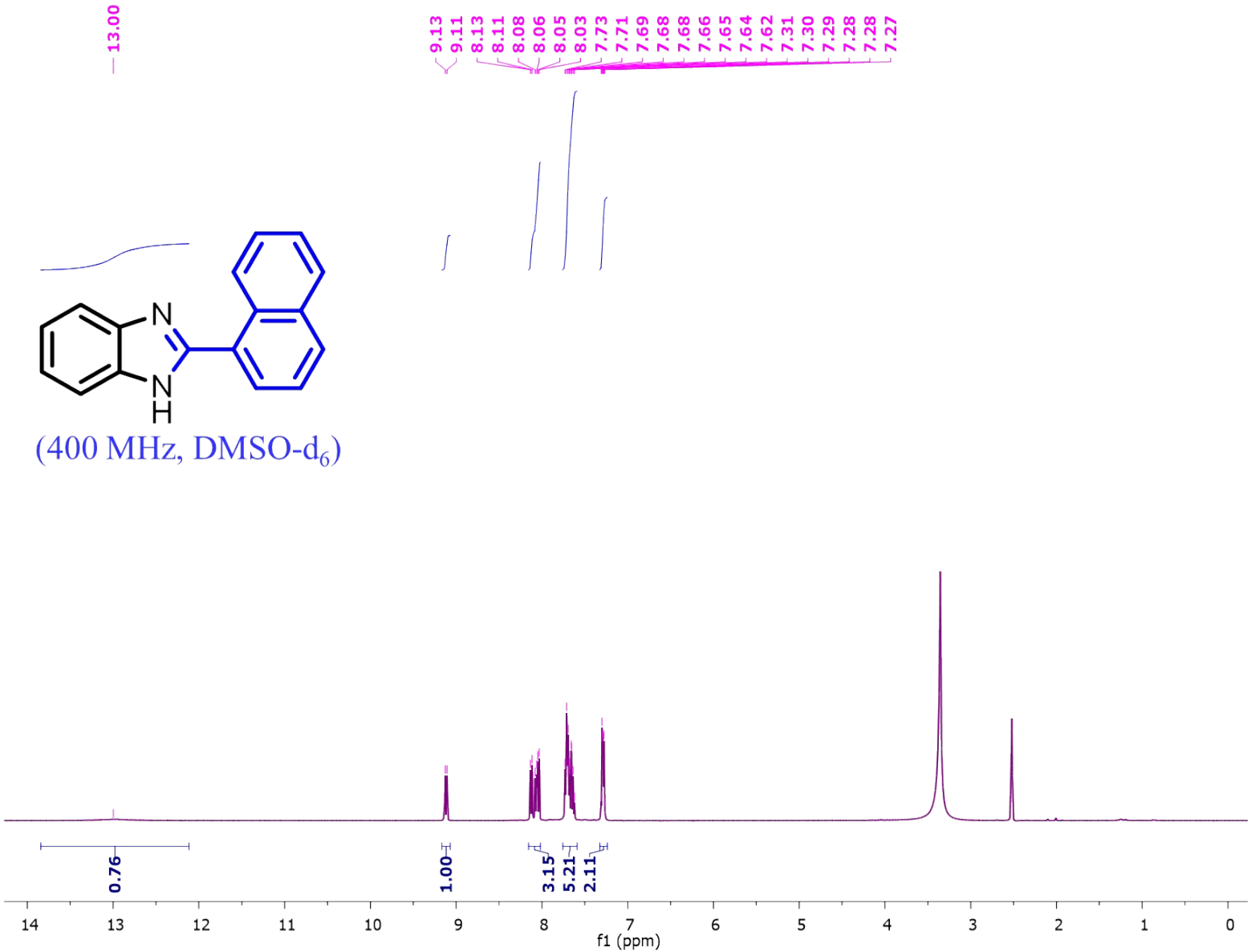

Fig. S38. [1]H NMR spectra of 2-(naphthalen-1-yl)-1H-benzo[d]imidazole (**3h**) in DMSO-d_6.

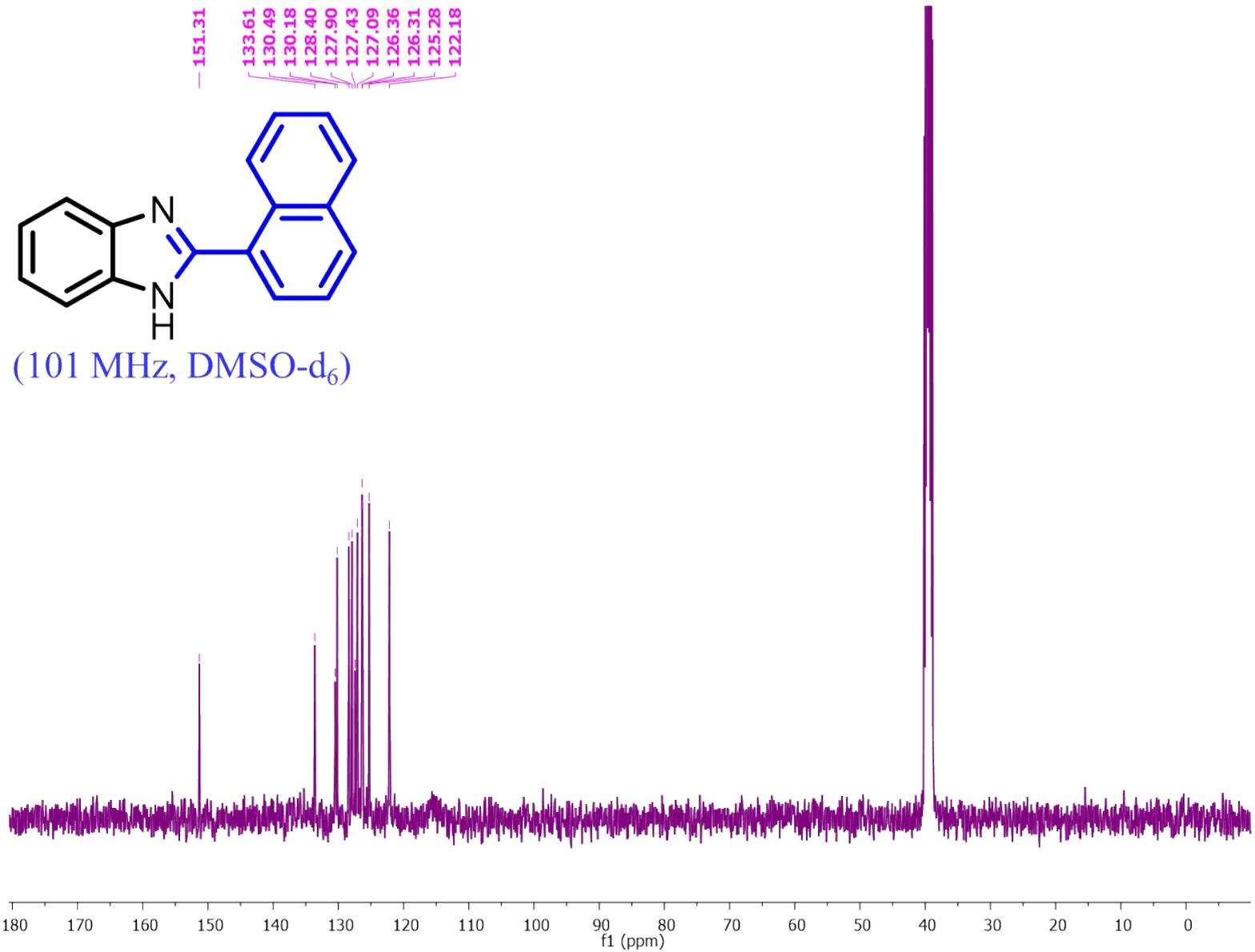

Fig. S39. ^{13}C NMR spectra of 2-(naphthalen-1-yl)-1H-benzo[d]imidazole (**3h**) in DMSO-d_6.

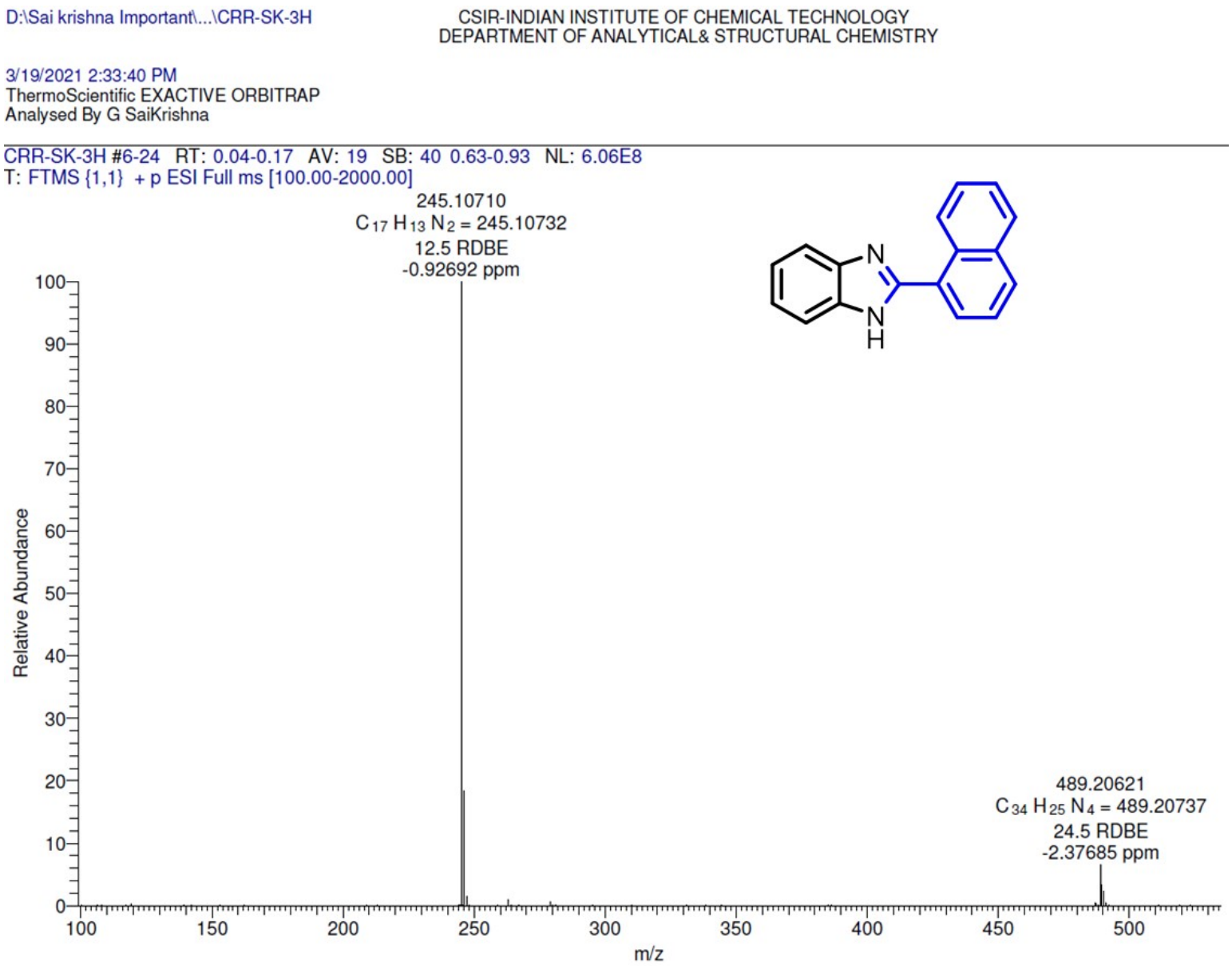

Fig. S40. HRMS spectra of 2-(naphthalen-1-yl)-1H-benzo[d]imidazole (**3h**).

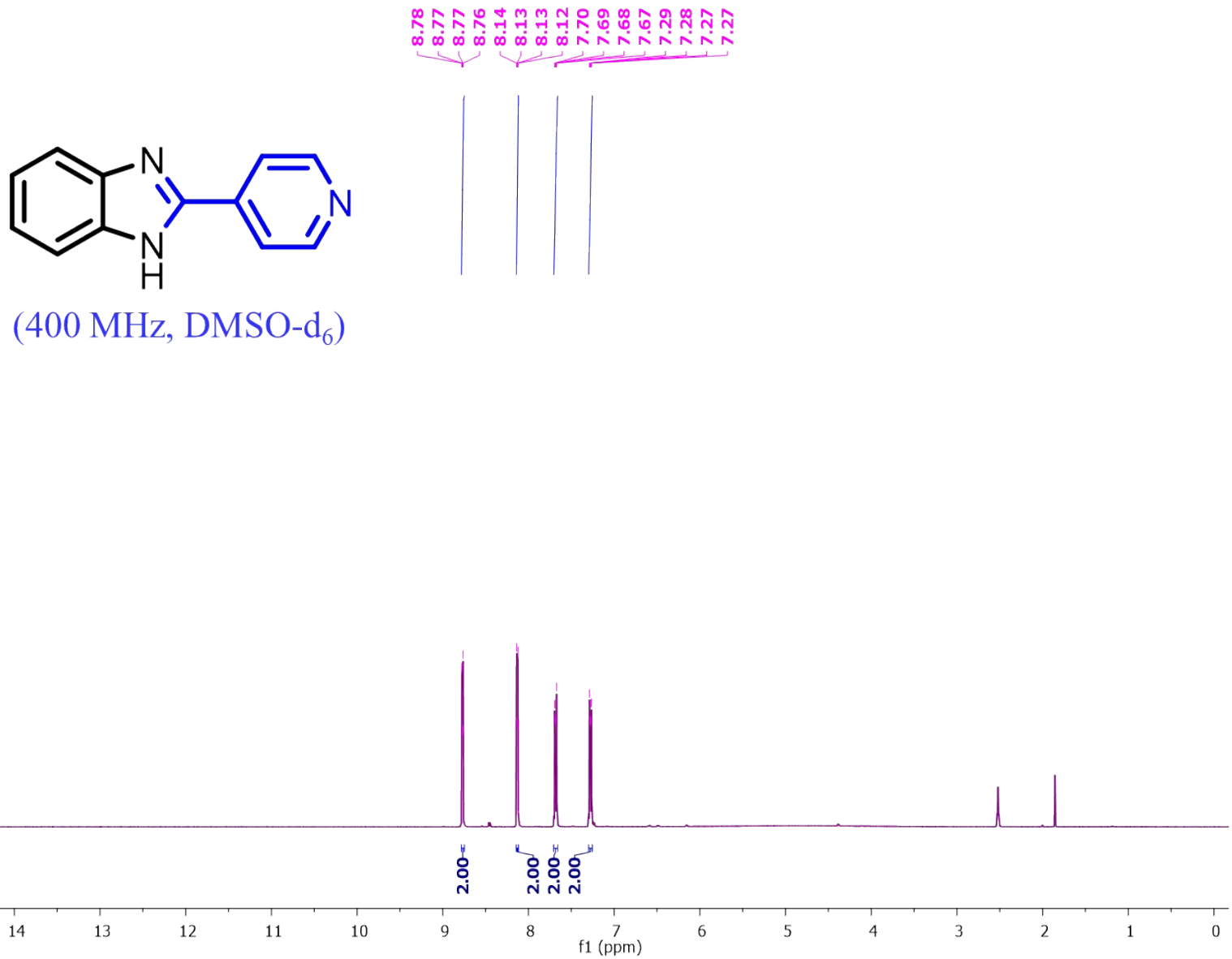

Fig. S41. [1]H NMR spectra of 2-(pyridin-4-yl)-1H-benzo[d]imidazole (**3i**) in DMSO-d_6.

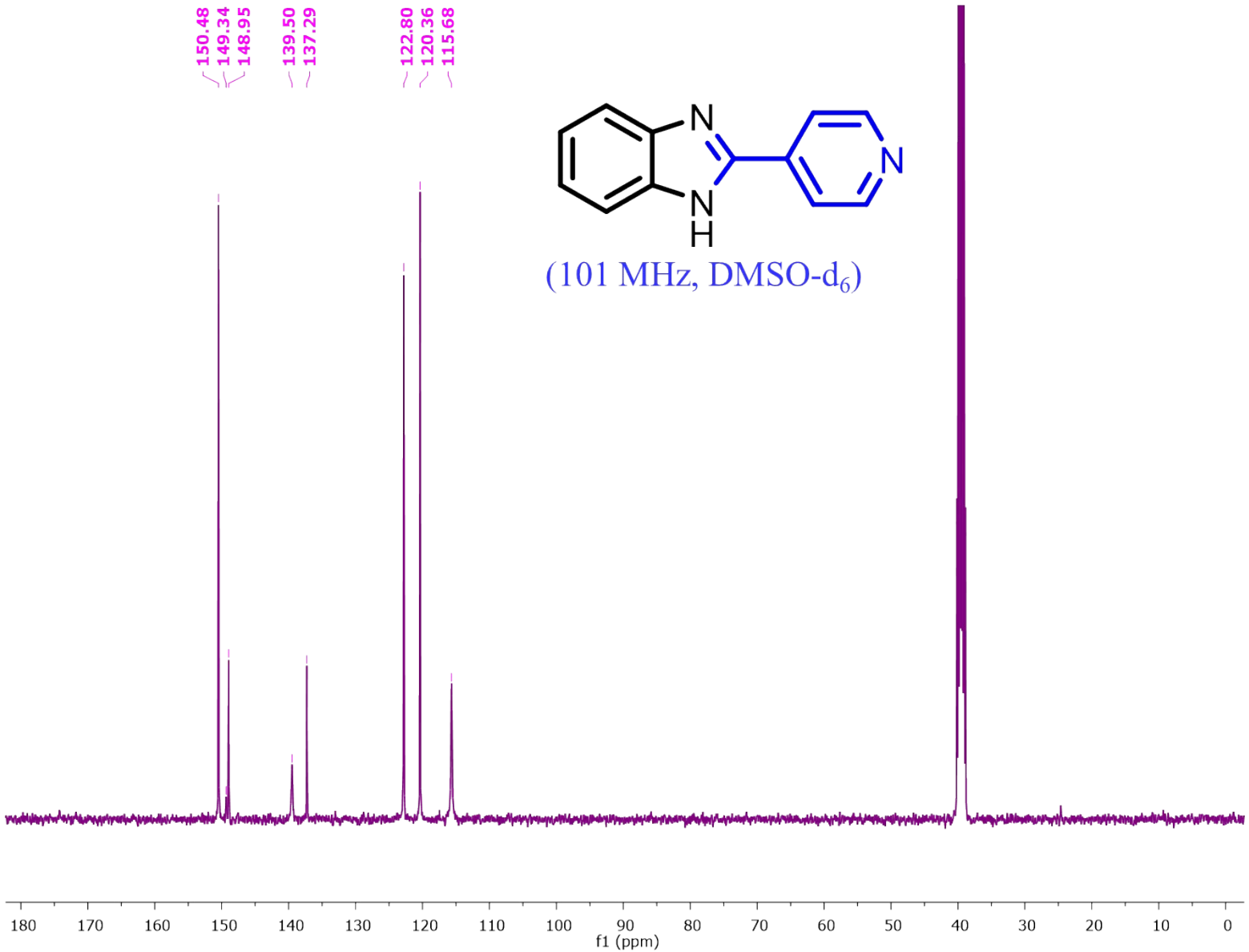

Fig. S42. ^{13}C NMR spectra of 2-(pyridin-4-yl)-1H-benzo[d]imidazole (**3i**) in DMSO-d_6.

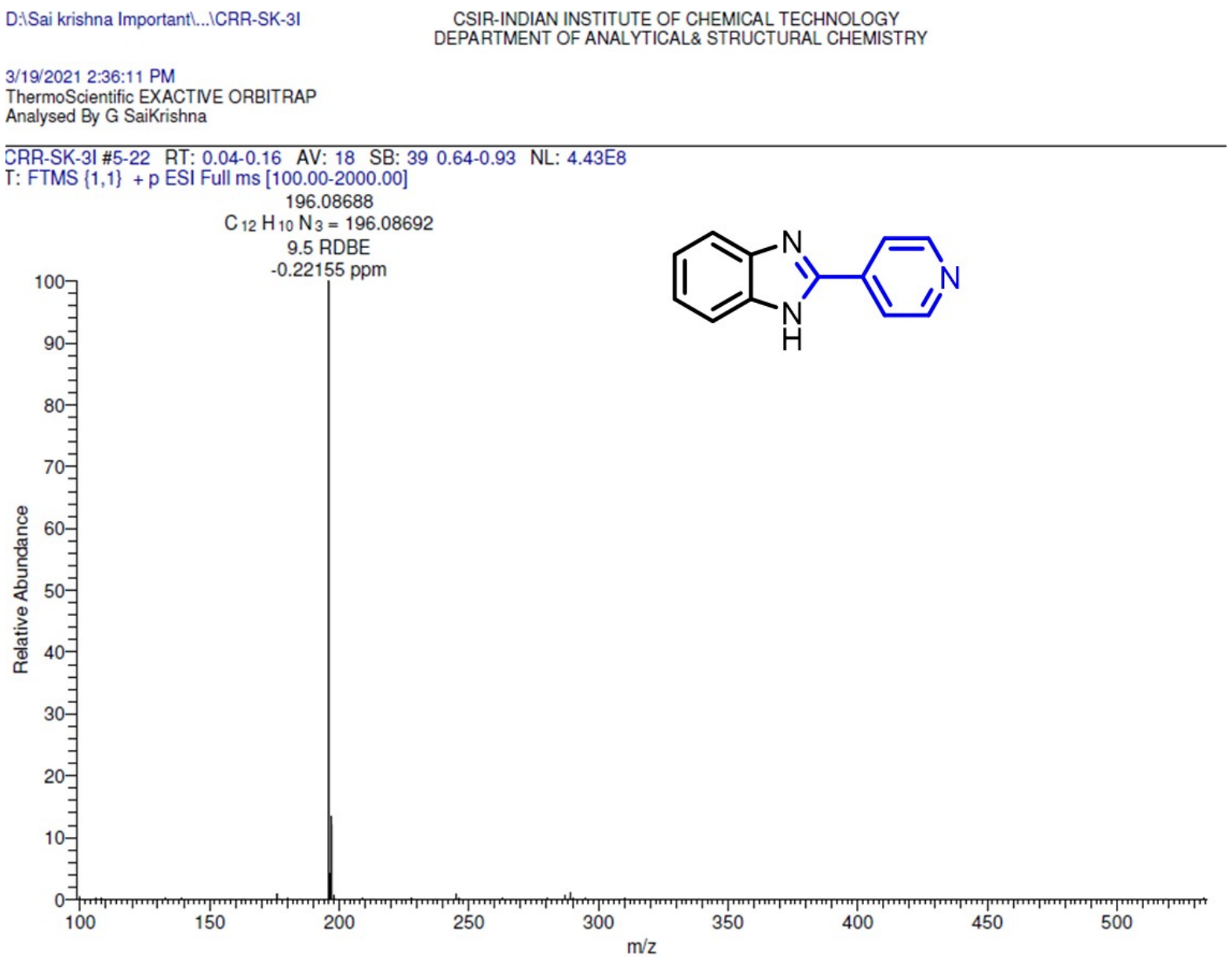

Fig. S43. HRMS spectra of 2-(pyridin-4-yl)-1H-benzo[d]imidazole (**3i**).

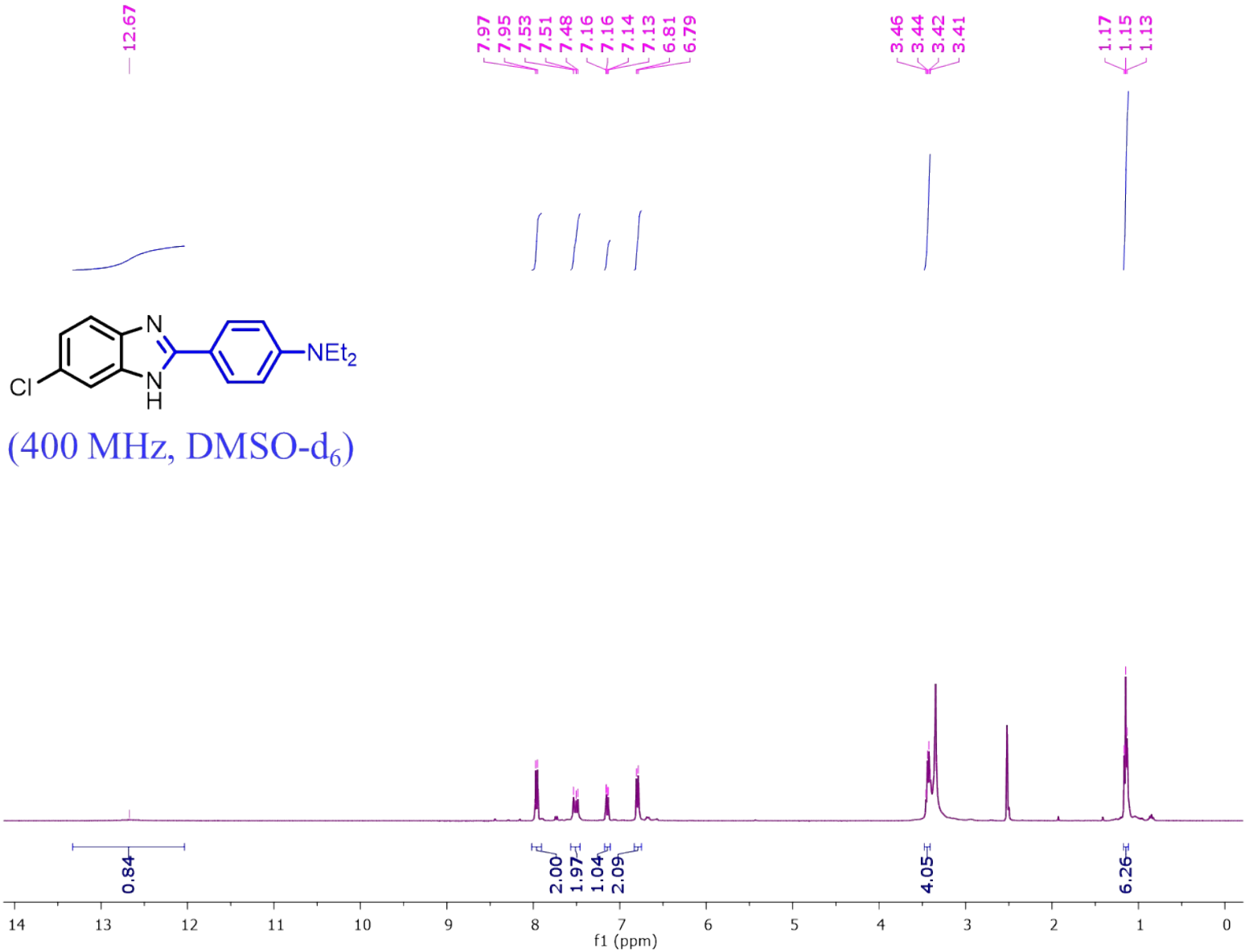

Fig. S44. [1]H NMR spectra of 4-(6-chloro-1H-benzo[d]imidazol-2-yl)-N, N-diethyl aniline (**3j**) in DMSO-*d*$_6$.

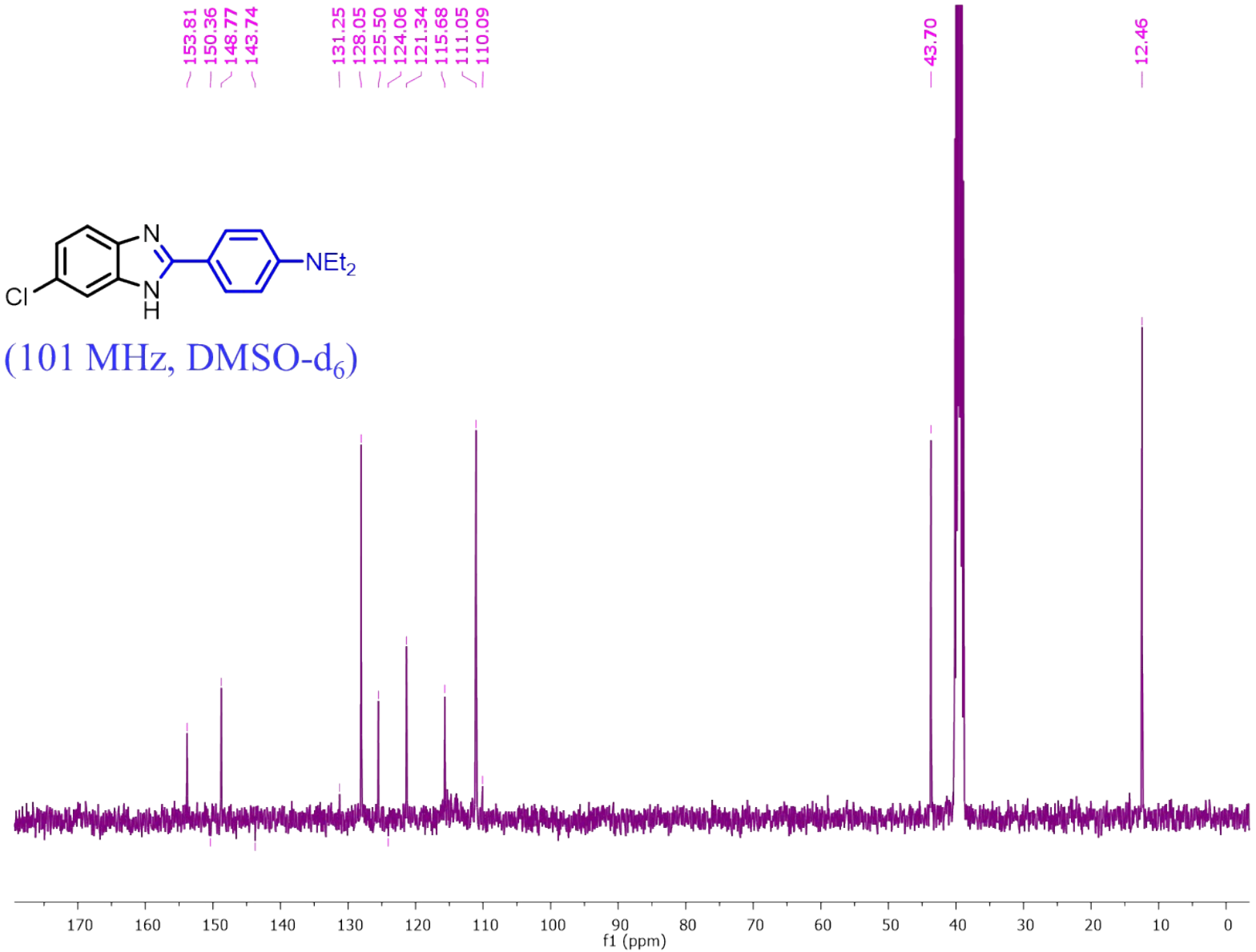

Fig. S45. ^{13}C NMR spectra of 4-(6-chloro-1H-benzo[d]imidazol-2-yl)-N, N-diethyl aniline (**3j**) in DMSO-d_6.

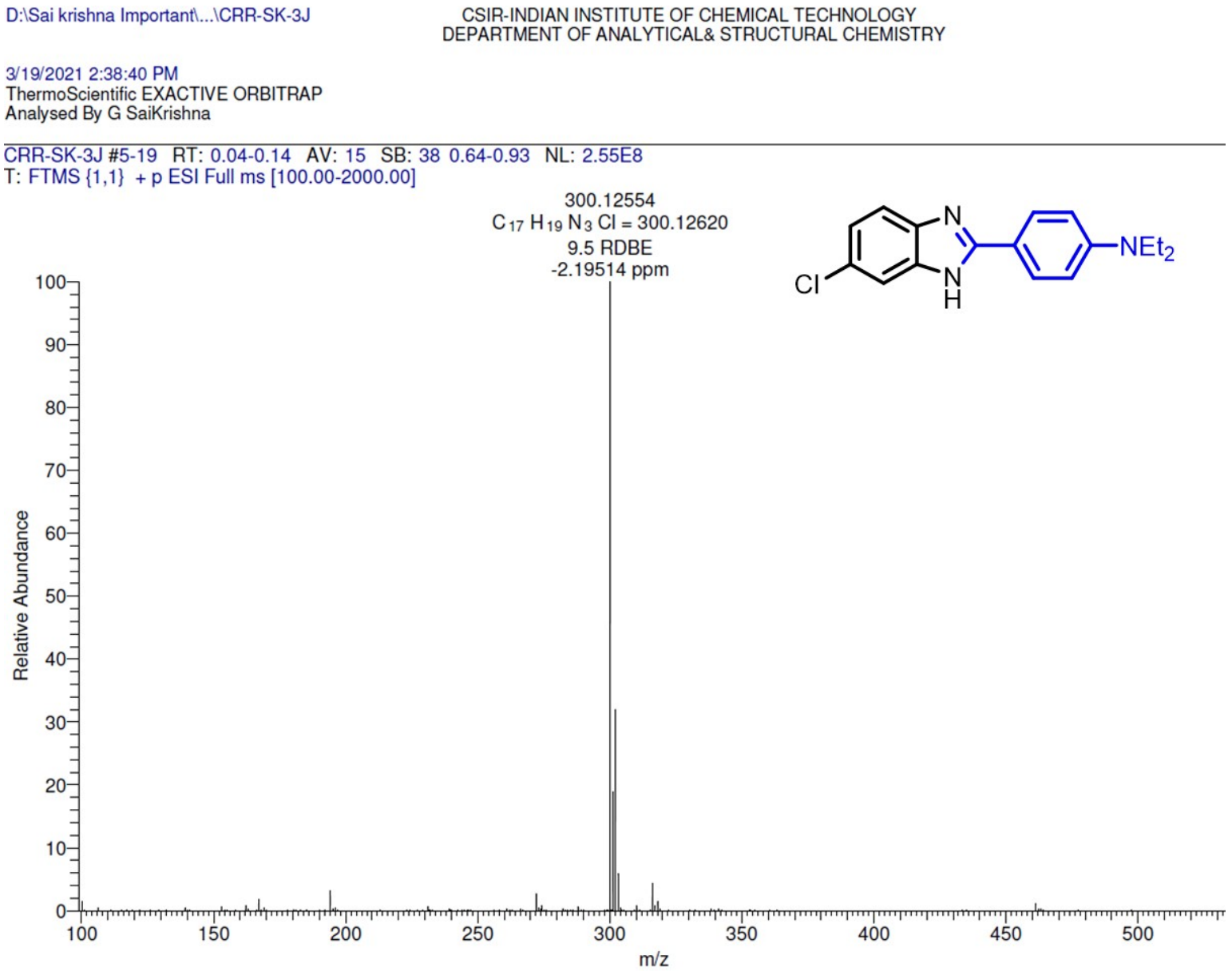

Fig. S46. HRMS spectra of 4-(6-chloro-1H-benzo[d]imidazol-2-yl)-N, N-diethyl aniline (**3j**).

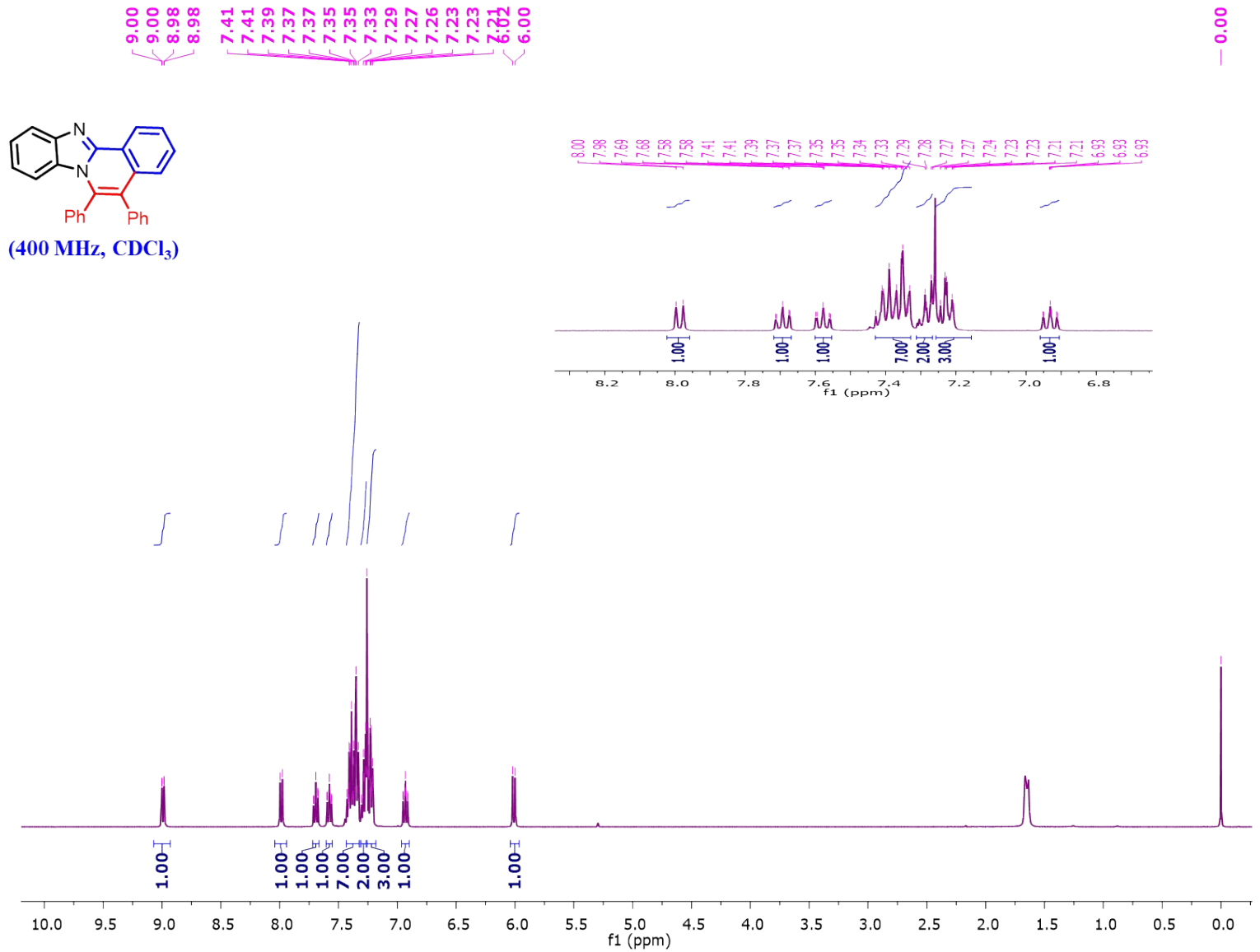

Fig. S47. ^{1}H NMR spectra of 5,6-diphenylbenzo[4,5]imidazo[2,1-a]isoquinoline (**5a**) in $CDCl_3$.

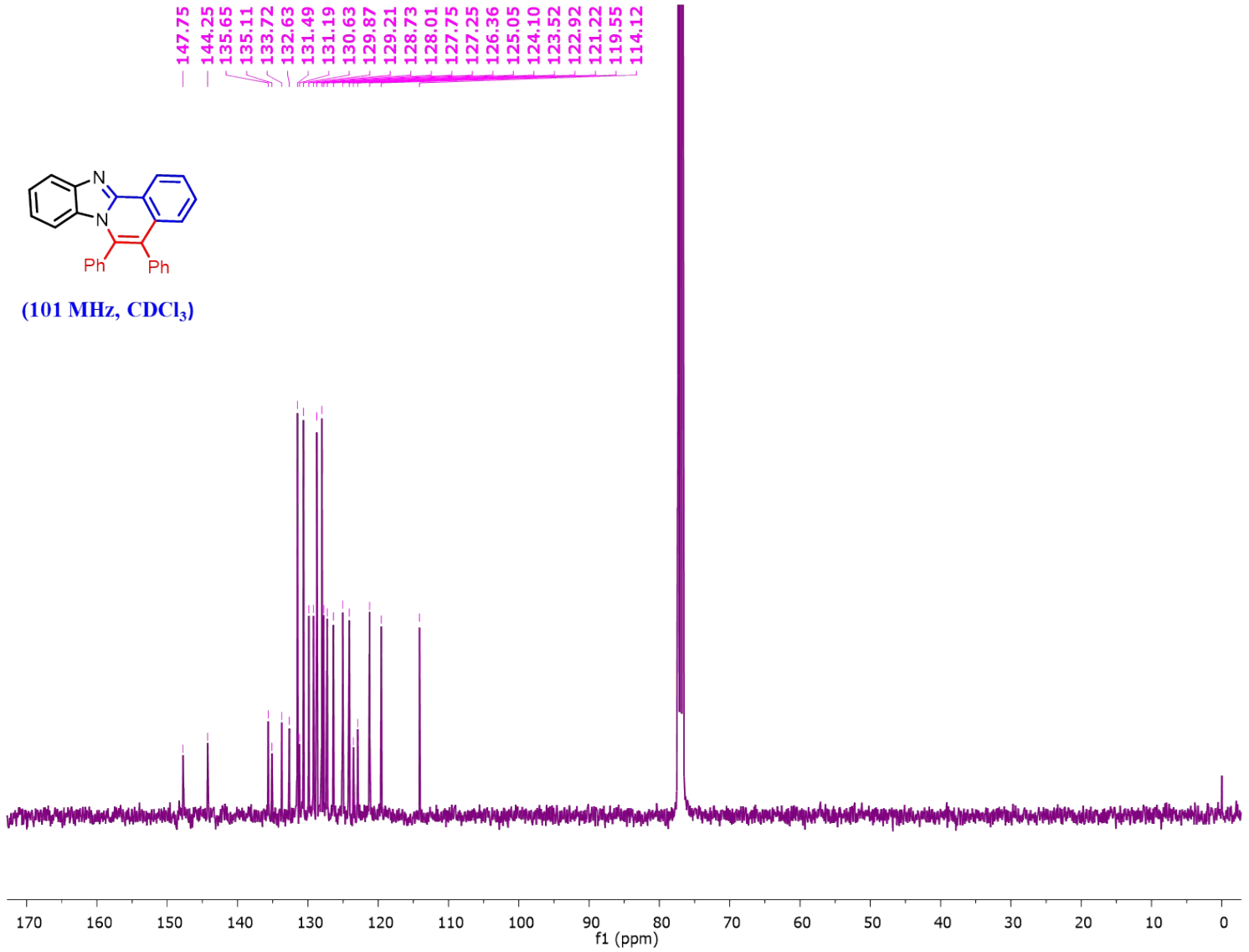

Fig. S48. ^{13}C NMR spectra of 5,6-diphenylbenzo [4,5] imidazo[2,1-a] isoquinoline (**5a**) in $CDCl_3$.

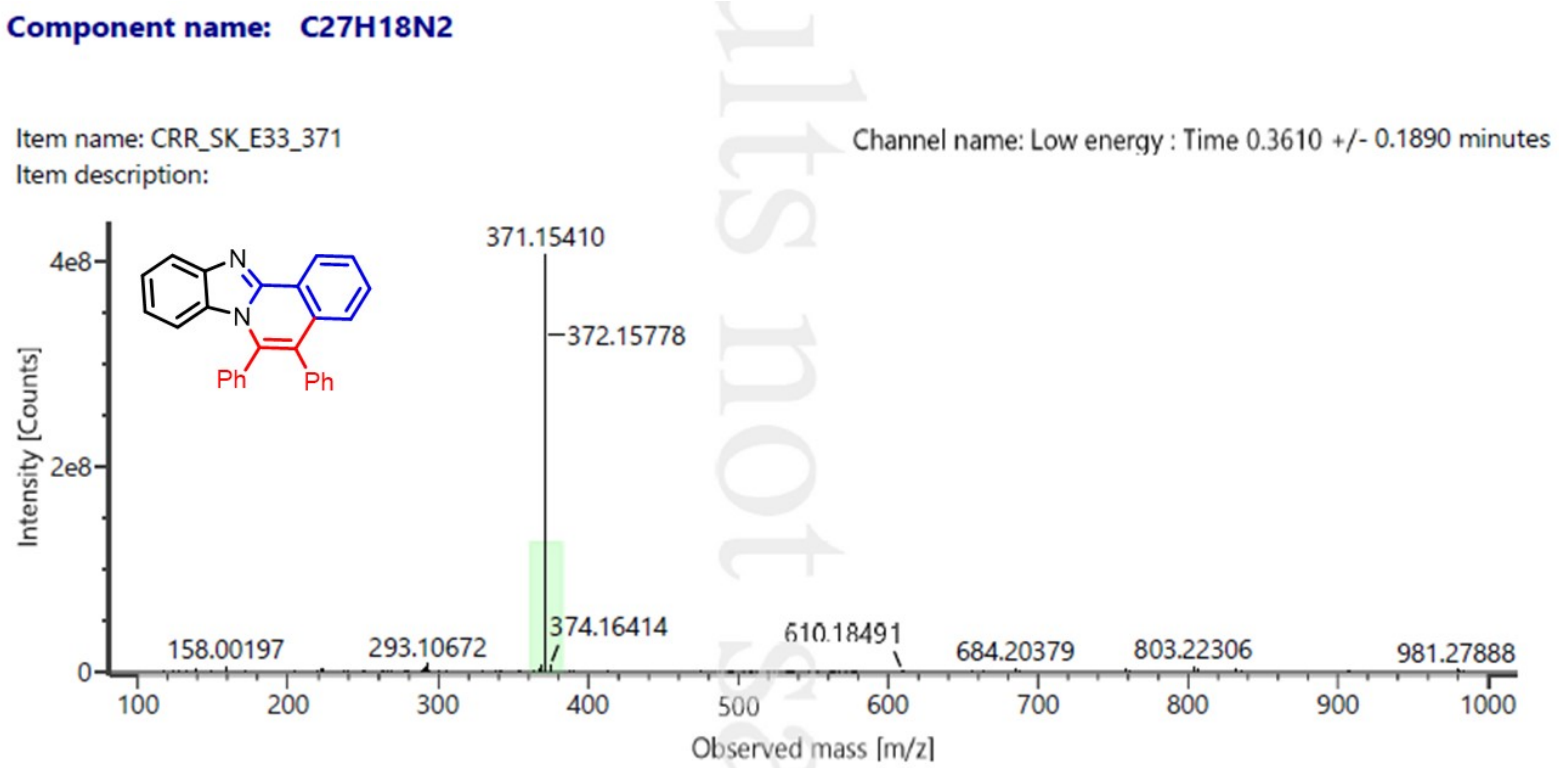

Fig. S49. HRMS spectra of 5,6-diphenylbenzo [4,5] imidazo[2,1-a] isoquinoline (**5a**).

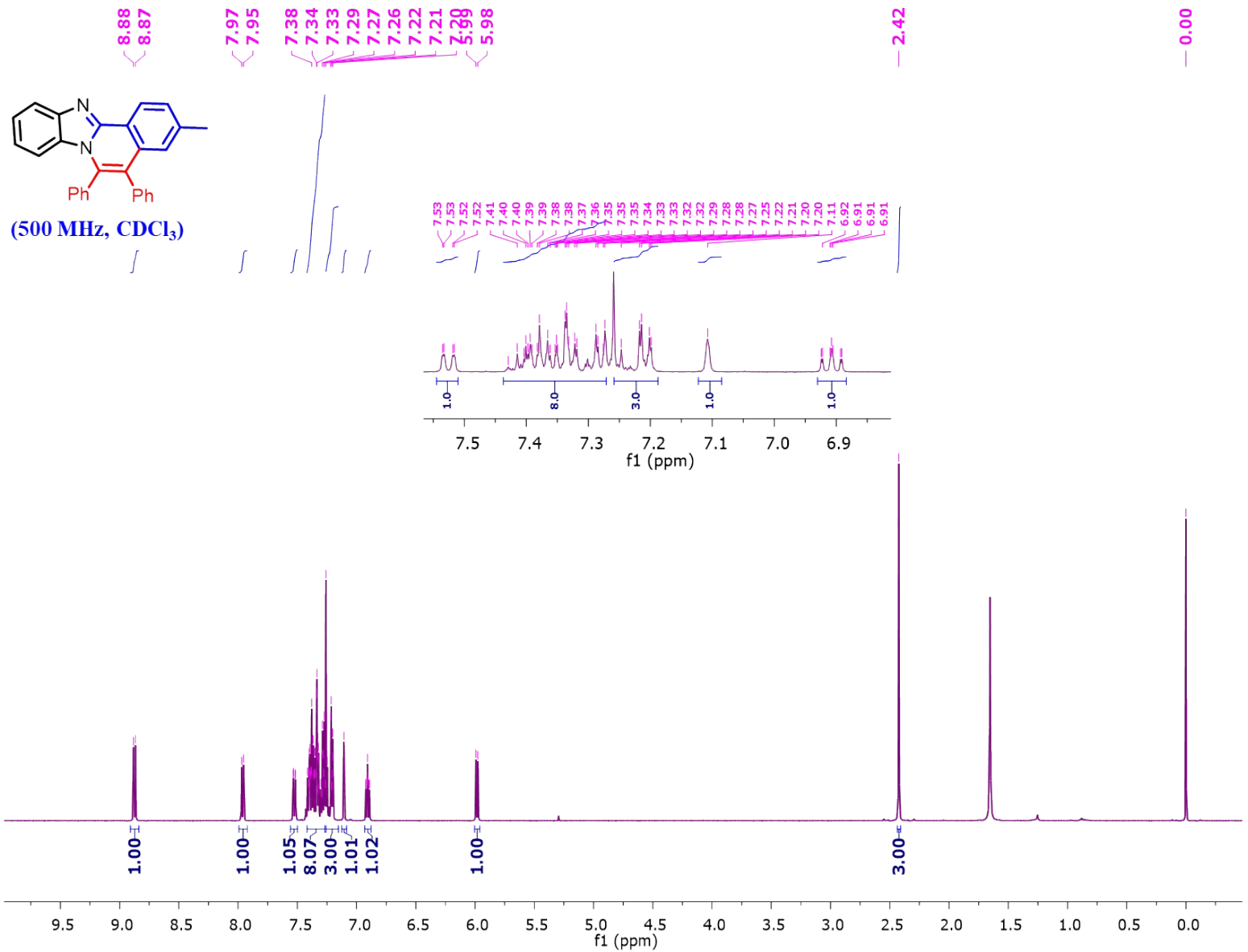

Fig. S50. ^{1}H NMR spectra of 3-methyl-5,6-diphenylbenzo [4,5] imidazo[2,1-a] isoquinoline (**5b**) in $CDCl_3$.

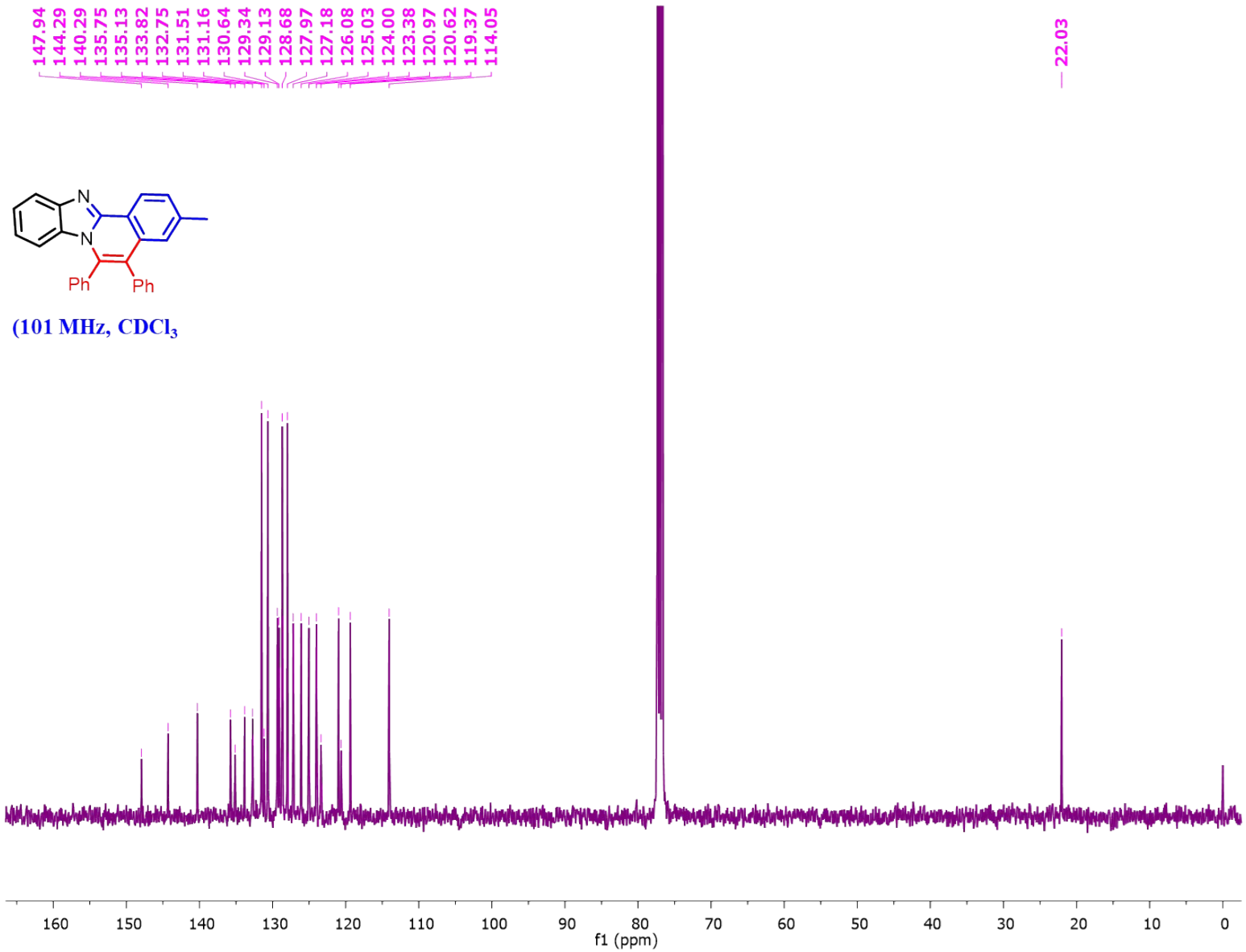

Fig. S51. ^{13}C NMR spectra of 3-methyl-5,6-diphenylbenzo [4,5] imidazo[2,1-a] isoquinoline (**5b**) in $CDCl_3$.

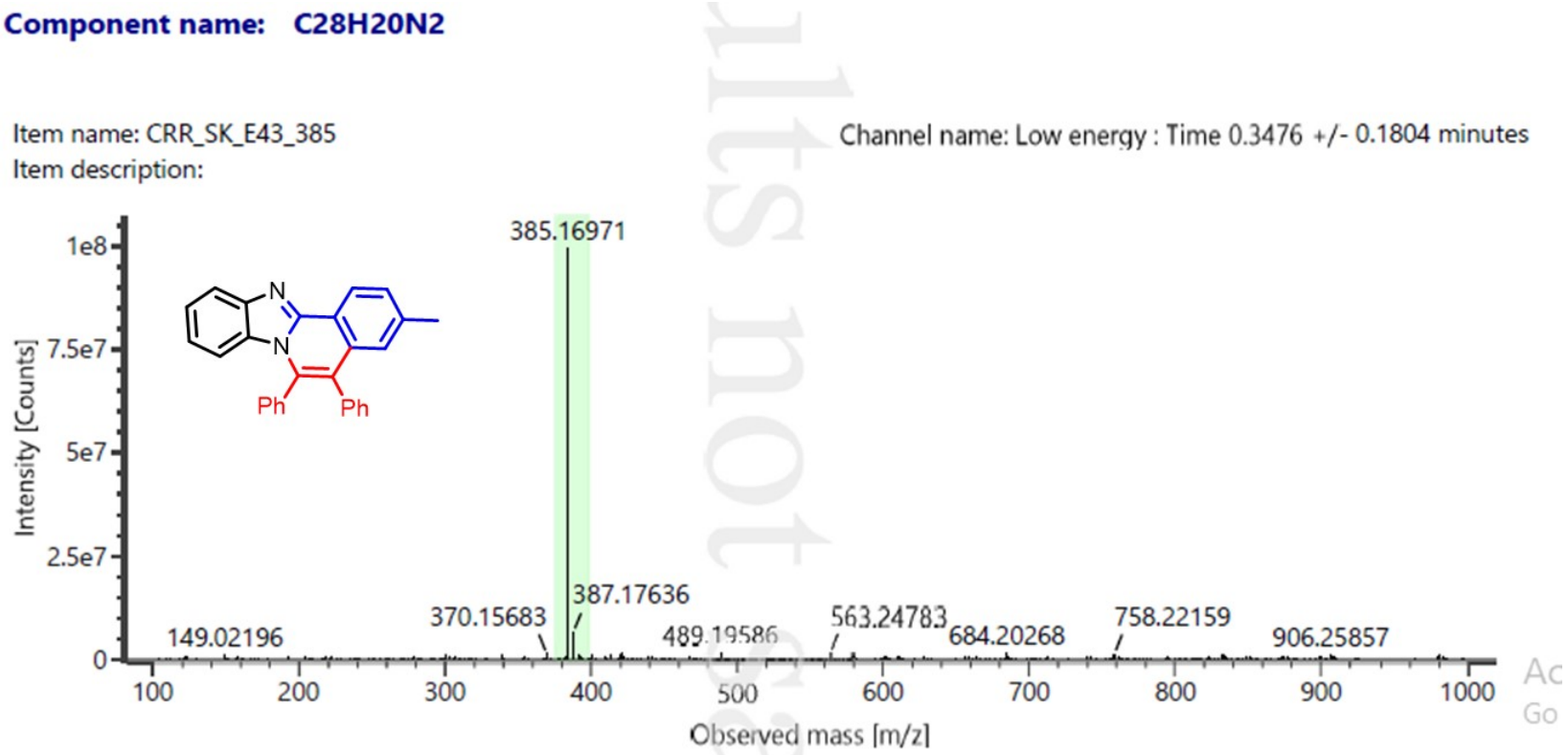

Fig. S52. HRMS spectra of 3-methyl-5,6-diphenylbenzo [4,5] imidazo[2,1-a] isoquinoline (**5b**).

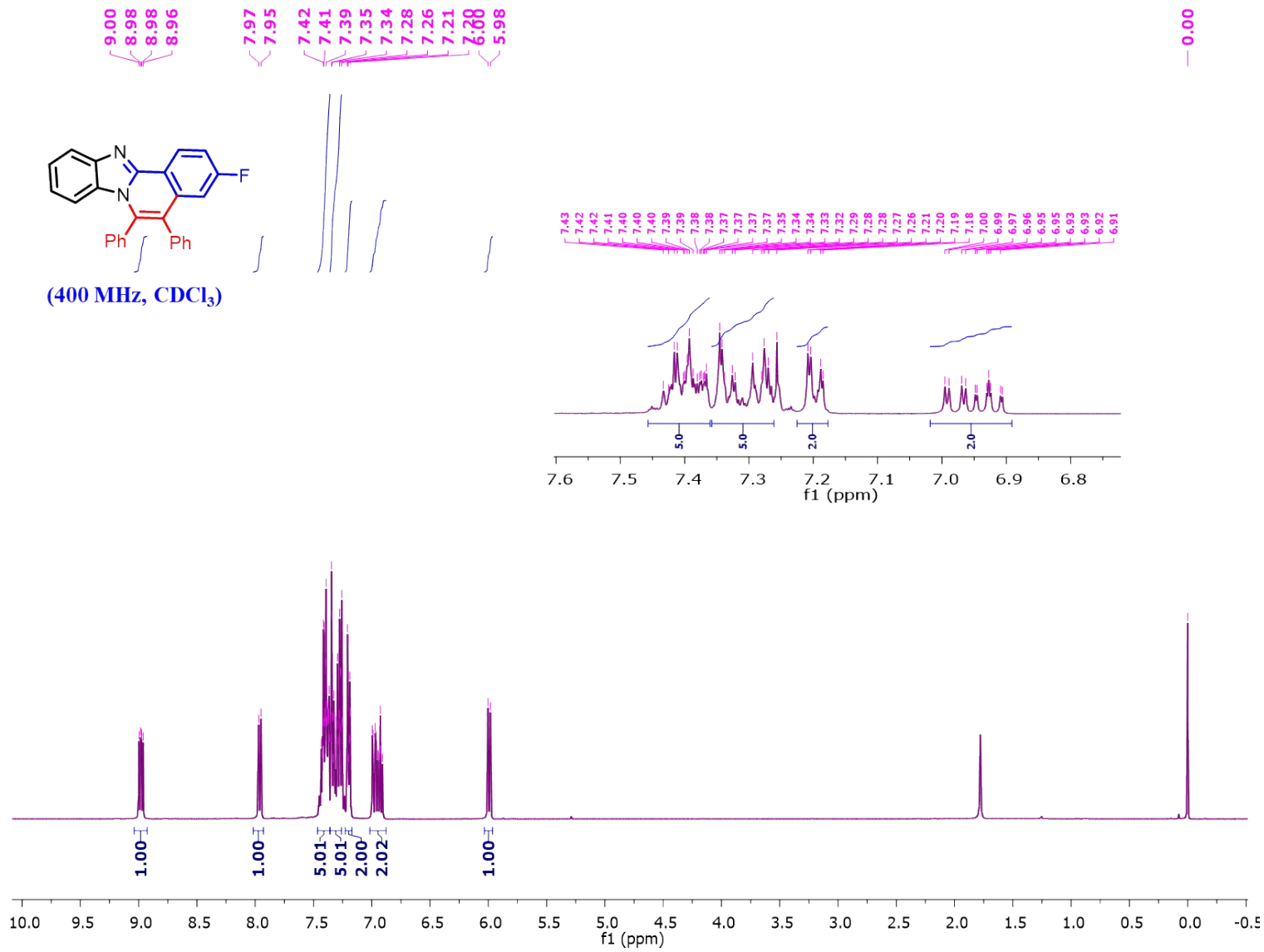

Fig. S53. ^{1}H NMR spectra of 3-fluoro-5,6-diphenylbenzo [4,5] imidazo[2,1-a] isoquinoline (**5c**) in $CDCl_3$.

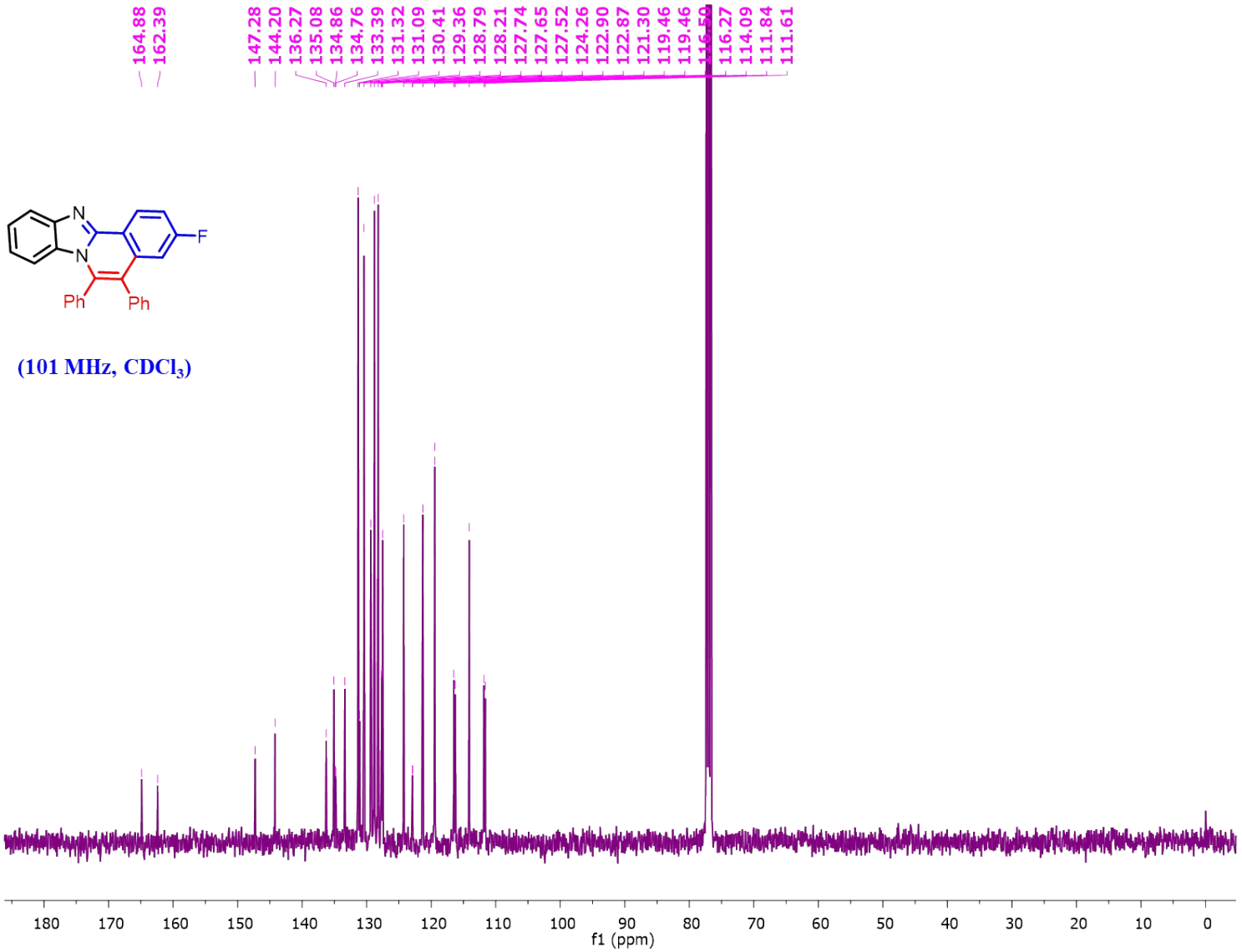

Fig. S54. ^{13}C NMR spectra of 3-fluoro-5,6-diphenylbenzo [4,5] imidazo[2,1-a] isoquinoline (**5c**) in $CDCl_3$.

Fig. S55. ^{19}F NMR spectra of 3-fluoro-5,6-diphenylbenzo [4,5] imidazo[2,1-a] isoquinoline (**5c**) in $CDCl_3$.

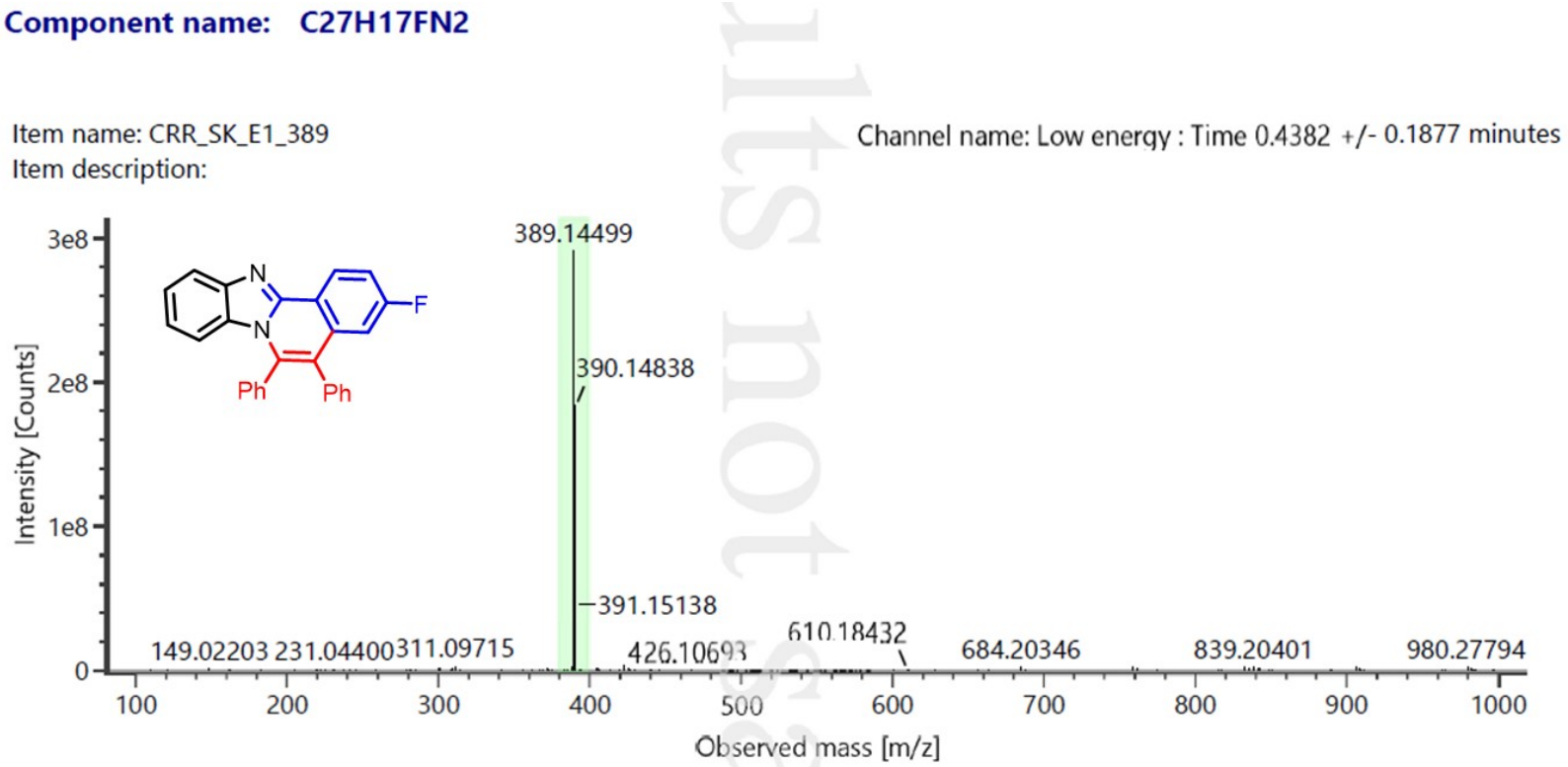

Fig. S56. HRMS Spectra of 3-fluoro-5,6-diphenylbenzo [4,5] imidazo[2,1-a] isoquinoline (**5c**).

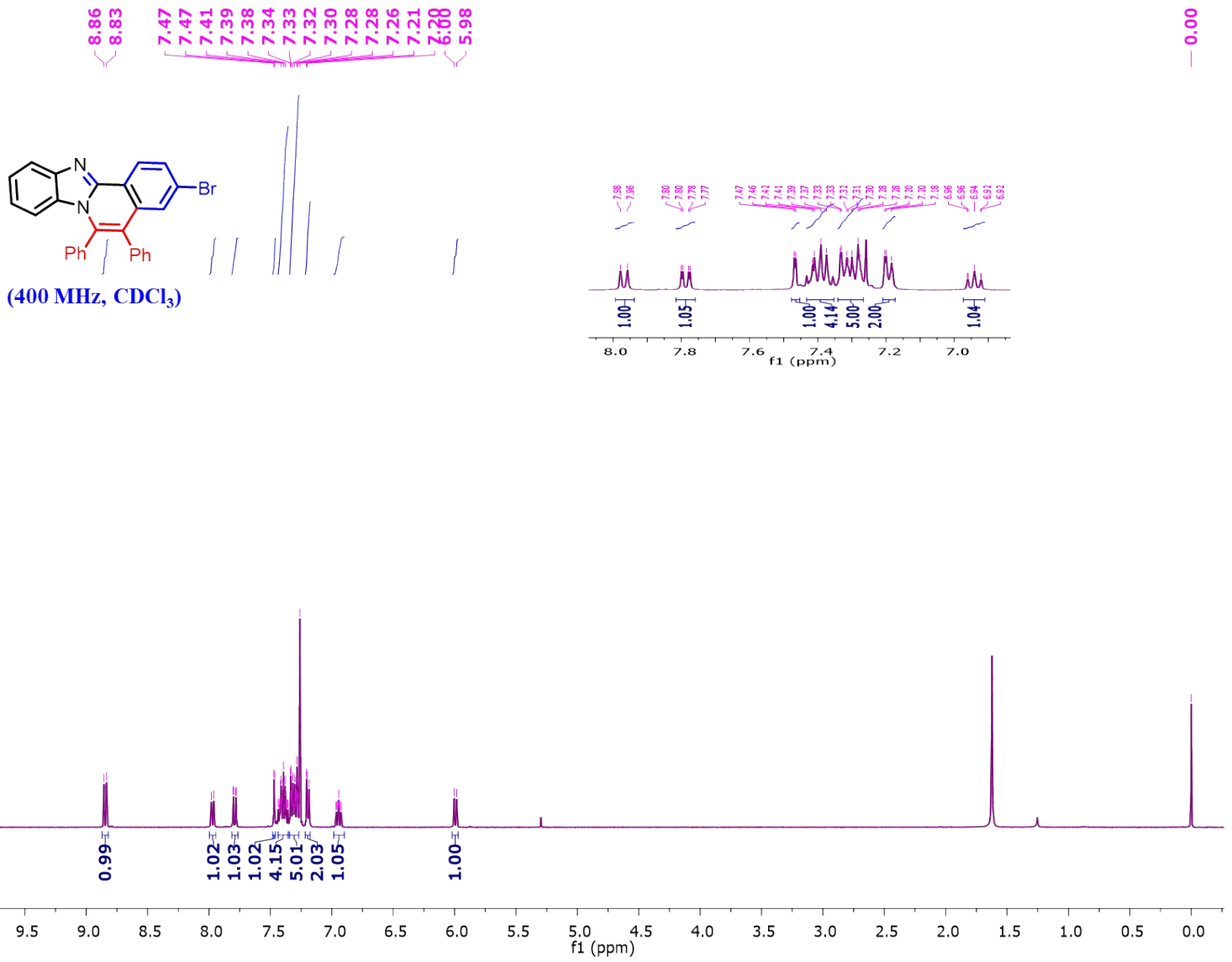

Fig. S57. ^{1}H NMR spectra of 3-bromo-5,6-diphenylbenzo [4,5] imidazo[2,1-a] isoquinoline (**5d**) in $CDCl_3$.

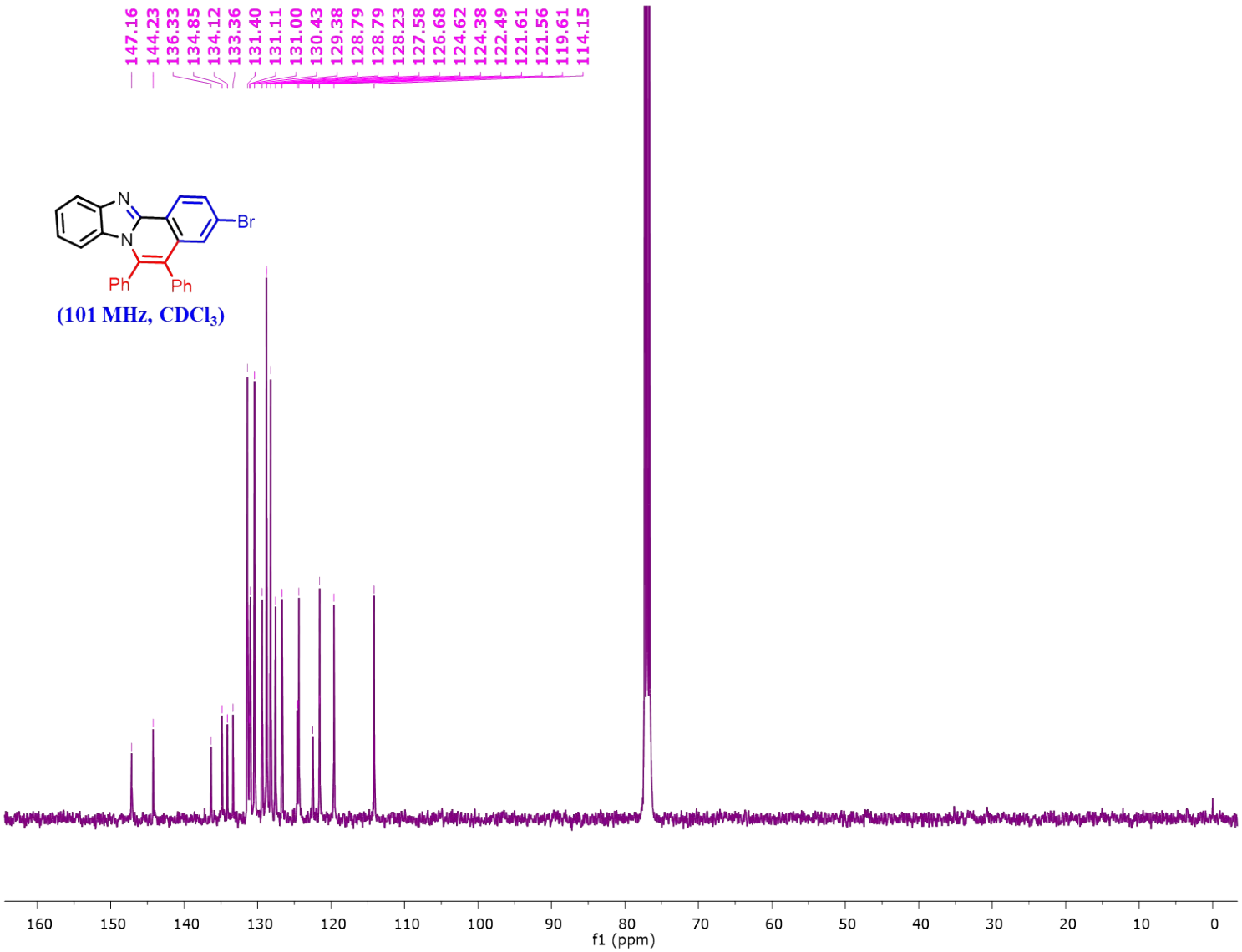

Fig. S58. ^{13}C NMR spectra of 3-bromo-5,6-diphenylbenzo [4,5] imidazo[2,1-a] isoquinoline (**5d**) in $CDCl_3$.

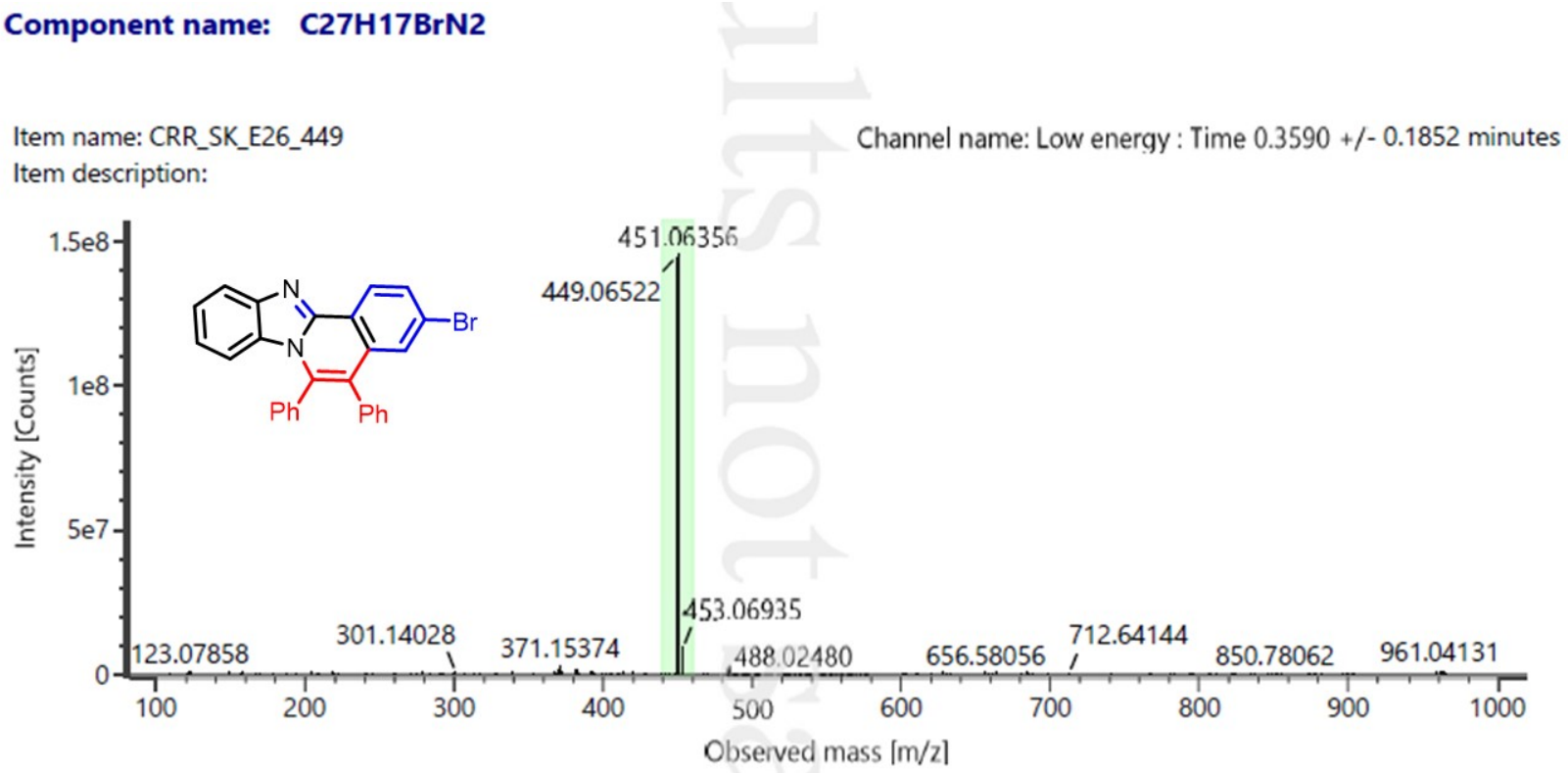

Fig. S59. HRMS spectra of 3-bromo-5,6-diphenylbenzo [4,5] imidazo[2,1-a] isoquinoline (**5d**).

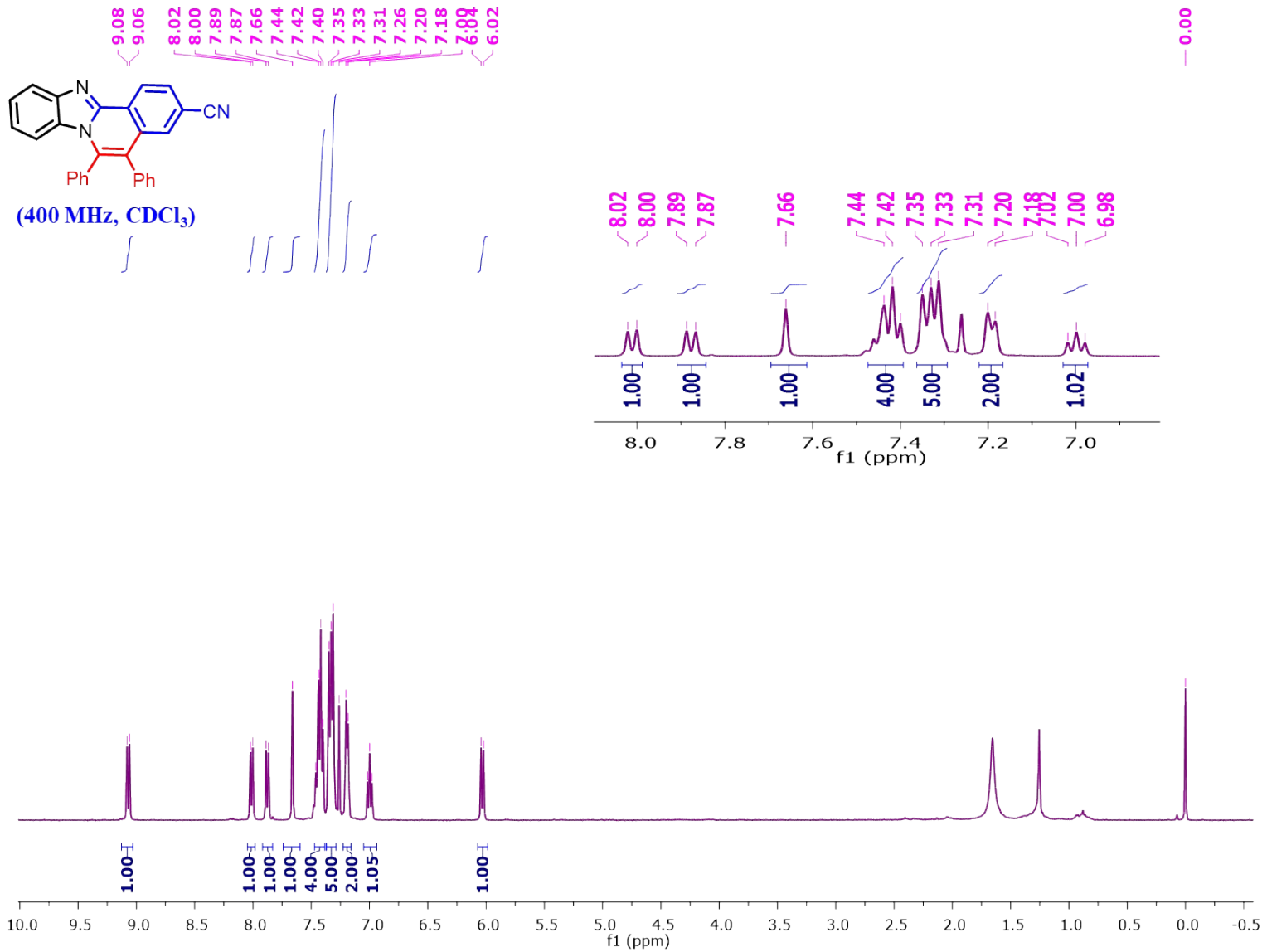

Fig. S60. ^{1}H NMR spectra of 5,6-diphenylbenzo[4,5]imidazo[2,1-a]isoquinoline-3-carbonitrile (**5e**) in $CDCl_3$.

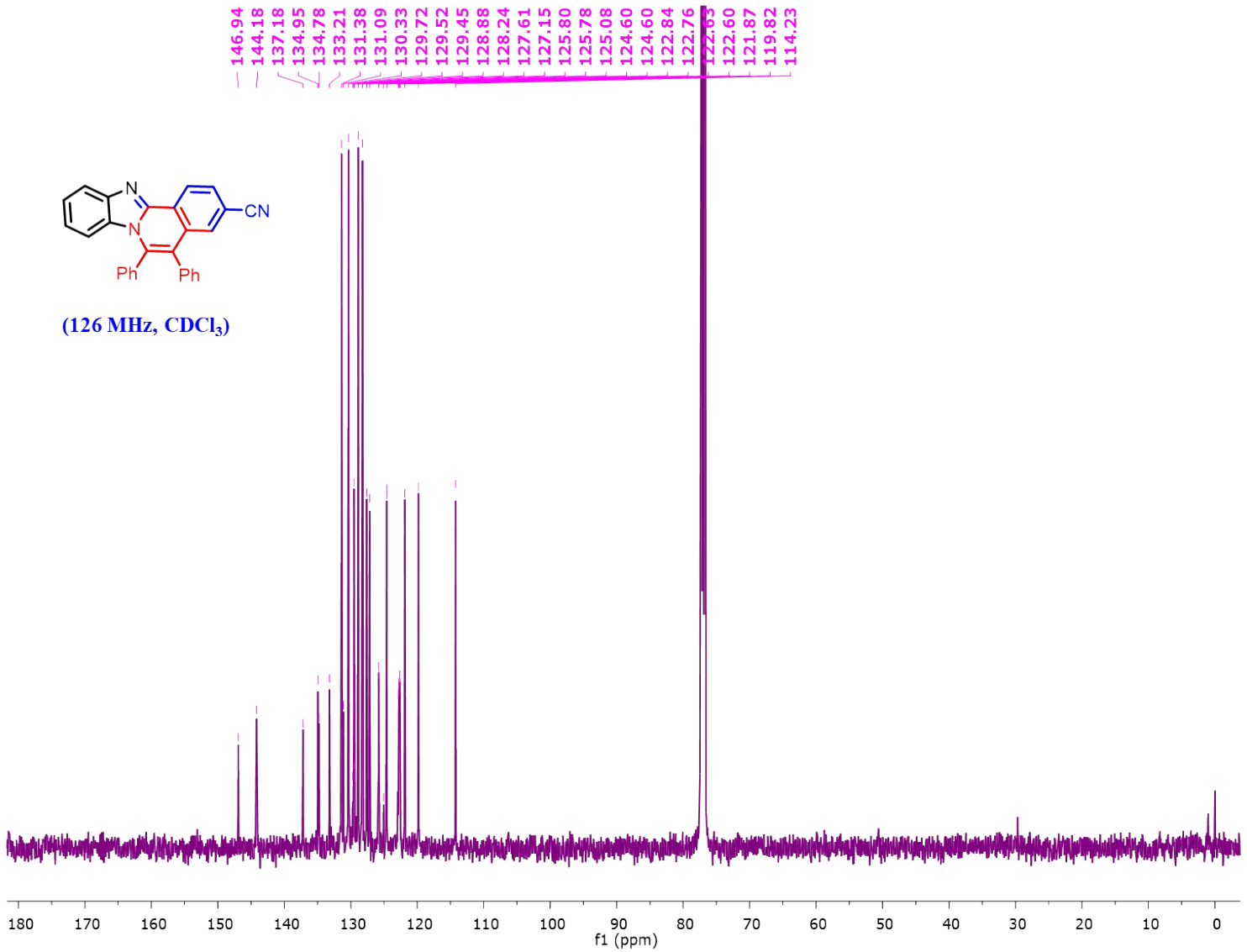

Fig. S61. ^{13}C NMR spectra of 5,6-diphenylbenzo[4,5]imidazo[2,1-a]isoquinoline-3-carbonitrile (**5e**) in $CDCl_3$.

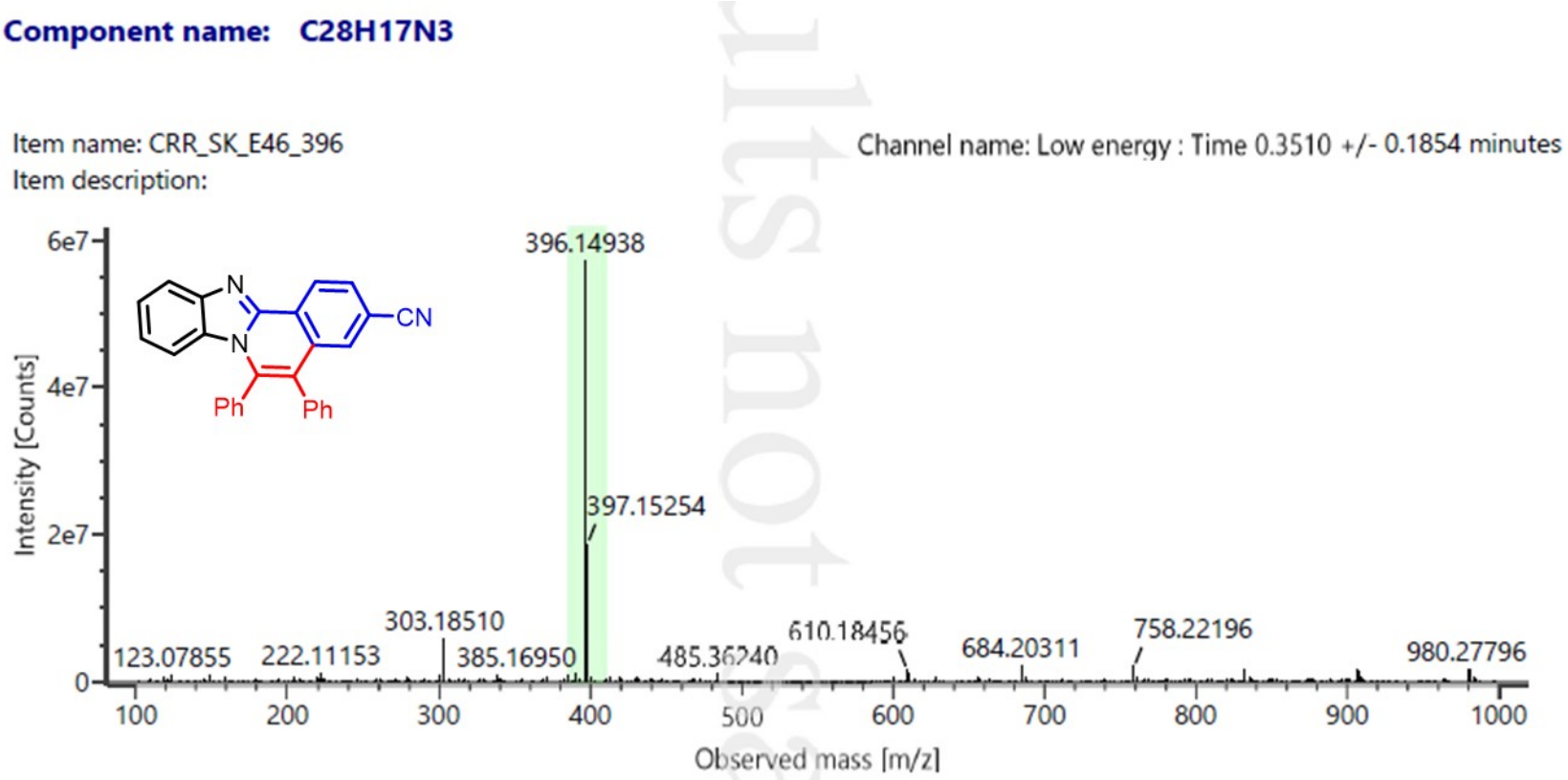

Fig. S62. HRMS spectra of 5,6-diphenylbenzo [4,5] imidazo[2,1-a] isoquinoline-3-carbonitrile (**5e**).

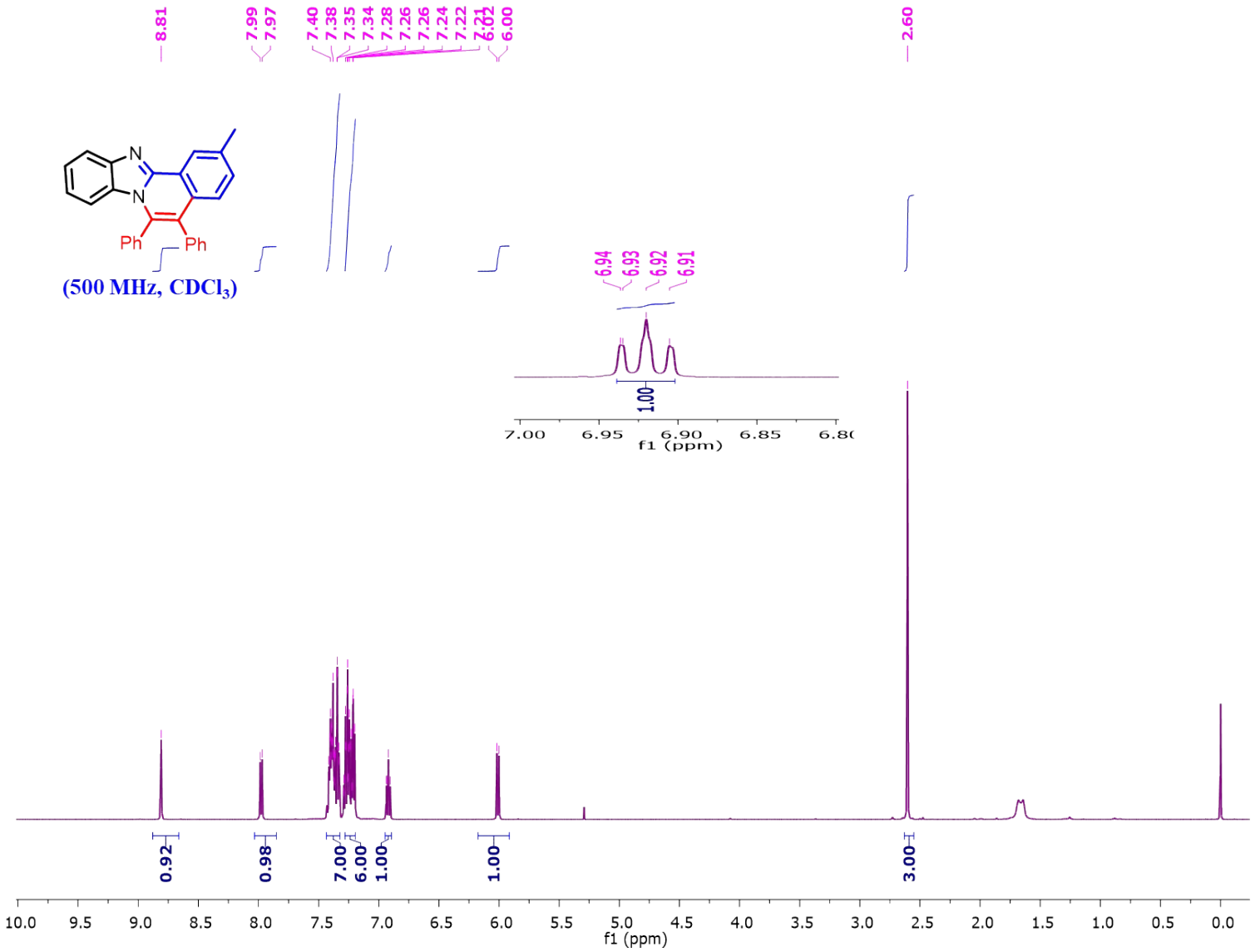

Fig. S63. ^{1}H NMR spectra of 2-methyl-5,6-diphenylbenzo [4,5] imidazo[2,1-a] isoquinoline (**5f**) in $CDCl_3$.

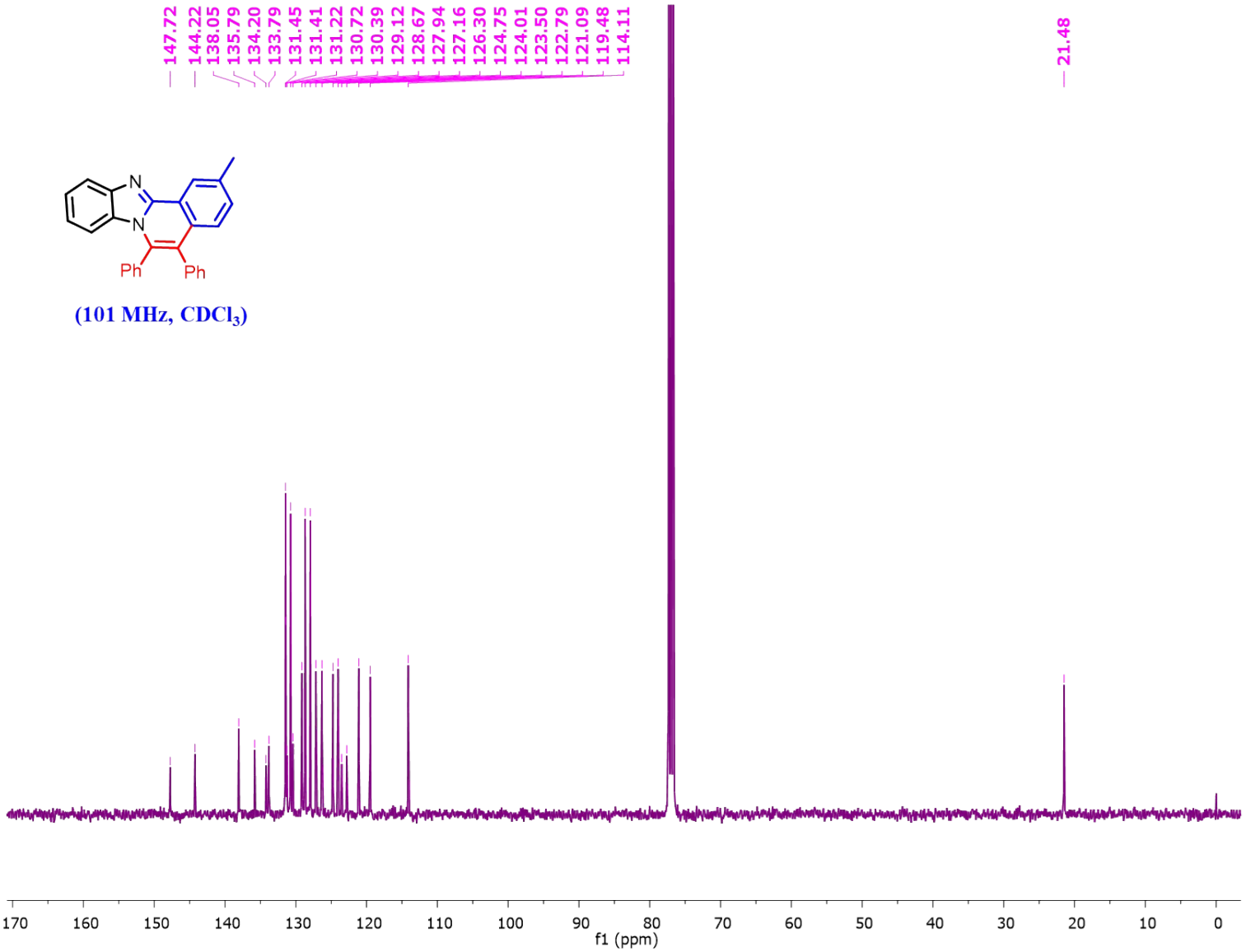

Fig. S64. ^{13}C NMR spectra of 2-methyl-5,6-diphenylbenzo [4,5] imidazo[2,1-a] isoquinoline (**5f**) in $CDCl_3$.

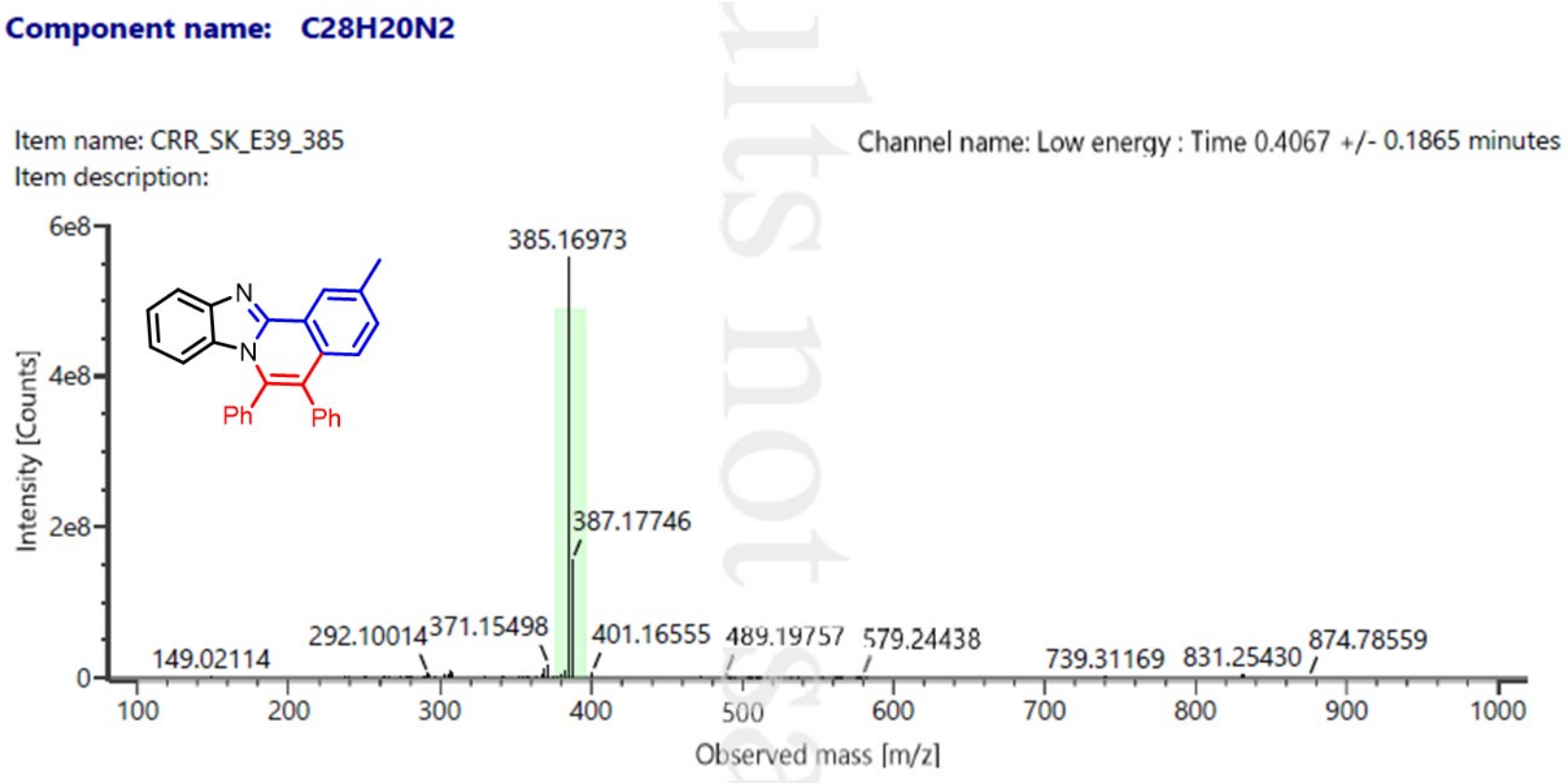

Fig. S65. HRMS spectra of 2-methyl-5,6-diphenylbenzo [4,5] imidazo [2,1-a] isoquinoline (**5f**).

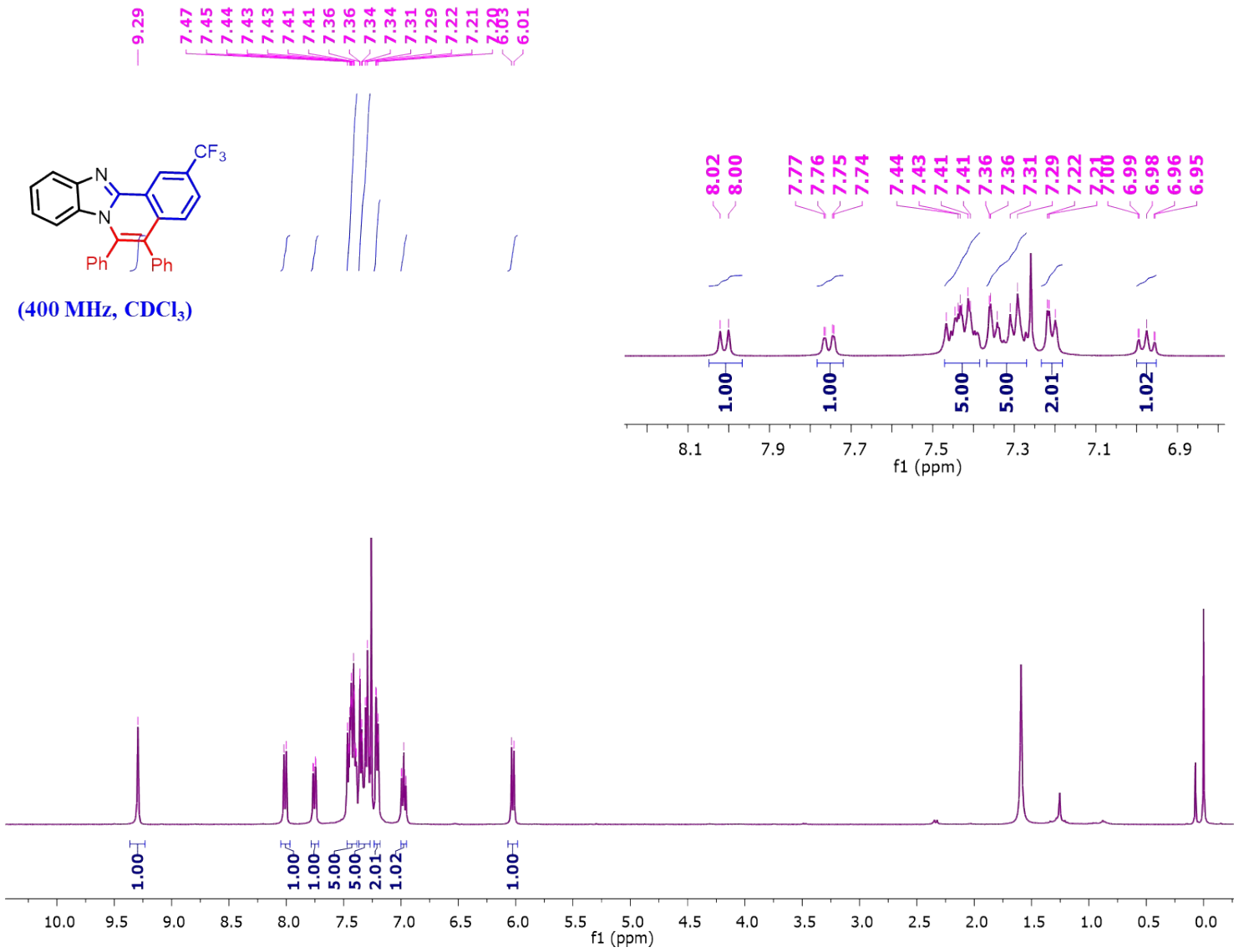

Fig. S66. ^{1}H NMR spectra of 5,6-diphenyl-2-(trifluoromethyl) benzo [4,5] imidazo [2,1-a] isoquinoline (**5g**) in $CDCl_3$.

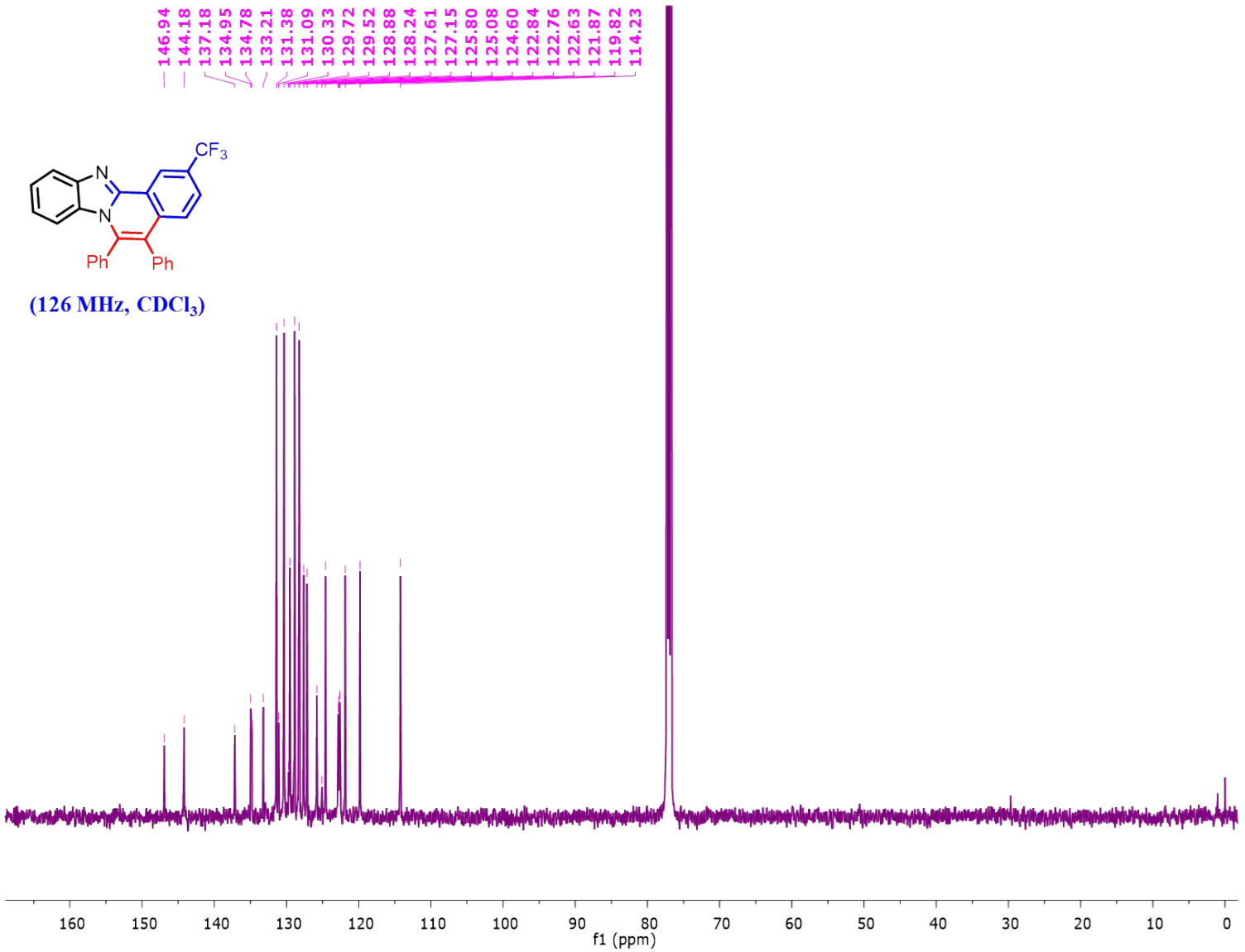

Fig. S67. ^{13}C NMR spectra of 5,6-diphenyl-2-(trifluoromethyl) benzo [4,5] imidazo[2,1-a] isoquinoline (**5g**) in $CDCl_3$.

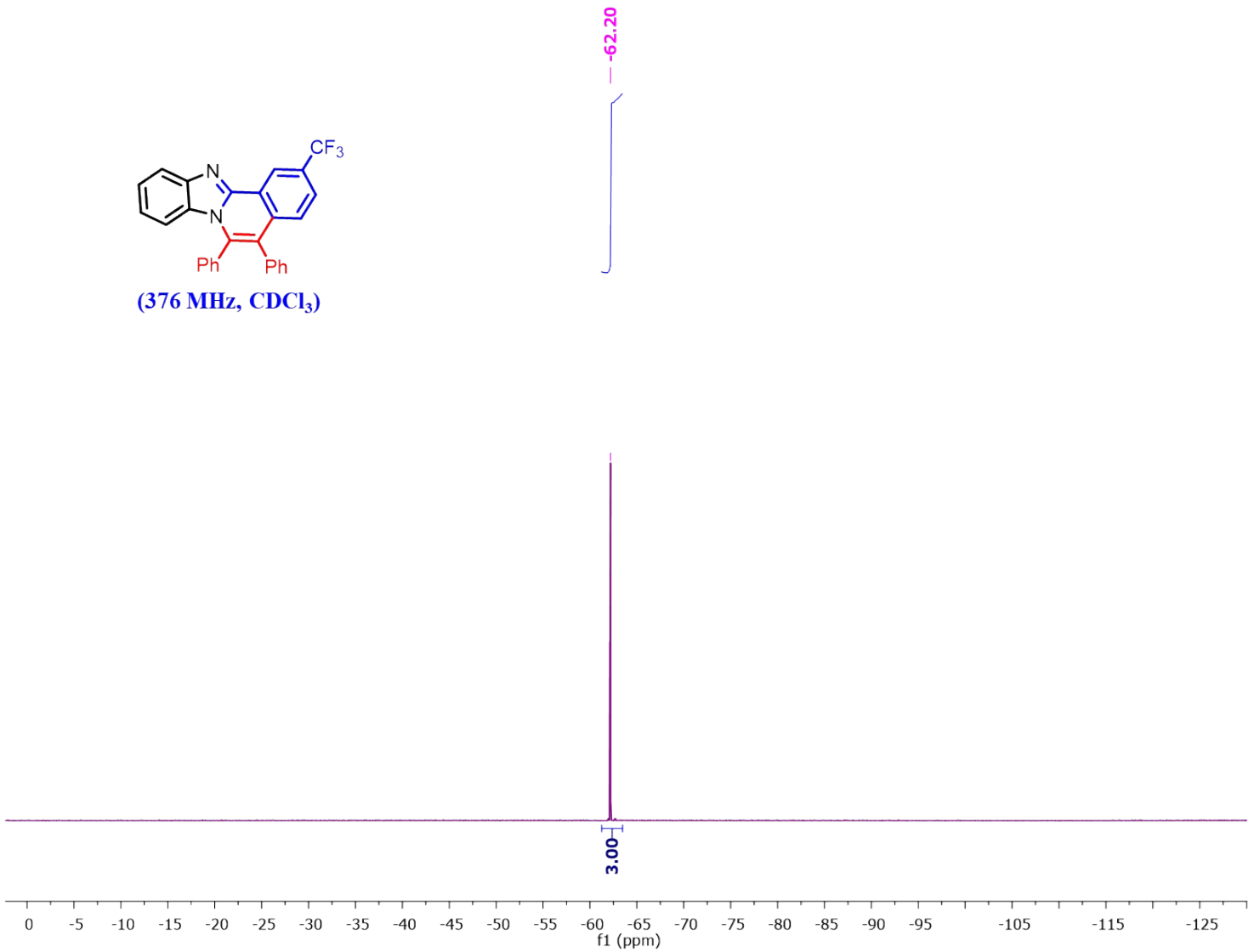

Fig. S68. ^{19}F NMR spectra of 5,6-diphenyl-2-(trifluoromethyl) benzo [4,5] imidazo[2,1-a] isoquinoline (**5g**) in $CDCl_3$.

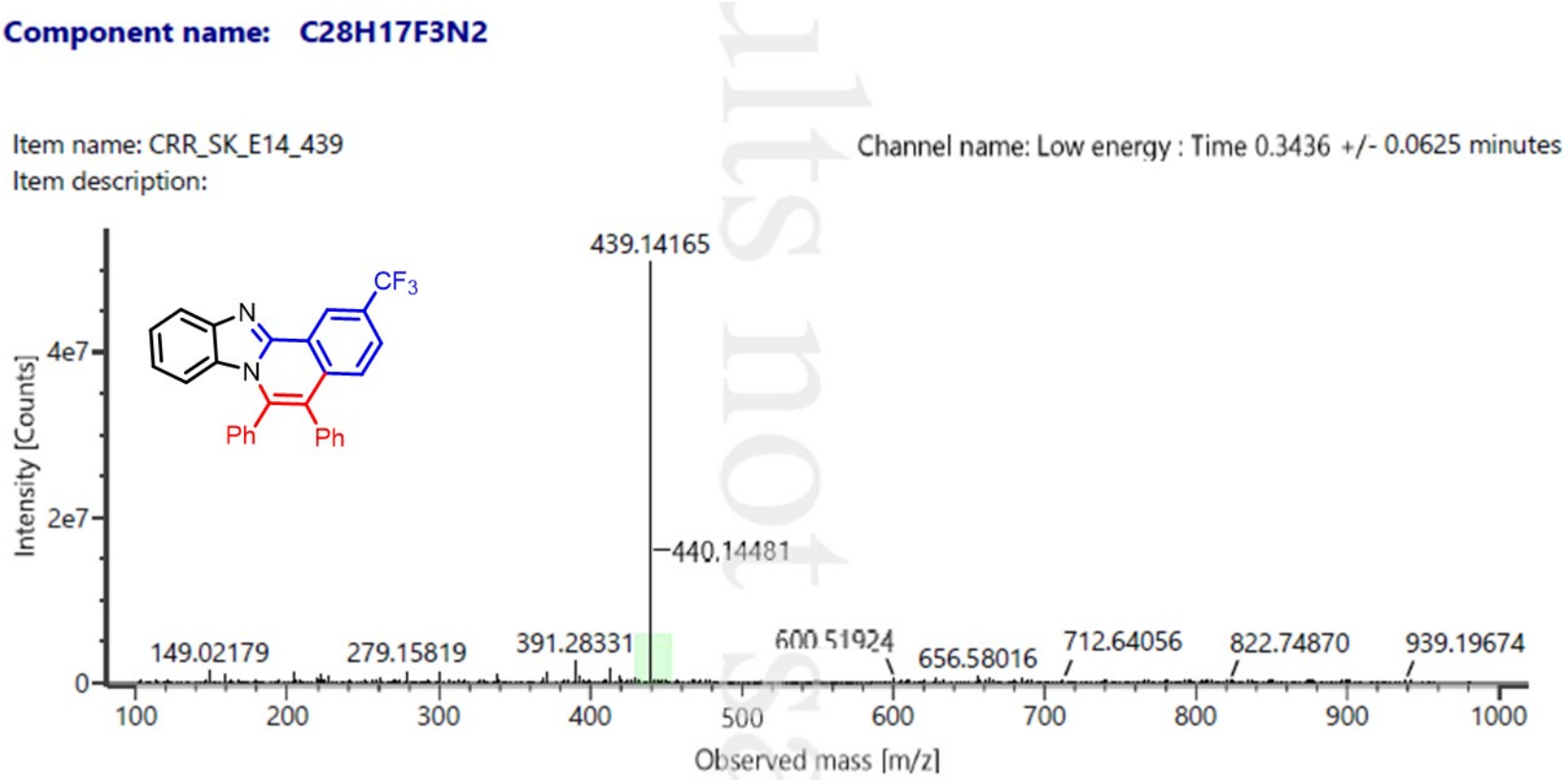

Fig. S69. HRMS spectra of 5,6-diphenyl-2-(trifluoromethyl) benzo [4,5] imidazo[2,1-a] isoquinoline (**5g**).

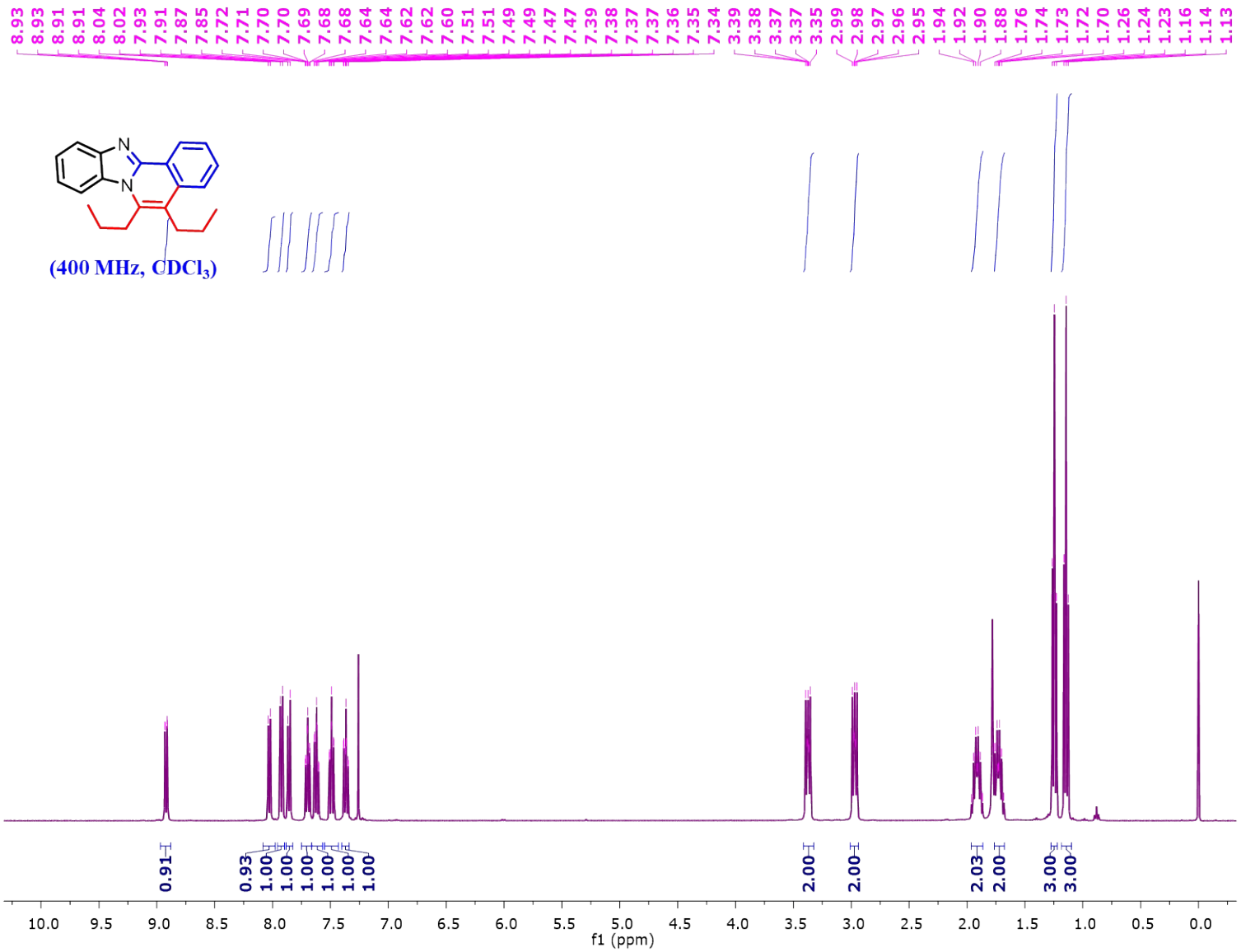

Fig. S70. ^{1}H NMR spectra of 5,6-dipropylbenzo [4,5] imidazo [2,1-a] isoquinoline (**5h**) in $CDCl_3$.

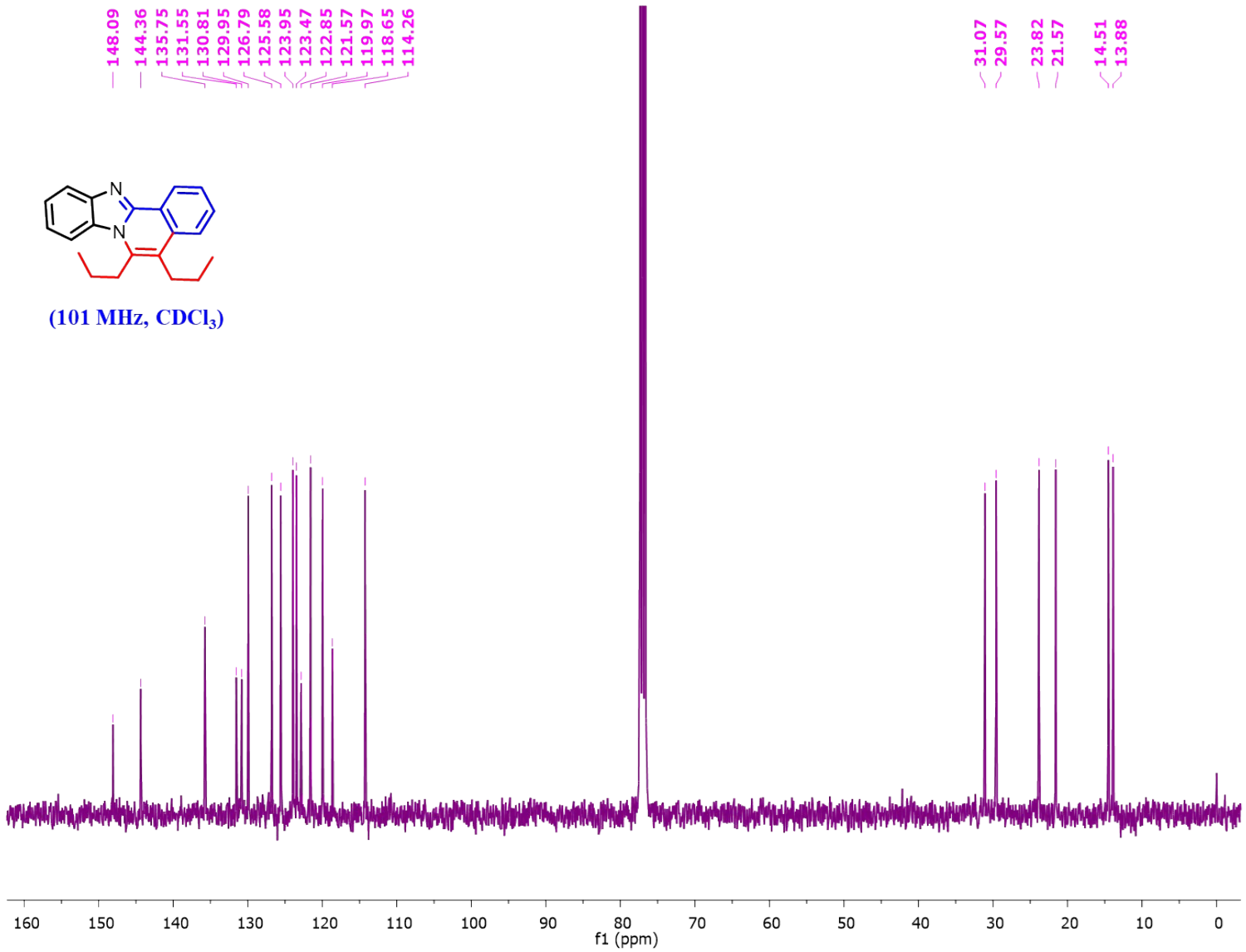

Fig. S71. ^{13}C NMR spectra of 5,6-dipropylbenzo [4,5] imidazo[2,1-a] isoquinoline (**5h**) in $CDCl_3$.

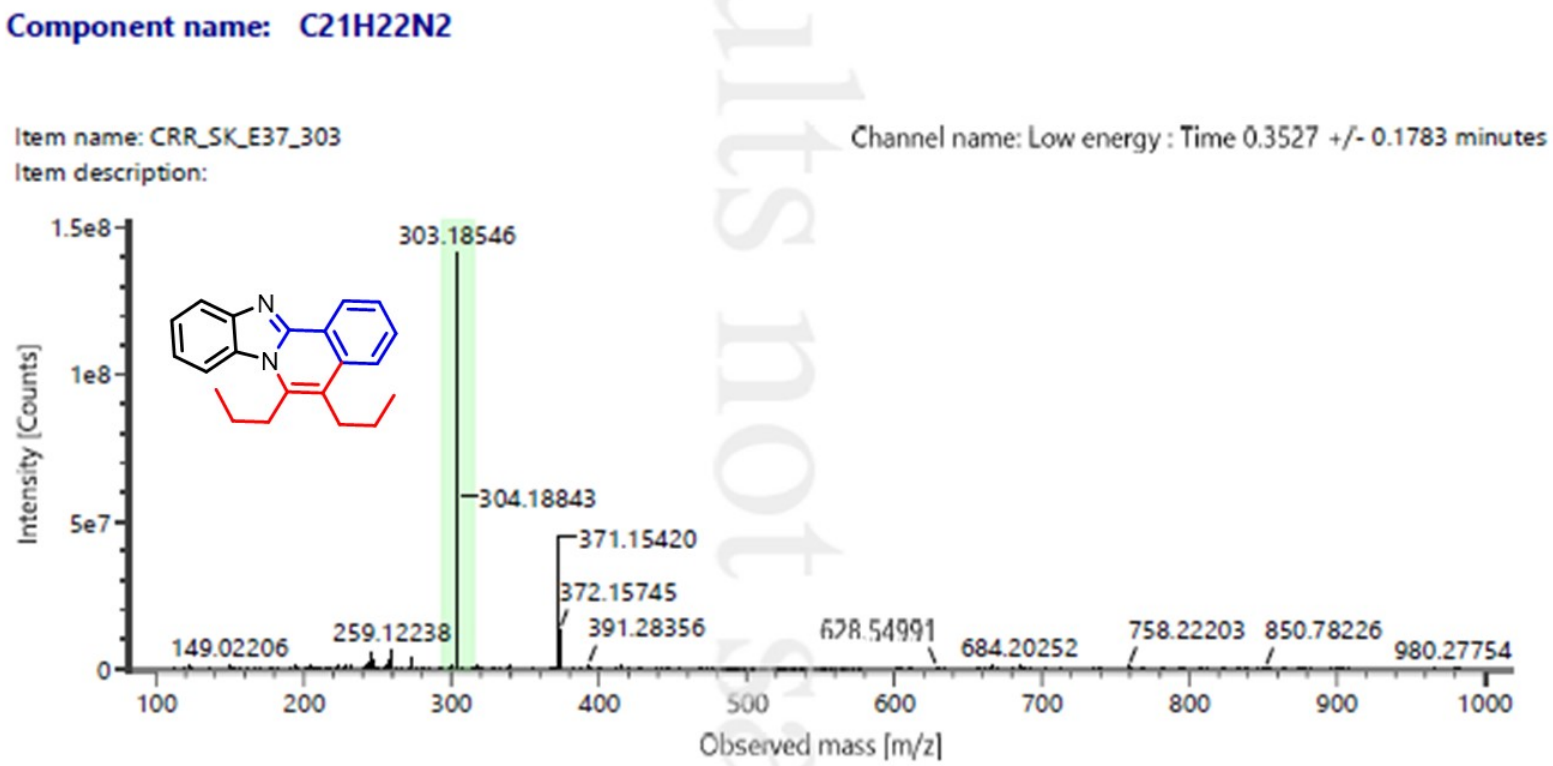

Fig. S72. HRMS spectra of 5,6-dipropylbenzo [4,5] imidazo[2,1-a] isoquinoline (**5h**).

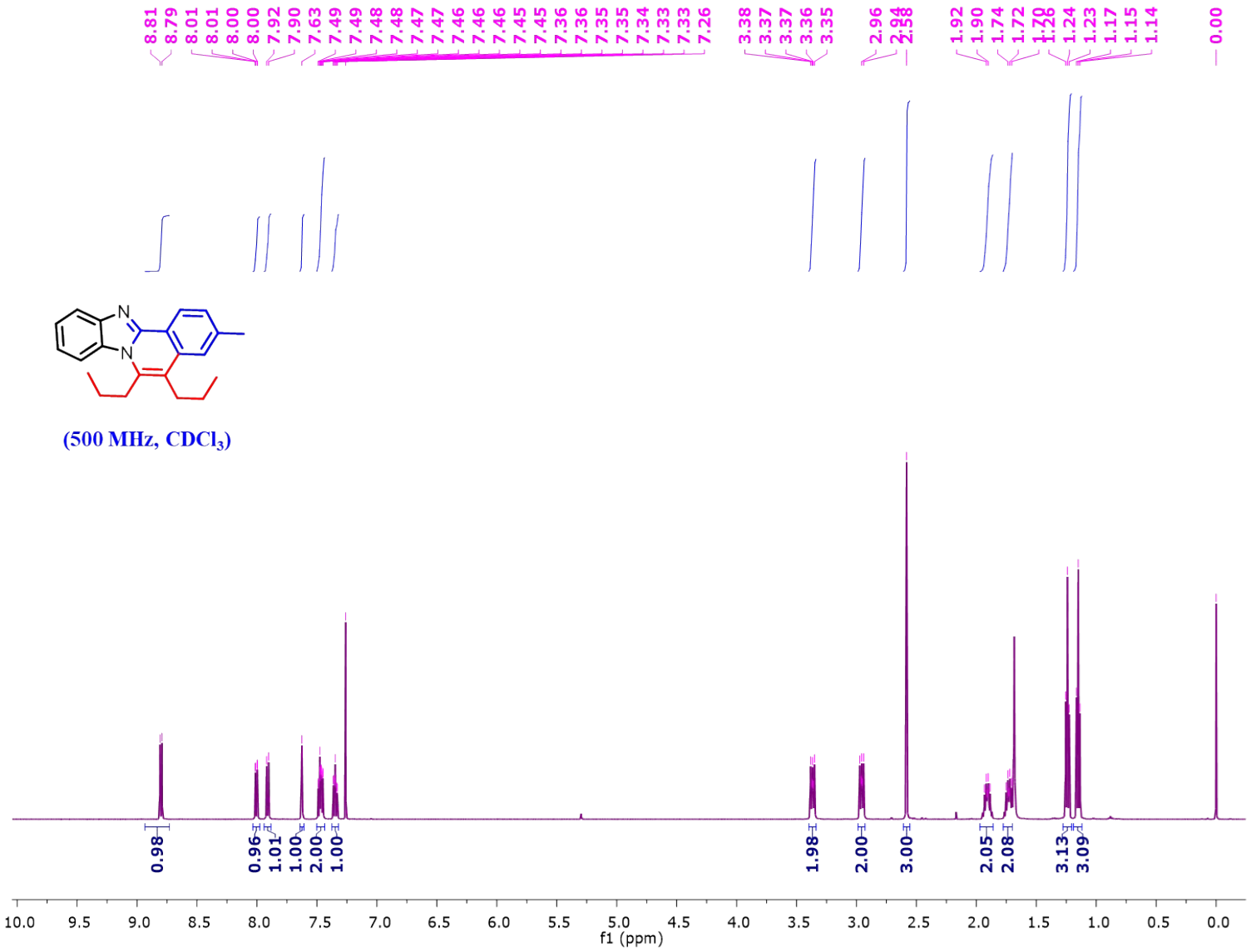

Fig. S73. ^{1}H NMR spectra of 3-methyl-5,6-dipropylbenzo [4,5] imidazo[2,1-a] isoquinoline (**5i**) in $CDCl_3$.

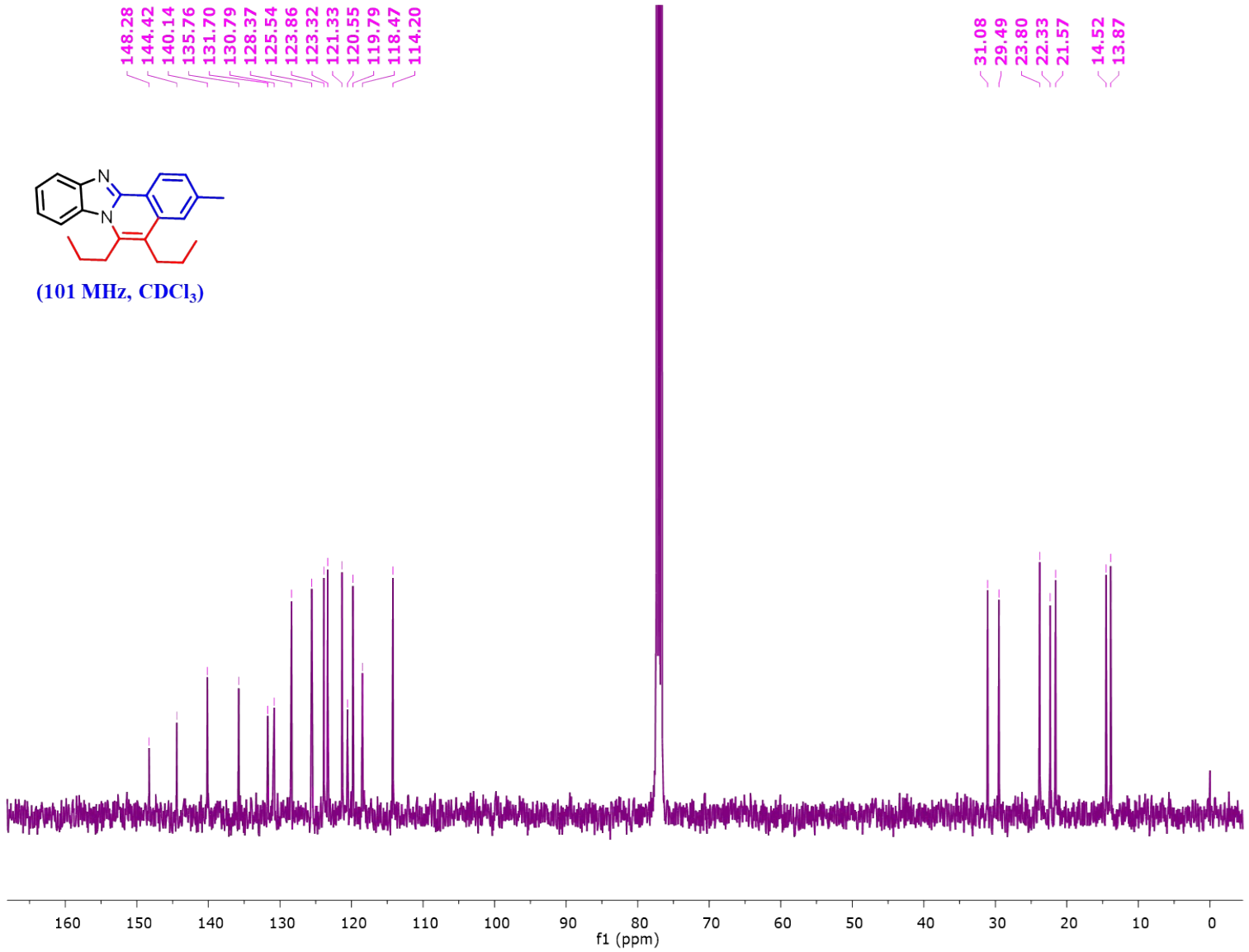

Fig. S74. ^{13}C NMR spectra of 3-methyl-5,6-dipropylbenzo [4,5] imidazo[2,1-a] isoquinoline (**5i**) in $CDCl_3$.

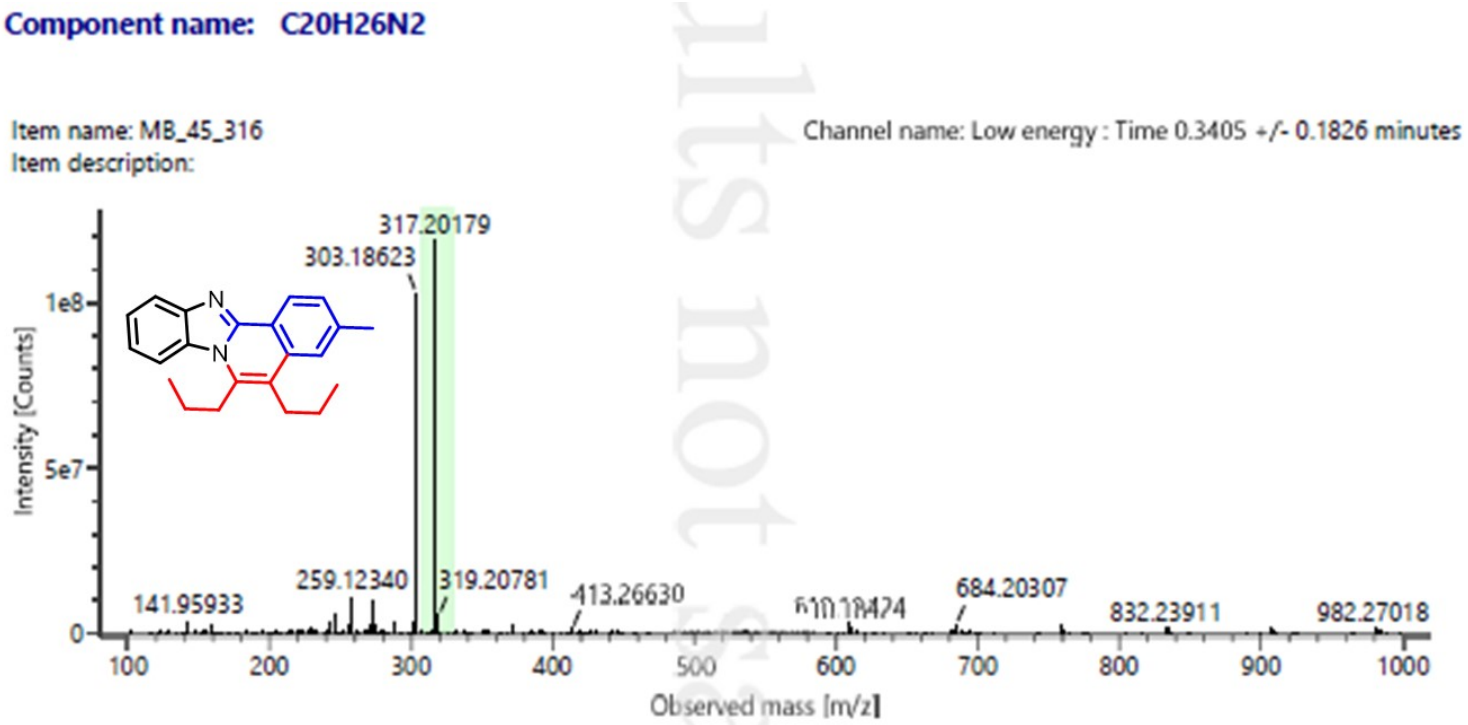

Fig. S75. HRMS spectra of 3-methyl-5,6-dipropylbenzo [4,5] imidazo[2,1-a] isoquinoline (**5i**).

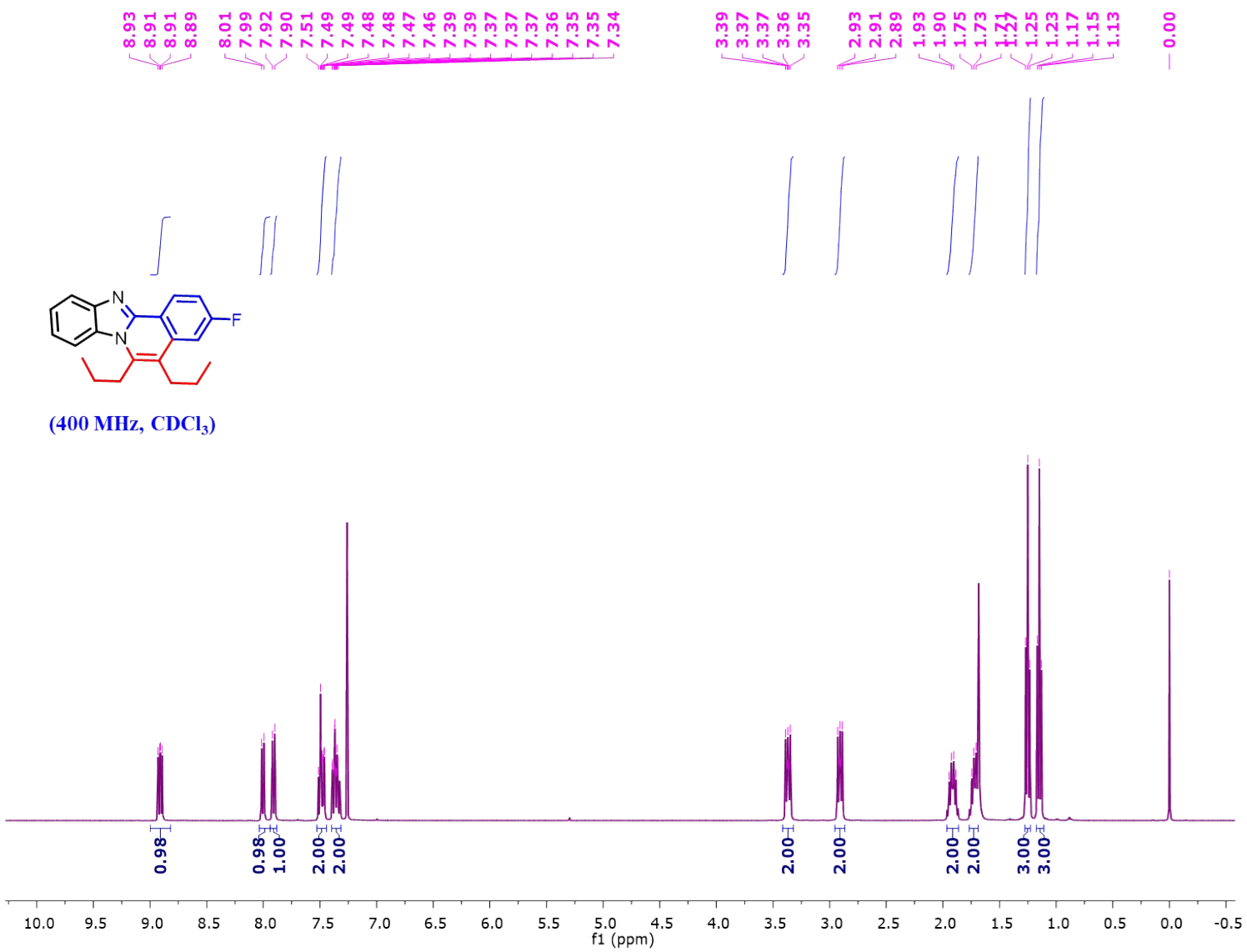

Fig. S76. ^{1}H NMR spectra of 3-fluoro-5,6-dipropylbenzo [4,5] imidazo [2,1-a] isoquinoline (**5j**) in $CDCl_3$.

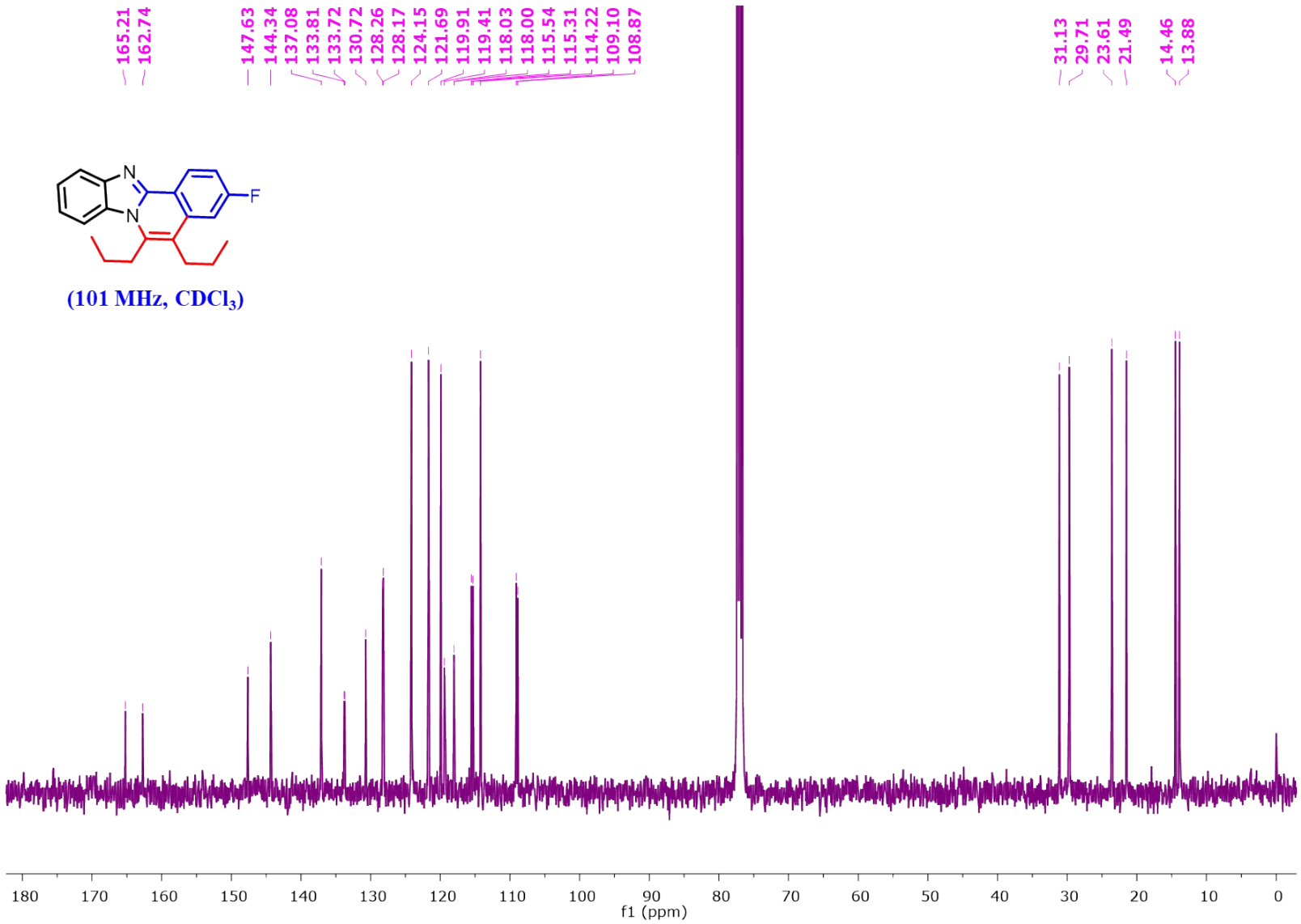

Fig. S77. ^{13}C NMR spectra of 3-fluoro-5,6-dipropylbenzo [4,5] imidazo[2,1-a] isoquinoline (**5j**) in $CDCl_3$.

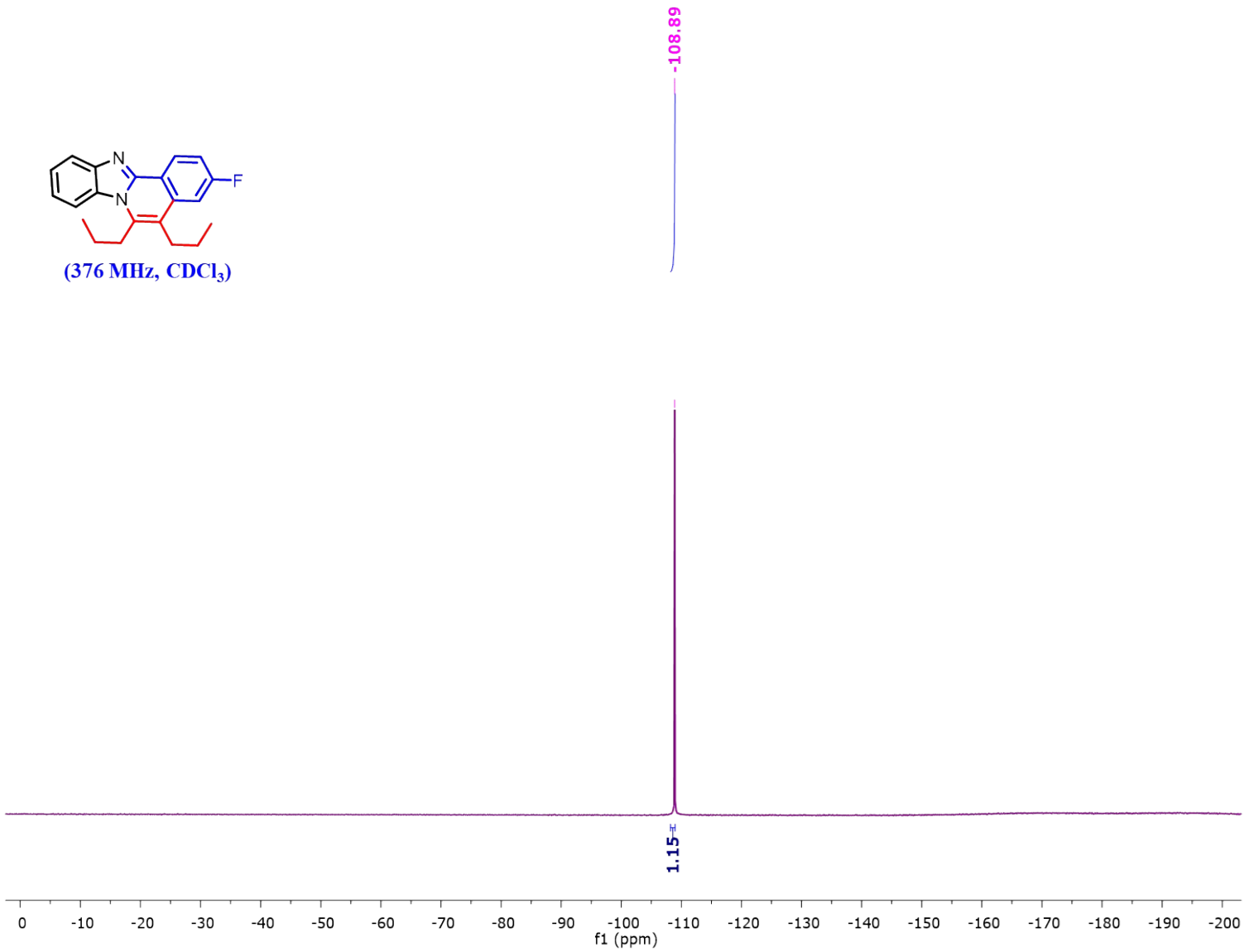

Fig. S78. IR spectra of 3-fluoro-5,6-dipropylbenzo [4,5] imidazo [2,1-a] isoquinoline (**5j**) in $CDCl_3$.

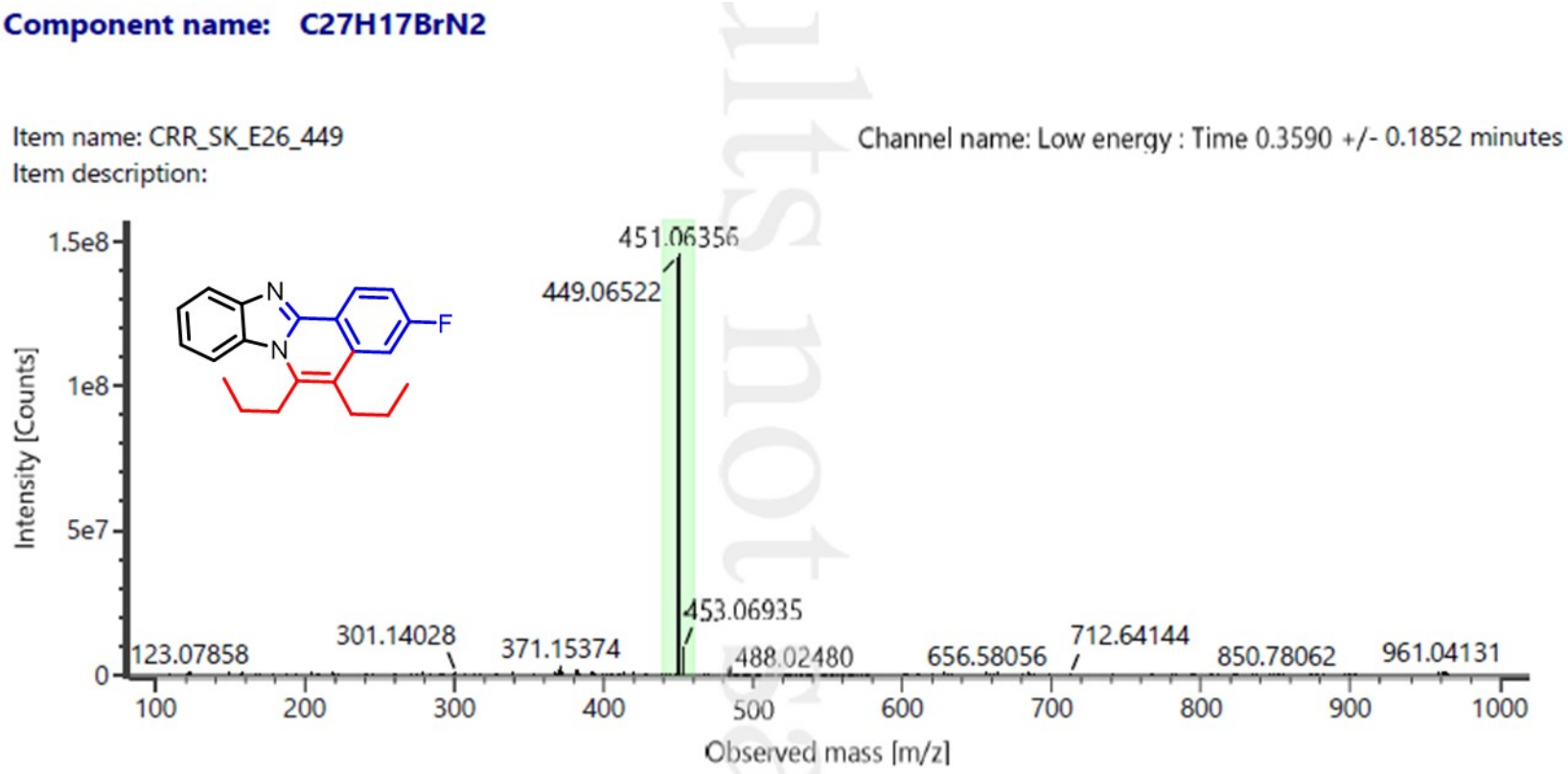

Fig. S79. HRMS spectra of 3-fluoro-5,6-dipropylbenzo [4,5] imidazo [2,1-a] isoquinoline (**5j**).

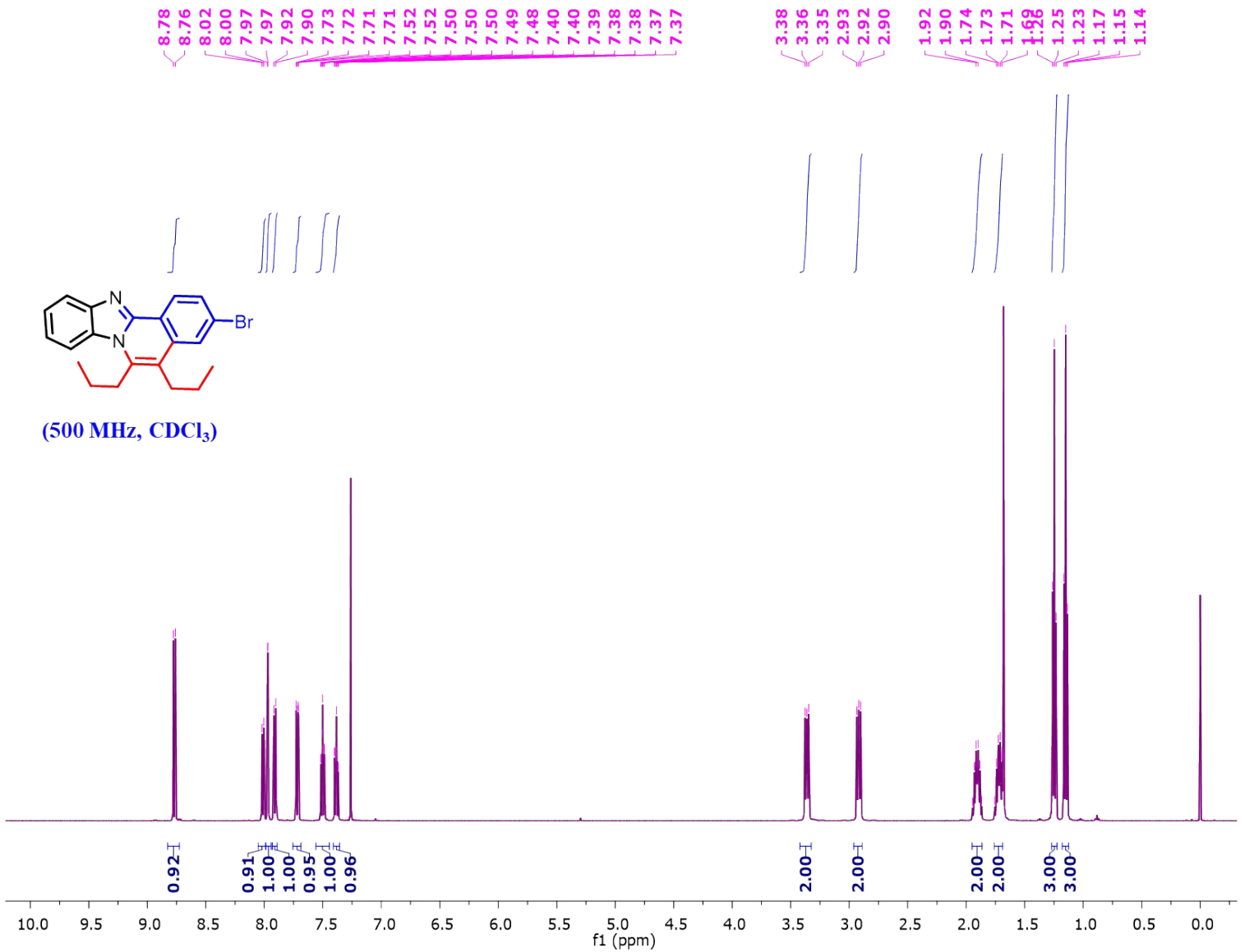

Fig. 80. ^{1}H NMR spectra of 3-bromo-5,6-dipropylbenzo [4,5] imidazo[2,1-a] isoquinoline (**5k**) in $CDCl_3$.

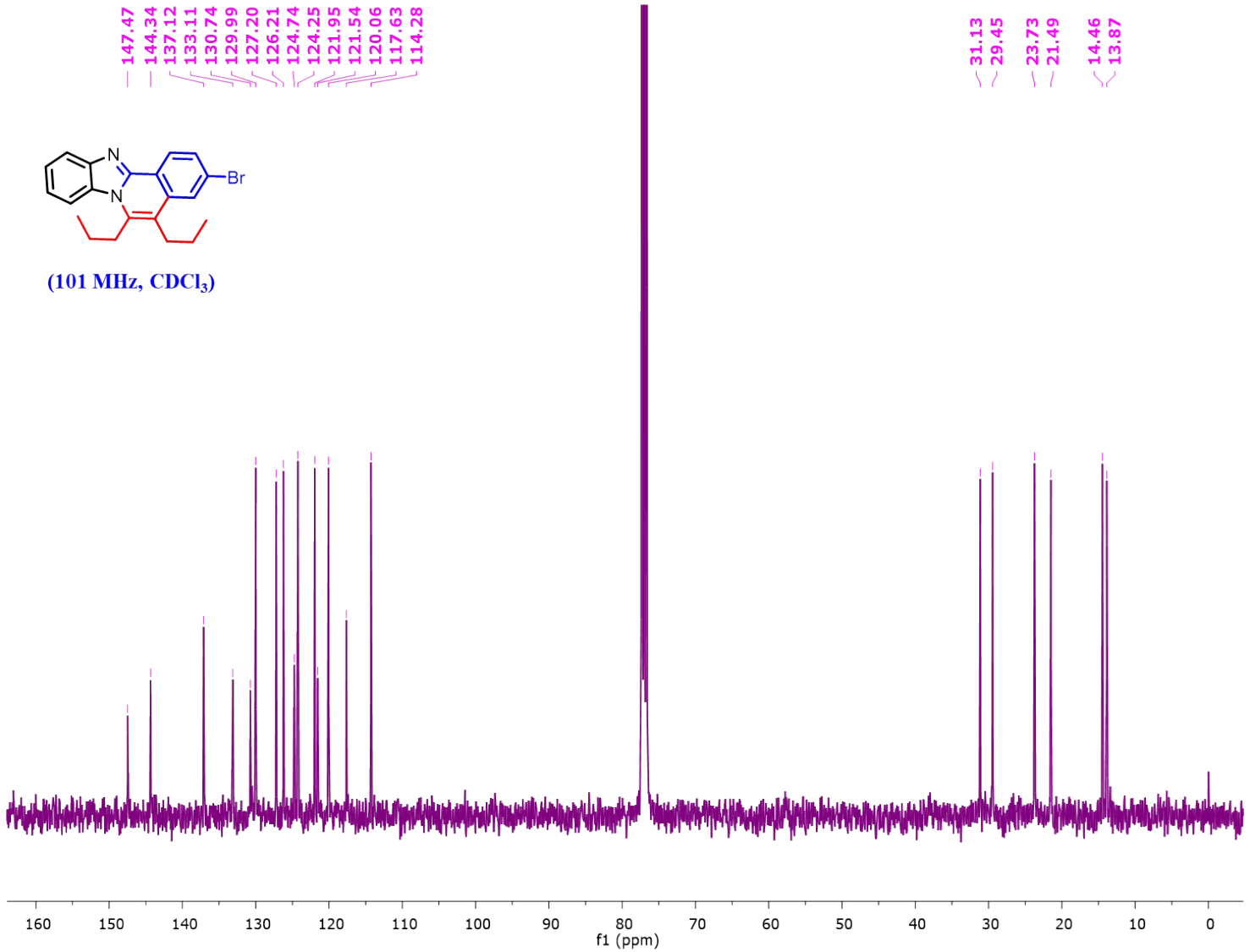

Fig. S81. ^{13}C NMR spectra of 3-bromo-5,6-dipropylbenzo [4,5] imidazo[2,1-a] isoquinoline (**5k**) in $CDCl_3$.

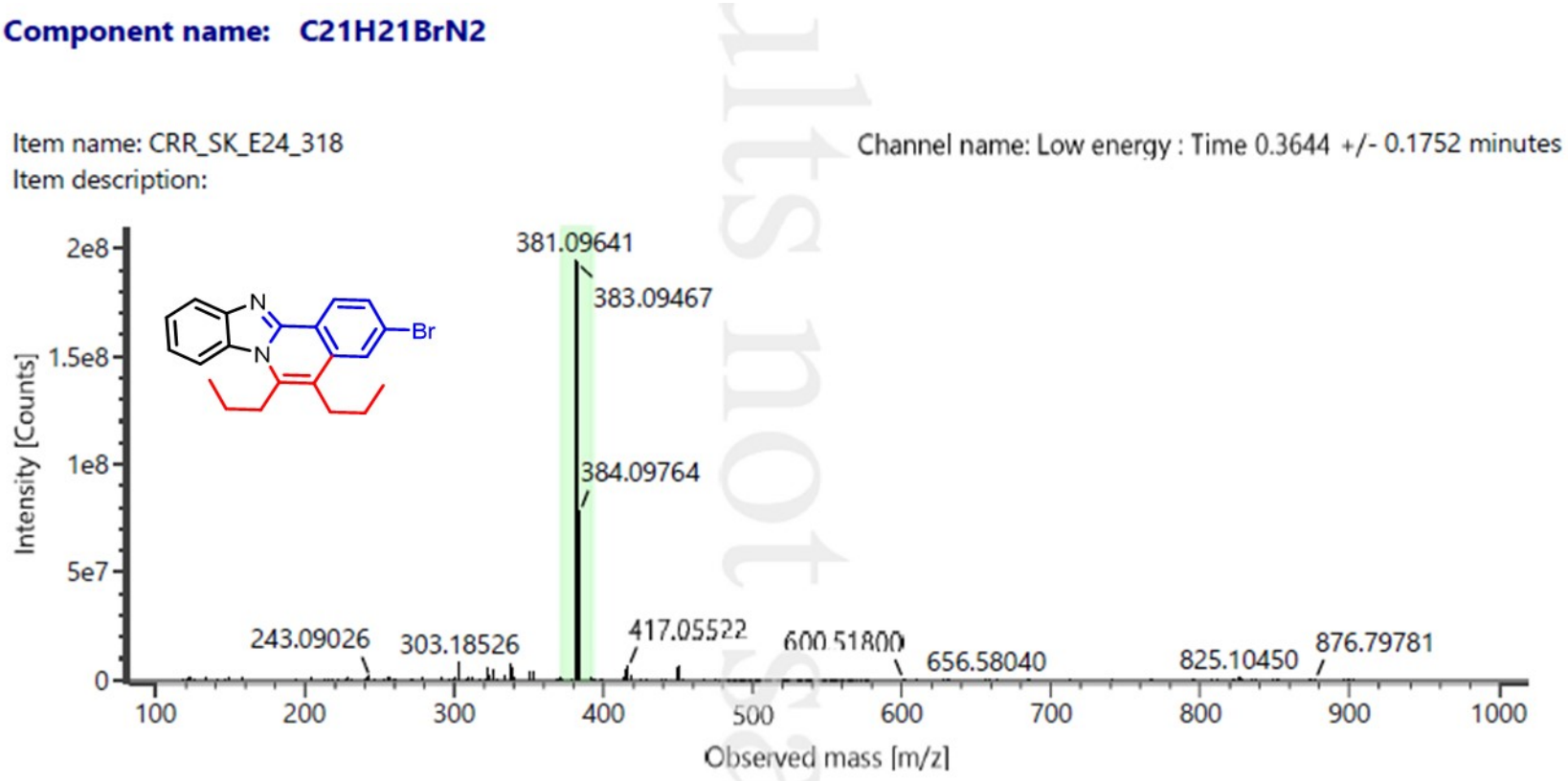

Fig. S82. HRMS spectra of 3-bromo-5,6-dipropylbenzo [4,5] imidazo[2,1-a] isoquinoline (**5k**).

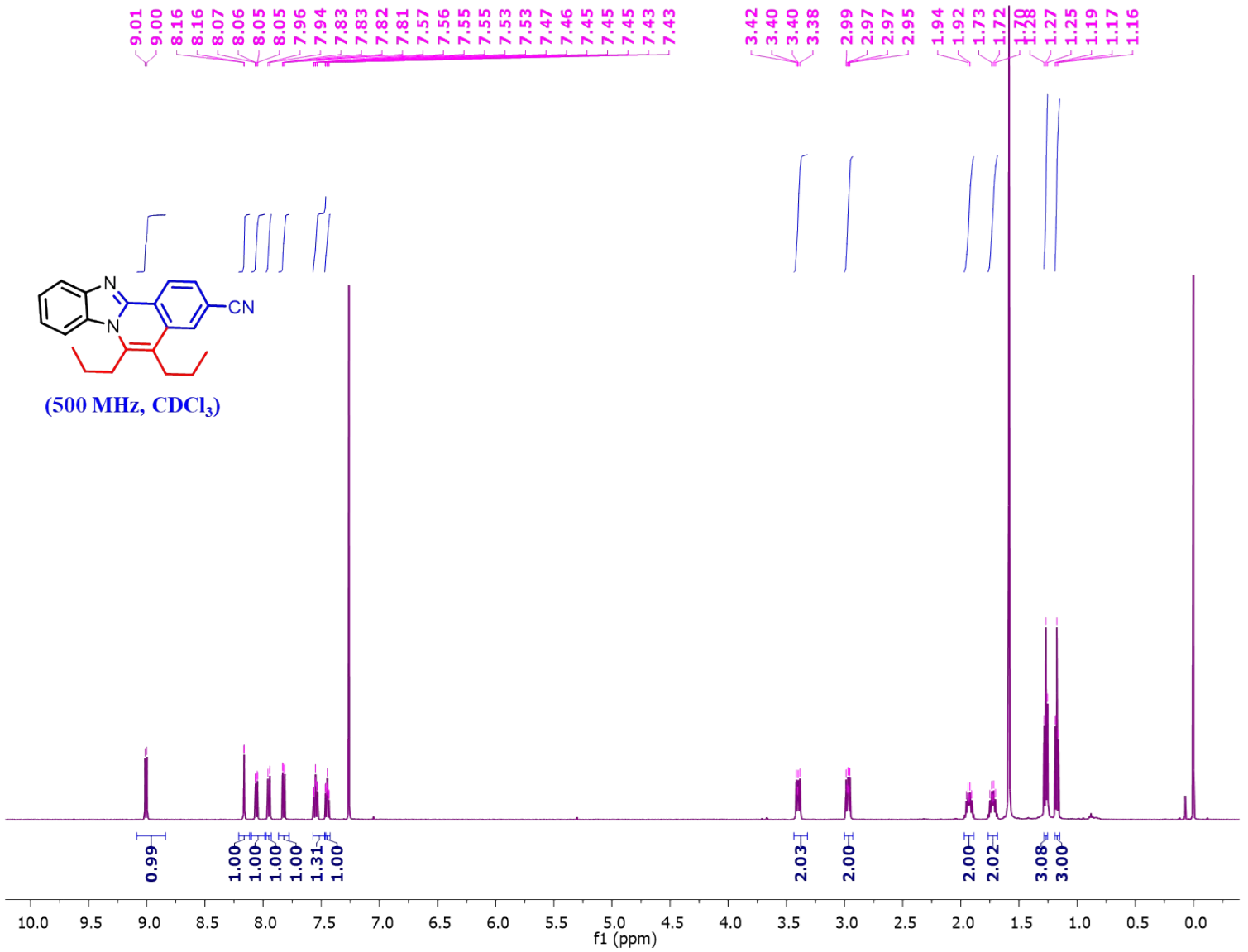

Fig. S83. ^{1}H NMR spectra of 5,6-dipropylbenzo [4,5] imidazo[2,1-a] isoquinoline-3-carbonitrile (**5l**) in $CDCl_3$.

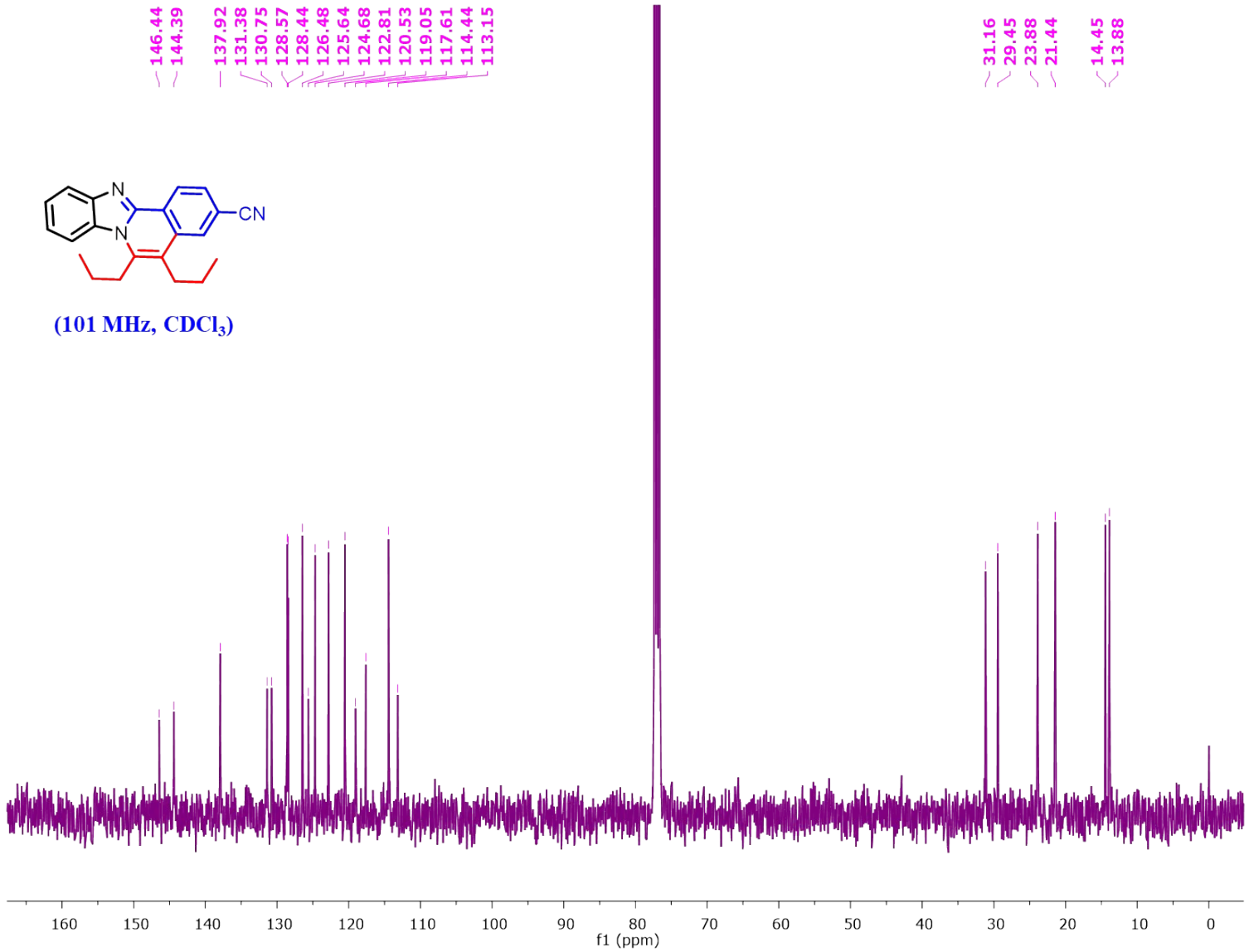

Fig. S84. ^{13}C NMR spectra of 5,6-dipropylbenzo [4,5] imidazo[2,1-a] isoquinoline-3-carbonitrile (**5l**) in $CDCl_3$.

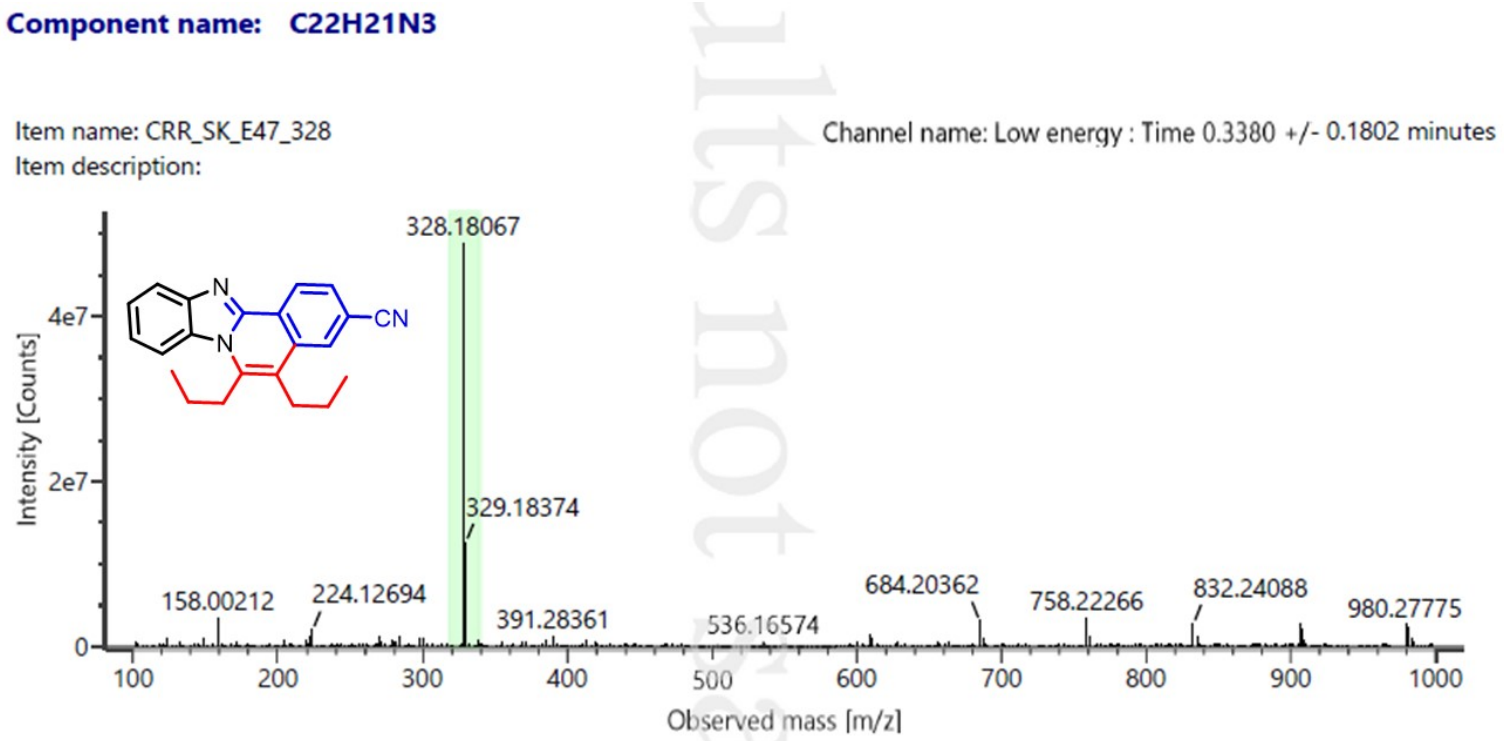

Fig. S85. HRMS spectra of 5,6-dipropylbenzo [4,5] imidazo[2,1-a] isoquinoline-3-carbonitrile (**5l**).

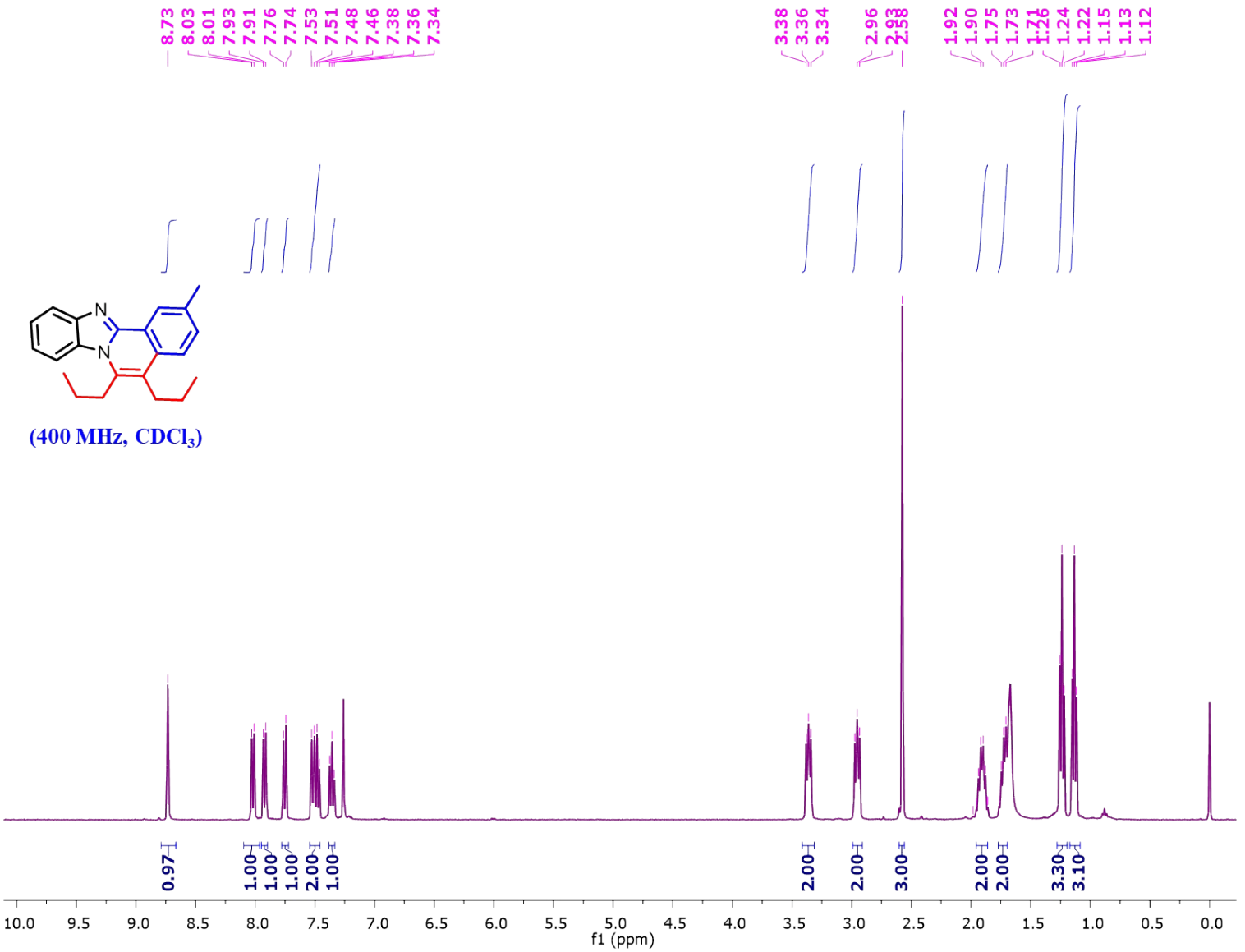

Fig. S86. ^{1}H NMR spectra of 2-methyl-5,6-dipropylbenzo [4,5] imidazo [2,1-a] isoquinoline (**5m**) in $CDCl_3$.

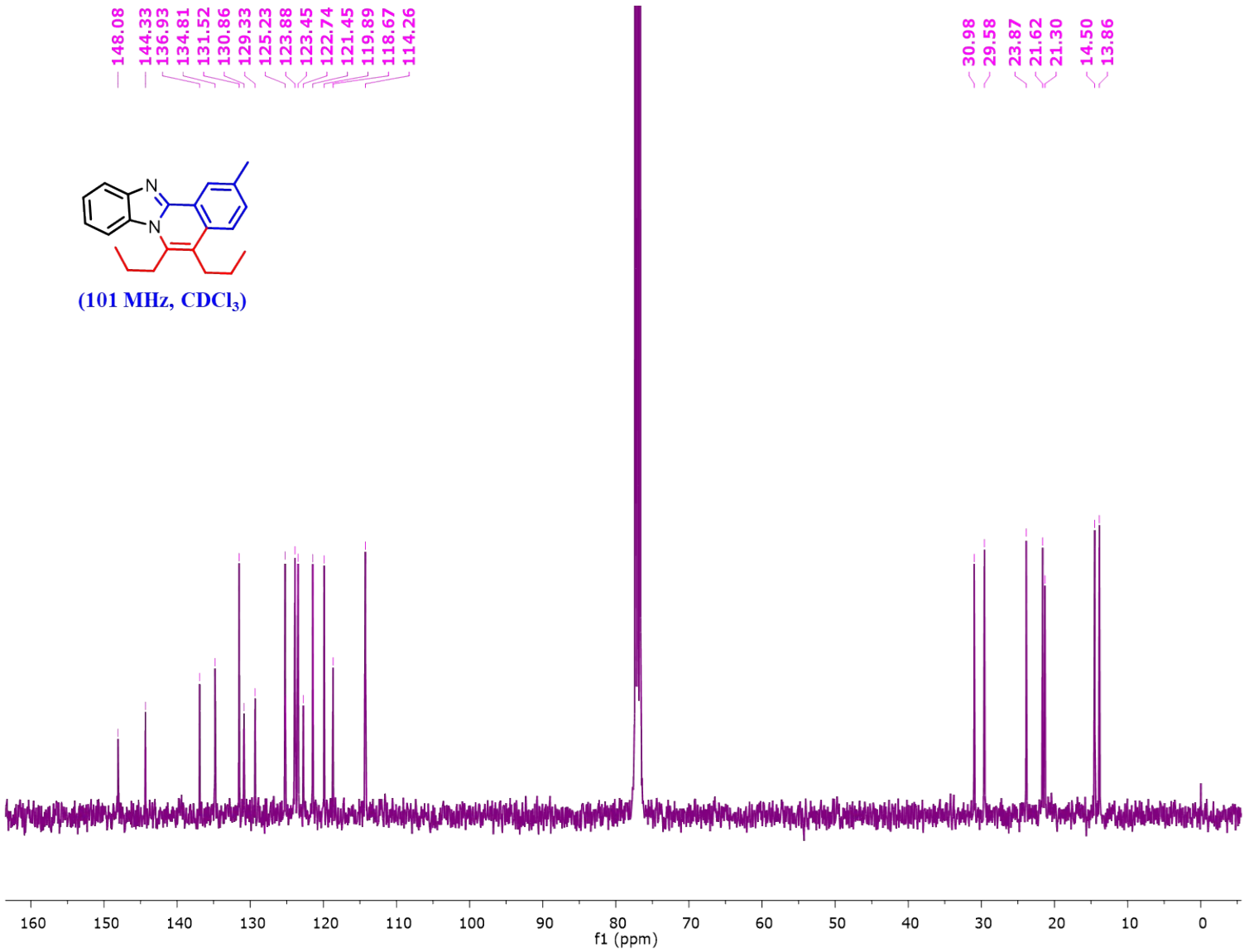

Fig. S87. ^{13}C NMR spectra of 2-methyl-5,6-dipropylbenzo [4,5] imidazo[2,1-a] isoquinoline (**5m**) in $CDCl_3$.

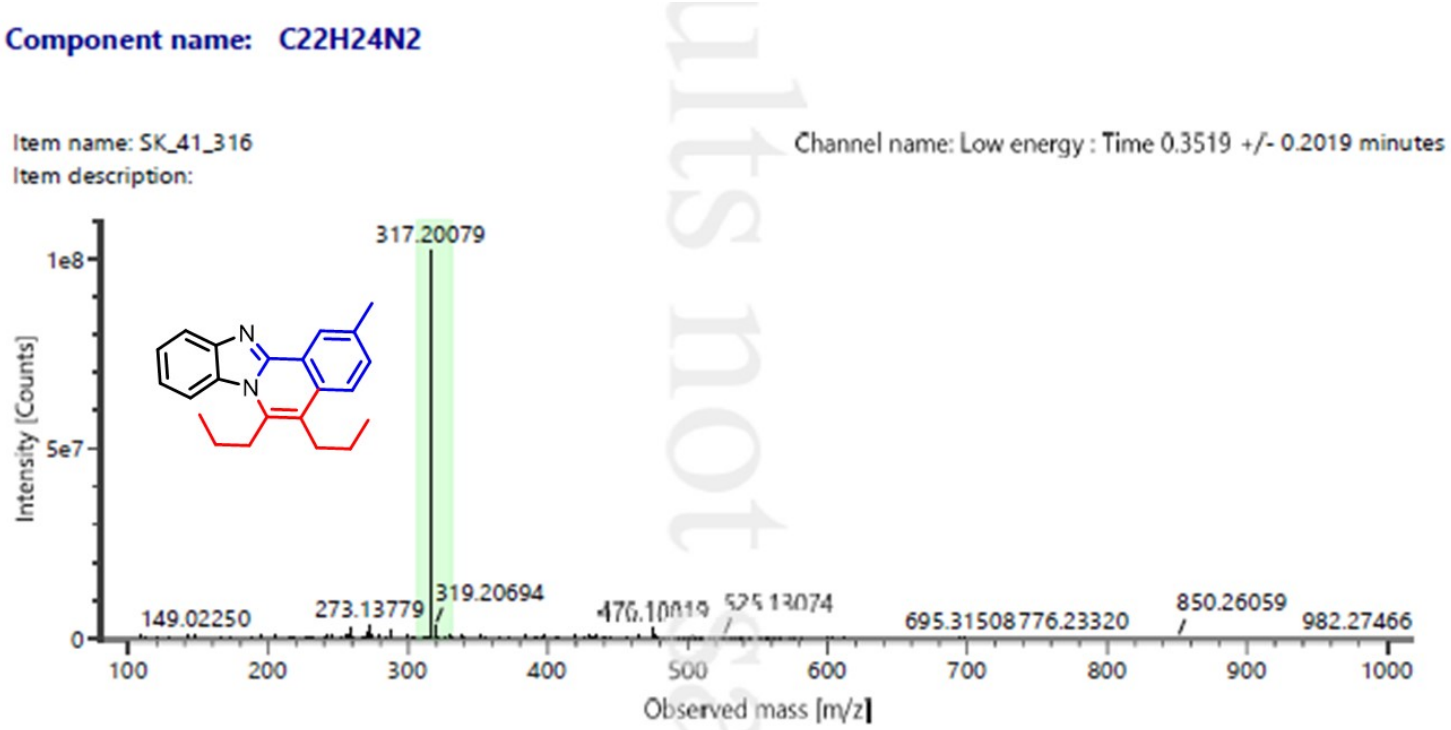

Fig. S88. HRMS spectra of 2-methyl-5,6-dipropylbenzo [4,5] imidazo [2,1-a] isoquinoline (**5m**).

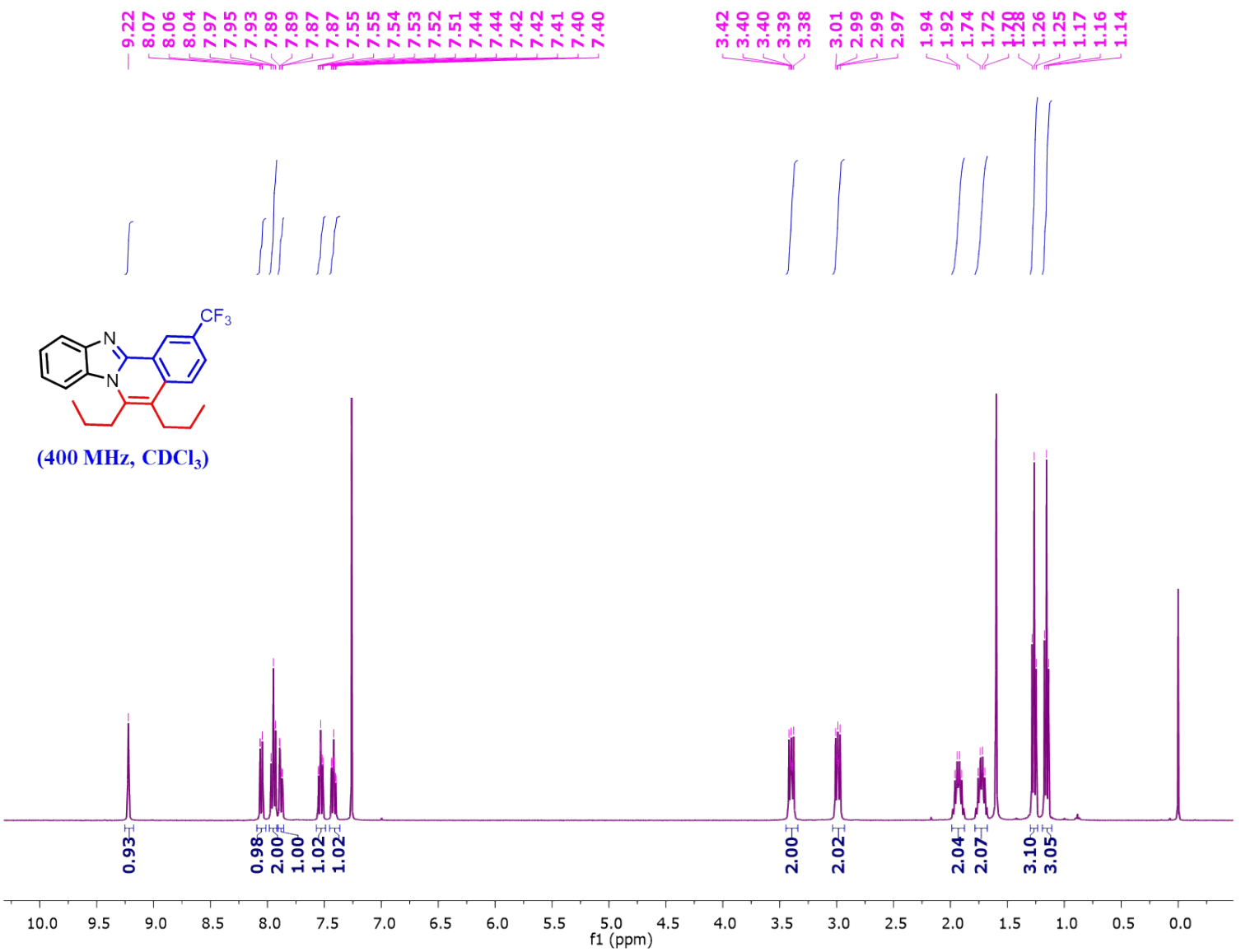

Fig. S89. ^{1}H NMR spectra of 5,6-dipropyl-2-(trifluoromethyl) benzo [4,5] imidazo[2,1-a] isoquinoline (**5n**) in $CDCl_3$.

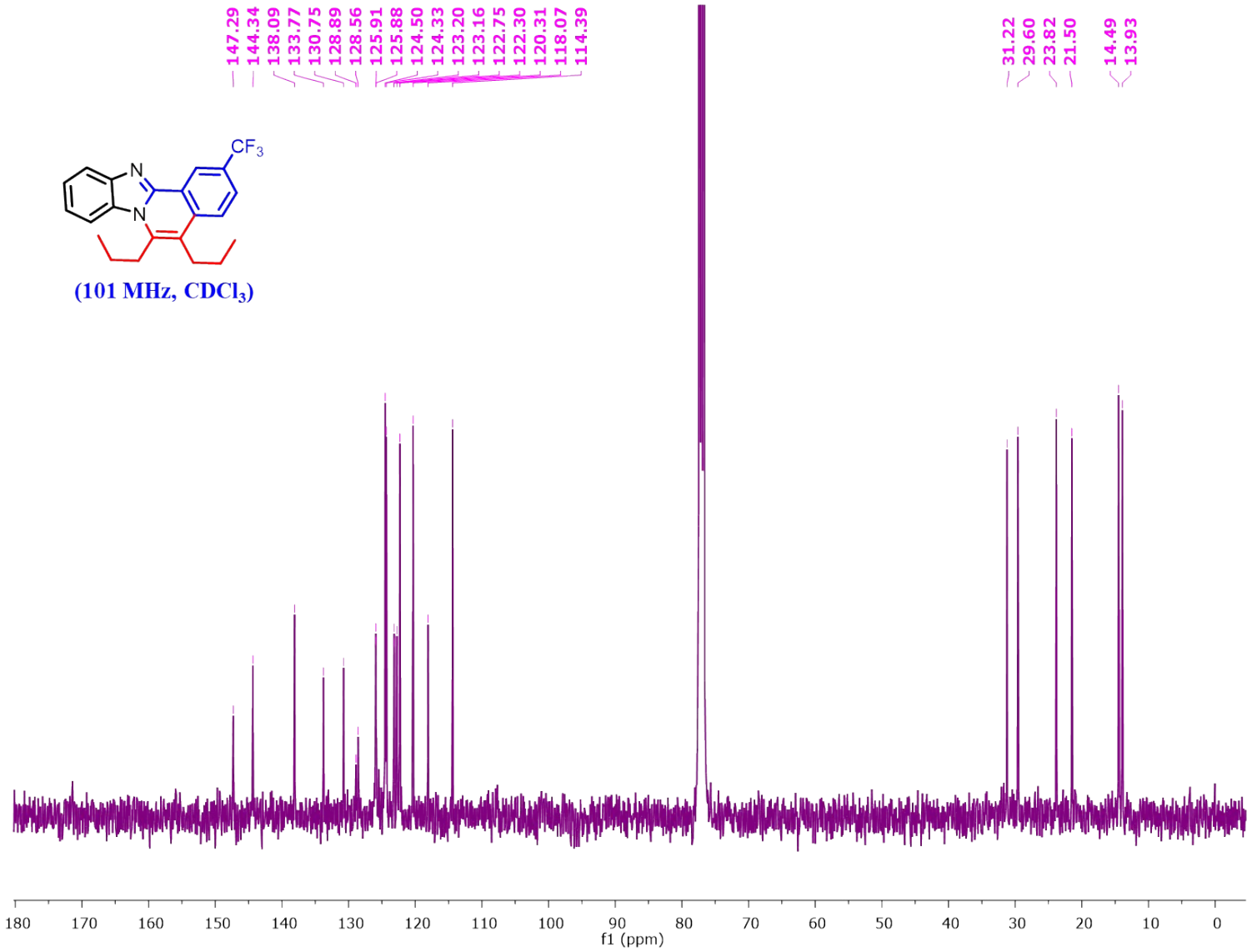

Fig. S90. ^{13}C NMR spectra of 5,6-dipropyl-2-(trifluoromethyl) benzo [4,5] imidazo[2,1-a] isoquinoline (**5n**) in $CDCl_3$.

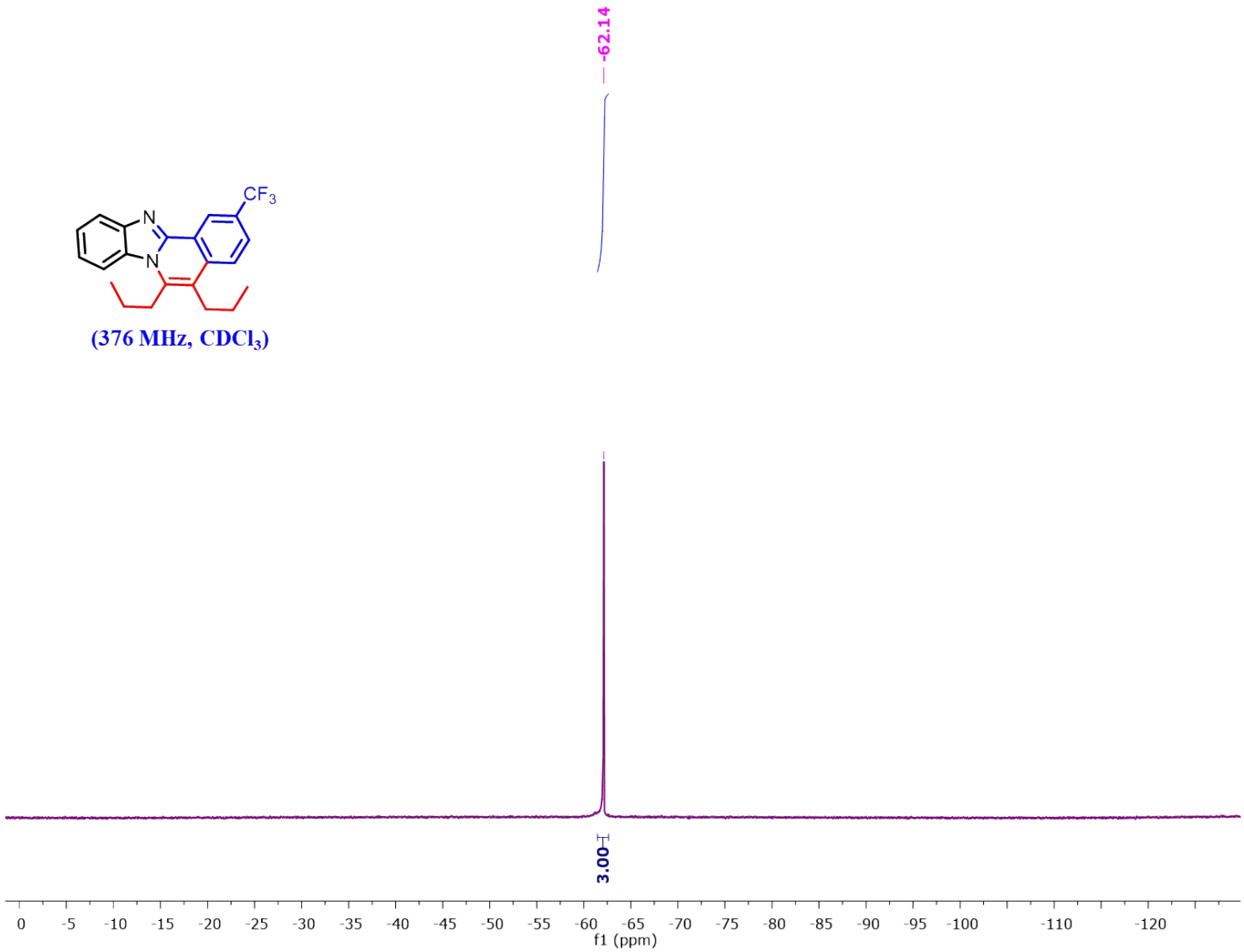

Fig. S91. ^{19}F NMR spectra of 5,6-dipropyl-2-(trifluoromethyl) benzo [4,5] imidazo [2,1-a] isoquinoline (**5n**) in $CDCl_3$.

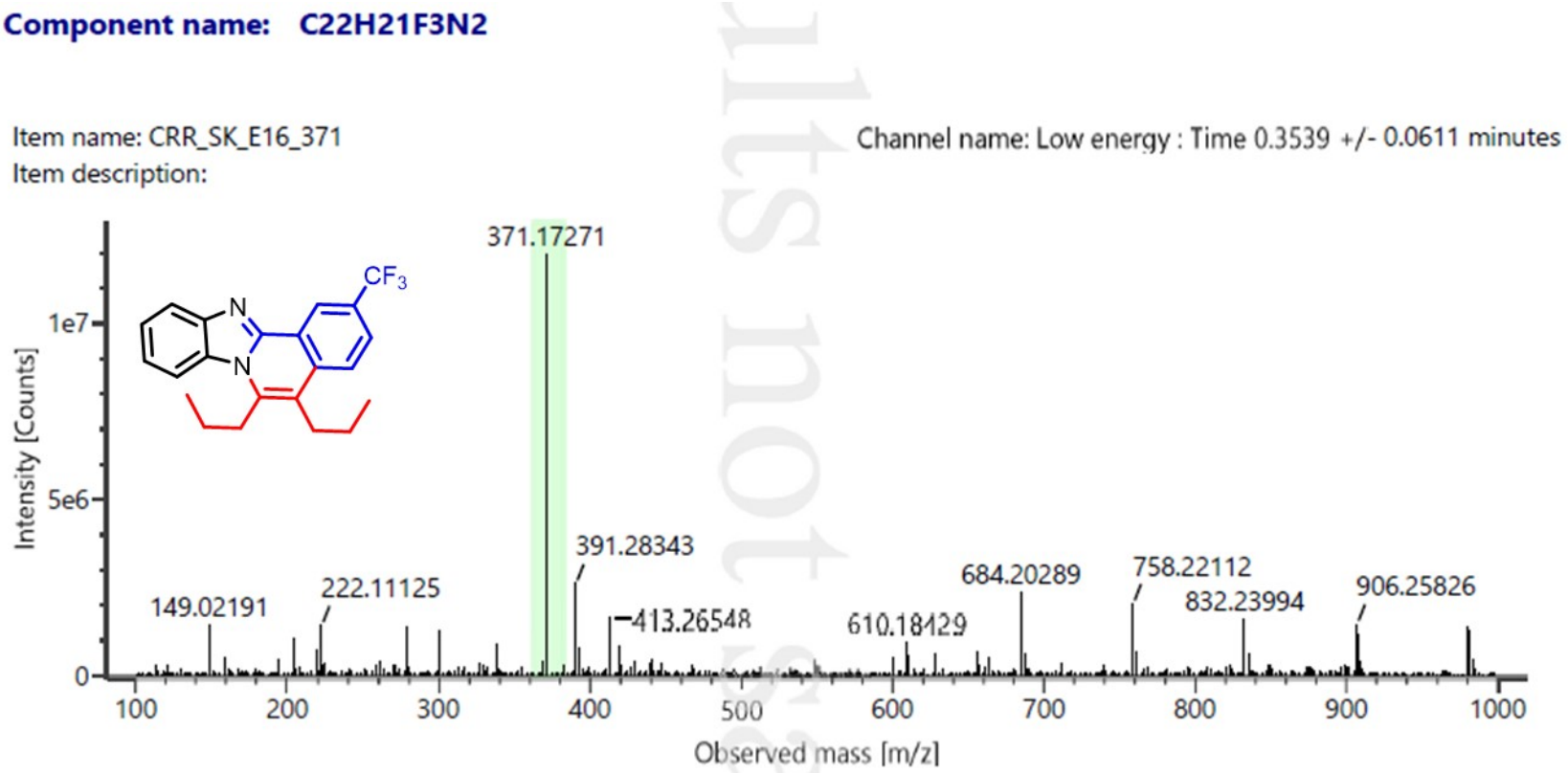

Fig. S92. HRMS spectra of 5,6-dipropyl-2-(trifluoromethyl) benzo [4,5] imidazo [2,1-a] isoquinoline (**5n**).

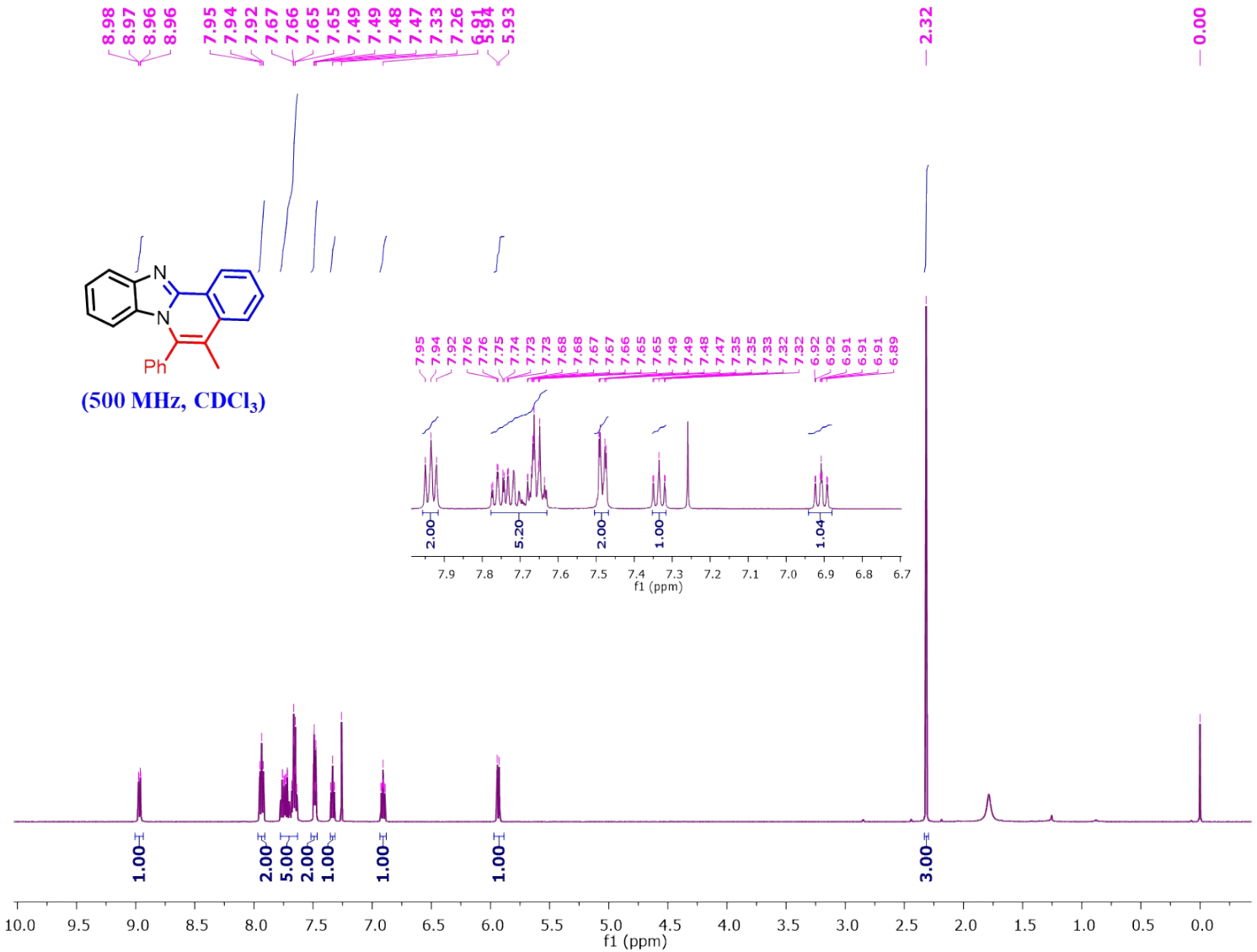

Fig. S93. ^{1}H NMR spectra of 5-methyl-6-phenylbenzo [4,5] imidazo [2,1-a] isoquinoline (**5o**) in $CDCl_3$.

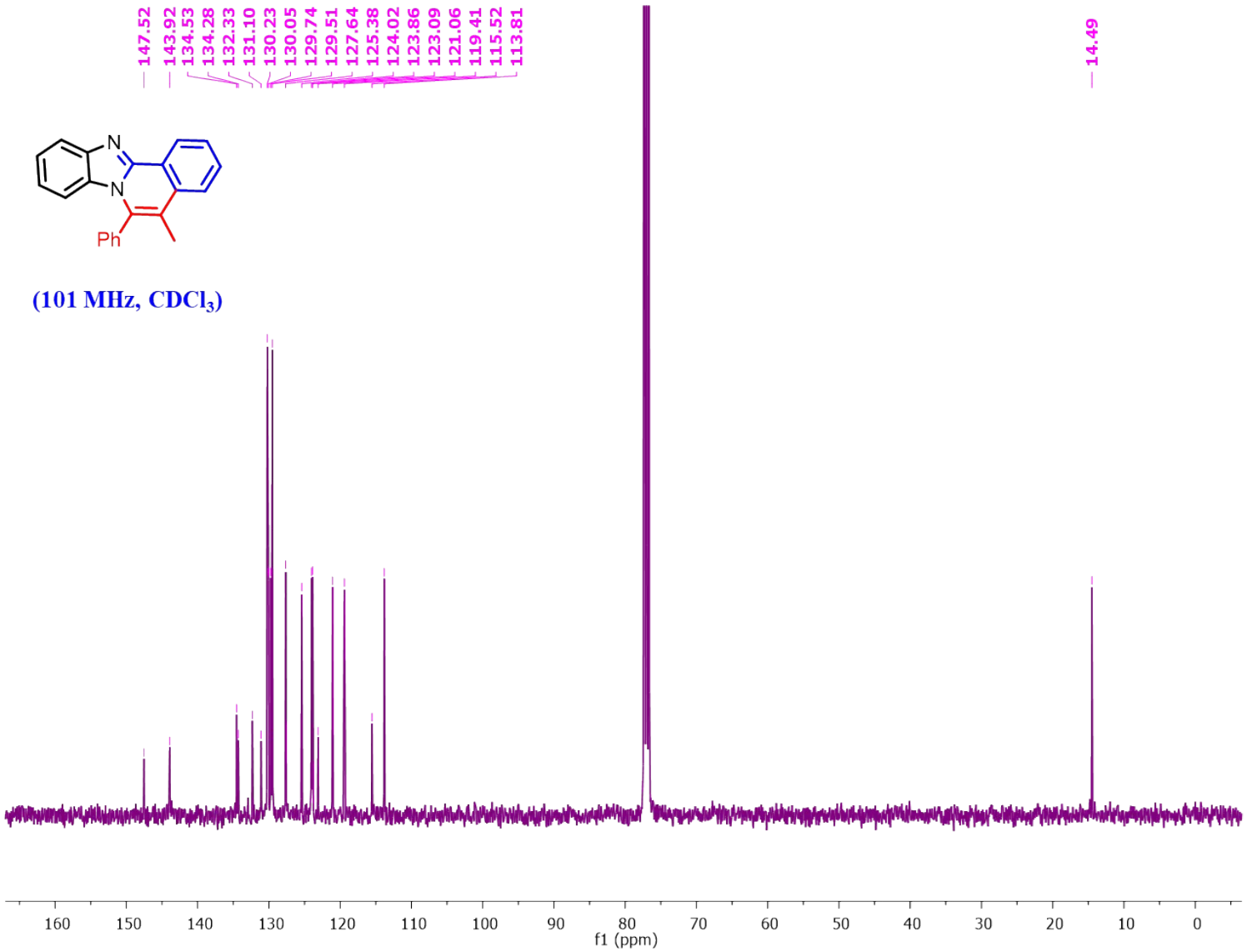

Fig. S94. ^{13}C NMR spectra of 5-methyl-6-phenylbenzo [4,5] imidazo [2,1-a] isoquinoline (**5o**) in $CDCl_3$.

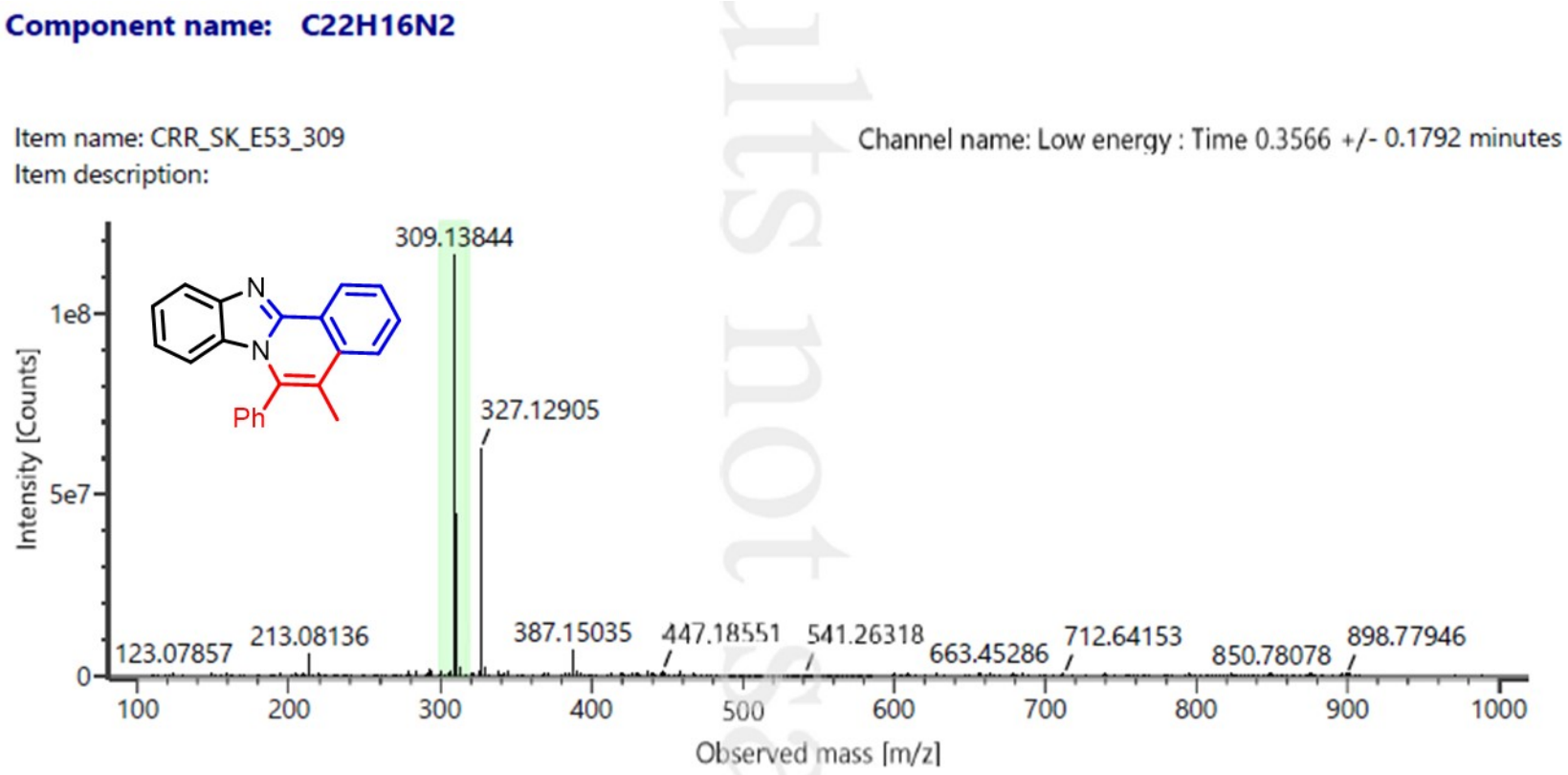

Fig. S95. HRMS spectra of 5-methyl-6-phenylbenzo [4,5] imidazo [2,1-a] isoquinoline (**5o**).

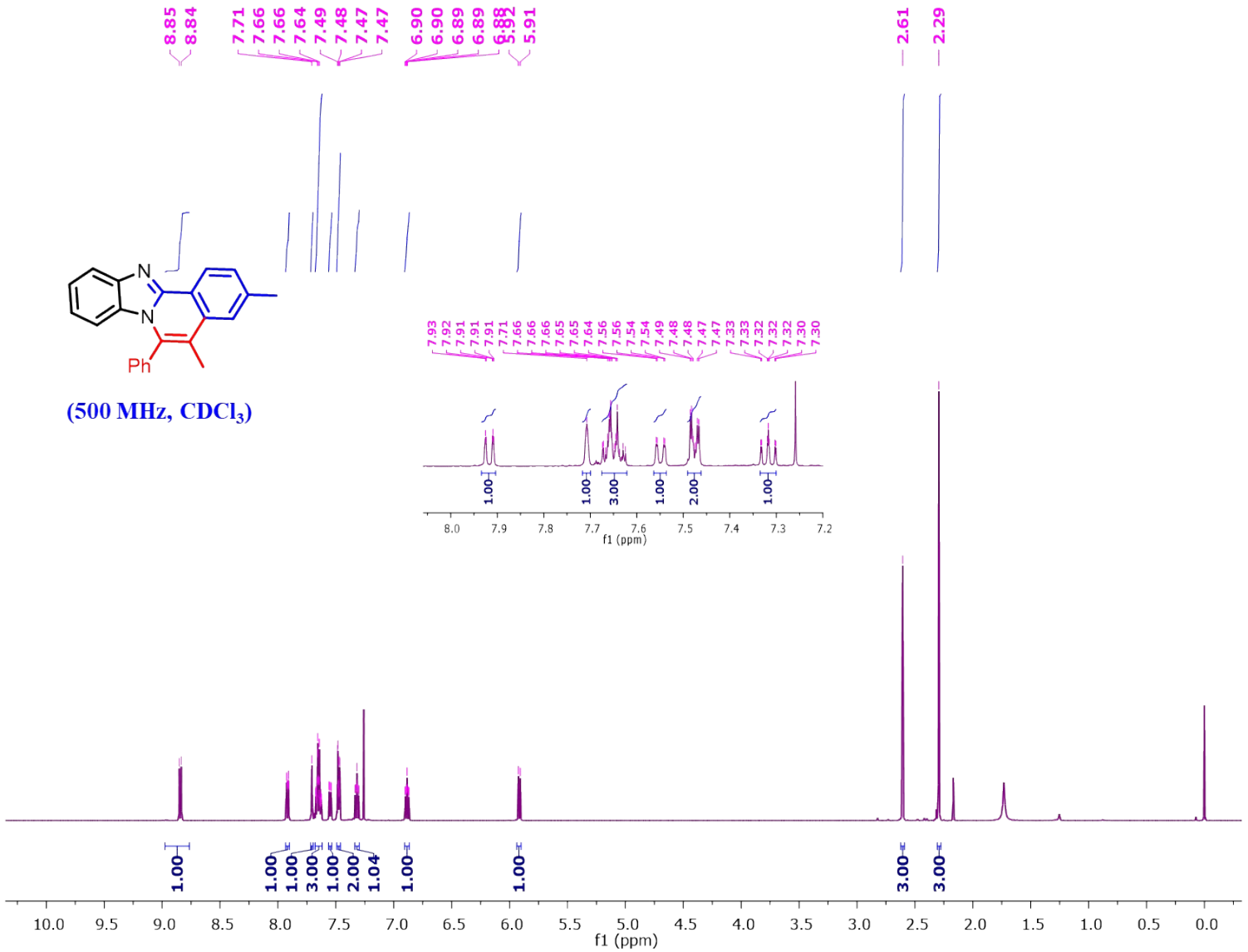

Fig. S96. ^{1}H NMR spectra of 3,5-dimethyl-6-phenylbenzo [4,5] imidazo [2,1-a] isoquinoline (**5p**) in $CDCl_3$.

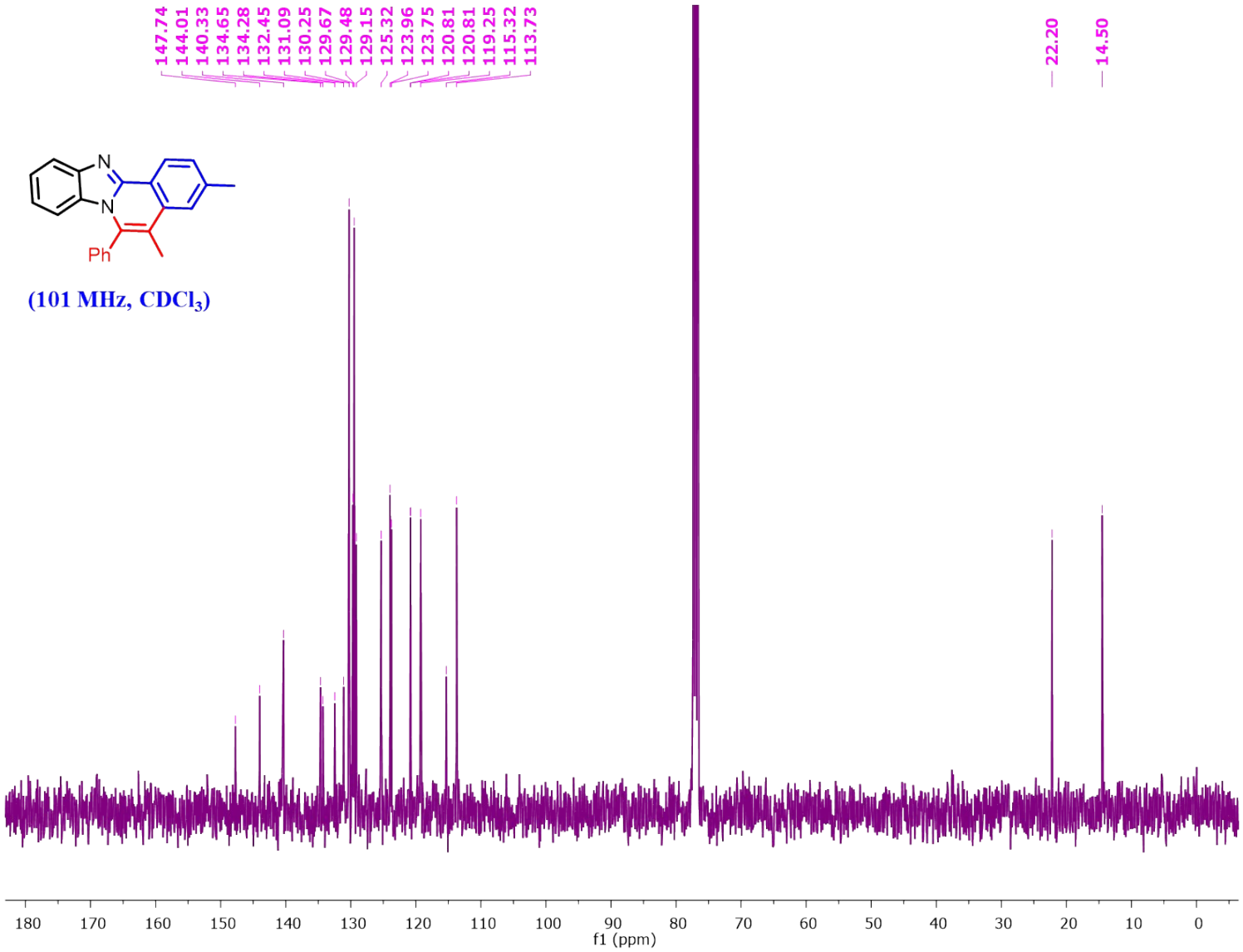

Fig. S97. ^{13}C NMR spectra of 3,5-dimethyl-6-phenylbenzo [4,5] imidazo [2,1-a] isoquinoline (**5p**) in $CDCl_3$.

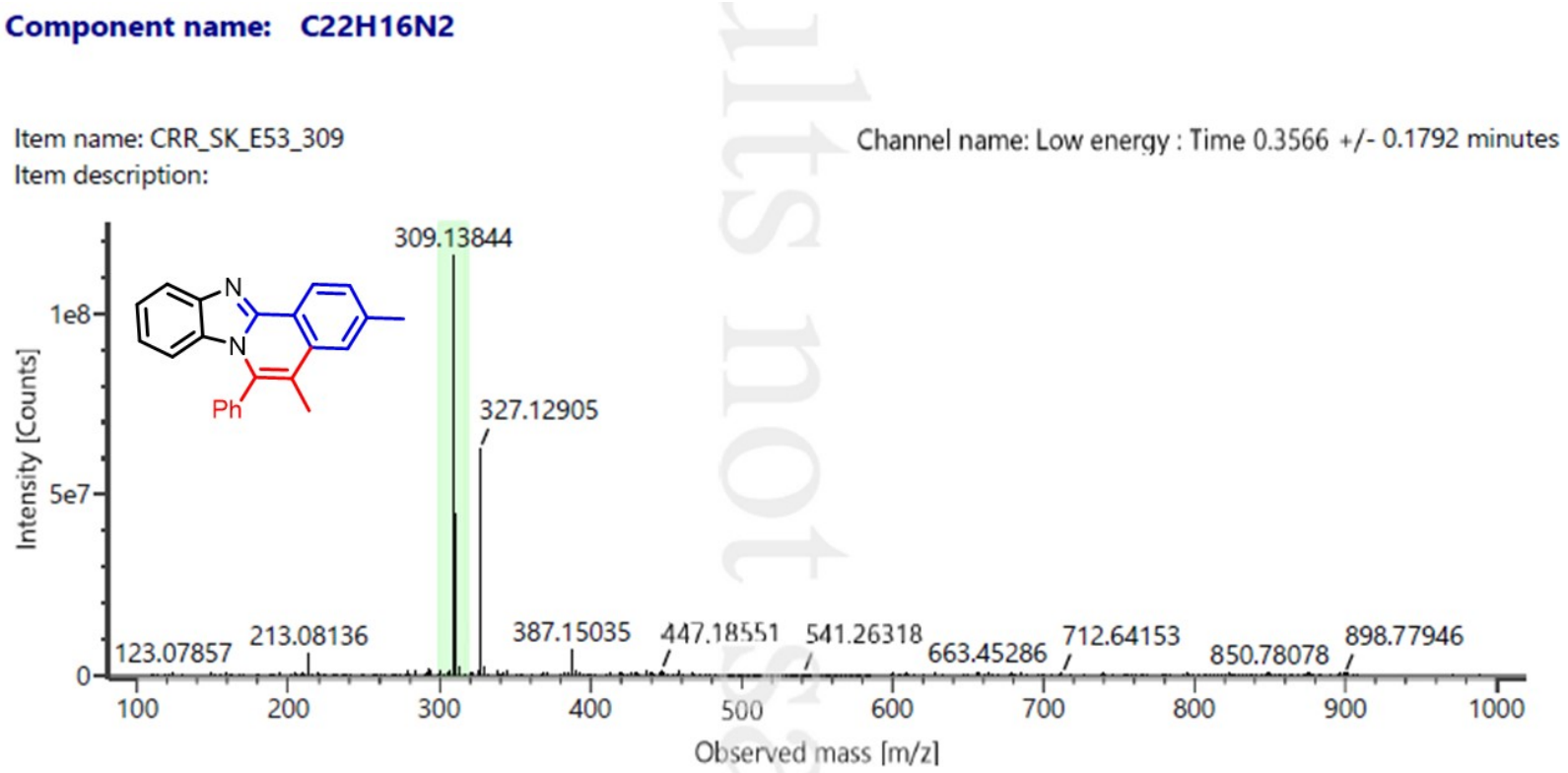

Fig. S98. HRMS spectra of 3,5-dimethyl-6-phenylbenzo [4,5] imidazo[2,1-a] isoquinoline (**5p**).

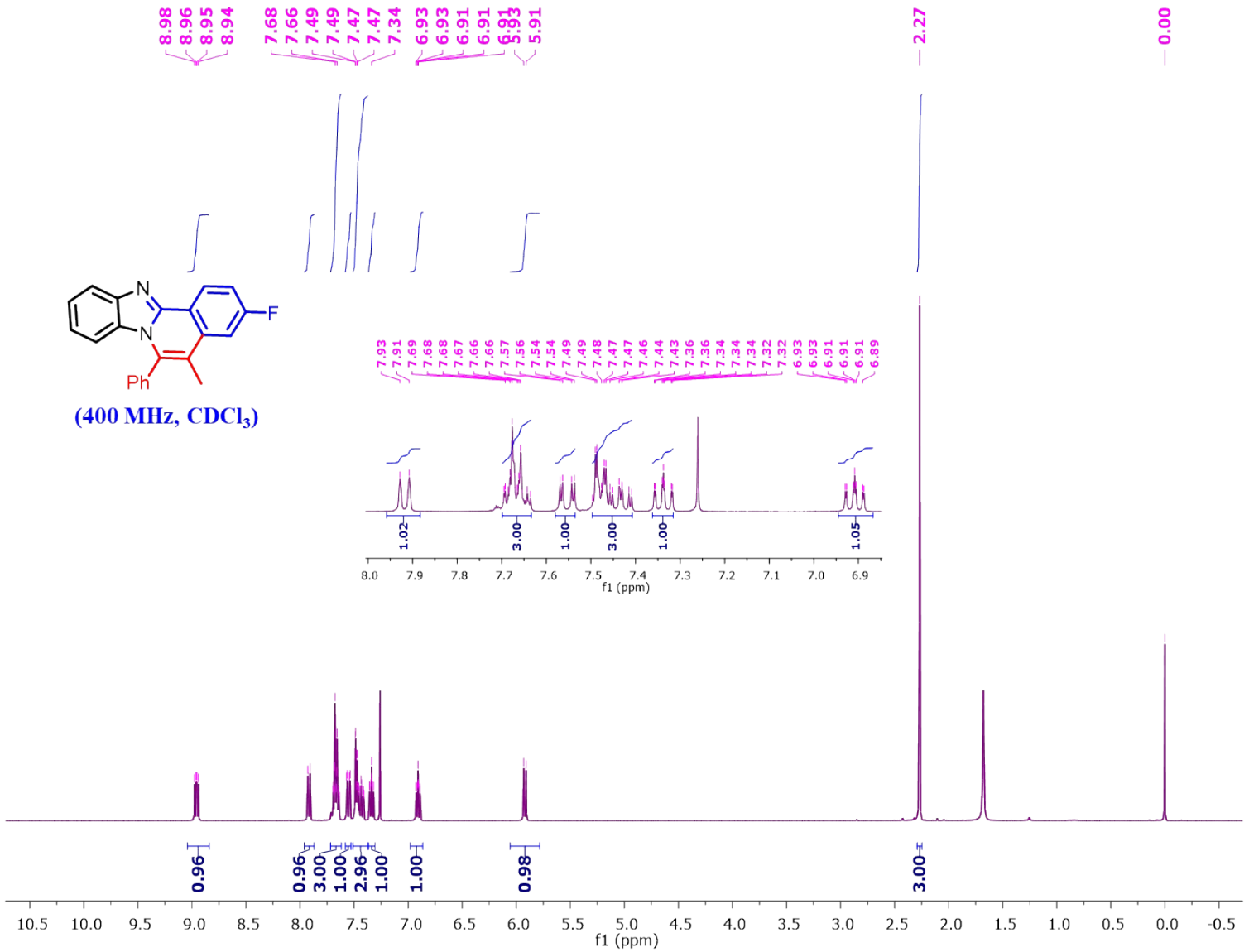

Fig. S99. ^{1}H NMR spectra of 3-fluoro-5-methyl-6-phenylbenzo [4,5] imidazo [2,1-a] isoquinoline (**5q**) in $CDCl_3$.

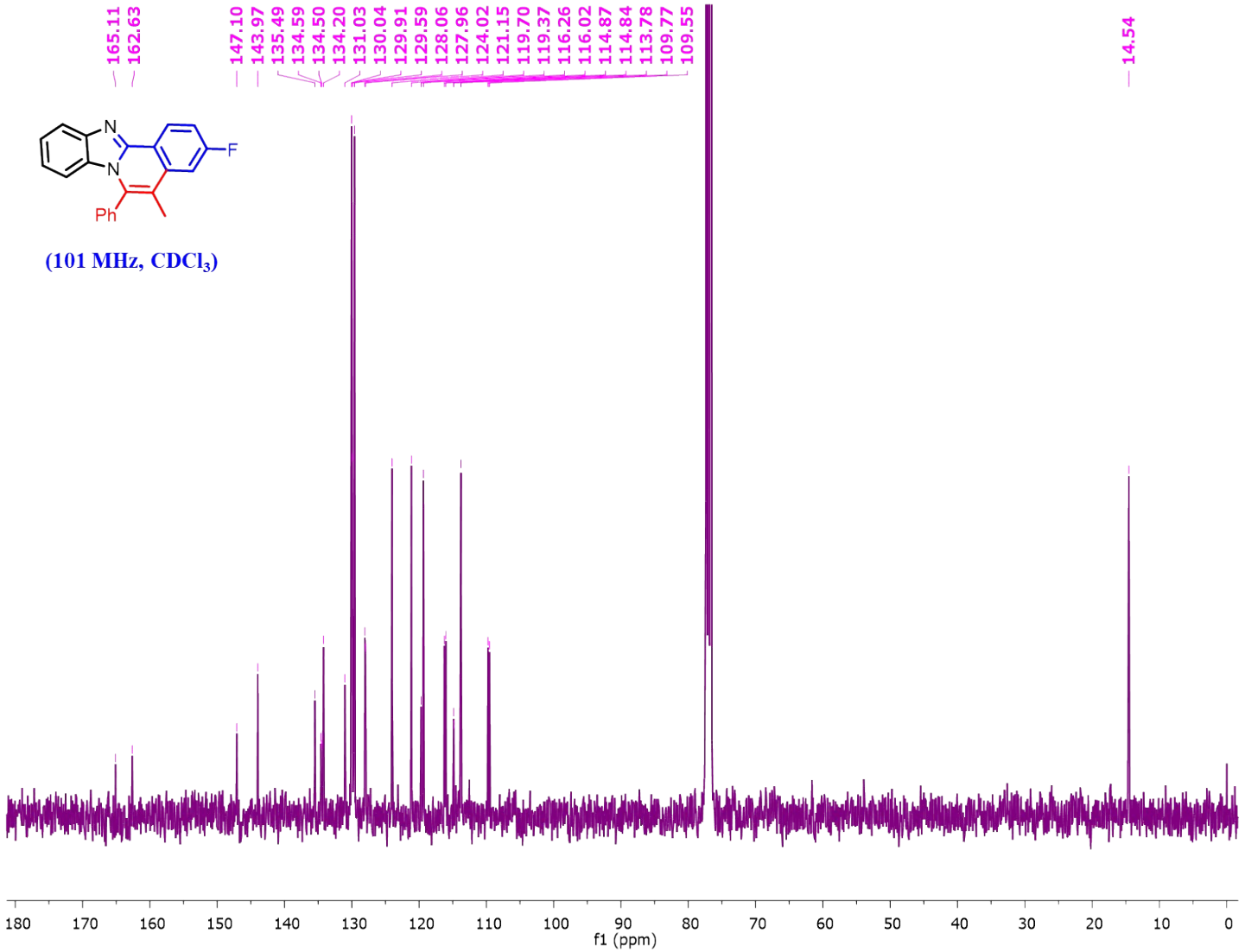

Fig. S100. ^{13}C NMR spectra of 3-fluoro-5-methyl-6-phenylbenzo [4,5] imidazo[2,1-a] isoquinoline (**5q**) in $CDCl_3$.

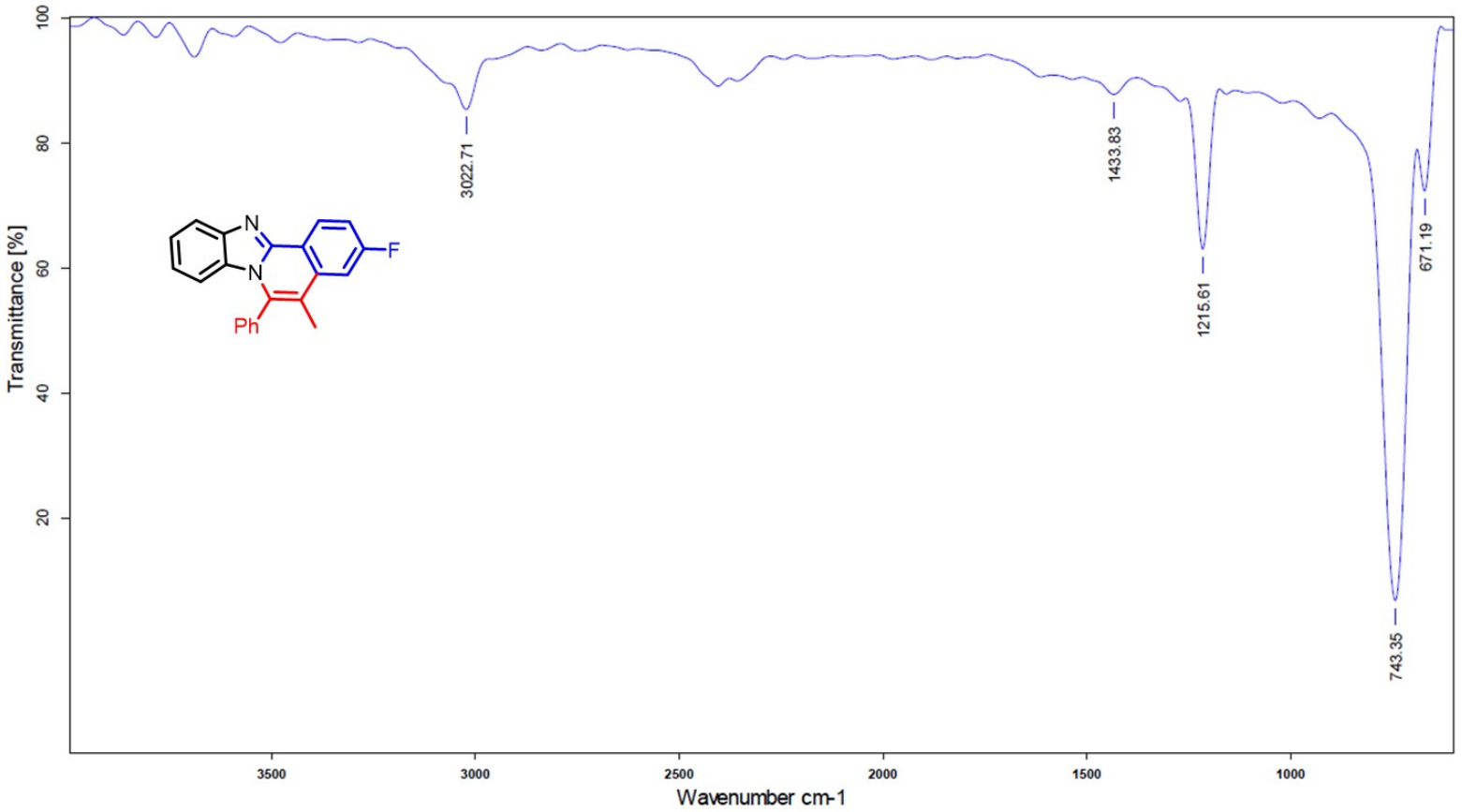

Fig. S101. IR spectra of 3-fluoro-5-methyl-6-phenylbenzo [4,5] imidazo[2,1-a] isoquinoline (**5q**).

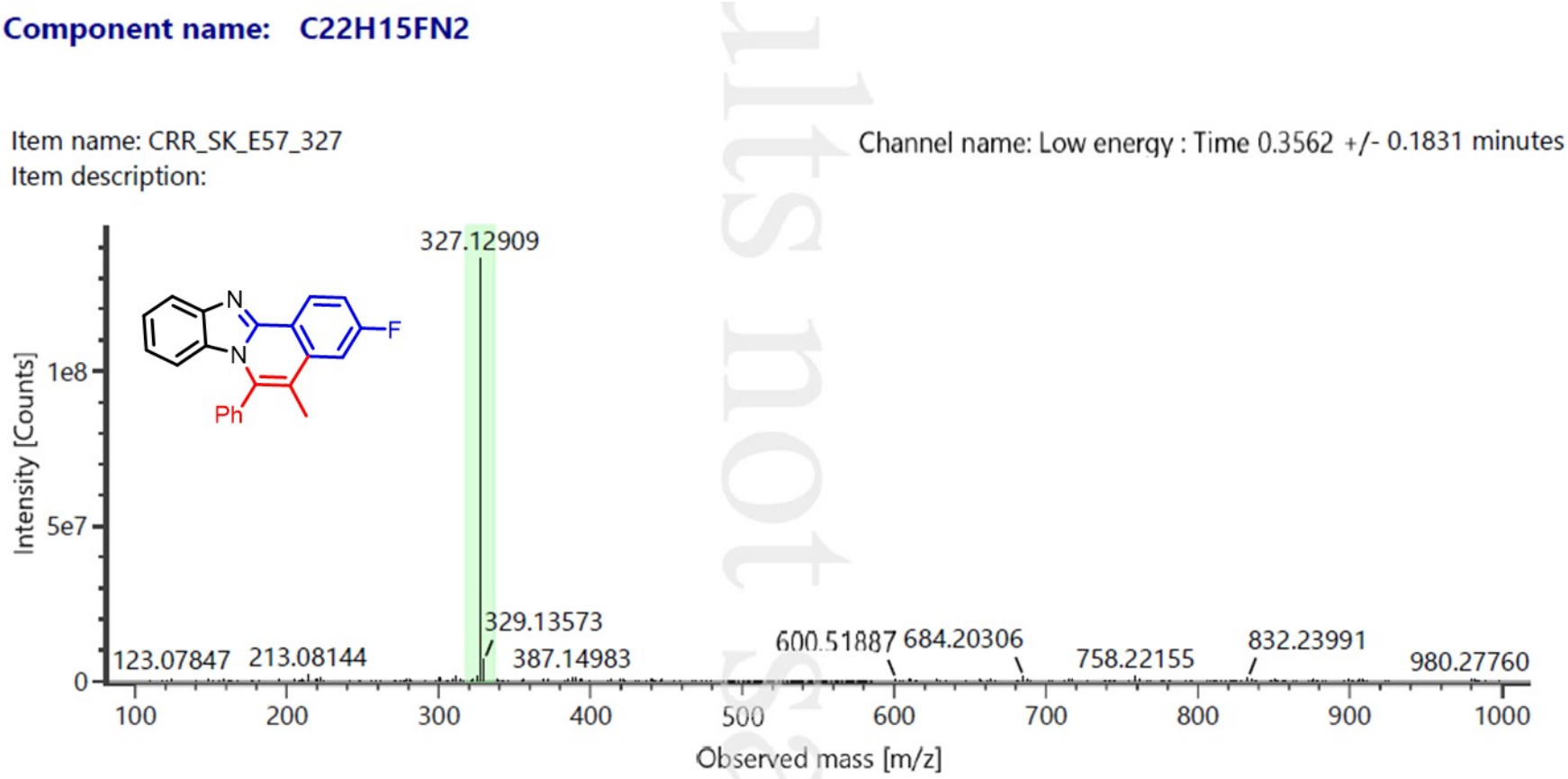

Fig. S102. HRMS spectra of 3-fluoro-5-methyl-6-phenylbenzo [4,5] imidazo[2,1-a] isoquinoline (**5q**).

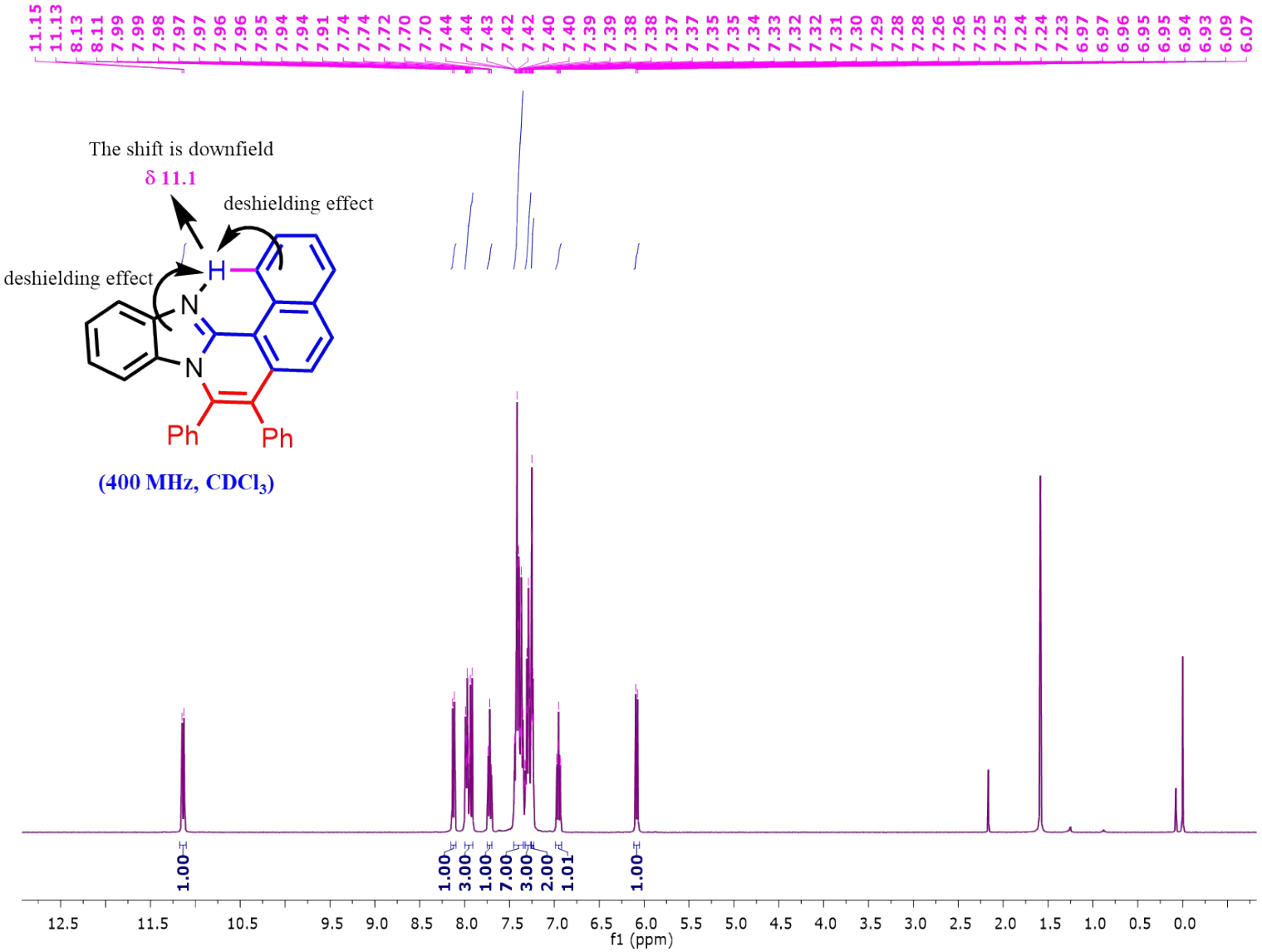

Fig. S103. ^{1}H NMR spectra of 7,8-diphenylbenzo[h]benzo [4,5] imidazo[2,1-a] isoquinoline (**5r**) in $CDCl_3$.

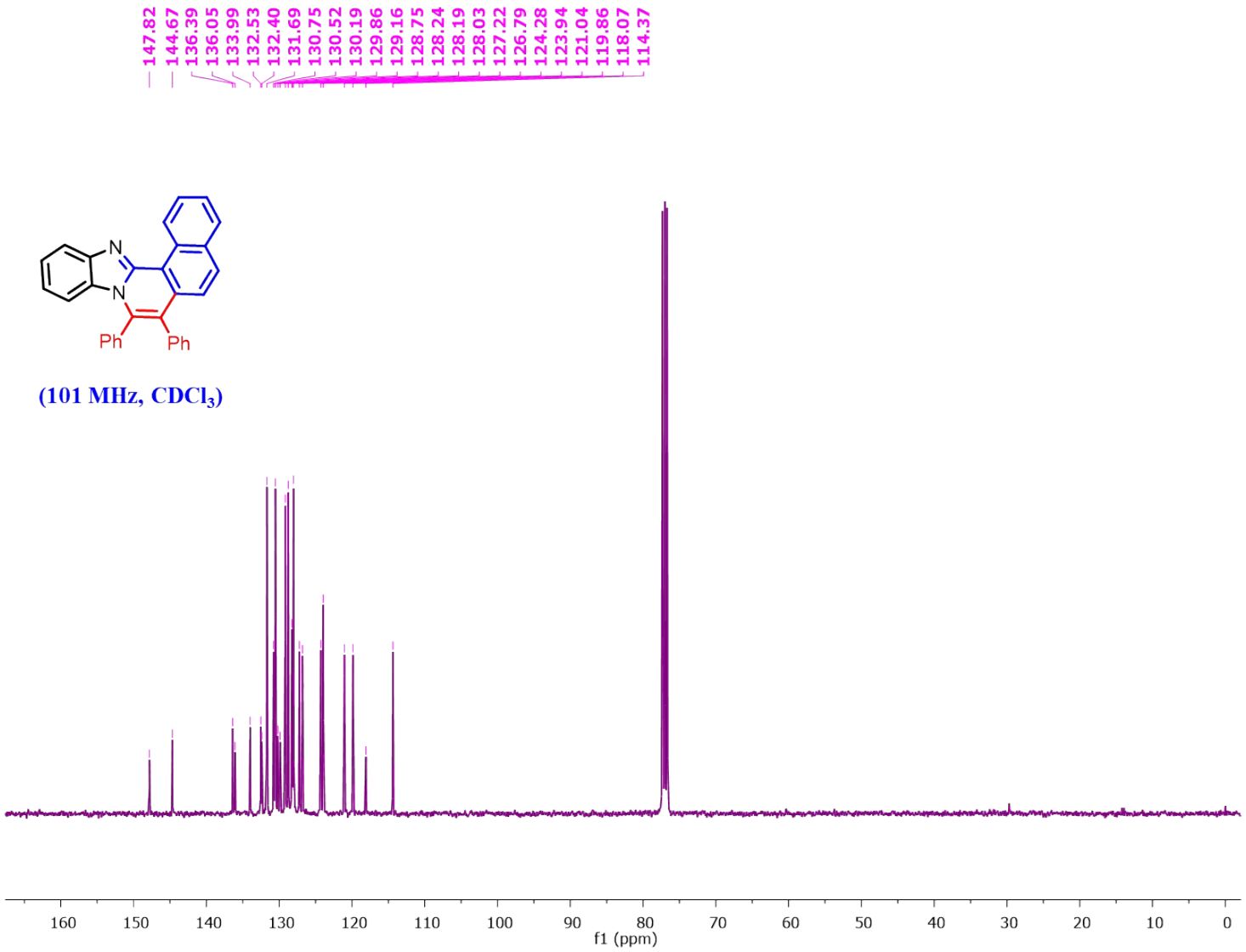

Fig. S104. ^{13}C NMR spectra of 7,8-diphenylbenzo[h] benzo [4,5] imidazo [2,1-a] isoquinoline (**5r**) in $CDCl_3$.

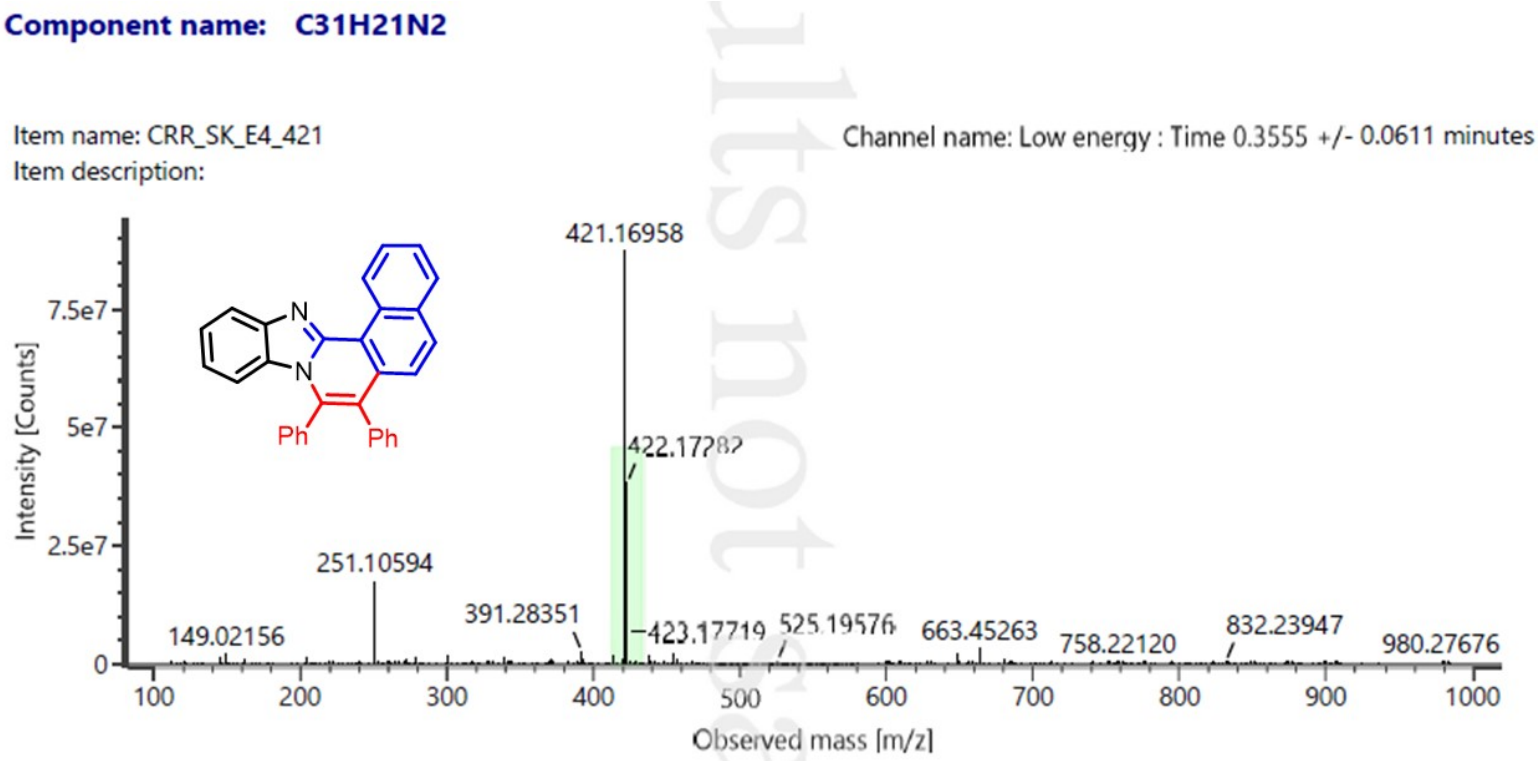

Fig. S105. HRMS spectra of 7,8-diphenylbenzo[h]benzo [4,5] imidazo[2,1-a] isoquinoline (**5r**).

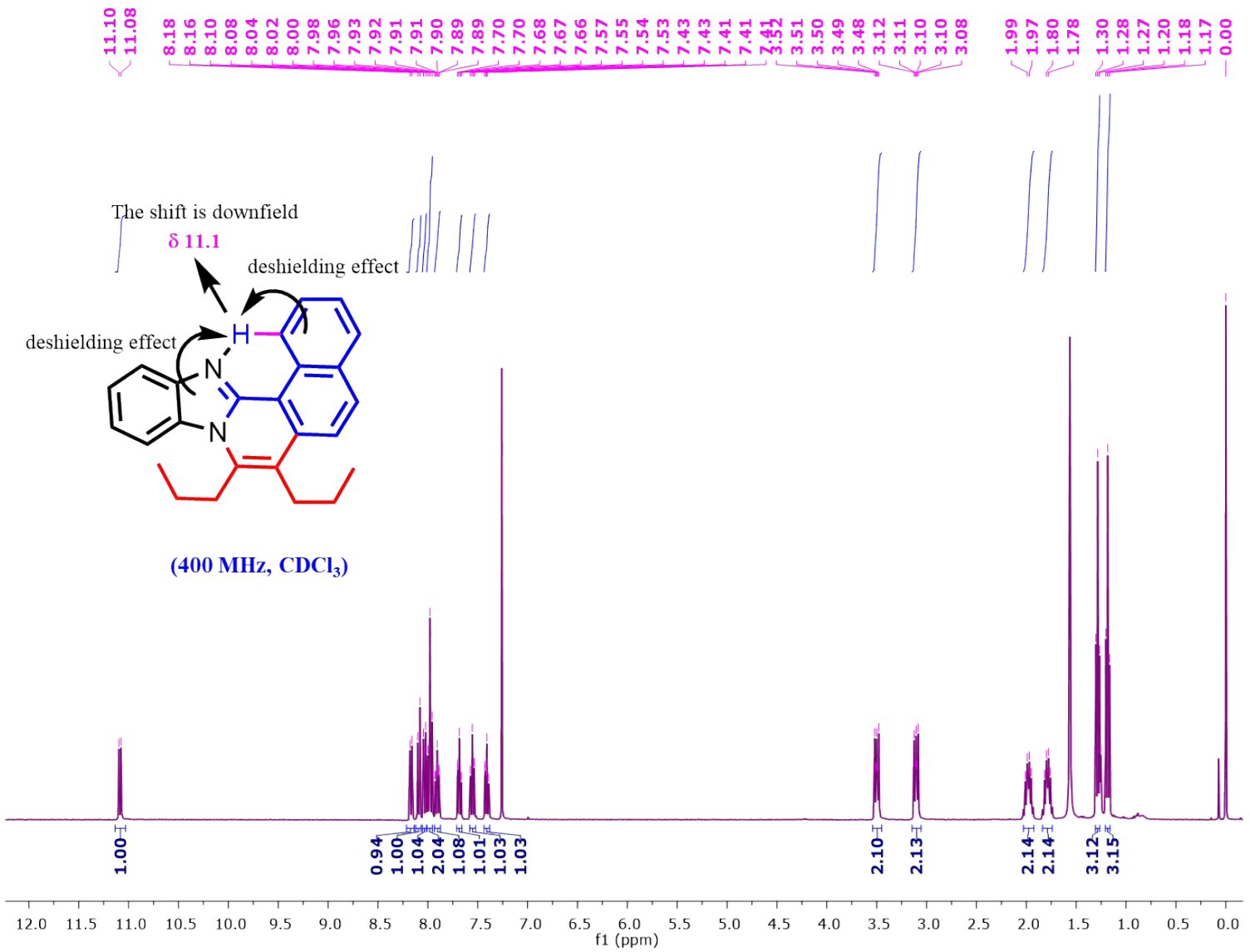

Fig. S106. ^{1}H NMR spectra of 7,8-dipropylbenzo[h]benzo [4,5] imidazo[2,1-a] isoquinoline (**5s**) in $CDCl_3$.

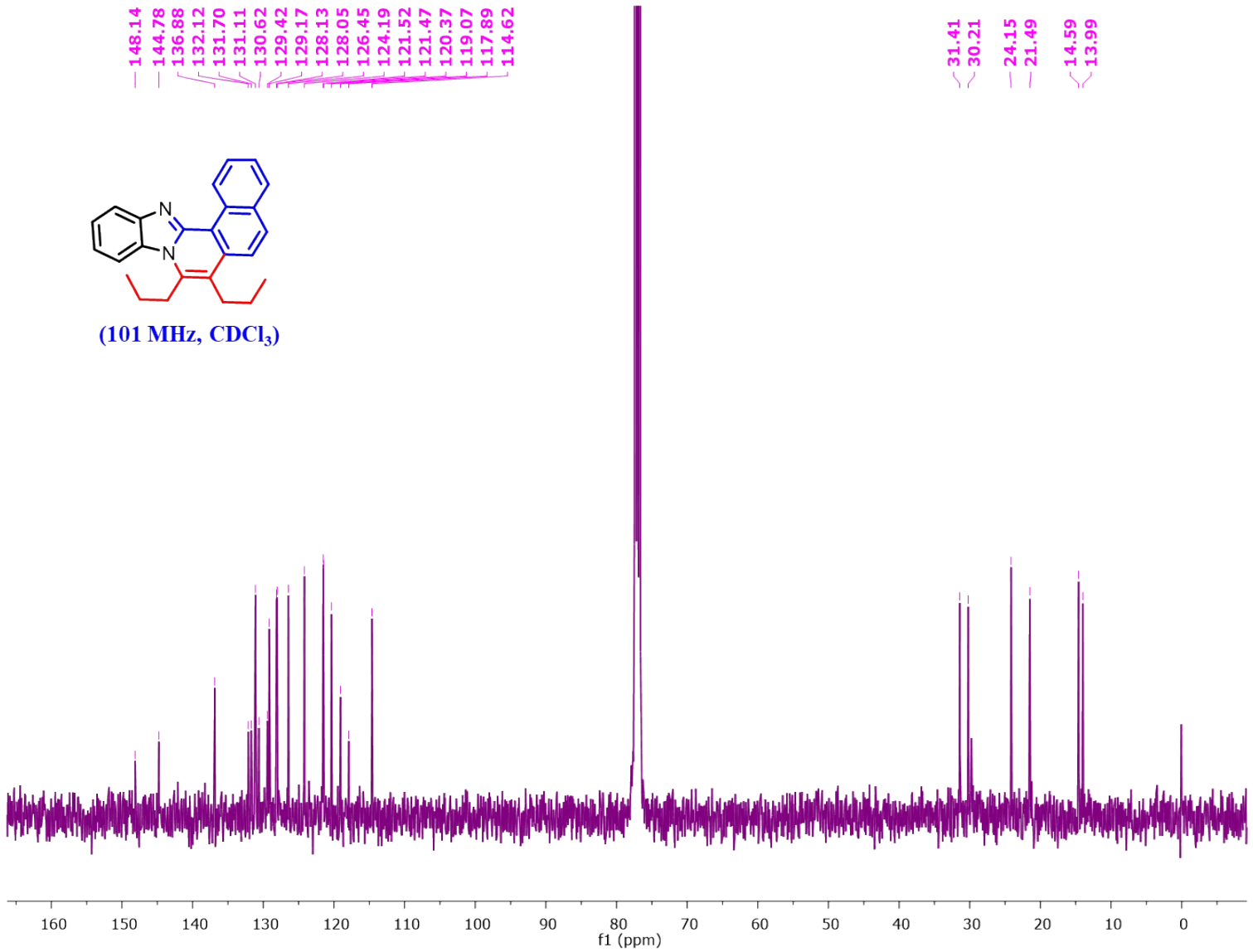

Fig. S107. ^{13}C NMR spectra of 7,8-dipropylbenzo[h]benzo [4,5] imidazo[2,1-a] isoquinoline (**5s**) in $CDCl_3$.

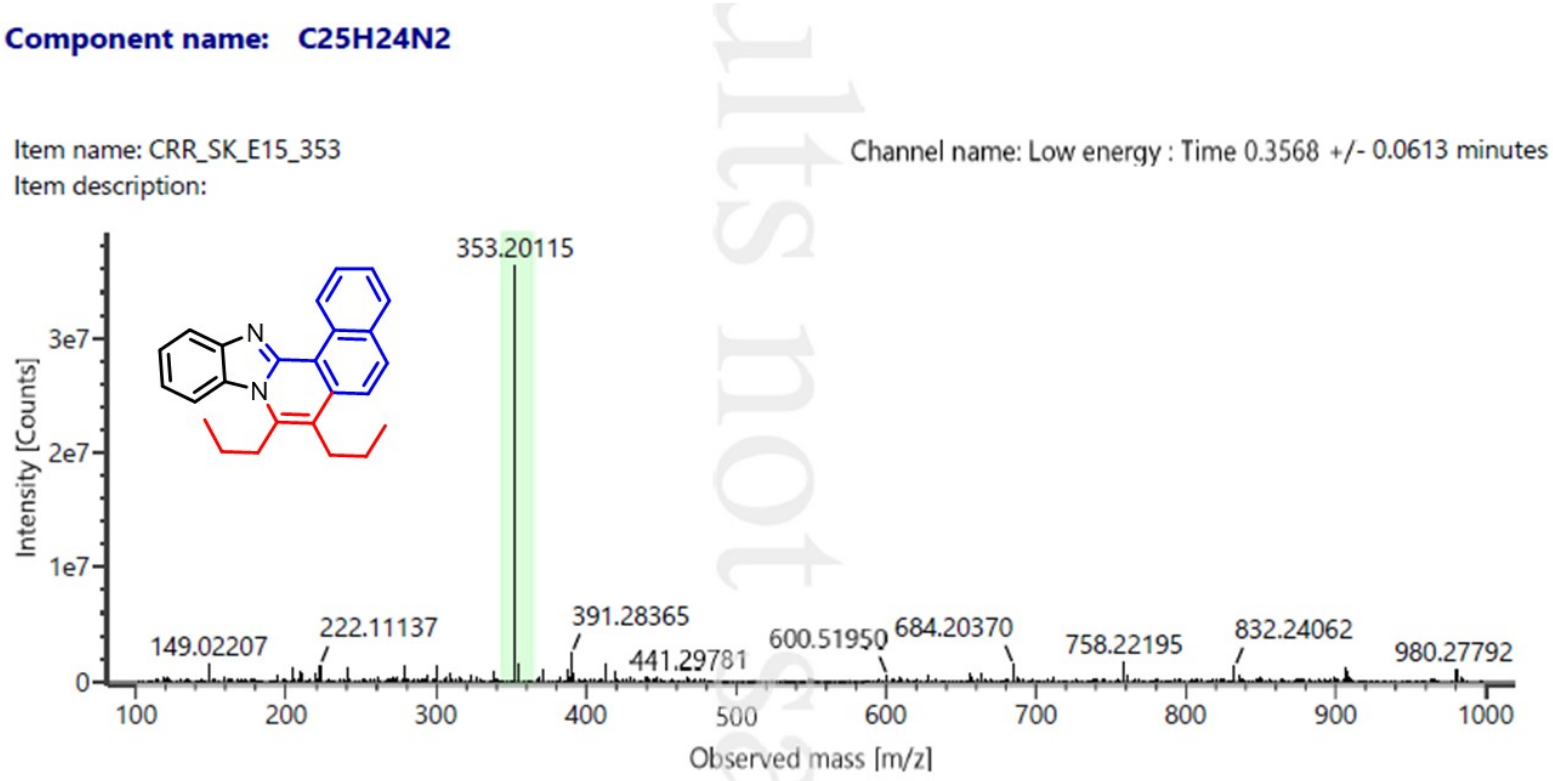

Fig. S108. HRMS spectra of 7,8-dipropylbenzo[h]benzo [4,5] imidazo[2,1-a] isoquinoline (**5s**).

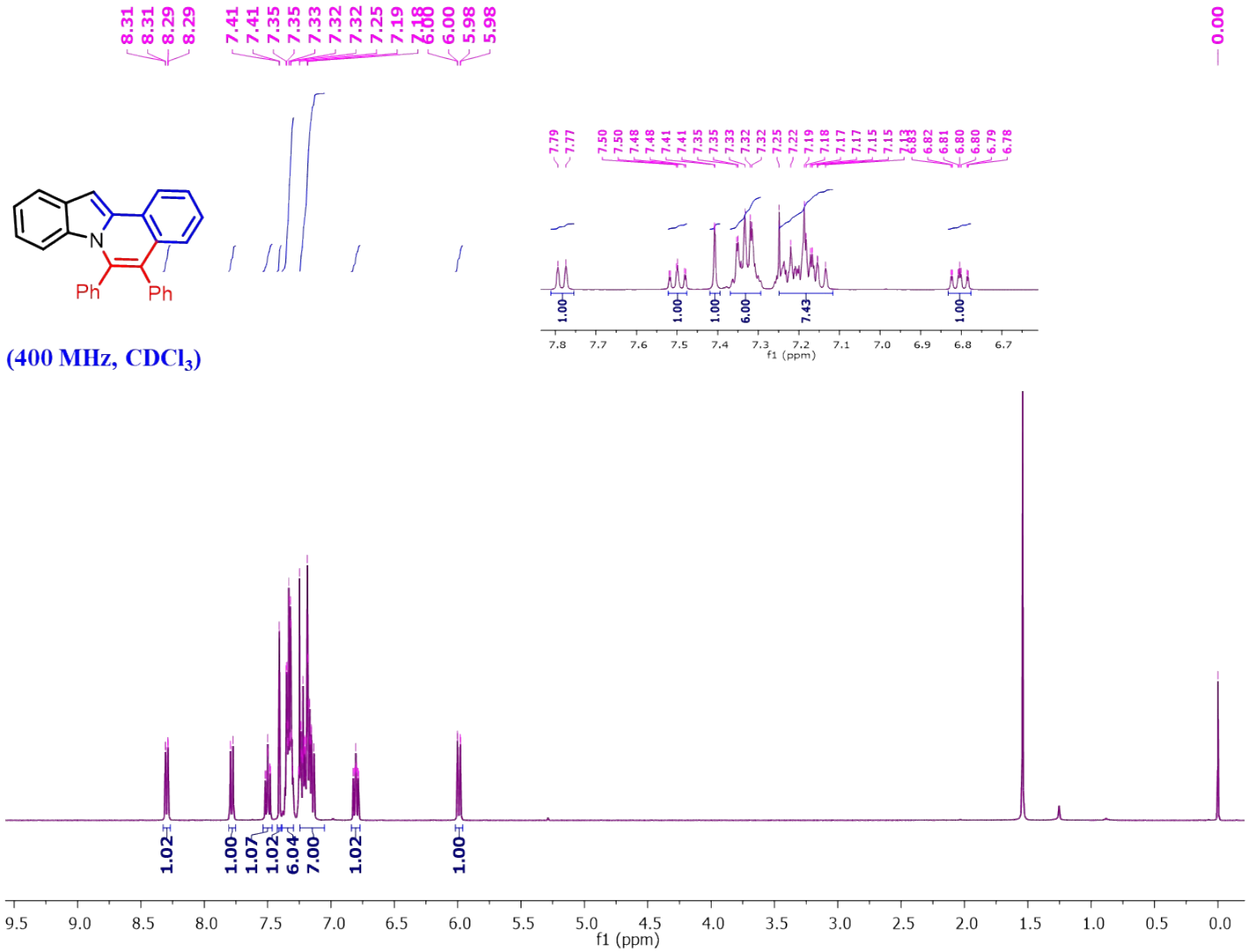

Fig. S109. ^{1}H NMR spectra of diphenylindolo [2,1-a] isoquinoline (**5t**) in $CDCl_3$.

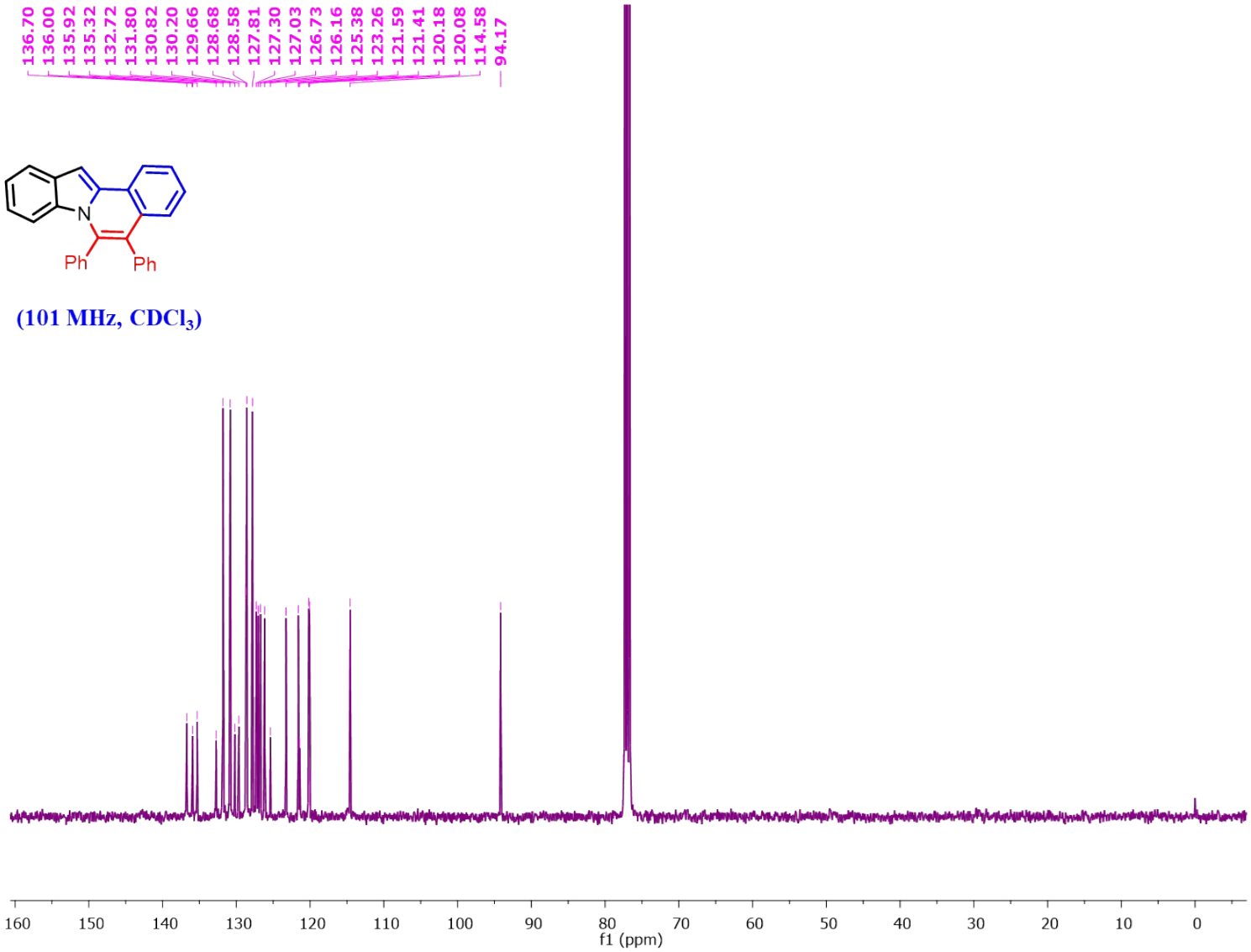

Fig. S110. ^{13}C NMR spectra of diphenylindolo [2,1-a] isoquinoline (**5t**) in $CDCl_3$.

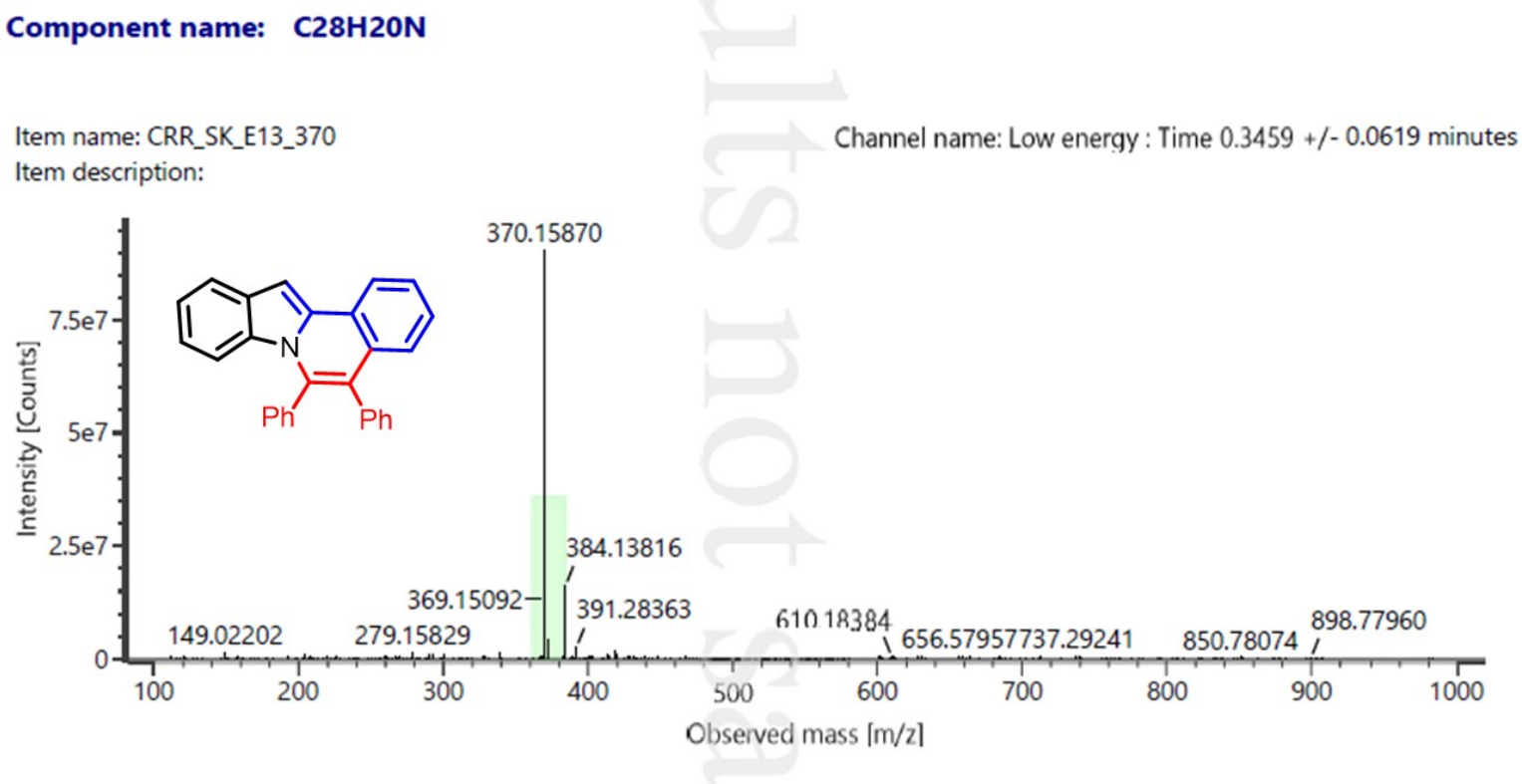

Fig. S111. HRMS spectra of diphenylindolo[2,1-a]isoquinoline (**5t**).

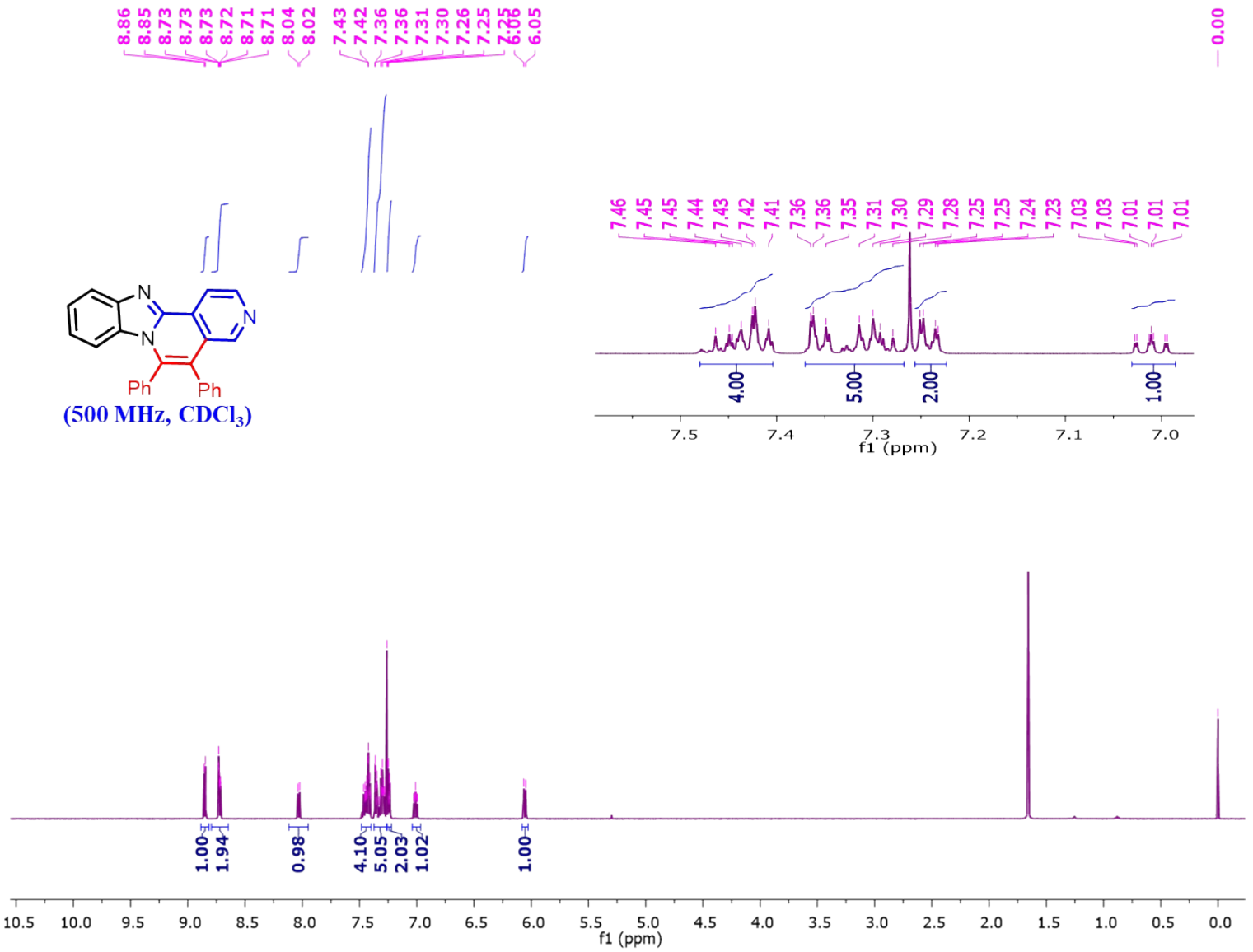

Fig. S112. ^{1}H NMR spectra of 5,6-diphenylbenzo [4,5] imidazo[2,1-a] [2,6] naphthyridine (**5u**) in $CDCl_3$.

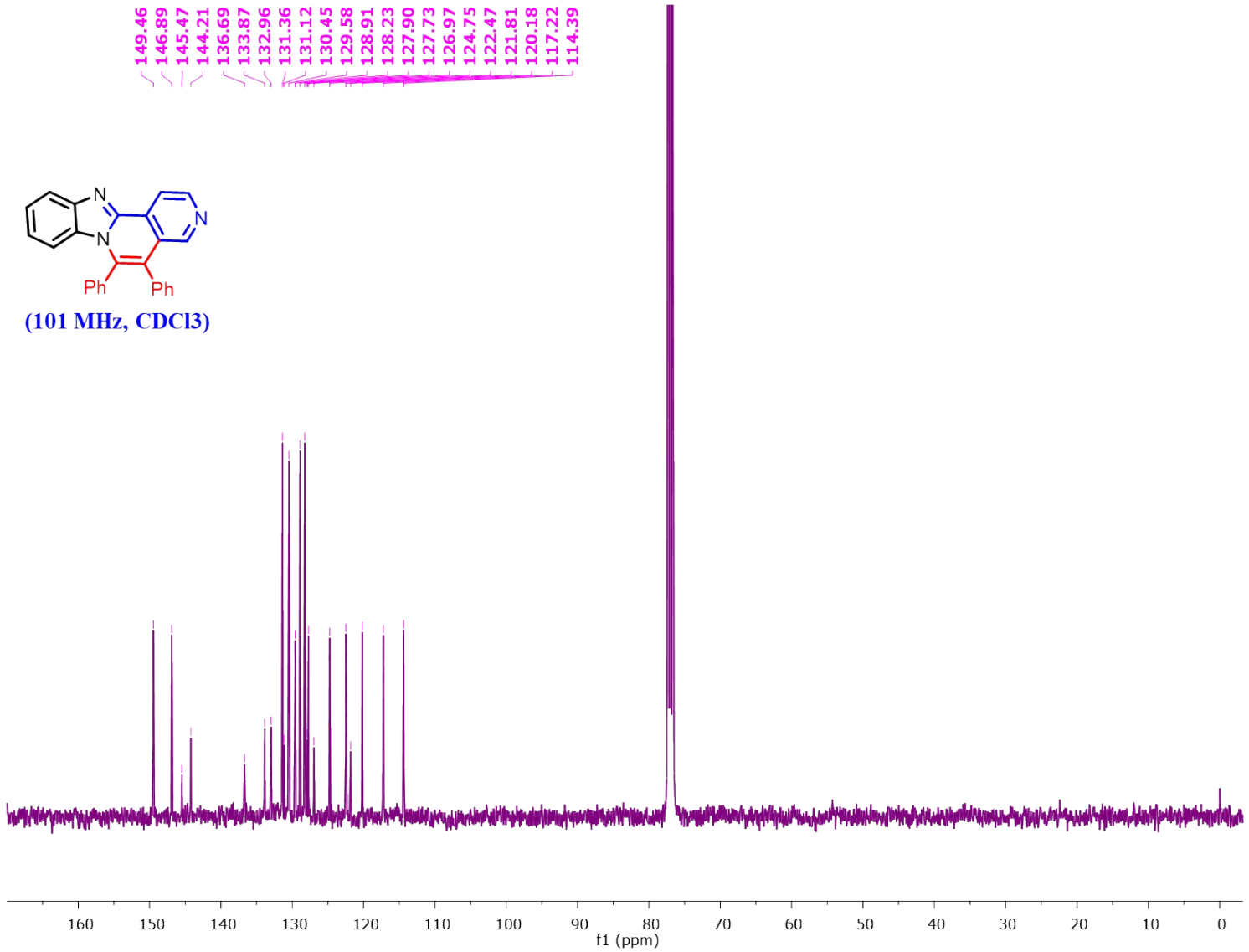

Fig. S113. ^{13}C NMR spectra of 5,6-diphenylbenzo [4,5] imidazo[2,1-a] [2,6] naphthyridine (**5u**) in $CDCl_3$.

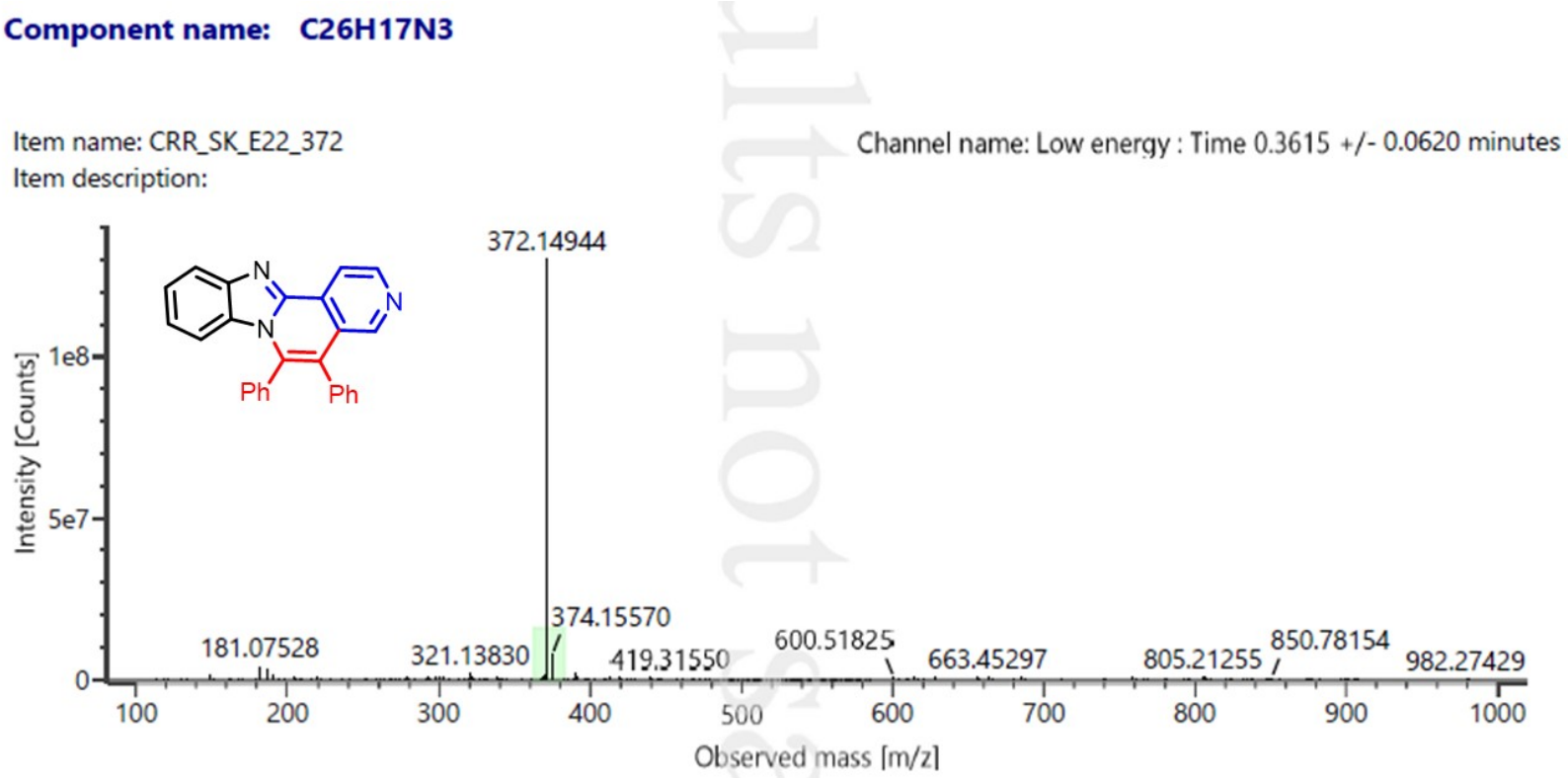

Fig. S114. HRMS spectra of 5,6-diphenylbenzo [4,5] imidazo[2,1-a] [2,6] naphthyridine (**5u**).

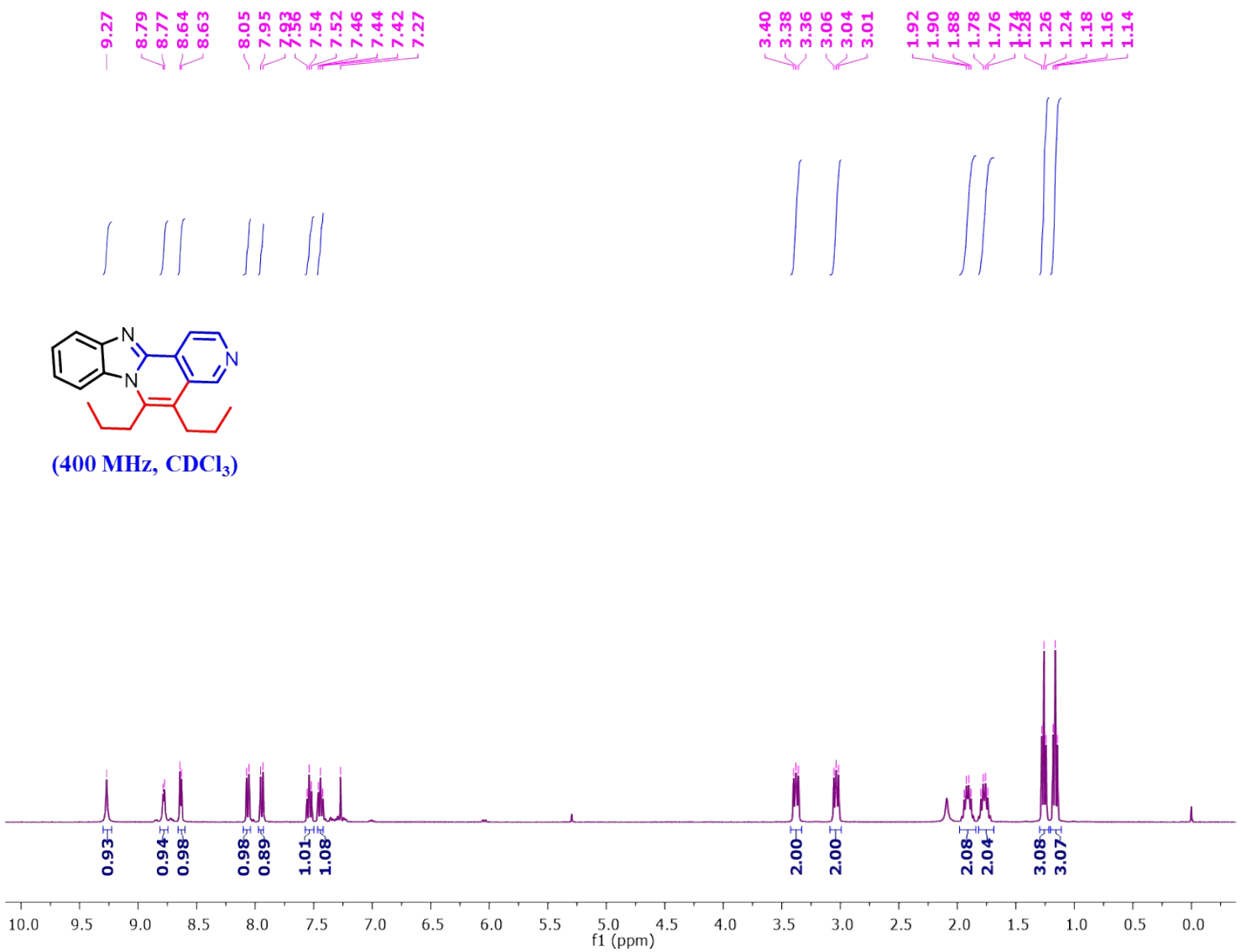

Fig. S115. ^{1}H NMR spectra of 5,6-dipropylbenzo [4,5] imidazo[2,1-a] [2,6] naphthyridine (**5v**) in $CDCl_3$.

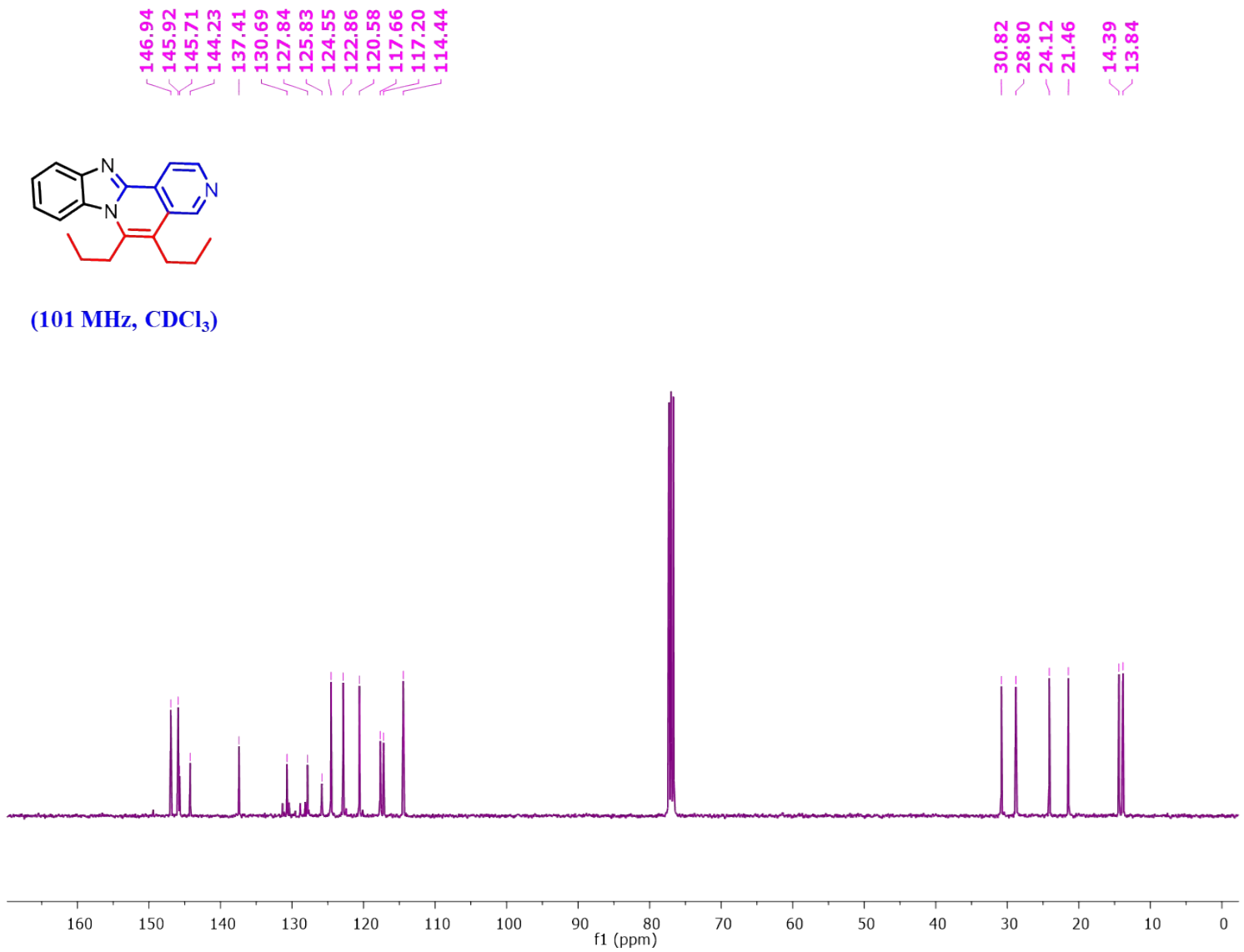

Fig. S116. ^{13}C NMR spectra of 5,6-dipropylbenzo [4,5] imidazo [2,1-a] [2,6] naphthyridine (**5v**) in $CDCl_3$.

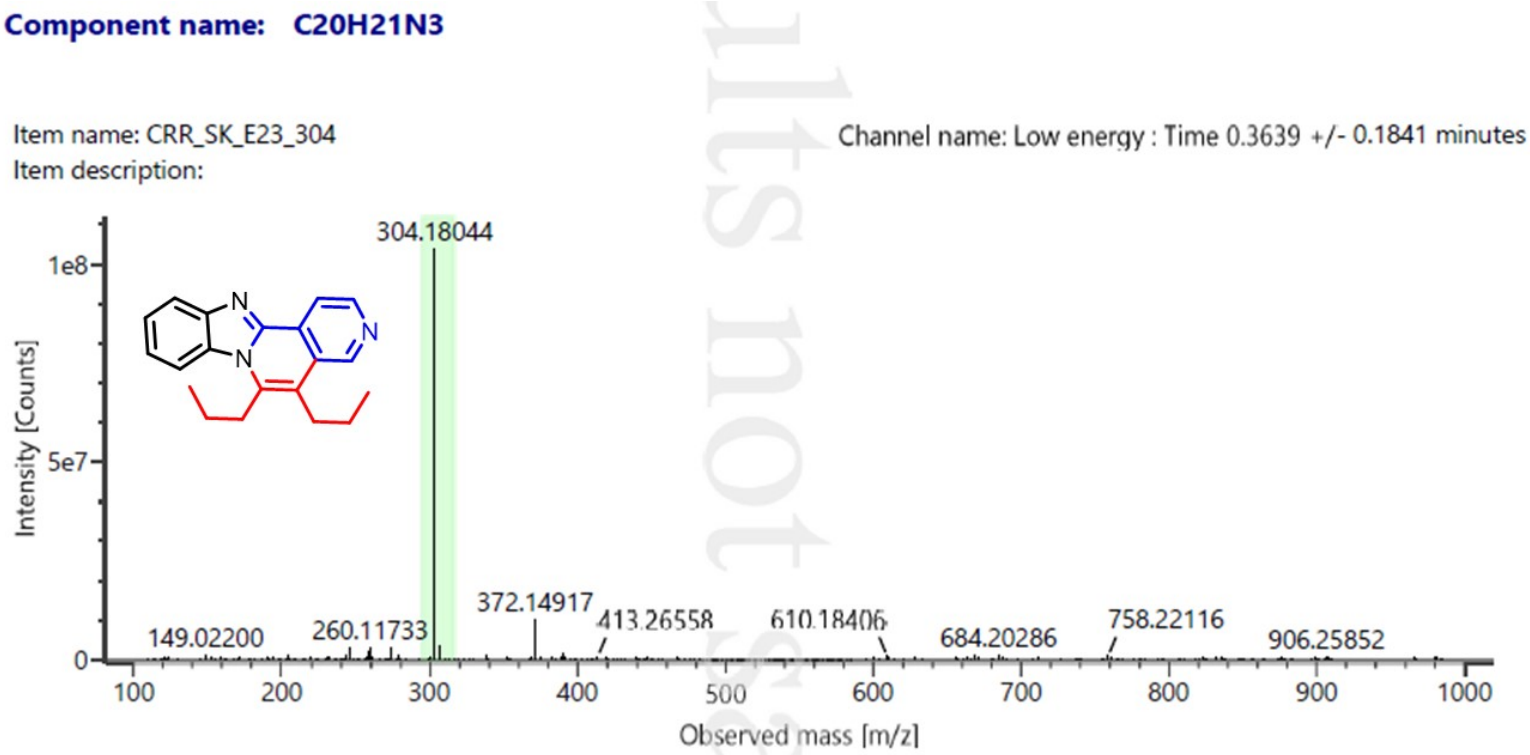

Fig. S117. HRMS spectra of 5,6-dipropylbenzo [4,5] imidazo[2,1-a] [2,6] naphthyridine (**5v**).

Fig. S118. ^{1}H NMR spectra of N, N-diethyl-5,6-diphenylbenzo [4,5] imidazo [2,1-a] isoquinolin-3 amine (**5w**) in $CDCl_3$.

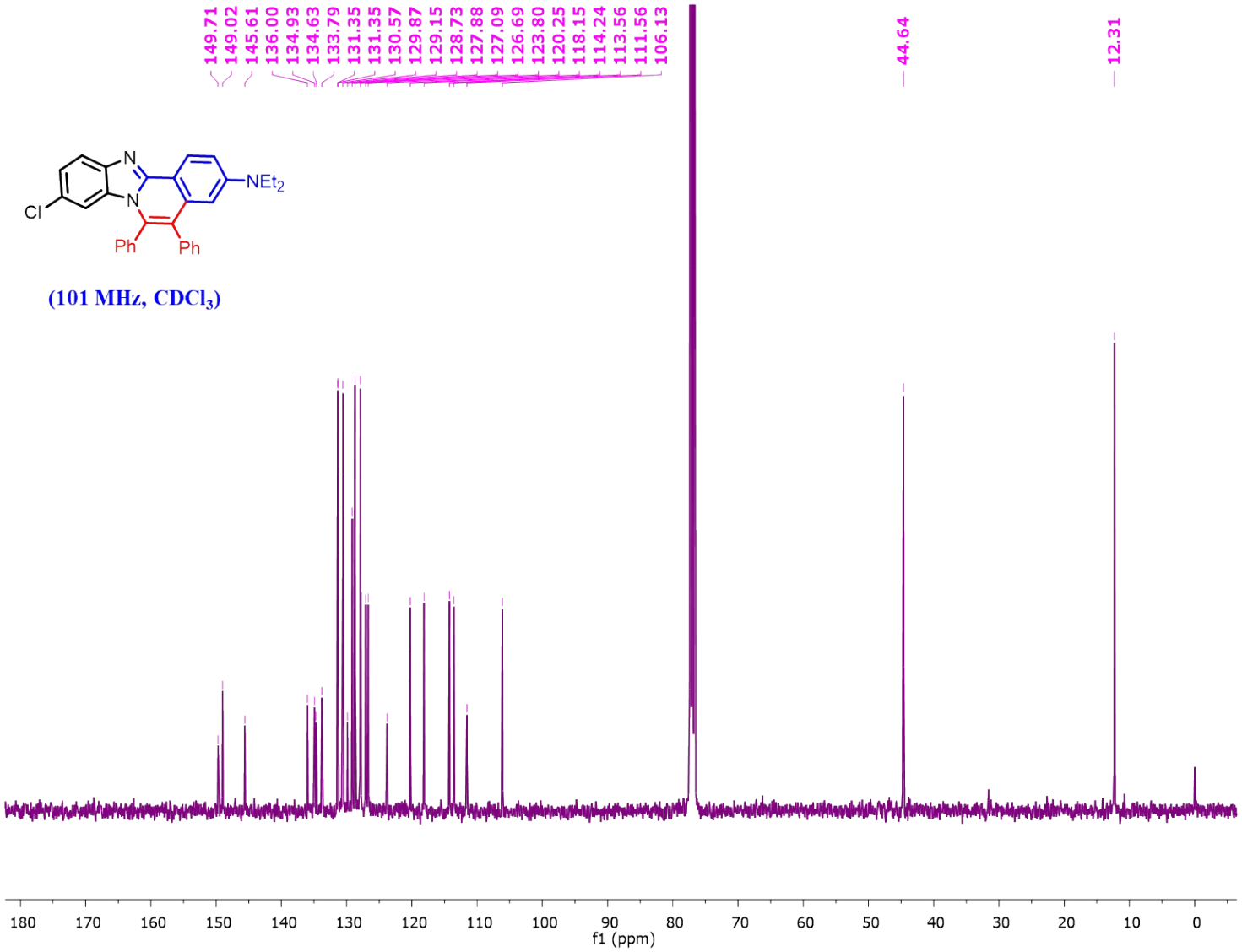

Fig. S119. ^{13}C NMR spectra of N, N diethyl-5,6-diphenylbenzo [4,5] imidazo[2,1-a] isoquinolin-3 amine (**5w**) in $CDCl_3$.

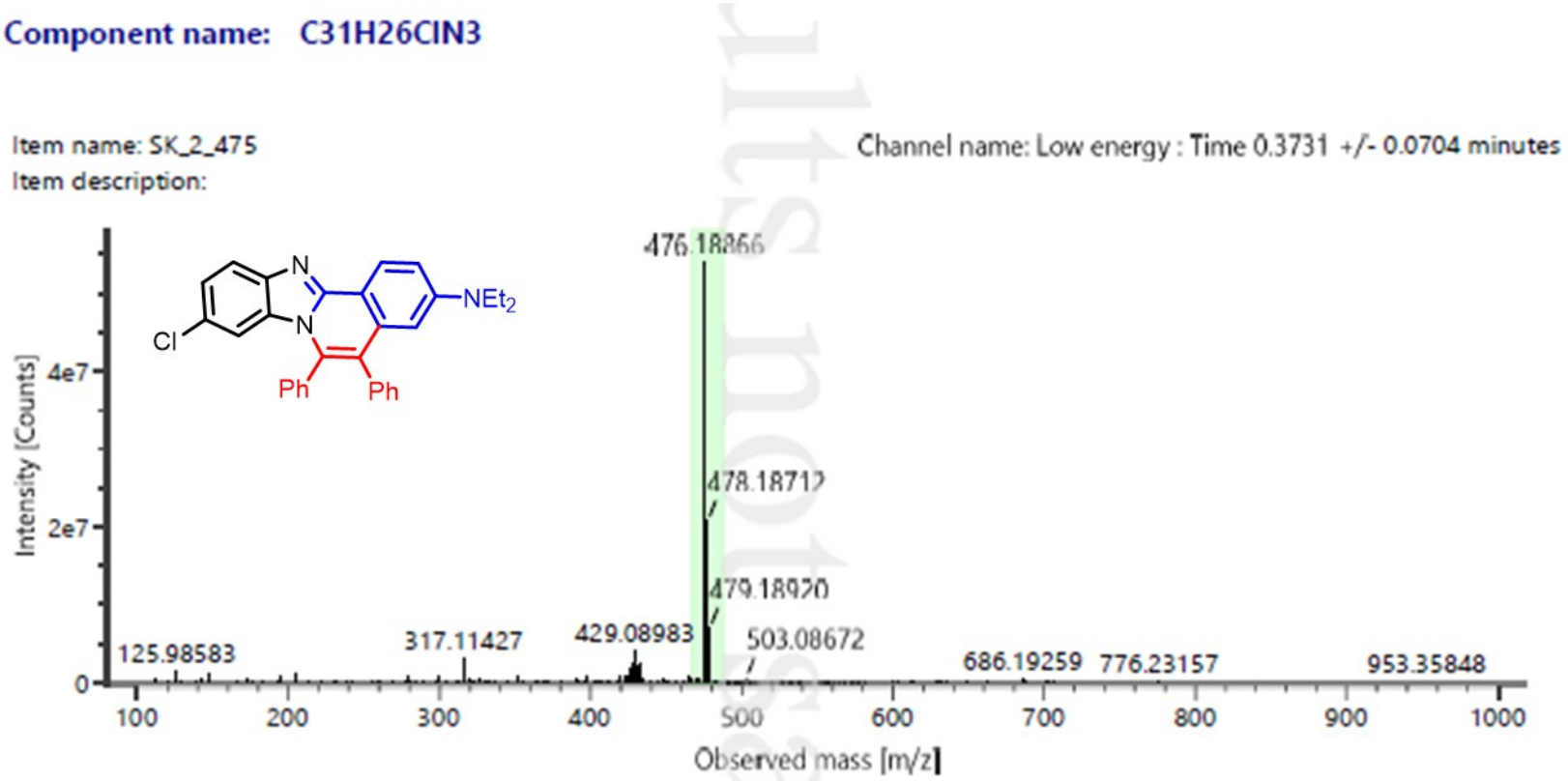

Fig. S120. HRMS spectra of N, N diethyl-5,6-diphenylbenzo [4,5] imidazo[2,1-a] isoquinolin-3 amine (**5w**).

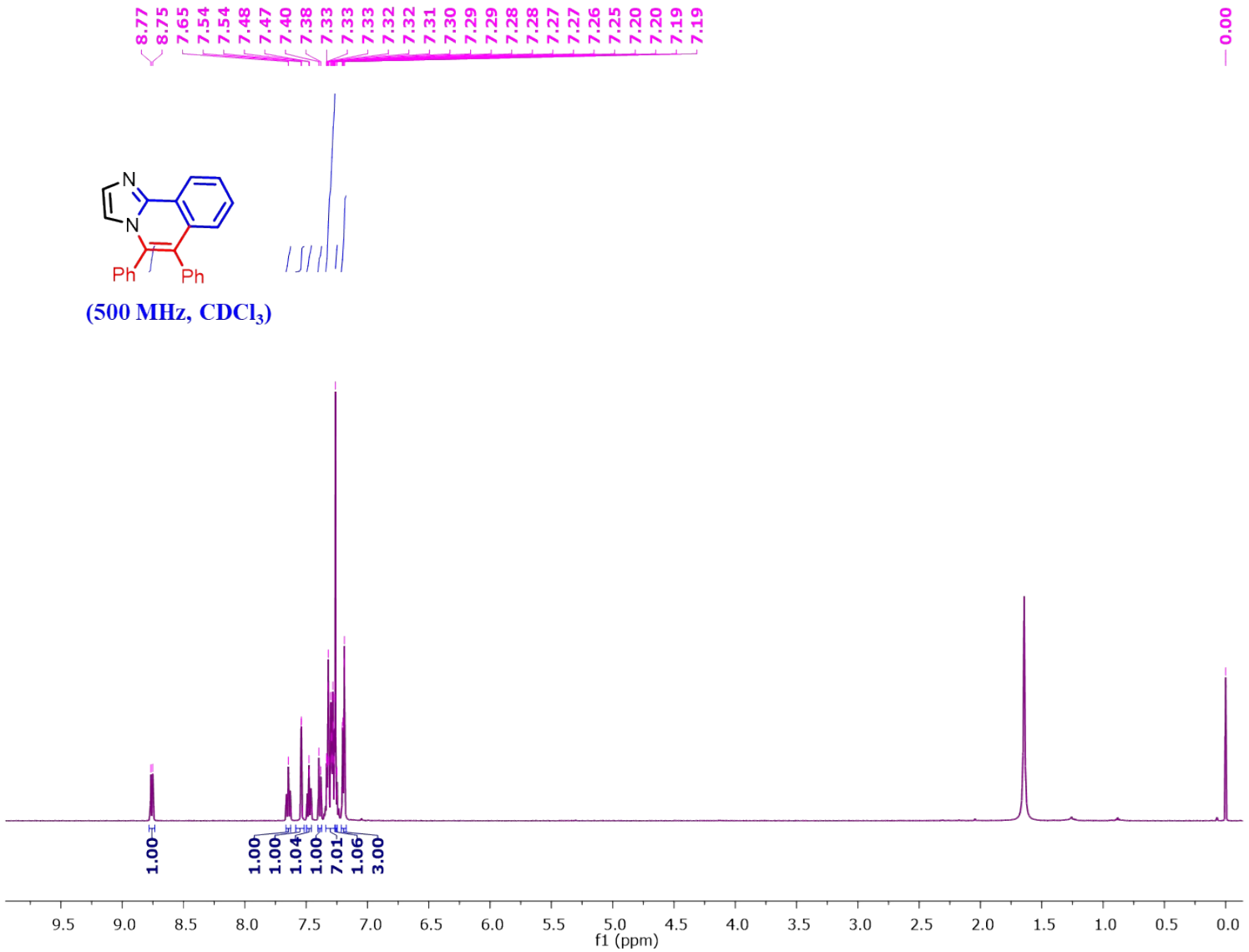

Fig. S121. ^{1}H NMR spectra of5,6-diphenylimidazo[2,1-a] isoquinoline (**5x**) in CDC_{l3}.

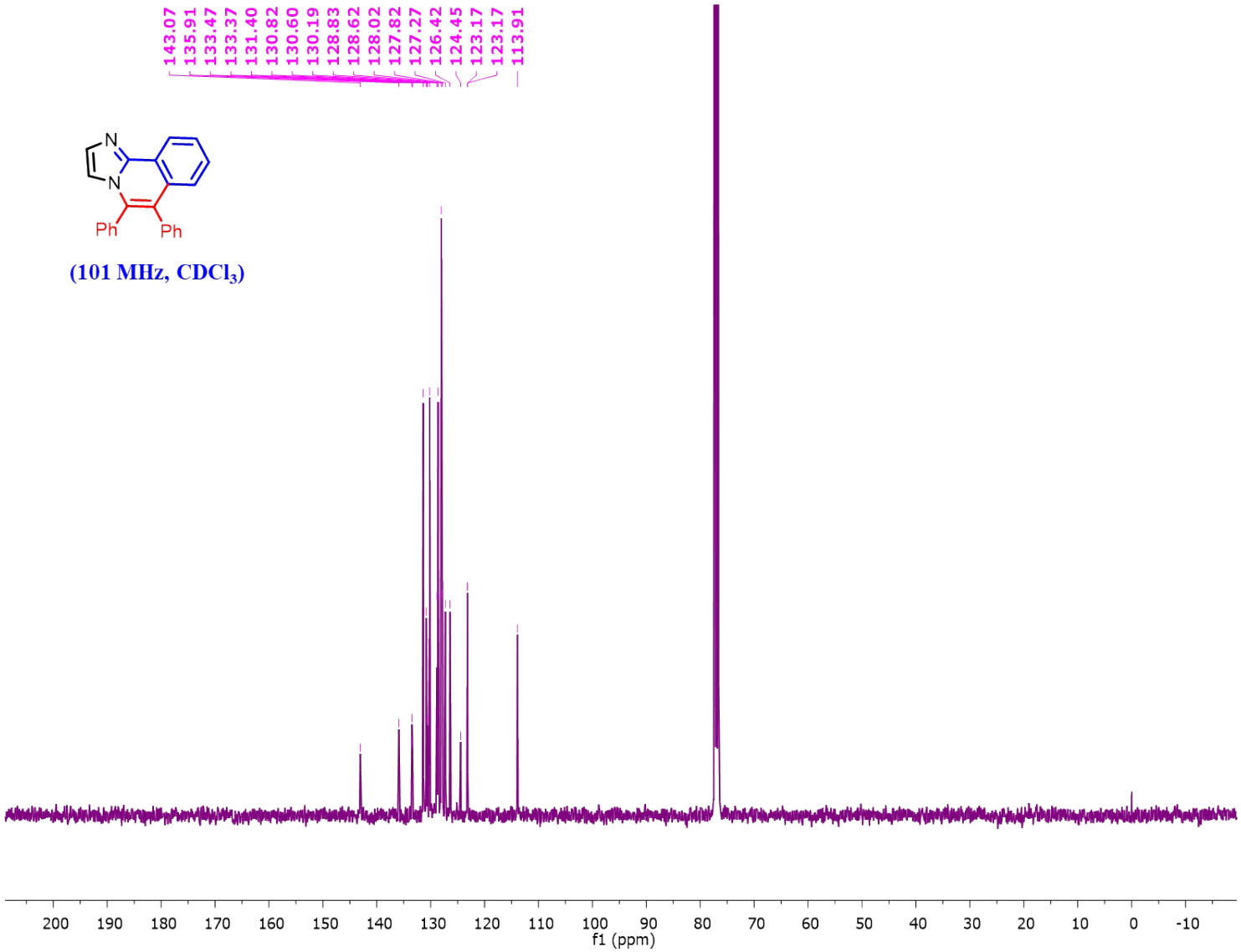

Fig. S122. ^{13}C NMR spectra of5,6-diphenylimidazo[2,1-a] isoquinoline (**5x**) in $CDCl_3$.

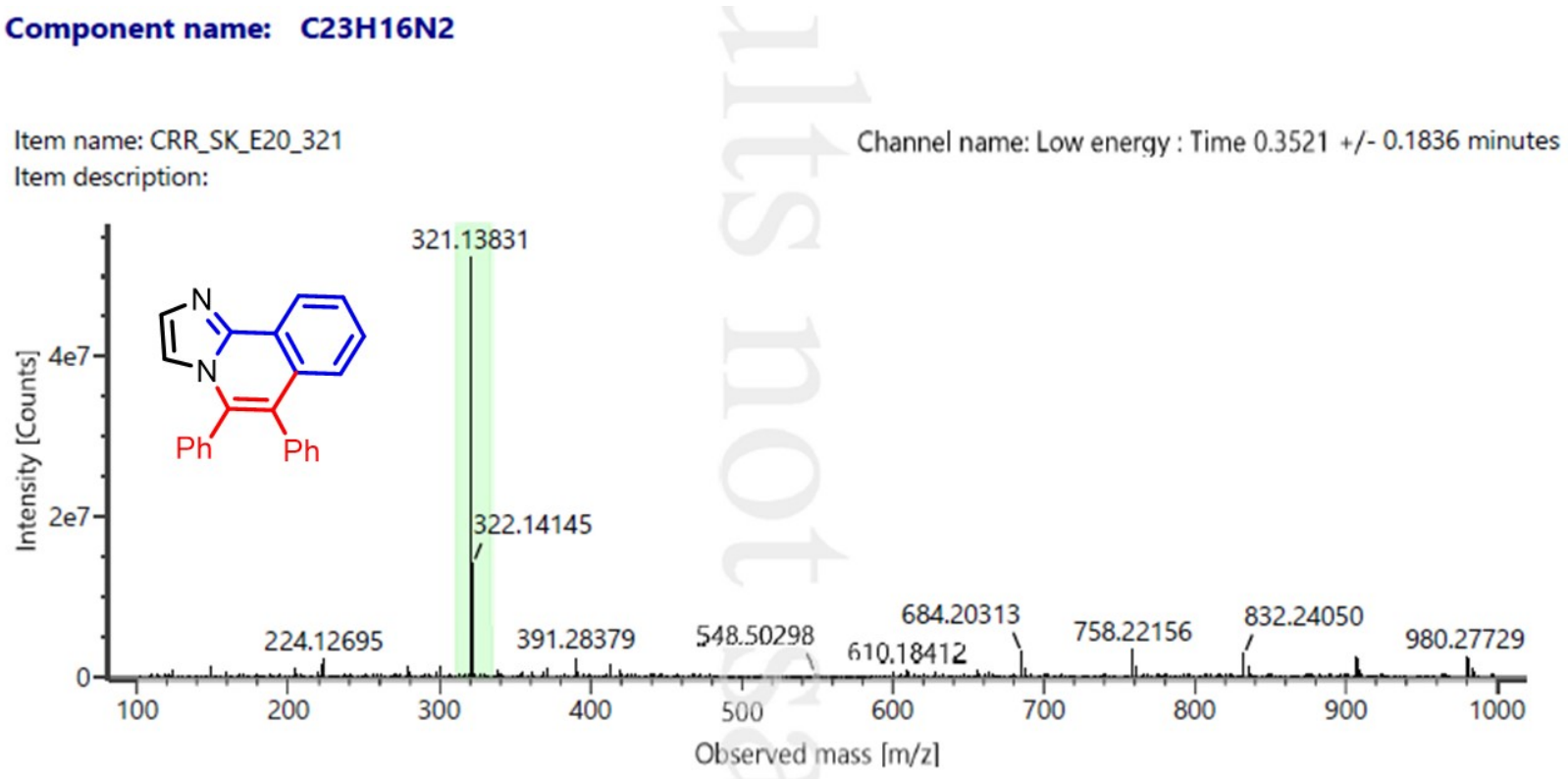

Fig. S123. HRMS spectra of5,6-diphenylimidazo[2,1-a] isoquinoline (**5x**).

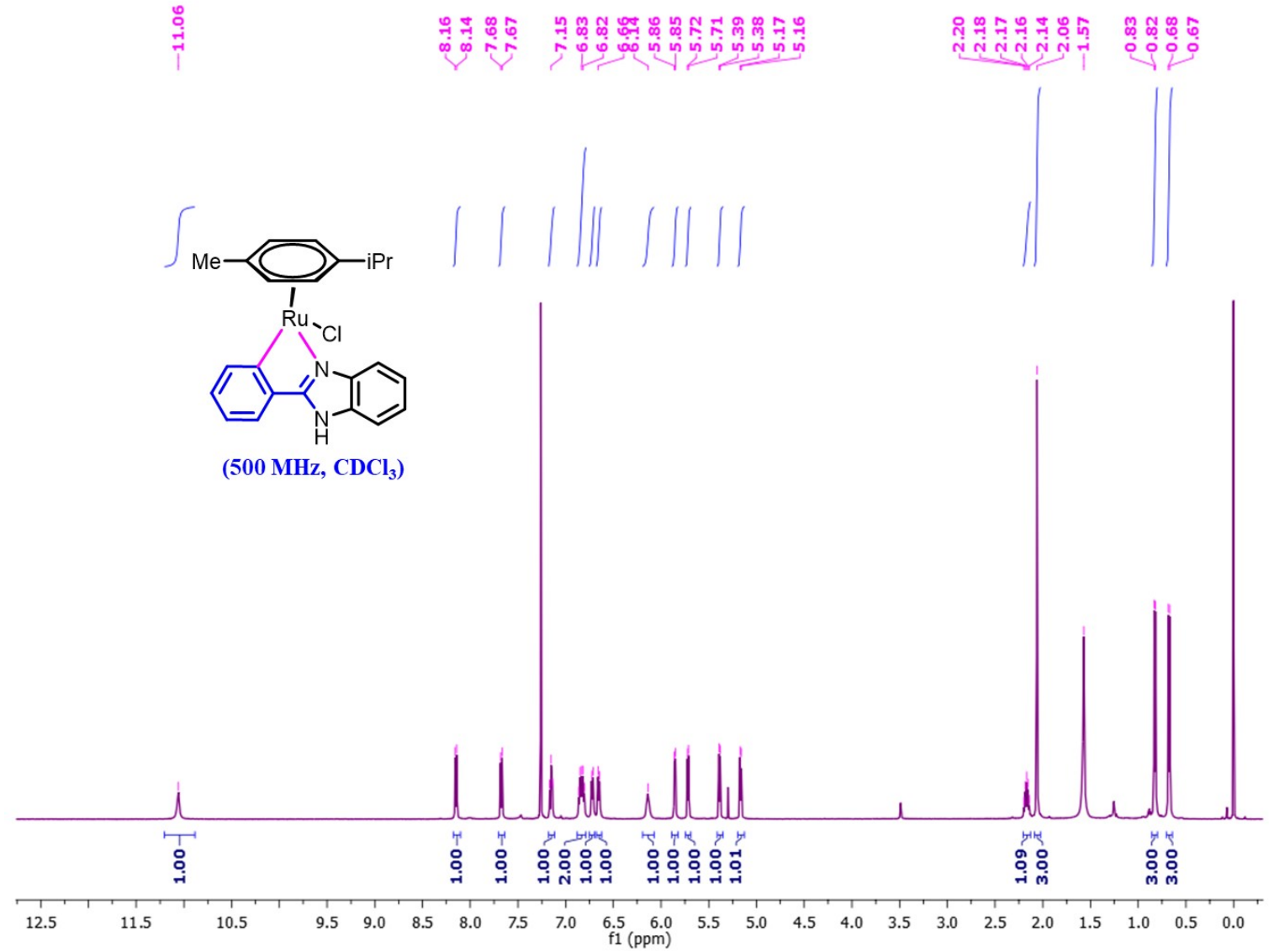

Fig. S124. ^{1}H NMR spectra of **Ru-II** complex in $CDCl_3$.

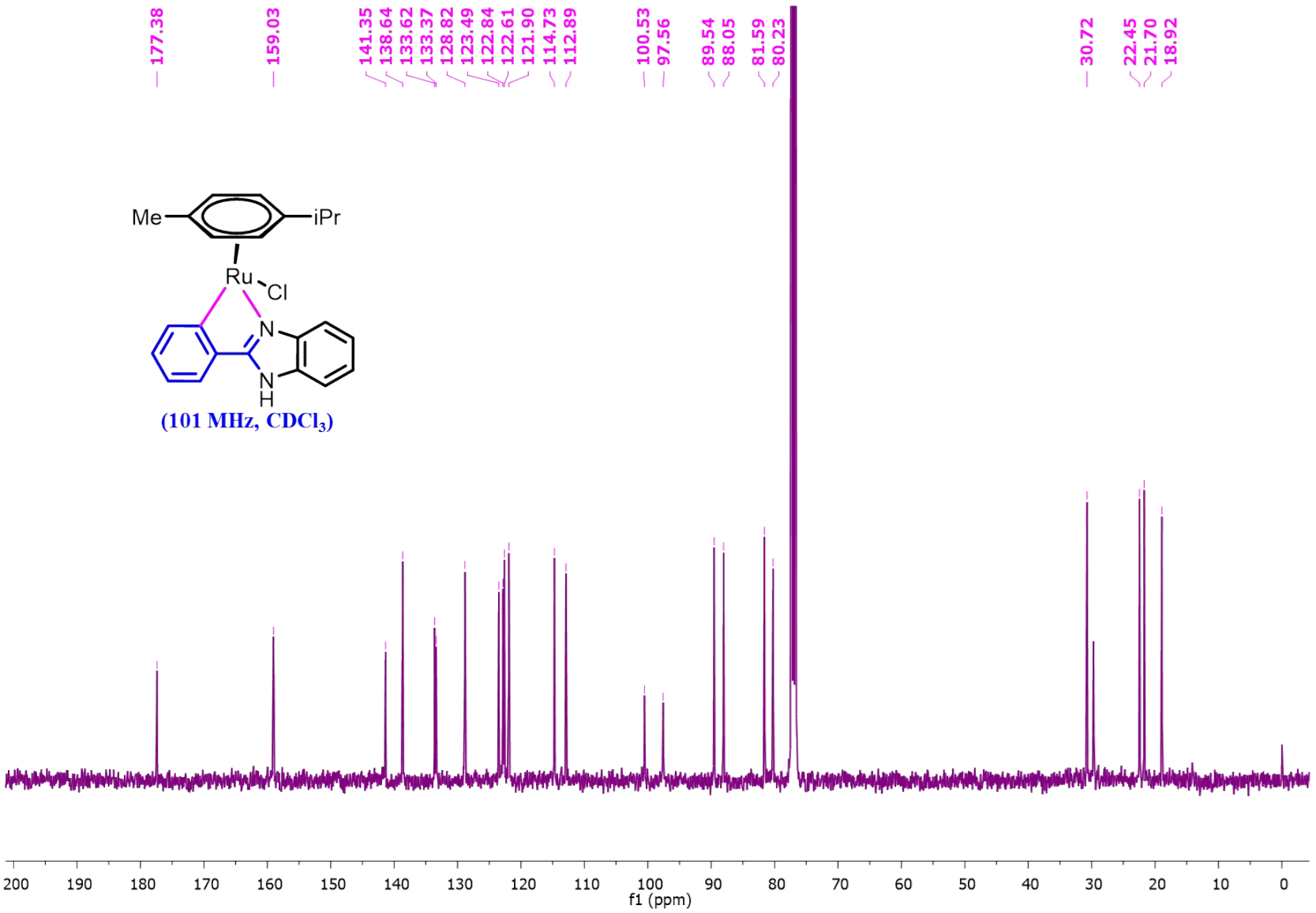

Fig. S125. ^{13}C NMR spectra of **Ru-II** complex in $CDCl_3$.

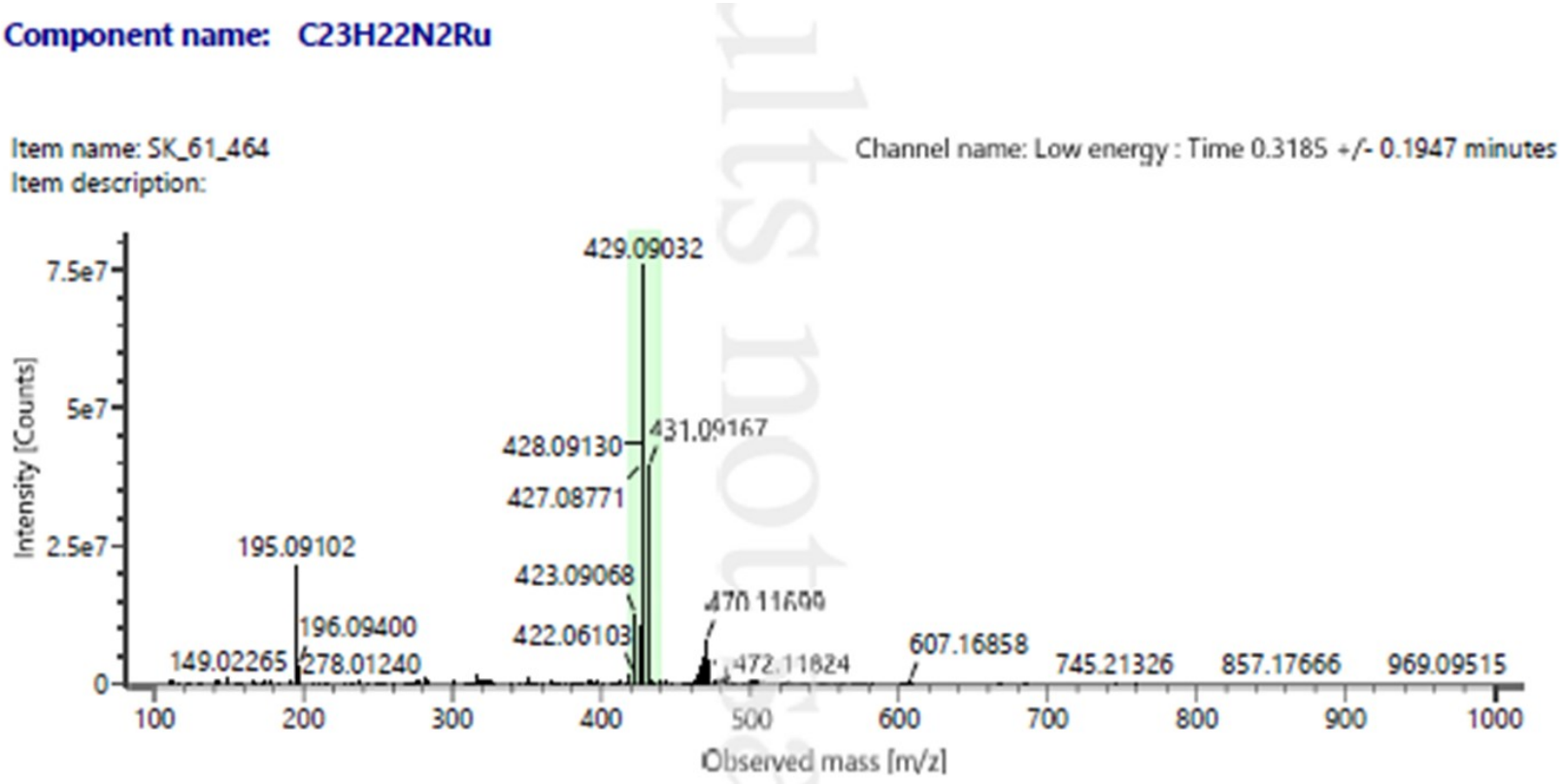

Fig. S126. HRMS spectra of **Ru-II** complex.

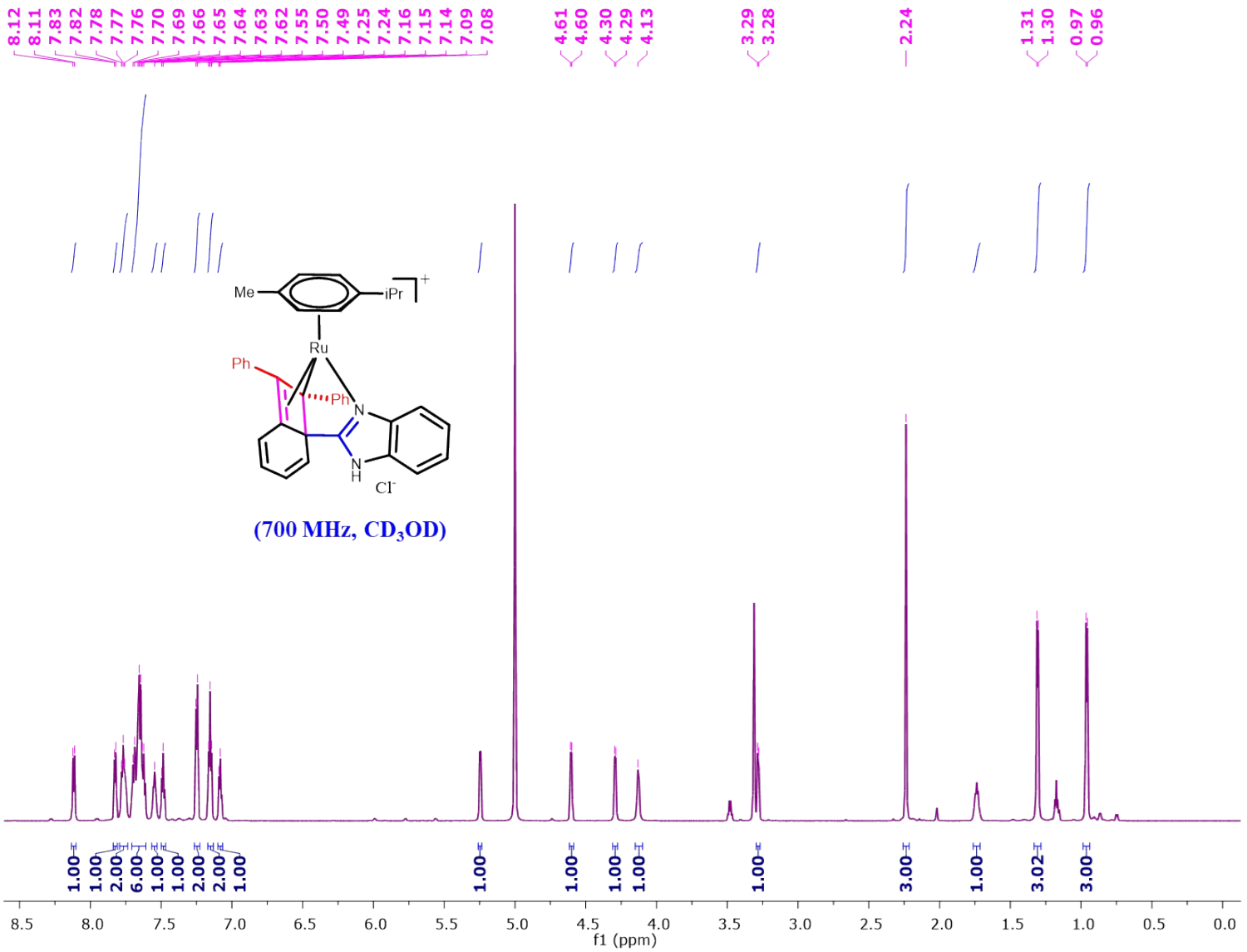

Fig. S127. ^{1}H NMR spectra of **Ru-IV** complex in CD_3OD.

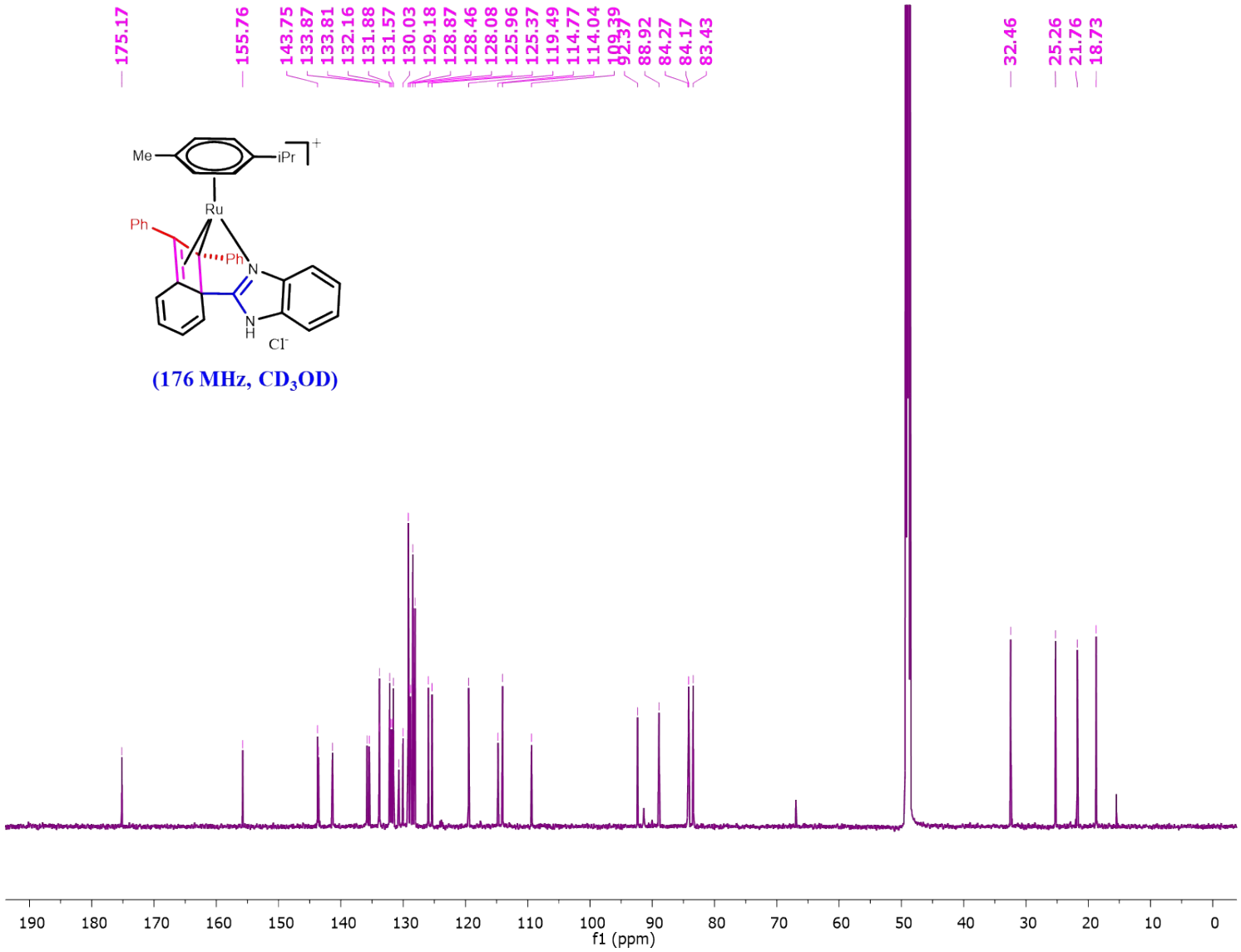

Fig. S128. ^{13}C NMR spectra of **Ru-IV** complex in CD_3OD.

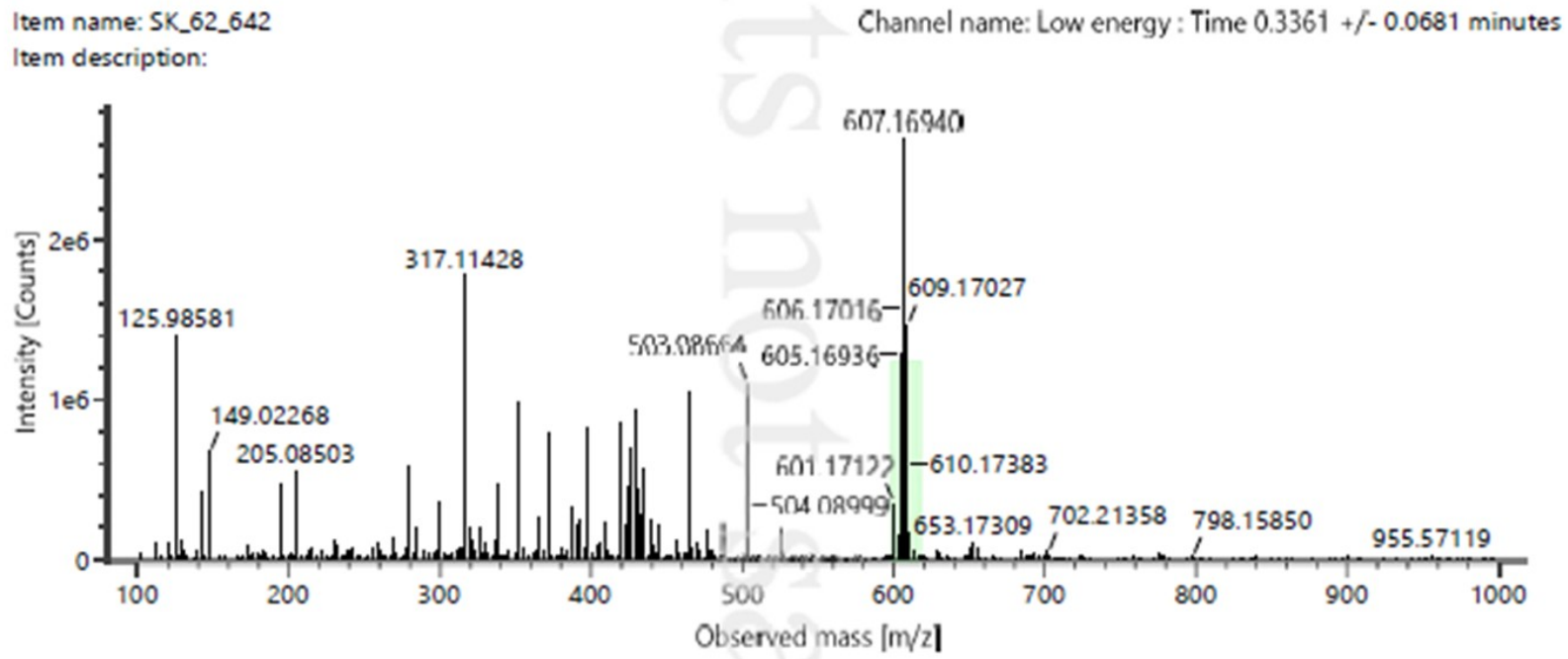

Fig. S129. HRMS spectra of **Ru-IV** complex.